Prepared in cooperation with the Nuclear Regulatory Commission

Recurrence Intervals for Great Earthquakes of the Past 3,500 Years at Northeastern Willapa Bay, Washington

Professional Paper 1576

epartment of the Interior
eological Survey

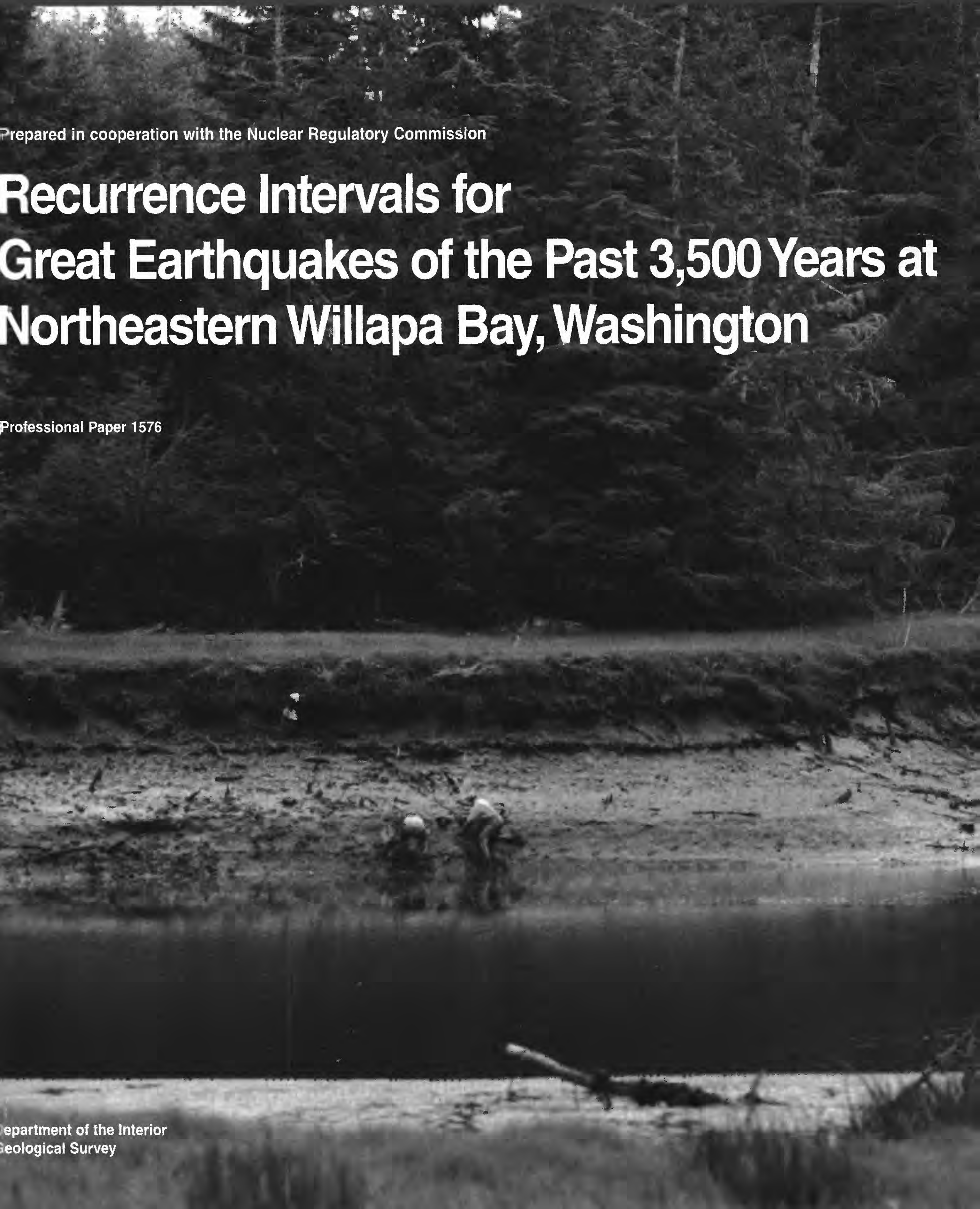

AVAILABILITY OF PUBLICATIONS OF THE U.S. GEOLOGICAL SURVEY

Order U.S. Geological Survey (USGS) publications from the offices listed below. Detailed ordering instructions, along with prices of the last offerings, are given in the current-year issues of the catalog "New Publications of the U.S. Geological Survey."

BOOKS, MAPS, AND OTHER PUBLICATIONS

By Mail

Books, maps, and other publications are available by mail from—

USGS Information Services
Box 25286, Federal Center, Denver, CO 80225

Publications include Professional Papers, Bulletins, Water-Supply Papers, Techniques of Water-Resources Investigations, Circulars, Fact Sheets, publications of general interest, single copies of permanent USGS catalogs, and topographic and thematic maps.

Over the Counter

Books, maps, and other publications of the U.S. Geological Survey are available over the counter at the following USGS Earth Science Information Centers (ESIC's), all of which are authorized agents of the Superintendent of Documents:

- **Anchorage, Alaska**—Rm. 101, 4230 University Dr.
- **Denver, Colorado**—Bldg. 810, Federal Center
- **Menlo Park, California**—Rm. 3128, Bldg. 3, 345 Middlefield Rd.
- **Reston, Virginia**—Rm. 1C402, USGS National Center, 12201 Sunrise Valley Dr.
- **Salt Lake City, Utah**—2222 West, 2300 South
- **Spokane, Washington**—Rm. 135, U.S. Post Office Building, 904 West Riverside Ave.
- **Washington, D.C.**—Rm. 2650, Main Interior Bldg., 18th and C Sts., NW.

Maps only may be purchased over the counter at the following USGS office:

- **Rolla, Missouri**—1400 Independence Rd.

Electronically

Some USGS publications, including the catalog "New Publications of the U.S. Geological Survey" are also available electronically on the USGS's World Wide Web home page at

http://www.usgs.gov

PRELIMINARY DETERMINATION OF EPICENTERS

Subscriptions to the periodical "Preliminary Determination of Epicenters" can be obtained only from the Superintendent of Documents. Check or money order must be payable to the Superintendent of Documents. Order by mail from—

Superintendent of Documents
Government Printing Office
Washington, DC 20402

INFORMATION PERIODICALS

Many Information Periodicals products are available through the systems or formats listed below:

Printed products: Printed copies of the Minerals Yearbook and the Mineral Commodities Summaries can be ordered from the Superintendent of Documents, Government Printing Office (address above). Printed copies of Metal Industry Indicators and Mineral Industry Surveys can be ordered from the Center for Disease Control and Prevention, National Institute for Occupational Safety and Health, Pittsburgh Research Center, P.O. Box 18070, Pittsburgh, PA 15236–0070.

Mines FaxBack: Return fax service.

1. Use the touch-tone handset attached to your fax machine's telephone jack. (ISDN [digital] telephones cannot be used with fax machines.)
2. Dial (703) 648–4999.
3. Listen to the menu options and punch in the number of your selection, using the touch-tone telephone.
4. After completing your selection, press the start button on your fax machine.

CD-ROM: A disc containing chapters of the Minerals Yearbook (1993–95), the Mineral Commodity Summaries (1995–97), a statistical compendium (1970–90), and other publications is updated three times a year and sold by the Superintendent of Documents, Government Printing Office (address above).

World Wide Web: http://minerals.er.usgs.gov/minerals/

SUBSCRIPTION TO THE CATALOG "NEW PUBLICATIONS OF THE U.S. GEOLOGICAL SURVEY"

Those wishing to be placed on a free subscription list for the catalog "New Publications of the U.S. Geological Survey" should write to the U.S. Geological Survey, 903 National Center, Reston, VA 20192.

Recurrence Intervals for Great Earthquakes Of the Past 3,500 Years at Northeastern Willapa Bay, Washington

By Brian F. Atwater and Eileen Hemphill-Haley

A geologic history of earthquakes
at the Cascadia subduction zone

U.S. GEOLOGICAL SURVEY PROFESSIONAL PAPER 1576

Prepared in cooperation with the
Nuclear Regulatory Commission

U.S. DEPARTMENT OF THE INTERIOR
MARCH 3, 1849

UNITED STATES GOVERNMENT PRINTING OFFICE, WASHINGTON : 1997

U.S. DEPARTMENT OF THE INTERIOR
BRUCE BABBITT, Secretary

U.S. GEOLOGICAL SURVEY
MARK SCHAEFER, Interim Director

For sale by U.S. Geological Survey, Information Services
Box 25286, Federal Center, Denver, CO 80225

Published in the Western Region, Menlo Park, Calif.
Manuscript approved for publication August 21, 1997.

Library of Congress Cataloging in Publication Data

Atwater, Brian F.
Recurrence intervals for great earthquakes of the past 3,500 years at northeastern Willapa Bay, Washington / by Brian F. Atwater and Eileen Hemphill-Haley.
p. cm. — (U.S. Geological Survey professional paper ; 1576)
"A geologic history of earthquakes at the Cascadia subduction zone."
"Prepared in cooperation with the Nuclear Regulatory Commission."
Includes bibliographical references.
Supt. of Docs. no.: I 19.16: 1576
1. Paleoseismology—Holocene. 2. Paleoseismology—Washington (State)—Willapa Bay Region. I. Hemphill-Haley, Eileen. II. U.S. Nuclear Regulatory Commission. III. Title. IV. Series.
QE539.2.P34A88 1997
551.22'09797'92—dc21 97–34929
CIP

CONTENTS

FIGURES

TABLES

Recurrence Intervals for Great Earthquakes of the Past 3,500 Years at Northeastern Willapa Bay, Washington

By Brian F. Atwater and Eileen Hemphill-Haley

ABSTRACT

Plate-boundary earthquakes have occurred repeatedly in the past several thousand years at the Cascadia subduction zone, where they are widely recorded by buried marsh and forest soils beneath estuarine wetlands. This report adds to previous accounts of such soils along the Pacific coast of southern Washington State. Our new evidence comes from outcrop surveys, diatom analyses, and radiocarbon dating of soils exposed about 10 km apart in banks of the Niawiakum and Willapa Rivers, tidal arms of Willapa Bay. This new evidence clarifies the timing of great (magnitude 8 or larger) earthquakes during the past 3,500 years at this part of the Cascadia subduction zone.

All the surveyed outcrops display buried soils that probably record tectonic subsidence during earthquakes. Although in many cases we cannot rule out every alternative to such coseismic subsidence, we found no buried soil that is better explained by stream migration, storm, river flood, sea-level rise, barrier breaching, or sediment compaction.

Each of the soils probably represents a marsh or forest that suddenly became a tidal flat and consequently was buried by tidal mud. In nearly every case the soils have too much lateral continuity and too little relief to record cutting and filling by tidal streams. Vascular-plant fossils preserved within and above many of the soils show that storms or floods, if unaccompanied by lasting submergence, cannot account for burial of the soils. Where their remains are preserved, plants that had lived on the soils belong to species indicative of high parts of tidal marshes, or of tidal swamps or uplands. By contrast, the main vascular-plant species preserved in mud above the soils is *Triglochin maritimum*, a colonist of saltwater mudflats in southern coastal Washington. Assemblages of diatoms verify vascular-plant evidence for lasting submergence and show that such submergence is recorded also by buried soils with which vascular-plant fossils are not preserved. In an outcrop along the Niawiakum River, for example, diatoms show that each of six successive soils represents a high marsh or an upland, and that mud above each of these soils represents an intertidal or subtidal mudflat.

Fossils further show that the change from high marsh or upland to mudflat probably happened too fast to have resulted from a gradual rise in sea level. For every soil studied for fossil diatoms, diatom assemblages imply that this change happened suddenly, without transition through low marsh. Gradual sea-level rise is further precluded for some soils by remains of vascular plants that had lived on buried soils. These remains include stems and leaves that were surrounded by mudflat deposits before they had time to decompose.

Other alternatives to coseismic subsidence can be discounted as well. Submergence from breaching of a baymouth barrier is ruled out by soils of brackish marshes that require tidal connection with the sea. Localized settlement from earthquake-induced compaction of unconsolidated Holocene deposits does not explain the presence of buried soils directly above well-consolidated Pleistocene deposits. Evidence against alternative explanations at one outcrop can be extrapolated to other outcrops by radiocarbon and stratigraphic correlation of buried soils.

Plate-boundary earthquakes probably account for all the subsidence events. The plate boundary is the only recognized fault common to all areas having evidence for coseismic subsidence in southern coastal Washington. Although some of these areas coincide with mapped late Cenozoic synclines, where coseismic subsidence might accompany earthquakes on faults in the North America plate, others are outside such synclines.

The coseismically subsided areas include part of welt of Eocene basement rock 40 km long and 15 km wide, herein termed the South Bend antiform. This structural high, the largest in southern coastal Washington, has probably grown in late Cenozoic time. The South Bend antiform should subside during plate-boundary earthquakes that flex the North America plate throughout southern coastal Washington. By contrast, the antiform might grow upward during an upper-plate earthquake that produces subsidence only in late Cenozoic synclines that flank the antiform. With these expectations in mind, we compared outcrops off the South Bend antiform (Niawiakum River) with outcrops on the antiform (Willapa River). We found no difference in sense

or timing of earthquake-induced changes in land level. Like the surveyed outcrops along the Niawiakum River, the surveyed outcrops along the Willapa River contain buried soils indicative of earthquake-induced subsidence. The longest stratigraphic sequences exposed along both streams contain six or seven soils less than 3,500 years old, and these sequences correlate with one another on the basis of soil horizons, spruce roots, and radiocarbon ages.

Though every buried soil identified in the surveyed outcrops probably records a plate-boundary earthquake, not every plate-boundary earthquake is widely recorded by a buried soil. One buried soil was obliterated at many sites through centuries of decomposition, probably because shallow burial left the soil high in the weathering profile of a succeeding soil. Such decomposition also destroyed most of the organic matter associated with two other soils. In addition, a widespread soil might not be available for burial if an earthquake occurs too soon after its predecessor for much rebuilding of tidal marshes. Despite these limitations, the composite record from buried soils in large outcrops of northeastern Willapa Bay probably includes every earthquake in the area during the past 3,500 years that caused at least ½ m of widespread coseismic subsidence and followed the preceding great earthquake by more than a century.

Willapa Bay's earthquake history in the past 3,500 years probably includes seven events, each comprising a single rupture or multiple contiguous ruptures on the Washington part of the Cascadia plate boundary. Each event probably included at least one great earthquake, as judged from likely rupture widths inferred from modern geophysical evidence, likely rupture lengths inferred from coastwise correlation of buried soils, extensive sea-floor displacement inferred from a tsunami in Japan, and seismic-moment release deduced from plate motions and average recurrence intervals. The history begins with three events between 3,300–3,500 years ago and 2,400–2,800 years ago (ranges include estimated 95-percent confidence interval). The next recorded events occurred 1,500–1,700 and 1,130–1,350 years ago. They were followed by a poorly dated event that probably occurred before 900 years ago and may have been associated with rupture on inland faults in the North America plate 1,000–1,100 years ago. The most recent of the events happened close to 300 years ago, probably in January 1700.

The six intervals between events in this inferred history average 500–540 years but range from about one to three centuries to about a millenium. The earliest two intervals sum to 540–1,100 years. The first of them may have been the longer, as judged from spruce roots that may indicate prolonged interseismic emergence. Next came an interval of 700–1,300 years, when spruce forests spread onto emerging tidal marshes and decomposition largely destroyed an underlying buried soil. This exceptionally long interval was followed by two short ones that together spanned no more than 800 years. The most recent complete interval, marked by another spreading of spruce forests and decomposition of earlier buried soils, lasted 600–1,000 years.

This pattern of long and short recurrence intervals at Willapa Bay may match the pattern of intervals between turbidity currents in Cascadia Channel, on the abyssal sea floor 200 km off the central Oregon coast. Previous work showed that these currents largely originated at submarine canyon heads about 50 km west of Willapa Bay, and that great earthquakes may have generated 13 currents in the past 7,500 years. Although pelagic layers between the turbidites have been interpreted as evidence for recurrence intervals of fairly uniform duration, burrows in the turbidites suggest variability in recurrence intervals and allow one-for-one correlation with recurrence intervals inferred from buried soils at Willapa Bay.

INTRODUCTION

Plate-boundary earthquakes at the Cascadia subduction zone are known primarily from geologic evidence for prehistoric land-level changes, tsunamis, and shaking (figs. 1, 2). Average recurrence intervals estimated from this geologic evidence, as summarized in figure 3, range from a few hundred to more than one thousand years (Adams, 1990; Clarke and Carver, 1992; Atwater and others, 1995; Geomatrix Consultants, 1995; Darienzo and Peterson, 1995; Nelson and others, 1996a).

Much of this broad range in average recurrence intervals is due to problems with identifying and dating earthquakes (fig. 4). Such problems affect the strongest of the evidence for prehistoric plate-boundary earthquakes at the Cascadia subduction zone—buried marsh and swamp soils at estuaries along the Pacific coast between southern British Columbia and northern California. Many of these soils represent sudden tectonic subsidence of coastal land during plate-boundary earthquakes; the subsidence caused frequent tidal submergence and consequent burial of the soils by estuarine mud and sand (Atwater and others, 1995). However, burial of some of the soils may have resulted from nonseismic events, such as storms or rapid sea-level rise (fig. 4*B*) (Nelson and others, 1996a, b), or from earthquakes on faults in the North America plate (fig. 4*C*) (Nelson, 1992a; Clarke and Carver, 1992; McCaffrey and Goldfinger, 1995). Still other soils may have disappeared through decomposition or erosion, or may have escaped burial through insufficient tidal submergence or sediment supply (fig. 4*D*). Moreover, the combined geologic and analytical errors in radiocarbon dating of the earthquakes can approach or exceed the lengths of time between them, with consequently large uncertainty in the duration of recurrence intervals (fig.4*E*) (Nelson, 1992b; Atwater, 1992).

We reduced such uncertainties in identifying and dating earthquakes by studying sequences of buried soils in low-tide outcrops at northeastern Willapa Bay (figs. 5, 6). We took advantage of large outcrops to make stratigraphic and paleontologic tests of alternatives to sudden tectonic subsidence and to identify poorly preserved soils that might be overlooked in isolated borings. We also used the varied

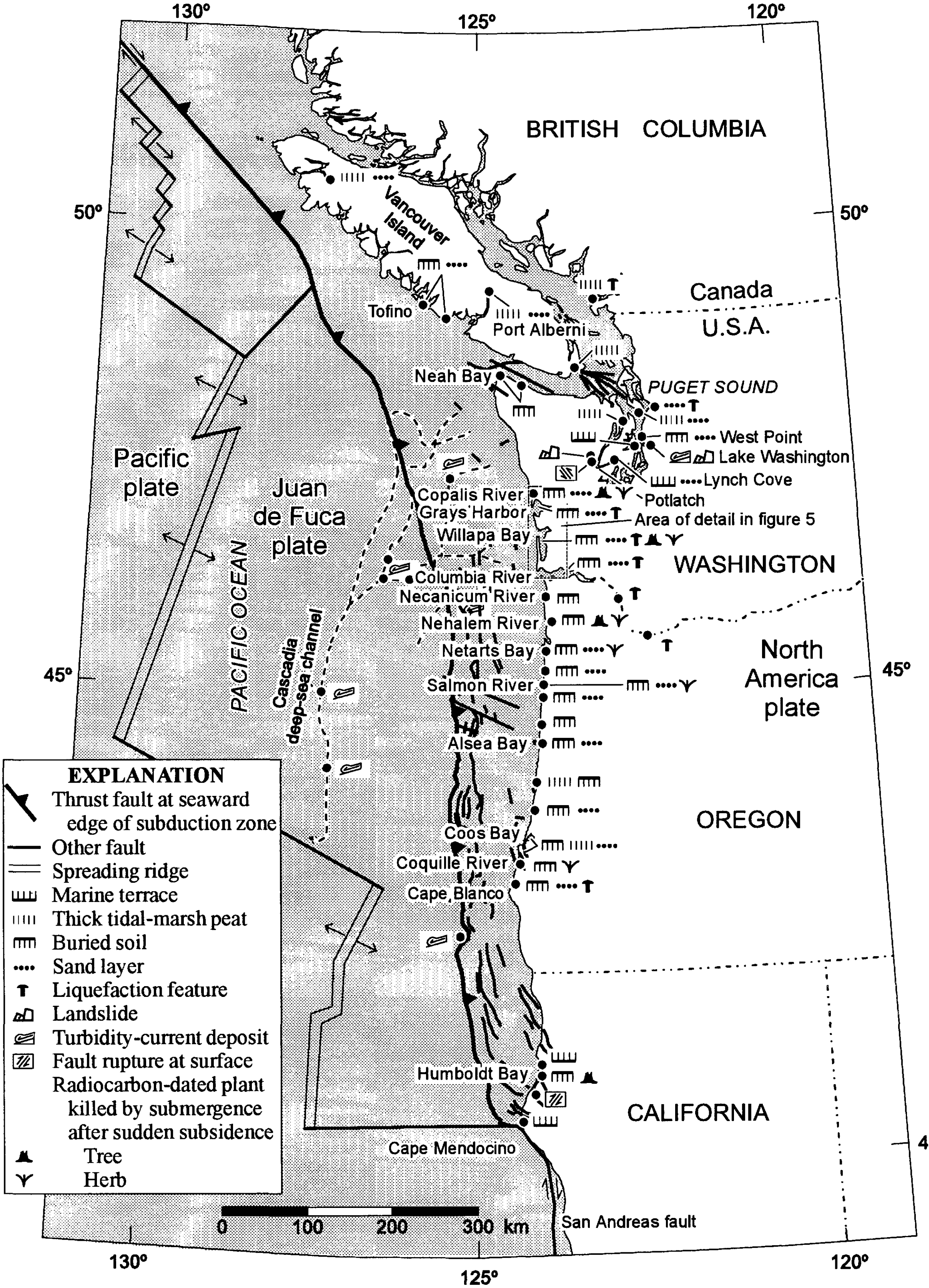

Figure 1. Cascadia subduction zone. Symbols explained at lower left depict plate boundaries, faults active or probably active in the Quaternary, and evidence bearing on occurrence of Holocene earthquakes. Modified from compilations by Atwater and others (1995) and, for the Puget Sound area, by Bucknam and others (1992). Includes additions from Benson and others (1997) and unpublished data from Oregon provided by Alan R. Nelson.

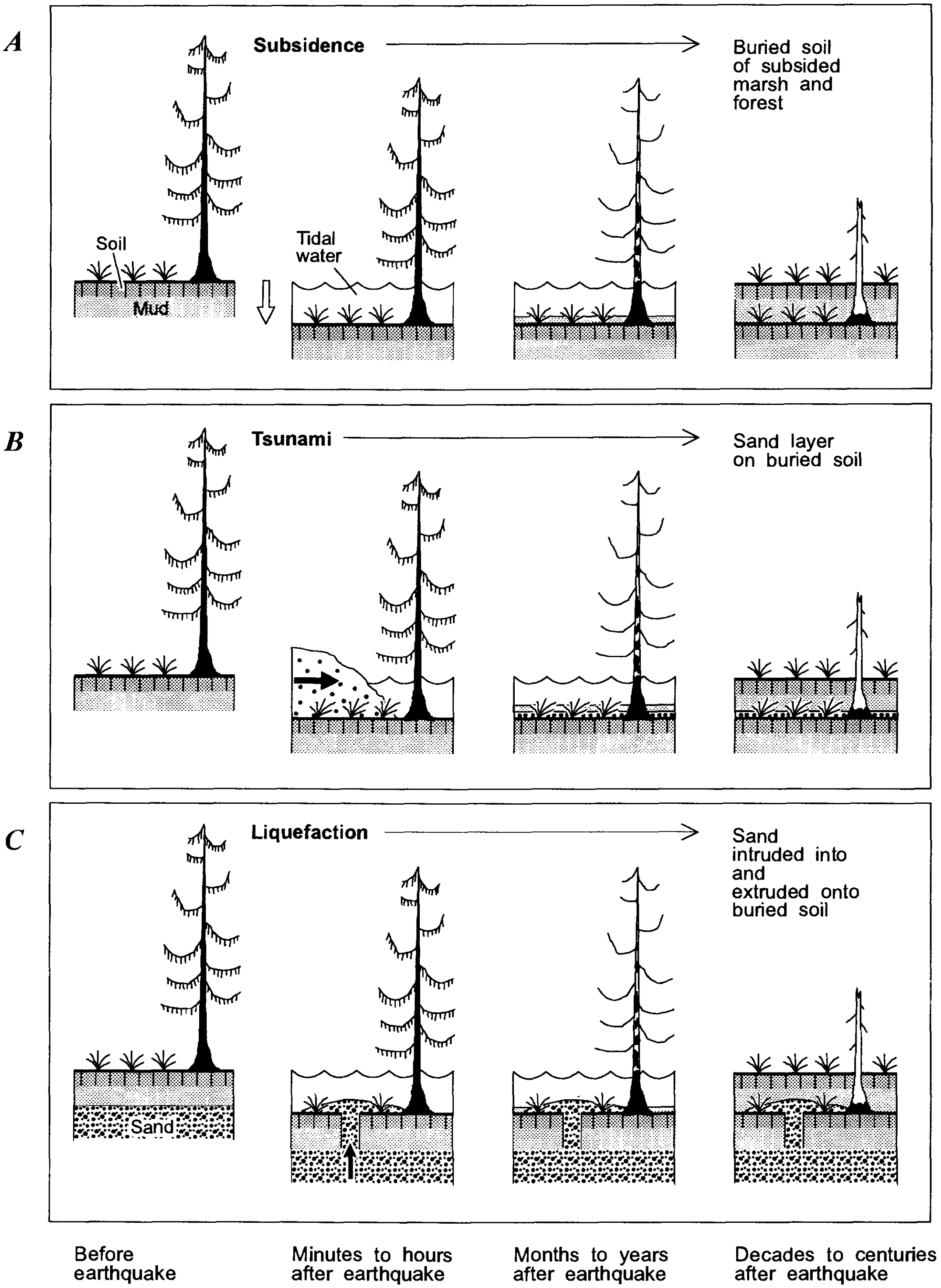

Figure 2. Inferred origin of the main coastal features cited as evidence for prehistoric earthquakes at the Cascadia subduction zone. *A*, Forest soil buried by tidal mud after subsidence during an earthquake allows tidal water to inundate the soil frequently. *B*, Sand sheet is deposited on a subsided soil by a tsunami that comes ashore minutes to hours after an earthquake. *C*, Liquefied sand erupts through and onto a subsided soil as a result of seismic shaking. After Atwater and others (1995).

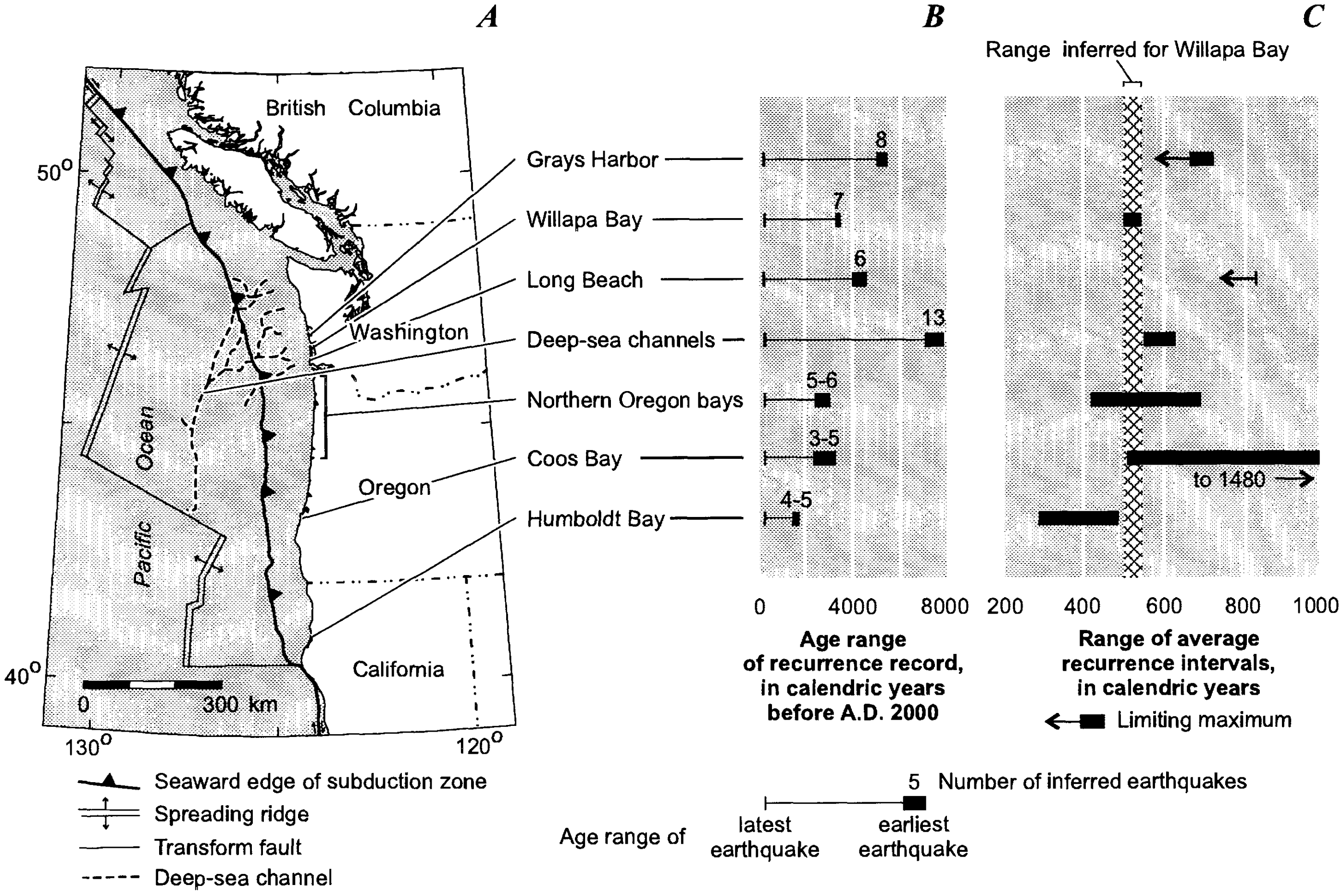

Figure 3. Comparison among average recurrence intervals estimated from geologic evidence for prehistoric earthquakes at the Cascadia subduction zone. In *B*, narrow lines denote total age range of the inferred earthquakes, and wide lines denote age ranges of latest and earliest of the inferred earthquakes. For details see section "Previous Estimates of Recurrence Intervals for Plate-Boundary Earthquakes at the Cascadia Subduction Zone" (p. 7). Sources: Grays Harbor, Shennan and others (1996); Willapa Bay, this report; deep-sea channels, Adams (1990); northern Oregon bays, Darienzo and Peterson (1995); Coos Bay, Nelson and others (1996a); Humboldt Bay, Clarke and Carver (1992).

structural setting of the outcrops to check for earthquakes on faults in the North America plate. We found that all the buried soils in the outcrops can be explained most simply by submergence and burial following regional coseismic subsidence from plate-boundary earthquakes. This finding, along with several new radiocarbon ages having unusually small geologic and analytical errors, shows that about 500 years probably elapsed, on average, between earthquakes of magnitude 8 or larger (great earthquakes) in the past 3,500 years at northeastern Willapa Bay. The buried-soil record of these earthquakes, however, is locally incomplete. We also checked the possibility that the earthquakes happened at regular intervals as diagrammed in figure 4*F*. We found instead that the earthquakes probably occurred at variable intervals (fig. 4*G*) ranging from a few centuries to about 1,000 years.

ACKNOWLEDGMENTS

We thank David Lewis, John Shulene, Jamie Hill, Boyd Benson, Mark Hemphill-Haley, Alan Carter Mortimer, Judith Boughner, Roger Lewis, Maria Ferrier, Patricia Atwater, Yumei Wang, and Bernice Wuethrich for help in surveys of stratigraphy and modern vegetation; Minze Stuiver, Phil Wilkinson, and Paula Reimer for high-precision radiocarbon ages; Hansjörg Streif for a reference to decomposed peat horizons in Germany; Mary Ann Reinhart and Steve McMullen for measurement of oriented plant fossils along the Niawiakum River; Chris Goldfinger, Lisa McNeill, George Plafker, Thomas Yelin, Ray Wells, and Robert Yeats for discussion of tectonics; Marie Hanak for photographic prints; and Alan Nelson, Harvey Kelsey, John Adams, Ian Shennan, John Tinsley, Kathleen Sayce, and

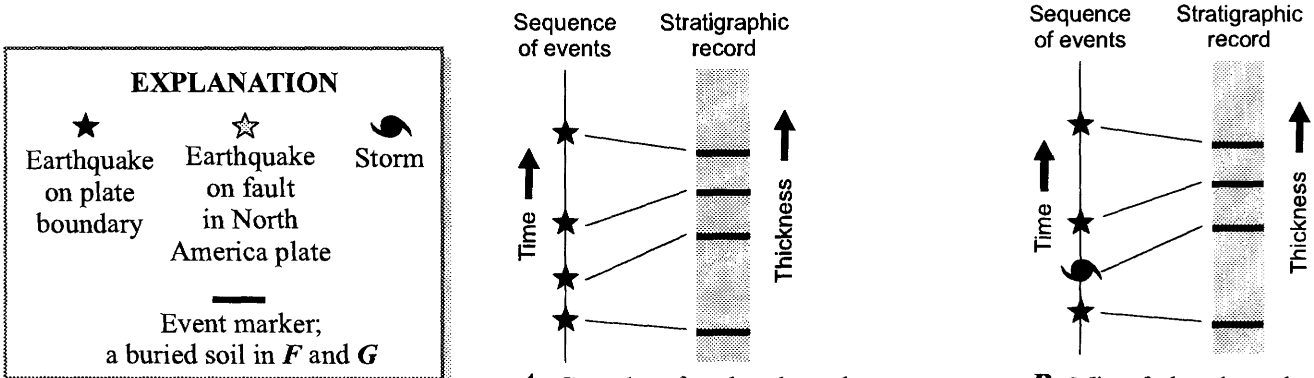

A Complete for plate-boundary earthquakes

B Mix of plate-boundary earthquakes and a storm

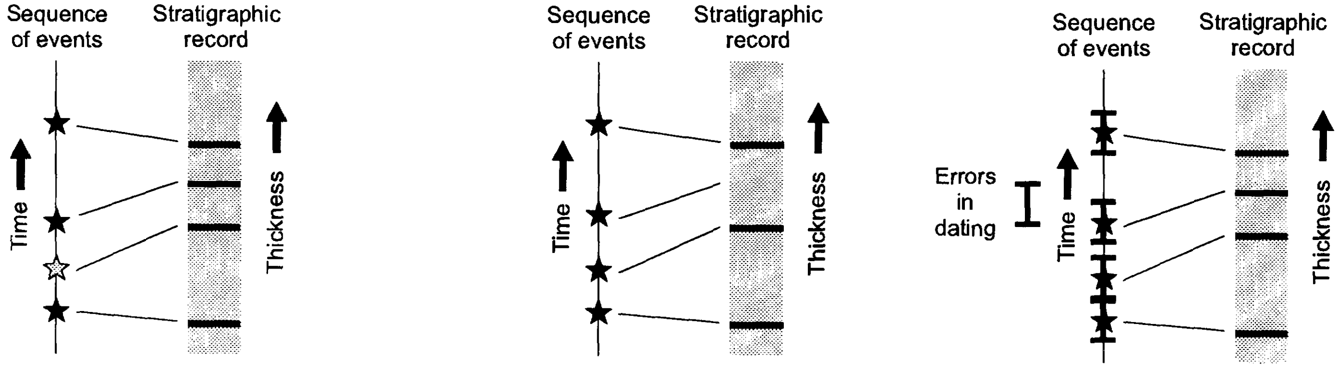

C Mix of plate-boundary earthquakes and an earthquake in the North America plate

D Incomplete for plate-boundary earthquakes

E Ages of earthquakes poorly known

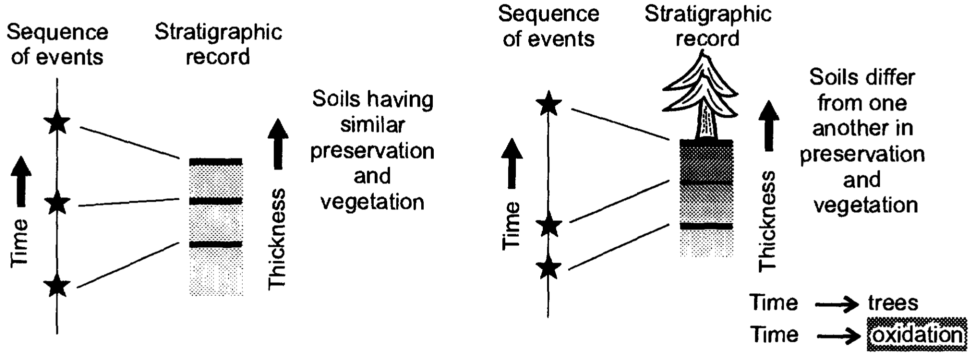

F Periodic, characteristic earthquakes

G Aperiodic, not necessarily characteristic earthquakes

Figure 4. Sources of error in using stratigraphic records to estimate recurrence intervals for plate-boundary earthquakes at the Cascadia subduction zone. *A*, One-for-one correspondence between plate-boundary earthquakes and stratigraphic markers. *B*, *C*, Records contaminated by stratigraphic markers for events other than plate-boundary earthquakes. *D*, Record lacking stratigraphic marker for one of the earthquakes. *E*, Complete record having large uncertainties in dating. *F*, Complete record of periodic, characteristic earthquakes. *G*, Complete record of aperiodic earthquakes for which passage of interseismic time promotes change in vegetation and decomposition of soils; see figure 35 for inferred examples.

Jeffrey Troll for critical reviews. The work was funded by earthquake programs of the U.S. Geological Survey and the Nuclear Regulatory Commission.

PREVIOUS ESTIMATES OF RECURRENCE INTERVALS FOR PLATE-BOUNDARY EARTHQUAKES AT THE CASCADIA SUBDUCTION ZONE

Geologic attempts to estimate recurrence intervals for great (magnitude 8 or larger) Cascadia earthquakes began in the middle 1980's with work by Adams (1990), who used deposits in deep-sea channels as recorders of earthquakes. Estimates of earthquake-recurrence intervals at coastal estuaries began to be made in the late 1980's and have appeared in refereed journals since the early 1990's, as reviewed by Atwater and others (1995). Atwater and Hemphill-Haley (1996) made preliminary estimates for northeastern Willapa Bay that are superseded in this report.

TURBIDITES IN DEEP-SEA CHANNELS OFF WASHINGTON AND OREGON

Adams (1990, 1996) cited deep-sea turbidites as evidence that great earthquakes off the Washington and Oregon coast have recurred at an average interval close to 600 years. This estimate was based on counting, in cores from sites in deep-sea channels (fig. 1), turbidites younger than Mazama ash, which erupted about 7,500 calendric years ago. Many of these cores contain 13 or 14 post-Mazama turbidites, both above and below junctions of tributary channels (Griggs and Kulm, 1970, p. 1375–1376). Griggs and Kulm (1970, p. 1382) ascribed these turbidites to "periodic earthquakes or severe storms" acting on unstable deposits at heads of submarine canyons. Adams (1990) argued that great earthquakes provide the simplest explanation for the uniformity in number of post-Mazama turbidites above and below channel junctions, and for the many-century intervals between turbidites.

Adams inferred a one-for-one correspondence between turbidites and great plate-boundary earthquakes. He acknowledged, however, that some great earthquakes may have been preceded by too little time for much sediment to accumulate in canyon heads (Adams, 1990, p. 580). He further stated that a few turbidites in some cores may have resulted from lesser earthquakes on faults in the North America plate. Such earthquakes, he argued, may account for tributary-channel cores that contain 14, 15, or 16 post-Mazama turbidites.

If the turbidites and plate-boundary earthquakes correspond one for one, the mean recurrence interval for 13 post-Mazama earthquakes is between about 550 and 630 years. This range is based on the assumption that the earliest post-Mazama turbidite—the lowest one containing Mazama ash accumulated between 6900 and 7800 years ago (Adams, 1990, p. 576), and that the most recent turbidite formed close to 300 years ago (Adams, 1990, p. 580). The 13 intervals inferred by Adams have a standard deviation of 170 years (Adams, 1990, 1996) or less (Weichert and Adams, 1995), as reviewed in the section beginning on page 102.

BURIED SOILS AT HUMBOLDT BAY, CALIFORNIA

Clarke and Carver (1992) cited buried soils exposed at low tide along Mad River Slough—an arm of Humboldt Bay—as evidence for earthquake recurrence intervals that average less than 500 years. They reported evidence for four or five earthquakes between about 1,450–1,750 years ago and about 300 years ago.

Clarke and Carver inferred that three of these events were accompanied by surface rupture of a nearby thrust fault in the North America plate. However, they proposed that this thrust faulting usually accompanies great earthquakes on the underlying plate boundary.

BURIED SOILS AT ESTUARIES IN NORTHERN OREGON

Darienzo and Peterson (1995) used buried soils less than 3,000 years old to estimate average recurrence intervals less than 600 calendric years for great earthquakes between the Necanicum River and Alsea Bay (Peterson and Darienzo, 1996). They reported that the average interval could be as little as about 200 calendric years.

The minimum average interval that we calculate from their data—about 400 years (fig. 3)—is longer for two reasons:

1. We use high-precision (quoted errors ±10–15 ^{14}C yr) radiocarbon ages that effectively lengthen the time between the most recent earthquake and its predecessors. The high-precision ages show that the most recent plate-boundary earthquake, or earthquake series, occurred close to 300 years ago along most or all of the Cascadia subduction zone (Nelson and others, 1995) (see p. 81). Darienzo and Peterson (1995) used less precise radiocarbon ages, according to which this seismicity occurred as much as 680 years ago.
2. We average the last five of the recurrence intervals inferred by Darienzo and Peterson (1995). The shortest recurrence intervals estimated by Darienzo and Peterson (1995) are based on only the last four intervals. These intervals exclude the interval between their events 5 and 6—the longest interval implied by their radiocarbon ages (Darienzo and Peterson, 1995, their fig. 4).

INTERBEDDED PEAT AND MUD AT COOS BAY, OREGON

Nelson and others (1996a) presented evidence for a broad range of earthquake-recurrence intervals at Winchester Creek, which is part of the South Slough arm of Coos Bay. They evaluated 10 couplets of peat and mud, observed in cores, as evidence for coseismic subsidence in the past 4,290–4,930 years.

Nelson and his coworkers inferred coseismic subsidence if a couplet met three main criteria: it records at least ½ m of relative sea-level rise, as judged from qualitative and quantitative analysis of foraminifera and diatoms; the submergence happened suddenly, as shown by abrupt changes in lithology and in microfossil assemblages; and the submergence also happened widely, as shown by stratigraphic correlation among cores and radiocarbon correlation among estuaries. They judged three of the couplets indicative of earthquakes but found insufficient evidence to determine whether six additional couplets represent earthquakes.

Nelson and others (1996a, p. 152) stated that an unknown fraction of the earthquakes occurred on the plate boundary; others may have occurred independently on faults in the North America plate.

All three of the confidently inferred earthquakes date from the past 2,350–3,240 years, and two other peaty layers that might or might not represent earthquakes also fall within this range. The corresponding average recurrence interval ranges from about 500 to 1,500 years (fig. 3). An average interval of at least 500 years is also indicated if the entire sequence of peat and mud records nine or fewer plate-boundary earthquakes between about 300 and 4,290–4,930 years ago.

BURIED SCARPS WEST OF WILLAPA BAY NEAR LONG BEACH, WASHINGTON

Meyers and others (1996) interpreted Pacific Ocean beach deposits as evidence for six plate-boundary earthquakes in the past 4,500 years. Using ground-penetrating radar, they identified eight different buried scarps near Long Beach, west of southern Willapa Bay (fig. 5). Meyers and others (1996) attributed each of these scarps to storm erosion consequent to earthquake-induced subsidence.

Six of the scarps are probably less than 4,500 years old; the other two, the earliest, are undated. Meyers and others (1996) acknowledged that their inferred record of earthquakes is incomplete if erosion following one earthquake removed the scarp that resulted from a previous earthquake. If the most recent scarp originated about 300 years ago, and if each of the six dated scarps records an earthquake, the average recurrence interval is no greater than 840 years.

BURIED SOILS AT GRAYS HARBOR, WASHINGTON

Shennan and others (1996) reported evidence for eight coseismic subsidence events less than 5,000–5,400 years old at the Johns River, an arm of Grays Harbor (fig. 5). They used assemblages of fossil diatoms, pollen, and foraminifera—all compared with assemblages on modern Johns River wetlands—to show that each of eight successive buried soils records sudden tidal submergence. The youngest five of these soils are preserved widely enough to provide a reliable record of earthquake recurrence. They can be seen in an outcrop several tens of meters long and in five correlated cores distributed along a transect that extends 250 m landward from the outcrop.

Shennan and others (1996) dated the subsidence events by obtaining radiocarbon ages on peat in the soils. Such peat can be younger or centuries older than the subsidence event that the peat is meant to date (Nelson, 1992b). Shennan and others (1996) interpreted the ages as "not dissimilar to others reported from the Cascadia subduction zone." The most recent of the eight earthquakes inferred by Shennan and others (1996) occurred close to 300 years ago, and the earliest of the earthquakes probably occurred no more than 5,000–5,400 years ago. This history implies an average recurrence interval no greater than 670–730 years.

STRUCTURAL SETTING AND MODERN TIDAL WETLANDS OF NORTHEASTERN WILLAPA BAY

GEOLOGIC STRUCTURE

The northeastern part of Willapa Bay flanks and crosses a late Cenozoic uplift herein termed the South Bend antiform (fig. 5). This structural high, which extends about 40 km in a north-northwestward direction, is defined mainly by an exposed core of Crescent Formation—Eocene pillow basalt, basaltic breccia, and basaltic sedimentary rock (Wagner, 1967a, b). Near the northern and southern ends of the antiform the Crescent is flanked to the east and west by younger sedimentary strata of Eocene and Oligocene age. North of Raymond, in the eastern part of the antiform, sedimentary rocks within the Crescent dip to the east and northeast, approximately parallel to dips in strata that probably rest conformably on the Crescent (Wagner, 1967a). The antiform may be bounded on the west by an east-dipping thrust fault (Cowan and Potter, 1986; Palmer and Lingley, 1989, p. 11; Snavely and Wells, 1996, p. 163). Small but abundant outcrops of the Crescent near the Willapa River demonstrate that the antiform crosses the Willapa River, which forms the easternmost arm of Willapa Bay (fig. 6).

The South Bend antiform has probably grown in post-Miocene time and has undergone net uplift, with or without continued folding, in the late Quaternary. Flanks of the antiform trend parallel to synclines that deform rocks as young as Miocene (fig. 5). Net Quaternary uplift is shown by estuarine and shallow marine deposits of probable Pleistocene age; Wagner (1967a, b) mapped such deposits on the antiform to altitudes of 180 m. However, this net uplift extended beyond the antiform into other areas bordering Willapa Bay

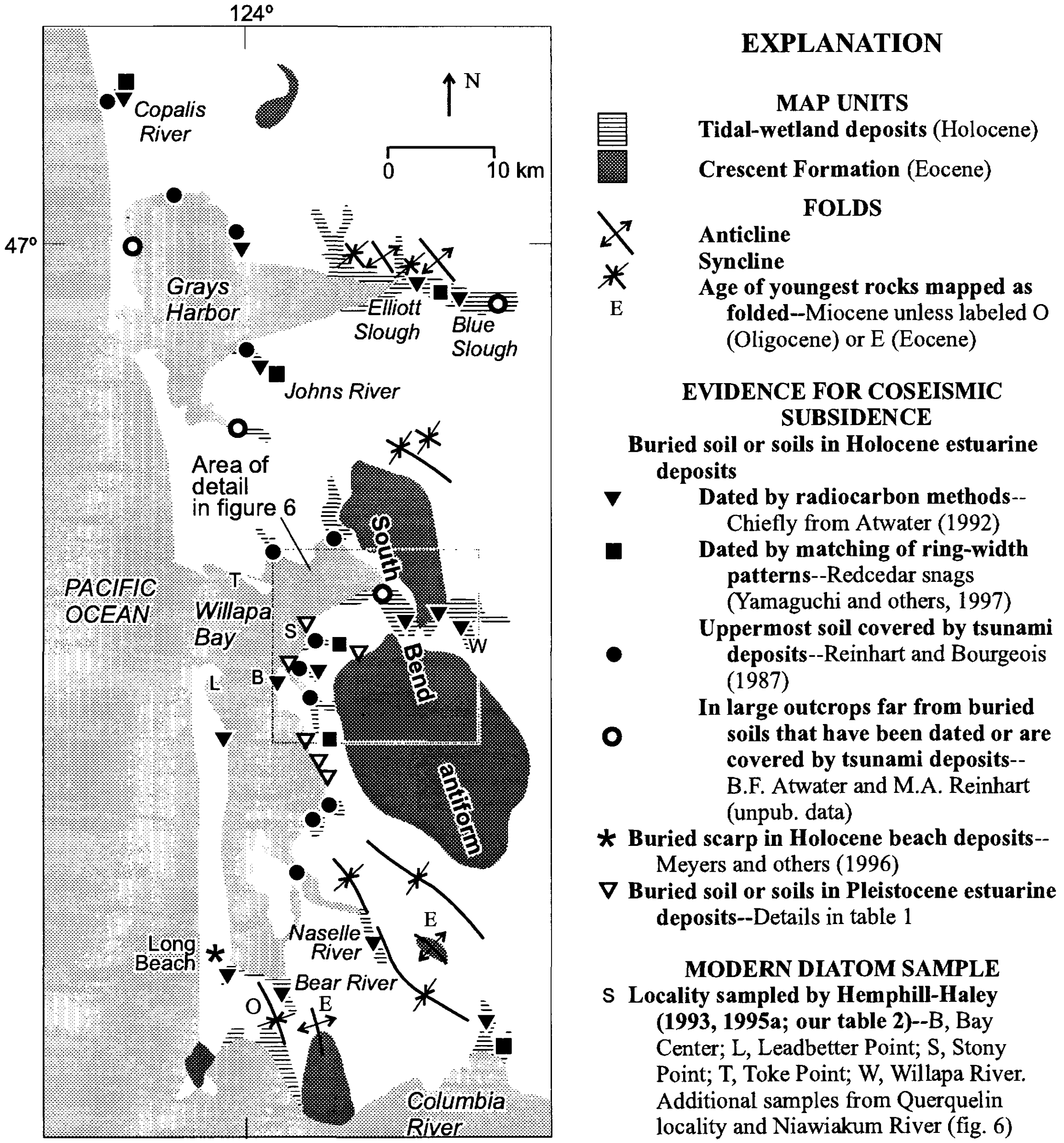

Figure 5. Cenozoic folds in relation to some of the sites having evidence for coseismic subsidence of Quaternary age in southern coastal Washington. Most sites plotted on the map comprise at least one outcrop tens of meters long that widely displays one or more successive buried soils. Many additional sites not plotted, mainly in areas of modern tidal wetlands. Folds in Tertiary rocks and limits of Crescent Formation are from compilation by Walsh and others (1987).

and Grays Harbor, as shown by Pleistocene marine and estuarine deposits tens of meters above present sea level (Walsh and others, 1987). Such areas include a Neogene syncline along the Naselle River (fig. 5), where Wells (1989) mapped a terrace of Pleistocene deposits. Consequently, the presence of uplifted Pleistocene deposits on the South Bend antiform need not signify that the antiform has grown in the late Quaternary.

We say "net" Quaternary uplift because estuarine deposits at Willapa Bay contain buried soils indicative of sudden subsidence. The soils, located both on and beside the South Bend antiform (fig. 5), demonstrate repeated coseismic subsidence of Holocene age (p. 73) and may also record repeated coseismic subsidence of Pleistocene age (table 1; Peterson and Darienzo, 1989). Such subsidence is compatible with net uplift if cumulative interseismic uplift exceeds cumulative coseismic subsidence (Atwater, 1987). Rates of present-day interseismic uplift at Willapa Bay are poorly known; geodetic estimates for the past 50 years range from near zero (Holdahl and others, 1989; Mitchell and others, 1994) to several millimeters per year (Ando and Balazs, 1979; Hyndman and Wang, 1995).

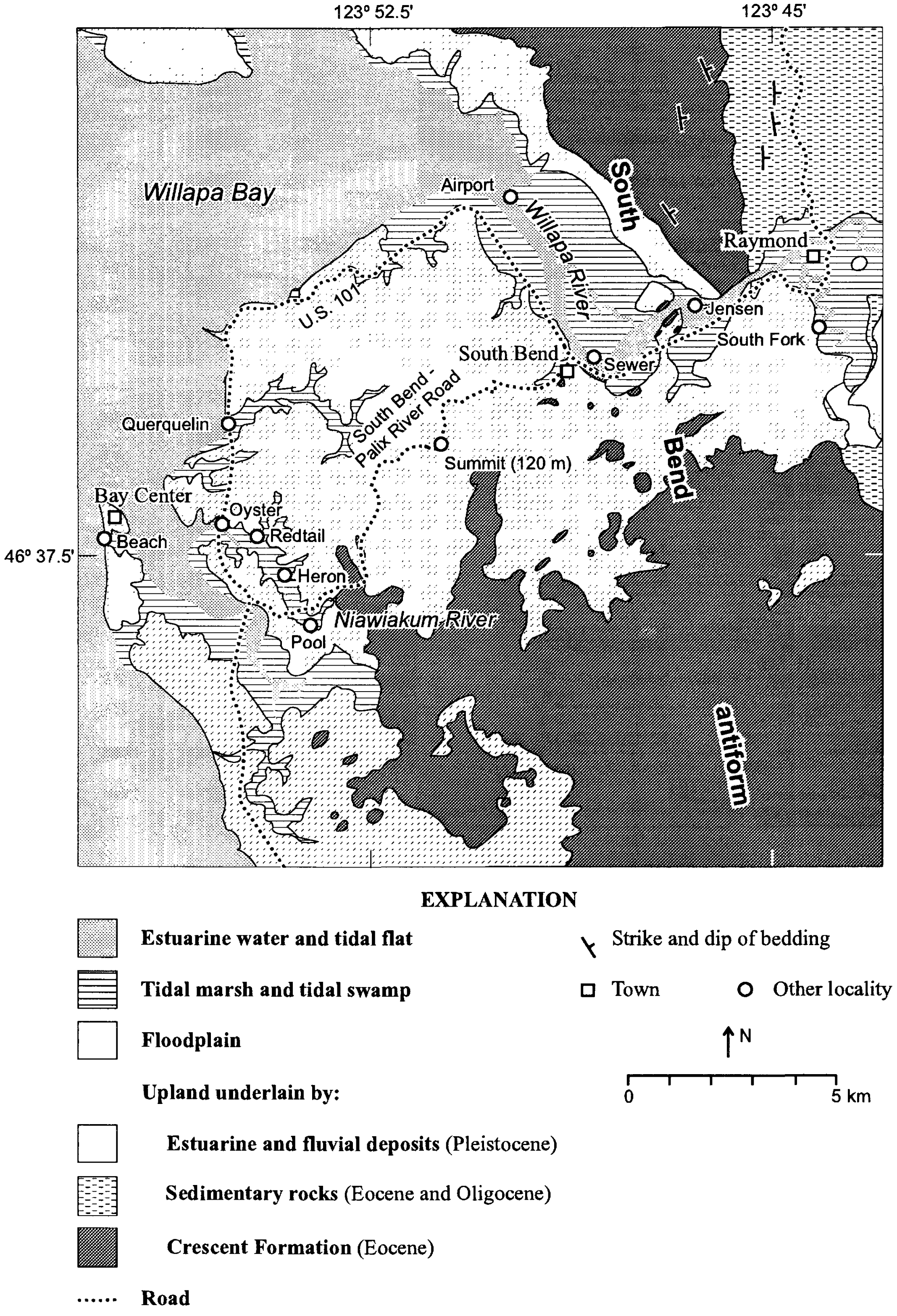

Figure 6. Index map of northeastern Willapa Bay. Geology generalized from Wagner (1967a, b).

Table 1. Buried soils in Pleistocene deposits near Willapa Bay

[Listed north to south, corresponding to open triangles in fig. 5 except for third entry, which is near solid triangle labeled B in fig. 5]

Location	Diagnostic features
NE/4 NE/4 sec. 33 and SE/4 SE/4 sec. 28, T.14N., R.10W., Bay Center 7.5-minute quadrangle; lowermost 2 m of bayside cliff	Woody organic horizon 5-15 cm thick, about 300 m long, abruptly overlain by mud; this mud contains a dark gray layer about 1 cm thick, perhaps the faint surficial horizon of a second buried soil
W/2 SW/4 sec. 1, T.13N., R.10W, South Bend 7.5-minute quadrangle; roadcuts along west side of South Bend - Palix River Road	At least two superposed carbonaceous layers 2-5 cm thick, separated from one another by mud
NW/4 SW/4 sec. 4, T.13N., R.10W., Bay Center 7.5-minute quadrangle (H.E. Clifton, oral commun., 1989); bayside cliff	Mud with many traces of roots and rhizomes, conformably overlain by lighter-colored mud that lacks such traces (Clifton, 1983, his fig. 9)
In sec. 37, T.13N., R.10W., 820 m south-southeast of Goose Point, Bay Center 7.5-minute quadrangle; lowermost 3 m of bayside cliff	Mud containing many rhizomes of *Triglochin maritimum*, abruptly overlain by locally woody mud that lacks rhizomes
NE/4 NW/4 SW/4 sec. 3, T.12N., R.10.W., Nemah 7.5-minute quadrangle; lowermost 2 m of bayside cliff	Three dark, probably carbonaceous layers 2-4 cm thick and about 0.5 m apart, separated from one another by mud. Horizontal laminations in the mud resemble those of the tidal-marsh deposits photographed by Clifton (1983, his figs. 9, 14); much of the mud also contains rhizomes of *Triglochin maritimum*
SE/4 SE/4 SW/4 sec. 3, T.12N., R.10W., Nemah 7.5-minute quadrangle; 2-6 m above base of bayside cliff	Dark, probably carbonaceous layers, at least two of them below and another above a surface of nondeposition marked by a woody, probably upland soil. Lowest layer conformably overlies silt and clay having low-angle crossbeds consistent with intertidal or subtidal origin
NW/4 SE/4 sec. 10, T.12N., R.10W., Nemah 7.5-minute quadrangle; 5 m above base of bayside cliff	Two successive beds, each about 0.3 m thick, in which mud with rhizomes grades upward into peaty mud or peat whose upper contact is abrupt. Lower bed abruptly overlies the A horizon of an upland soil. Bioturbated mud, probably deposited on a tideflat, conformably overlies the upper bed

TIDES

Willapa Bay is subject to two daily low tides and two daily high tides of unequal height. Mean lower low water, the standard datum for nautical charts in the western United States, is the average of the lower of the two daily low tides; mean higher high water similarly represents the average of the higher of the two daily high tides.

The typical difference between mean lower low water and mean higher high water is about 3 m. Extreme astronomical tides expand the height of the intertidal zone to as much as 4.5 m.

TIDAL-WETLAND ENVIRONMENTS

Many of the buried soils described in this report represent vegetated wetlands dominated by herbaceous plants (marshes) or by trees (swamps). Modern analogs for these wetlands can be found high in the intertidal zone along streams tributary to Willapa Bay (fig. 7).

Most modern tidal marshes at Willapa Bay form nearly horizontal surfaces at or slightly above mean higher high water (high marsh). Additional tidal marsh of lower altitude (low marsh) descends to tidal flats and channels (fig. 8). The high marsh is mostly about 1 m higher than tidal mud flats being colonized by *Triglochin maritimum*, a dominant low-marsh plant. This difference in level is labeled "D" in figure 8.

Tidal swamps of modern Willapa Bay are restricted to mostly freshwater reaches of the bay's tidal streams. Though they resemble uplands in some of their vegetation, they are not much if any higher in the intertidal zone than are high marshes farther downstream. We found no such difference in level by surveying the tidal marsh and tidal spruce swamp along the Niawiakum River near the Pool locality (fig. 8).

Vascular-plant species of the modern wetlands are commonly zoned with respect to tide level and salinity (Weinmann and others, 1984; Kunze and Cornelius, 1982). On brackish-water high marshes the dominant species are tufted hair-grass (*Deschampsia caespitosa*), Baltic rush (*Juncus balticus*), and Pacific silverweed (*Potentilla pacifica*). Pickleweed (*Salicornia virginica*) is common in saline parts of high marshes and in the transition between high marshes and low marshes. A mainly upland tree, Sitka spruce (*Picea sitchensis*), is joined by western crabapple

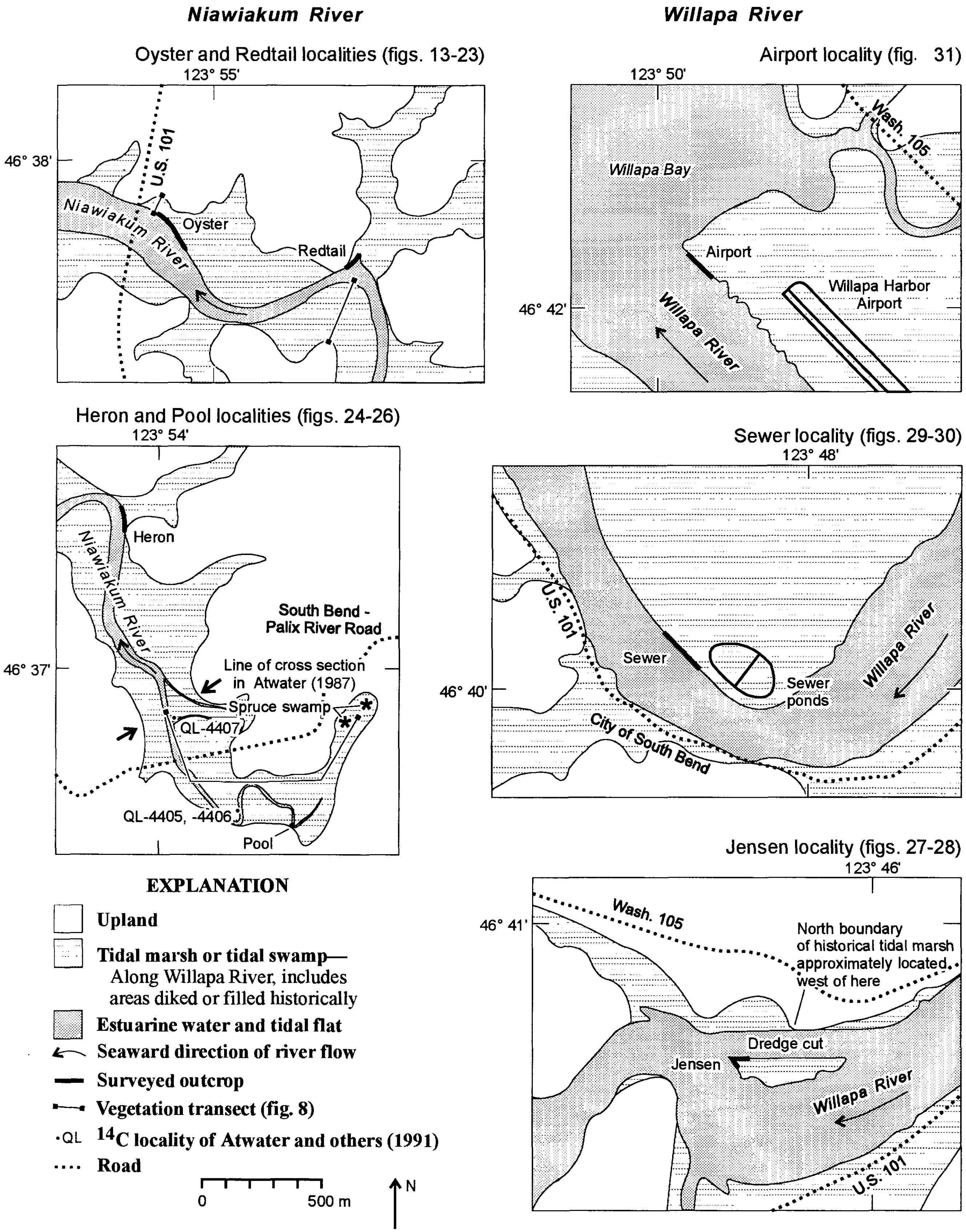
Niawiakum River

Oyster and Redtail localities (figs. 13-23)

Heron and Pool localities (figs. 24-26)

Willapa River

Airport locality (fig. 31)

Sewer locality (figs. 29-30)

Jensen locality (figs. 27-28)

Figure 7. Location and setting of outcrops and transects surveyed along the Willapa and Niawiakum Rivers.

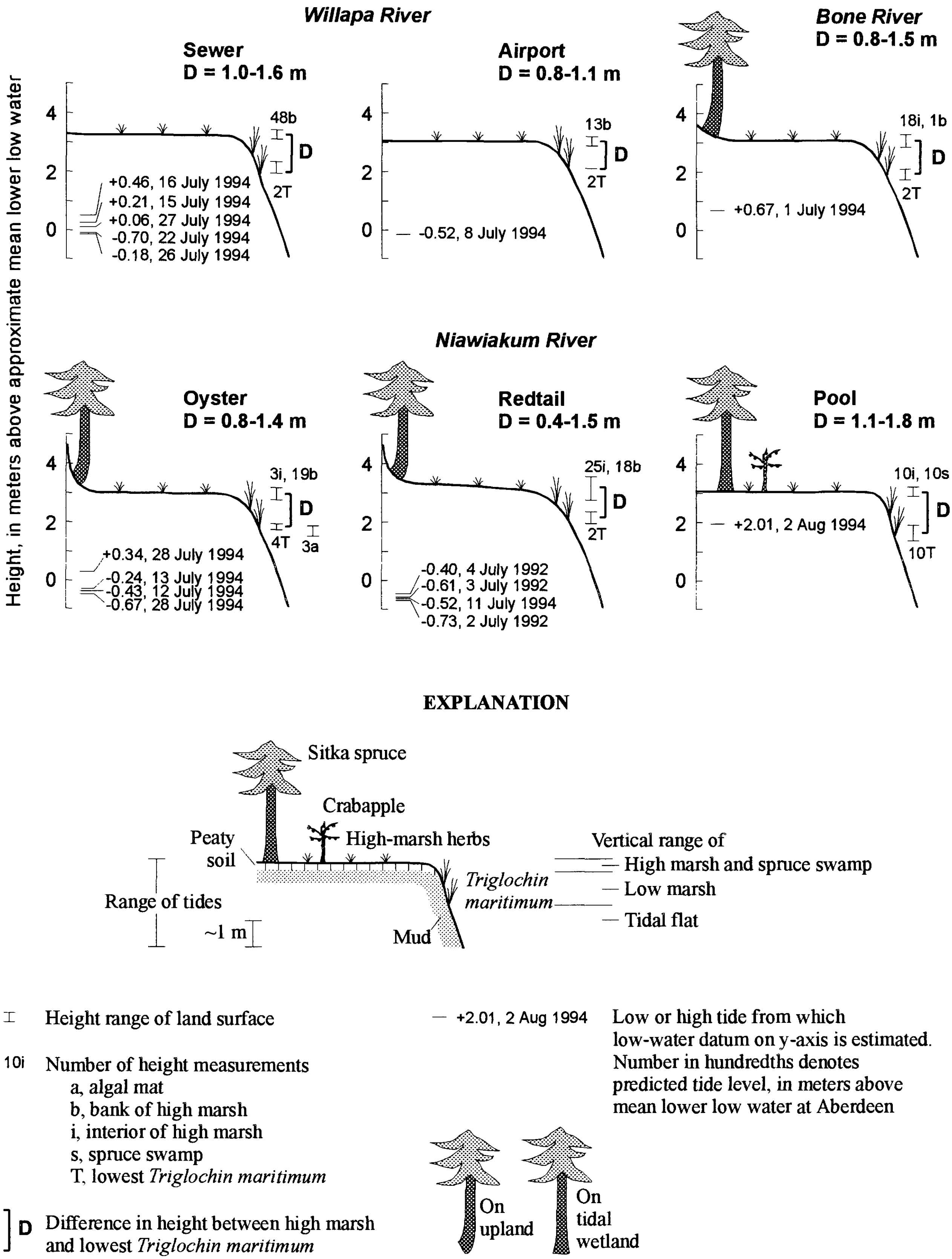

Figure 8. Vertical zonation of vascular plants in six tidal marshes and swamps at Willapa Bay. Zonation measured at surveyed outcrops and also, along the Niawiakum River, at transects plotted in figure 7. Topographic profiles schematic. Datum for each profile is mean lower low water estimated from tides tabulated under each profile.

(*Pyrus fusca*) in tidal swamps served mainly by freshwater. Seaside arrowgrass (*Triglochin maritimum*) is the chief vascular plant native to salt- and brackish-water low marshes; upstream it is supplanted by Lyngby's sedge (*Carex lyngbyei*), which is also common in brackish-water high marshes.

Diatoms also define vertical zones in wetlands at the Cascadia subduction zone, both in central Oregon (Nelson and Kashima, 1993) and at Willapa Bay (Hemphill-Haley, 1995a). Diatom assemblages at Willapa Bay differ between marshes and tidal flats, and they also differ between low marshes and high marshes. Examples of important members of these assemblages are shown in figures 9 and 10.

Several statistical methods have been used to relate assemblages of microscopic organisms to vertical position in the intertidal zone at the Cascadia subduction zone (Jennings and Nelson, 1992; Nelson and Kashima, 1993; Mathewes and Clague, 1994; Hemphill-Haley, 1995a; Guilbault and others, 1995; Shennan and others, 1996). We use a simple ratio, termed the brackish intertidal diatom index (BIDI), that is consistent with results of Hemphill-Haley's (1995a) Q-mode factor analysis of samples from modern marsh deposits at Willapa Bay.

The index, which ranges from 0 to 1, summarizes proportions of taxa found mainly in modern high marshes (H), low marshes (L), both high and low marshes (B), or tidal flats and shallow subtidal channels (T) (table 2):

$$\mathrm{BIDI} = (H + B + 0.5L)/(H + B + L + T).$$

The value for low-marsh taxa receives partial weight in the numerator to treat low marsh as transitional between tidal flat and high marsh.

The index ranges from 0 to 0.29 in tidal flats and tidal channels, 0.29 to 0.65 in low marshes, and 0.65 to 1.00 in high marshes. These ranges come from 63 intertidal sites at Willapa Bay and Puget Sound (table 3; fig. 11). One tidal-flat sample contained a low-marsh assemblage, probably because of diatoms transported from a nearby tidal marsh (table 3, sample SFW-1). Some of the sites are located along leveled transects at the Niawiakum River (fig. 12).

UPLANDS

We use "upland" to denote typically forested land at or above extreme high water. Unlike tidal marshes, such uplands at Willapa Bay are too shady and too dry in summer to support large numbers of herbaceous plants and diatoms.

The few diatoms found on uplands adjoining the bay's modern tidal marshes are poorly preserved marsh and tidal-flat species. Such assemblages were found at 10 upland sites at Willapa Bay, 8 of which adjoin tidal marshes of the Niawiakum River (table 3). Each site is located at the edge of tidal wetland, where it is probably subject to inundation by the highest astronomical tides, particularly those augmented by storm surges. The meager assemblages of diatoms at these upland sites contrast with abundant freshwater diatoms in freshwater tidal swamps along the Willapa River, upstream of Raymond (fig. 6).

METHODS

We made detailed studies of earthquake recurrence along two tidal streams: the Niawiakum River, at the western edge of the South Bend antiform; and the Willapa River where it crosses the antiform (fig. 6). Along each stream we studied buried soils in low-tide outcrops several meters high and tens or hundreds of meters long. Most of the field work was done in July 1994 except along the Niawiakum River at the Redtail locality (studied intermittently 1986–1992) and the Pool and Heron localities (surveyed 1995). From several of the outcrops we collected samples for study of fossil diatoms, and from most of the outcrops we also collected samples for radiocarbon dating. Results of the surveys, and of subsequent laboratory studies, are shown in figures 13–32.

DELINEATION OF STRATIGRAPHIC UNITS

We surveyed stratigraphy at each of seven localities. Details from these surveys are shown in outcrop diagrams (figs. 7, 13, 18, 24, 25, 27, 29, 31). We paid most attention to the identification and delineation of buried soils. We also noted where the soils are truncated by channel fills—bodies of mud that locally contain much woody detritus, inclined bedding, or both. In addition, at four localities we noted depths to the top of Pleistocene deposits, which we identified as mud that is markedly stiffer and greener or yellower than any of the overlying estuarine deposits of Holocene age.

IDENTIFICATION OF BURIED SOILS

Buried soils of former marshes and swamps punctuate the stratigraphy of the surveyed outcrops. Each buried soil has a dark uppermost layer interpreted as a buried A or O horizon. We refer to this layer as a "surficial horizon." We call a soil "bold" if its surficial horizon contains peaty mud or peat 2–10 cm thick. In a "faint" soil, by contrast, the surficial horizon consists of 1–2 cm of mud that is merely darker, by one value unit in the Munsell color system, than mud above and below it.

The interpretive term "soil" applies without question where a surficial horizon contains growth-position roots attached to tree stumps or herbaceous stems and leaves that are entombed in mud above the surficial horizon. Such fossils identify the surficial horizon as material on which plants grew.

Other, more subtle features justify the use of "soil" in faint soils, which typically lack growth-position fossils other than rootlets injected from higher in the stratigraphic section. Most of the faint soils resemble bold soils in lateral

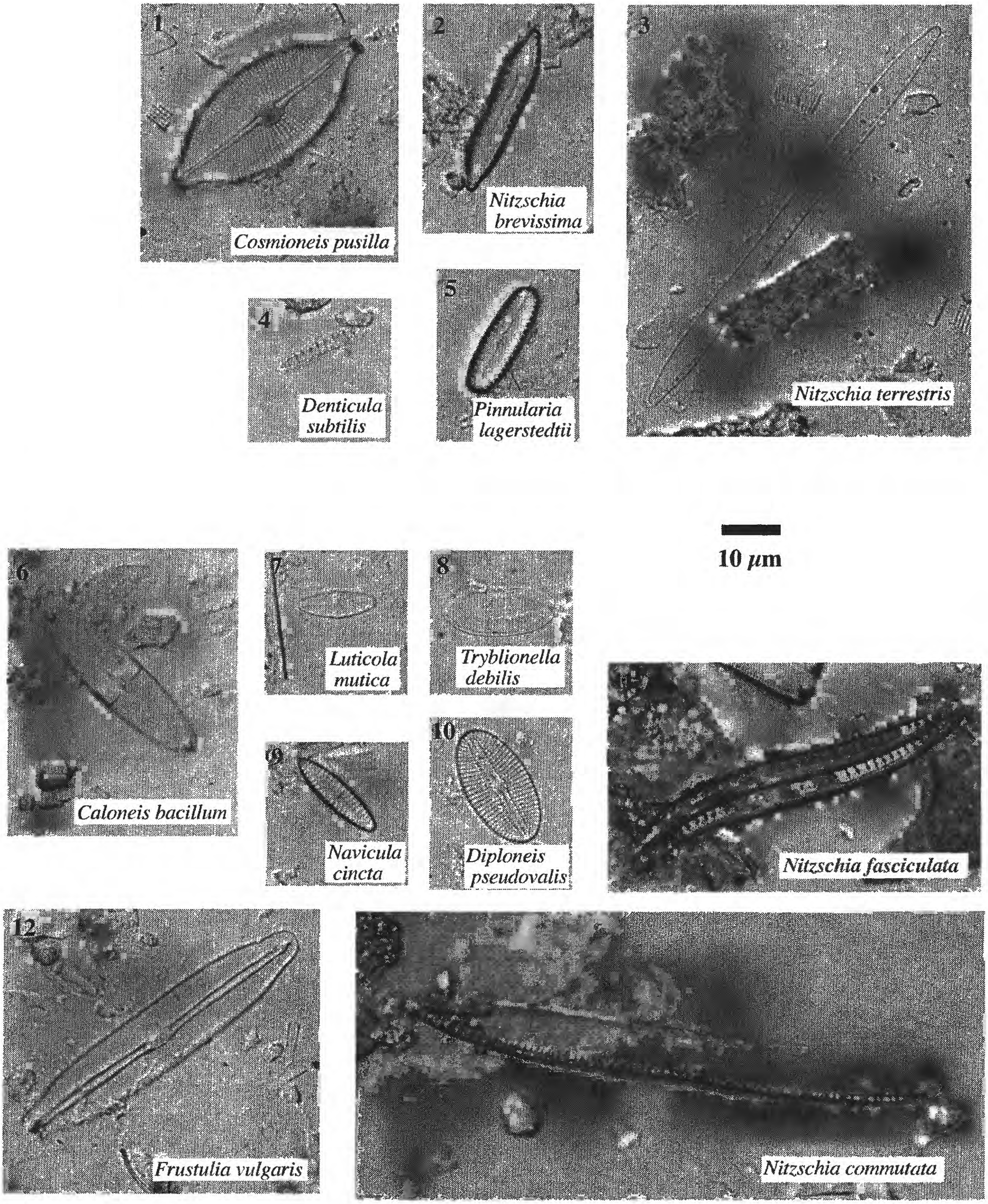

Figure 9. Examples of diatom species most commonly found in high marshes (1–5) or in both high and low marshes (6–13).

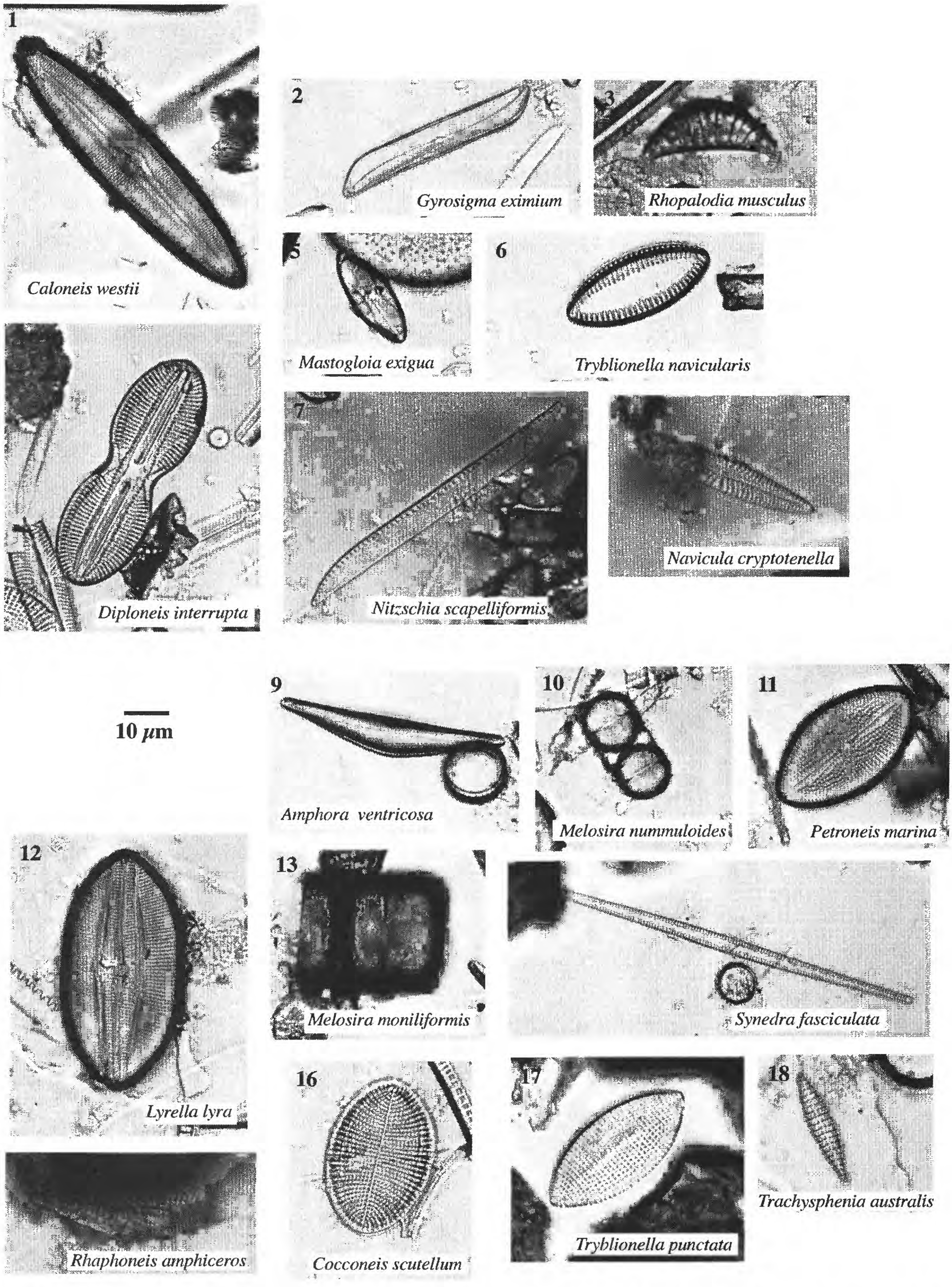

Figure 10. Examples of diatom species most commonly found in low marshes (1–8) or in tidal flats, tidal sloughs, and shallow subtidal channels (9–18).

Table 2. Diatom taxa used for the brackish intertidal diatom index

Diatoms representative of high marshes
- *Cosmioneis pusilla* (Wm. Smith) Mann and Stickle *in* Round and others, 1990
- *Denticula subtilis* Grunow, 1862
- *Navicula tenelloides* Hustedt, 1937
- *Nitzschia brevissima* Grunow in Van Heurck, 1881
- *Nitzschia pusilla* (Kützing) Grunow, 1862
- *Nitzschia terrestris* (Peterson) Hustedt, 1934
- *Pinnularia lagerstedtii* (Cleve) Cleve-Euler, 1934
- *Tryblionella aerophila* (Hustedt) Mann in Round and others, 1990

Diatoms representative of high or low marshes
- *Caloneis bacillum* (Grunow) Cleve, 1894
- *Diploneis pseudovalis* Hustedt, 1930
- *Frustulia vulgaris* (Thwaites) De Toni, 1891
- *Luticola mutica* (Kützing) Mann in Round and others, 1990
- *Navicula cincta* (Ehrenberg) Ralfs in Pritchard, 1861
- *Nitzschia commutata* Grunow in Cleve and Grunow, 1880
- *Nitzschia fasciculata* (Grunow) Grunow in Van Heurck, 1881
- *Tryblionella debilis* Arnott in O'Meara, 1873

Diatoms representative of low marshes
- *Caloneis westii* (W. Smith) Hendey, 1964
- *Diploneis interrupta* (Kützing) Cleve, 1894
- *Diploneis smithii* var. *rhombica* Mereschkowsky, 1902
- *Frustulia linkei* Hustedt, 1952
- *Gyrosigma eximium* (Thwaites) Boyer, 1927
- *Mastogloia exigua* Lewis, 1862
- *Navicula cryptotenella* Lange-Bertalot in Krammer and Lange-Bertalot, 1985
- *Nitzschia bilobata* W. Smith, 1853
- *Nitzschia scapelliformis* Grunow in Cleve and Grunow, 1880
- *Rhopaloda musculus* (Kützing) Müller, 1899
- *Scoliopleura tumida* (Brébisson ex Kützing) Rabenhorst, 1864
- *Tryblionella navicularis* (de Brébisson ex Kützing) Ralfs in Pritchard, 1861

Diatoms representative of muddy intertidal flats, sloughs, and shallow subtidal areas
- *Bacillaris paradoxa* Gmelin, 1791
- *Campylodiscus echineis* Ehrenberg, 1840
- *Catenula adhaerens* Mereschkowsky, 1903
- *Cerataulus turgidus* (Ehrenberg) Ehrenberg, 1843
- *Cocconeis scutellum* Ehrenberg, 1838
- *Cocconeis scutellum* var. *parva* Grunow ex Cleve, 1895
- *Gyrosigma acuminatum* (Kützing) Rabenhorst, 1853
- *Gyrosigma balticum* (Ehrenberg) Rabenhorst, 1853
- *Melosira moniliformis* (Müller) Agardh, 1824
- *Melosira nummuloides* Agardh, 1824
- *Navicula digitoradiata* (Gregory) Ralfs in Pritchard, 1861
- *Navicula tripunctata* (Müller) Bory, 1824
- *Nitzschia sigma* (Kützing) W. Smith, 1853
- *Nitzschia socialis* Gregory, 1857
- *Odontella aurita* (Lyngbye) Agardh, 1832
- *Opephora parva* Krasske, 1939
- *Plagiogramma staurophorum* (Gregory) Heiberg, 1863
- *Rhaphoneis amphiceros* (Ehrenberg) Ehrenberg, 1844
- *Rhaphoneis psammicola* Riznyk, 1973
- *Synedra fasciculata* (Agardh) Kützing, 1844
- *Trachyneis aspera* (Ehrenberg) Cleve, 1894
- *Tryblionella acuminata* W. Smith, 1853
- *Tryblionella apiculata* Gregory, 1857
- *Tryblionella coarctata* (Grunow) Mann in Round and others, 1990
- *Tryblionella levidensis* Wm. Smith, 1856
- *Tryblionella littoralis* (Grunow) Mann in Round and others, 1990
- *Tryblionella plana* (W. Smith) Mann in Round and others, 1990
- *Tryblionella punctata* W. Smith 1853
- *Tryblionella vexans* (Grunow) Mann in Round and others, 1990

Diatoms representative of sandy intertidal flats, sloughs, and shallow subtidal areas
- *Achnanthes delicatula* (Kützing) Grunow in Cleve and Grunow, 1880
- *Amphora proteus* Gregory, 1857
- *Amphora ventricosa* (Gregory) Hendey, 1951
- *Cocconeis diminuta* Pantocksek, 1902
- *Cocconeis peltoides* Hustedt, 1939
- *Dimeregramma minor* (Gregory) Ralfs in Pritchard, 1861
- *Fallacia cryptolyra* (Brockmann) Stickle and Mann in Round and others, 1990
- *Lyrellla lyra* (Ehrenberg) Karayeva, 1978
- *Navicula cancellata* Donkin, 1872
- *Petroneis granulata* (Bailey) Mann in Round and others, 1990
- *Petroneis marina* (Ralfs) Mann in Round and others, 1990
- *Trachyneis australis* (Ehrenberg) Cleve, 1894

extent and relief (figs. 13, 18, 24, 25, 27, 29, 31). Some grade laterally into bold soils in which vascular-plant fossils are preserved (p. 45, 69). In sections studied for fossil diatoms, faint soils contain diatom assemblages typical of tidal marshes (figs. 15, 20).

LETTER NAMES FOR BURIED SOILS

We assign each surveyed soil a name, such as "soil S," in which the capital letter denotes inferred position in a sequence of soils that we regard as correlative throughout the study area (p. 83; fig. 32). For the youngest soil we use a letter (Y) near the end of the alphabet; for progressively older soils we use letters nearer the front of the alphabet.

Our complete sequence of letter names is H, J, L, N, S, U, W, and Y. Gaps in the sequence of letters leave room for soils that we may have overlooked—a possibility evaluated in the section entitled "Additional, Unrecorded Events" (p. 94).

Table 3. Brackish intertidal diatom index (BIDI) of modern surface samples from Willapa Bay and Puget Sound

BIDI	Sample	Region	Site (figure number for location map or graph, in parentheses)	Environment
0.00	BC-1	Willapa Bay	Bay Center (6)	Sandy tidal flat
0.00	BC-2	Willapa Bay	Bay Center (6)	Sandy tidal flat
0.00	BC-4	Willapa Bay	Bay Center (6)	Sandy tidal flat
0.00	LC-3	Puget Sound	Lynch Cove (1)	Sandy tidal flat 10 m from edge of marsh
0.00	SP-2	Willapa Bay	Stony Point (5)	Muddy tidal flat
0.01	BR-1	Willapa Bay	Querquelin (6)	Muddy tidal flat
0.01	LC-1	Puget Sound	Lynch Cove (1)	Sandy tidal flat
0.01	T4-S	Willapa Bay	upper Niawiakum River (7, 12)	Shallow (~ 0.5 m) subtidal channel
0.03	BR-2	Willapa Bay	Querquelin (6)	Muddy tidal flat
0.03	LC-17	Puget Sound	Lynch Cove (1)	Floor of tidal slough
0.03	LC-7	Puget Sound	Lynch Cove (1)	Floor of tidal slough
0.03	SP-1	Willapa Bay	Stony Point (5)	Muddy tidal flat
0.08	LP-1	Willapa Bay	Leadbetter Point (5)	Tidal flat mud
0.09	T3-S	Willapa Bay	lower Niawiakum River (7, 12)	Shallow (~3 m) subtidal channel
0.12	SP-3	Willapa Bay	Stony Point (5)	Muddy tidal flat
0.12	T3-1	Willapa Bay	lower Niawiakum River (7, 12)	Muddy bank with *Zostera marina*
0.12	TP-1	Willapa Bay	Toke Point (5)	Muddy tidal flat
0.15	T3-2	Willapa Bay	lower Niawiakum River (7, 12)	Muddy bank of tidal stream
0.18	SFW-2	Willapa Bay	South Fork Willapa River (5)	Muddy bank of tidal stream
0.21	T3-3	Willapa Bay	lower Niawiakum River (7, 12)	Muddy bank with *Zostera japonica*
0.23	LC-14	Puget Sound	Lynch Cove (1)	Tidal slough with *Triglochin maritimum* on nearby slump block
0.27	T4-1	Willapa Bay	upper Niawiakum River (7, 12)	Muddy bank of tidal stream
0.28	T4-2	Willapa Bay	upper Niawiakum River (7, 12)	Muddy bank of tidal stream
0.30	LP-2	Willapa Bay	Leadbetter Point (5)	*Triglochin maritimum* low marsh at edge of tidal flat
0.30	SP-4	Willapa Bay	Stony Point (5)	Low marsh with *Triglochin maritimum* and *Salicornia virginica*
0.34	SFW-1	Willapa Bay	South Fork Willapa River (5)	Muddy bank of tidal stream
0.34	TP-2	Willapa Bay	Toke Point (5)	Low marsh with *Triglochin maritimum* and *Salicornia virginica*
0.44	TP-3	Willapa Bay	Toke Point (5)	Low marsh with *Triglochin maritimum* and *Salicornia virginica*
0.53	LC-11	Puget Sound	Lynch Cove (1)	Low marsh with *Distichlis spicata* and *Salicornia virginica*
0.56	LC-5	Puget Sound	Lynch Cove (1)	Low marsh with *Distichlis spicata* and *Salicornia virginica*
0.56	LP-3	Willapa Bay	Leadbetter Point (5)	Low marsh with *Distichlis spicata* and *Salicornia virginica*
0.56	T3-4	Willapa Bay	lower Niawiakum River (7, 12)	Low marsh on steep bank with *Salicornia* and *Jaumea*
0.58	T4-3	Willapa Bay	upper Niawiakum River (7, 12)	Low marsh on steep bank with *Carex lyngbyei*
0.61	PL-2	Puget Sound	Potlatch (1)	Low marsh with *Salicornia*, *Distichlis*, and *Jaumea*
0.62	LC-10	Puget Sound	Lynch Cove (1)	Low marsh with *Distichlis spicata* and *Salicornia virginica*
0.62	LC-9	Puget Sound	Lynch Cove (1)	Low marsh with *Distichlis spicata* and *Salicornia virginica*
0.62	PL-1	Puget Sound	Potlatch (1)	Low marsh with *Salicornia* and *Jaumea*
0.64	LC-8	Puget Sound	Lynch Cove (1)	Low marsh with *Distichlis spicata*
0.64	SFW-3	Willapa Bay	South Fork Willapa River (5)	Low marsh on steep bank with *Carex lyngbyei*
0.72	LC-15	Puget Sound	Lynch Cove (1)	Marsh transitional between low and high; *Juncus balticus* and *Distichlis spicata*
0.75	LC-12	Puget Sound	Lynch Cove (1)	Marsh transitional between low and high; *Juncus balticus* and *Distichlis spicata*
0.76	T4-4	Willapa Bay	upper Niawiakum River (7, 12)	Marsh transitional between low and high; *Carex lyngbyei*, *Deschampsia caespitosa*, and *Potentilla pacifica*

Table 3. Brackish intertidal diatom index (BIDI) of modern surface samples from Willapa Bay and Puget Sound—Continued

BIDI	Sample	Region	Site (figure number for location map or graph, in parentheses)	Environment
0.79	LC-18	Puget Sound	Lynch Cove (1)	Marsh transitional between low and high; *Juncus balticus* and *Distichlis spicata*
0.84	SFW-5	Willapa Bay	South Fork Willapa River (5)	High marsh of *Carex lyngbyei*
0.84	SFW-7	Willapa Bay	South Fork Willapa River (5)	High marsh of *Carex lyngbyei*
0.86	SP-5	Willapa Bay	Stony Point (5)	High marsh of *Potentilla pacifica*
0.89	T3-8	Willapa Bay	lower Niawiakum River (7, 12)	Landward edge of high marsh; *Carex obnuta, Achillea borealis*
0.90	SFW-4	Willapa Bay	South Fork Willapa River (5)	Landward edge of high marsh; *Potentilla, Aster,* grasses
0.91	T4-5	Willapa Bay	upper Niawiakum River (7, 12)	High marsh dominated by *Potentilla pacifica* and *Deschampsia caespitosa*
0.92	SFW-8	Willapa Bay	South Fork Willapa River (5)	High marsh; *Carex lyngbyei, Potentilla pacifica, Aster, Deschampsia*
0.93	SFW-6	Willapa Bay	South Fork Willapa River (5)	High marsh dominated by *Potentilla pacifica* and *Deschampsia caespitosa*
0.93	T4-6	Willapa Bay	upper Niawiakum River (7, 12)	High marsh dominated by *Potentilla pacifica* and *Deschampsia caespitosa*
0.94	T3-5	Willapa Bay	lower Niawiakum River (7, 12)	High marsh dominated by *Distichlis spicata* and *Deschampsia caespitosa*
0.96	T3-6	Willapa Bay	lower Niawiakum River (7, 12)	High marsh of *Deschampsia caespitosa*
0.97	LC-21	Puget Sound	Lynch Cove (1)	High marsh dominated by *Juncus* and *Aster*
0.97	LP-4	Willapa Bay	Leadbetter Point (5)	High marsh; *Carex lyngbyei* and *Distichlis spicata*
0.97	T3-7	Willapa Bay	lower Niawiakum River (7, 12)	High marsh; *Potentilla pacifica* and *Distichlis spicata*
0.97	T4-7	Willapa Bay	upper Niawiakum River (7, 12)	High marsh; *Potentilla pacifica* and *Deschampsia caespitosa*
0.98	T4-8	Willapa Bay	upper Niawiakum River (7, 12)	High marsh; *Potentilla pacifica* and *Juncus balticus*
0.99	LCT-5	Puget Sound	Lynch Cove (1)	Grassy meadow lacking halophytes but containing driftwood
0.99	LP-5	Willapa Bay	Leadbetter Point (5)	High marsh; *Potentilla pacifica* and *Deschampsia caespitosa*
0.99	PL-3	Puget Sound	Potlatch (1)	High marsh; *Juncus balticus* and *Deschampsia caespitosa*
1.00	LCT-6	Puget Sound	Lynch Cove (1)	Grassy meadow lacking halophytes but containing driftwood
none	T3-U1	Willapa Bay	Niawiakum River, near Oyster locality (7)	Upland forest <0.5 m above and <5 m landward from landward edge of high marsh
none	T3-U2	Willapa Bay	Niawiakum River, near Oyster locality (7)	Upland forest <0.5 m above and <5 m landward from landward edge of high marsh
none	T3-U3	Willapa Bay	Niawiakum River, near Oyster locality (7)	Upland forest <0.5 m above and <5 m landward from landward edge of high marsh
none	T3-U4	Willapa Bay	Niawiakum River, near Oyster locality (7)	Upland forest <0.5 m above and <5 m landward from landward edge of high marsh
none	RT-1	Willapa Bay	Niawiakum River, Redtail locality (7)	Upland forest <0.5 m above and <5 m landward from landward edge of high marsh
none	RT-2	Willapa Bay	Niawiakum River, Redtail locality (7)	Upland forest <0.5 m above and <5 m landward from landward edge of high marsh
none	H-1	Willapa Bay	Niawiakum River, Heron locality (7)	Upland forest <0.5 m above and <5 m landward from landward edge of high marsh
none	H-2	Willapa Bay	Niawiakum River, Heron locality (7)	Upland forest <0.5 m above and <5 m landward from landward edge of high marsh
none	T1-U1	Willapa Bay	Willapa River about 5 km east of Raymond (6)	Upland forest <0.5 m above and <5 m landward from landward edge of tidal swamp
none	T1-U2	Willapa Bay	Willapa River about 5 km east of Raymond (6)	Upland forest <0.5 m above and <5 m landward from landward edge of tidal swamp

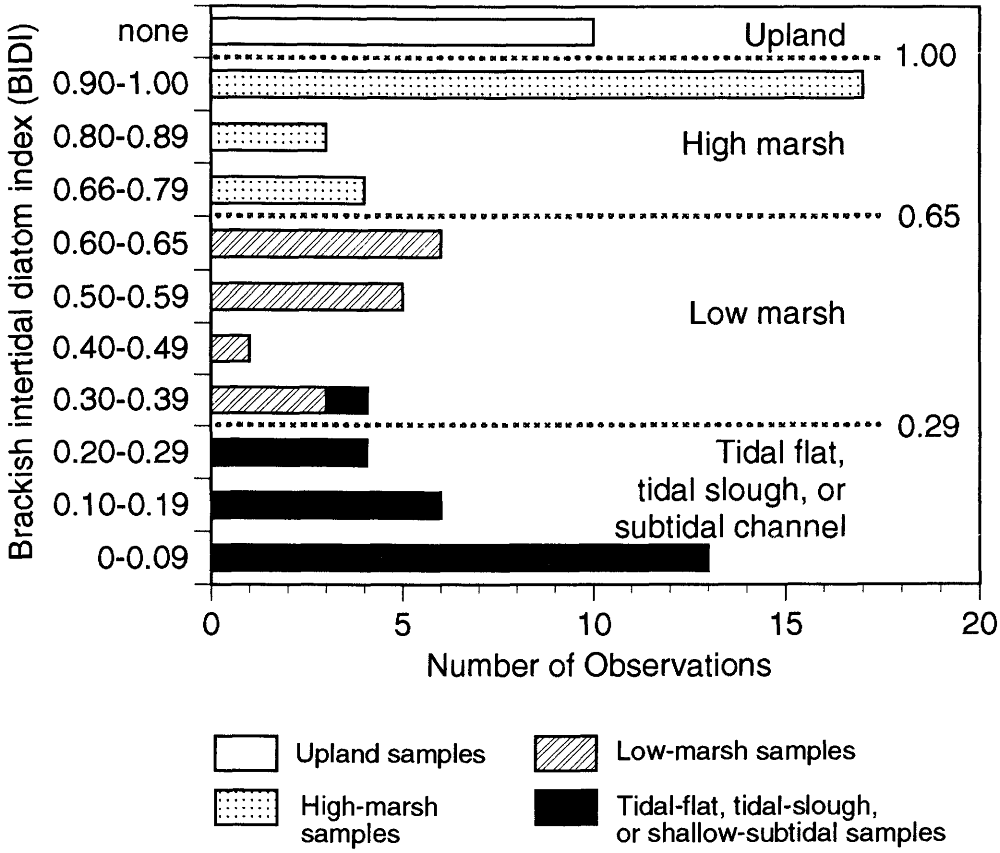

Figure 11. Brackish intertidal diatom index for modern samples from western Washington (table 3).

CONTINUITY OF STRATIGRAPHIC FEATURES

We observed stratigraphic features between some surveyed points and inferred their existence between others—a distinction shown by contrasting symbols in the outcrop diagrams. Soils depicted as continuously observed were apparent from differential erosion in natural outcrop (for example, soils J, L, S, and Y in fig. 14*B*; soil S in fig. 19*B*–*D*) or were exposed where cleaned with a shovel (soil U in fig. 14*C*; soil Y in fig. 19*D*, *E*; soils S, U, W, and Y in fig. 28*B*). Otherwise, we interpolated stratigraphic contacts between isolated exposures or borings.

We observed lateral continuity between bold and faint parts of soil N at the Redtail locality (fig. 13), soil U at the Oyster locality (fig. 18), and soil L at the Jensen locality (fig. 27). Although the outcrop diagrams show the change from bold to faint as abrupt, the changes are gradational across a few to many meters.

BORINGS AND DEPTH TO PLEISTOCENE DEPOSITS

We supplemented observations made in outcrop by using a gouge corer—a steel half-cylinder 2 cm in diameter and 1 m long—to find features not exposed at even the lowest tides. These features include soil H at the Redtail locality (fig. 13), soils H and J at the Pool locality (fig. 24) and at the southern part of the Jensen locality (fig. 27), parts of soils N and L and all of soil H at the Heron locality (fig. 25), and Pleistocene deposits at all these localities.

We did not core to Pleistocene deposits more than a few meters below the low tide levels. Deep cores have been taken, however, for a highway bridge near the Oyster locality (p. 45). We use these highway borings, along with our shallower cores of Pleistocene deposits (figs. 13, 24, 25, 27) and downward projection of valley walls, to infer differences in depth to Pleistocene deposits and to deduce consequent differences in settlement from gradual compaction of Holocene mud (see section "Thickness of Mud Between Soils," p. 82).

Figure 12. Variation in brackish intertidal diatom index → along leveled transects from high marsh to channel at the Niawiakum River. MHHW, mean higher high water; MLLW, mean lower low water; S, lowest sample. *A*, Transect Nl, which coincides with the vegetation transect at the Oyster locality (figs. 7, 8). *B*, Transect Nu, located about 0.5 km northwest of the Pool locality, just north of the South Bend–Palix River Road and on the east side of the Niawiakum River.

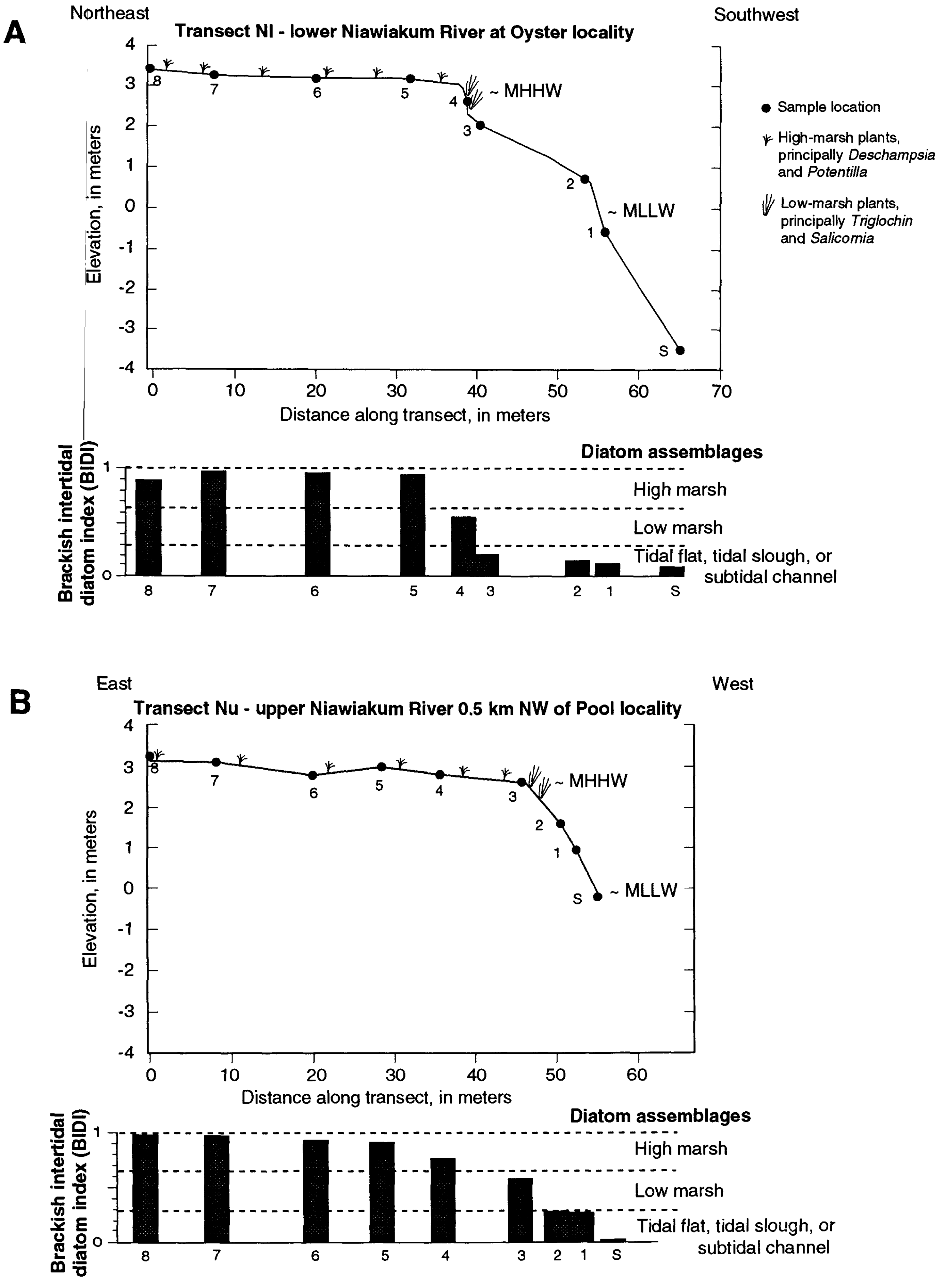
A
Northeast
Southwest
Transect Nl - lower Niawiakum River at Oyster locality
~ MHHW
~ MLLW
Elevation, in meters
4
3
2
1
0
-1
-2
-3
-4
0
10
20
30
40
50
60
70
Distance along transect, in meters
8
7
6
5
4
3
2
1
S
● Sample location
High-marsh plants, principally *Deschampsia* and *Potentilla*
Low-marsh plants, principally *Triglochin* and *Salicornia*
Brackish intertidal diatom index (BIDI)
1
0
Diatom assemblages
High marsh
Low marsh
Tidal flat, tidal slough, or subtidal channel
B
East
West
Transect Nu - upper Niawiakum River 0.5 km NW of Pool locality
~ MHHW
~ MLLW
Elevation, in meters
Distance along transect, in meters
Brackish intertidal diatom index (BIDI)
Diatom assemblages
High marsh
Low marsh
Tidal flat, tidal slough, or subtidal channel

PARTICLE SIZE

Mud above some of the soils—particularly soils S and Y—commonly contains more silt than does mud below their surficial horizons. This contrast is evident in well-washed outcrops in which layers of silt and sandy silt have been etched by water (fig. 30*B*). The contrast also can be seen on outcrops freshly faced with a shovel or machete; whereas the finer mud smears, the coarser mud peels roughly. This contrast aids in identification of buried soils.

Particle size was measured for samples from the Redtail locality (fig. 15). The samples, collected at an average interval of 6.5 cm, came from slabs sampled also for fossil diatoms. Organic matter was removed in 30 percent H_2O_2. Counts were made with a Cimax hydrophotometer and rapid settling analyzer at the U.S. Geological Survey in Palo Alto, California. Precision, estimated from calibration tests, is ±13 percent for the hydrophotometer and ±15 percent for the rapid settling analyzer. Particle-size distributions were determined with the technique of Torresan (1987).

ORGANIC CONTENT

Although we did not measure organic contents of the surficial horizons of the soils, such measurements have been made for a stratigraphic section containing three bold soils (probably correlative with soils L, S, and Y) and two faint soils (probably N and U) along the Johns River (figs. 5, 32; locality 14 of Atwater, 1992). The measurements, by means of loss on ignition, were made independently by James B. Phipps of Grays Harbor College (written commun., 1988) and by Shennan and others (1996, their fig. 3).

Both Phipps and the Shennan team reported organic contents of 30–50 percent of dry weight for 10 samples among bold soils L, S, and Y (horizons V, III, and I of Shennan and others, 1996). By contrast, they reported organic contents less than 10 percent for two samples each from faint soils N and U (horizons IV and II). They found little or no difference in organic content between the faint soils and the mud immediately above or below.

HORIZONTAL AND VERTICAL DATUMS

We used arbitrary points particular to each of the outcrops as datums for measuring positions of soils, channel fills, Pleistocene deposits, and fossils. Horizontal measurements were made by tape measure, vertical measurements with a tripod-mounted level.

The vertical measurements include the heights of one or more low slack tides at each locality. These tidal heights, and the tide level at Aberdeen (near Elliott Slough, fig. 5) as predicted in tide tables of the National Oceanic and Atmospheric Administration, are plotted on the outcrop diagrams.

FOSSILS

We depend mainly on vascular-plant fossils and diatom assemblages to assign ancient deposits to one of three depositional environments: high marsh, low marsh, and tidal flats or channels. We also use such evidence to estimate whether coseismic subsidence exceeded 1 m (p. 83).

VASCULAR PLANTS

Atwater and several coworkers identified vascular-plant fossils in the field, mainly in their growth position. They include woody roots, chiefly of Sitka spruce; formerly above-ground stems and basal leaves of *Deschampsia caespitosa*, *Potentilla pacifica*, *Juncus balticus*, and *Salicornia virginica*; and below-ground stems (rhizomes) of *Triglochin maritimum*, *Carex* (probably *Carex lyngbyei*), and *Distichlis spicata* (figs. 13, 18, 24, 25, 27, 29, 31). For species names we used the taxonomy of Hitchcock and Cronquist (1973).

DIATOMS

Hemphill-Haley studied diatom assemblages from vertical slabs collected at the Oyster, Redtail, and Sewer localities. The diatoms were sampled, separated, and identified by procedures previously described (Hemphill-Haley, 1995a, b). For the Oyster and Redtail localities, Hemphill-Haley counted an average of 388 diatom valves per sample, of which an average of at least 100 proved useful for inferring depositional environment.

Results of the diatom counts are listed in tables 4–6. In each of these tables the diatoms are listed alphabetically in two categories, benthic and planktonic. Each table concludes with summary data that include the brackish intertidal diatom index (BIDI). This index is defined on page 14 and is plotted in figures 15 and 20. Counts used to calculate the index are plotted in figures 16, 21, and 22, and photographs of important taxa are shown in figures 9 and 10.

CRITERIA FOR INFERRING UPLAND CONDITIONS

By analogy with diatom assemblages of modern uplands (p. 14), we interpret many fossil assemblages of sparse, poorly preserved diatoms as indicators of uplands that bordered tidal wetlands. Species typical of these assemblages have thick, sturdy valves that make them more resistant to breakage and dissolution than other diatoms. Some are species that live today in marshes, such as *Cosmioneis pusilla*, *Pinnularia lagerstedii*, and *Tryblionella debilis*. Others are typical of tidal flats—*Delphineis* cf. *D. surirella*, *Cocconeis scutellum*, *Tryblionella granulata*, and *Paralia sulcata*.

Several kinds of evidence generally confirm that such assemblages of fossil diatoms represent uplands at the Redtail locality. First, as discussed below under "Comparisons Between Diatoms and Vascular Plants" (p. 23), sparse, poorly preserved diatoms coincide with spruce roots in soils S and Y and with an archaeological site in soil Y. Second, upland conditions inferred for soils N and Y continue an upsection trend toward progressively higher land. This upsection trend is shown by upsection gradation from tidal-flat assemblages, through low-marsh assemblages, to high-marsh assemblages (figs. 15, 16). The same trend may be present for soil S if a 12-cm gap between samples accounts for the lack of a high-marsh assemblage between low-marsh and upland assemblages.

Without such independent evidence, however, assemblages of sparse, poorly preserved diatoms need not signify upland conditions. Fully estuarine deposits may contain sparse, poorly preserved diatoms where conditions during or after deposition favor removal of diatoms (Denys, 1984; Sherrod and others, 1989).

SIGNIFICANCE OF *PARALIA SULCATA*

Paralia sulcata, which abounds in most of our fossil samples, shows little about vertical position at the time of deposition but may serve as an indicator of later dissolution. Though the species lives mainly on tidal flats, its valves may be found at all intertidal levels and on uplands as well (Nelson and Kashima, 1994; Hemphill-Haley, 1995a; Shennan and others, 1996). This large vertical range is due partly to ease of transport; the valves form chains easily suspended by tides. The abundance of *Paralia sulcata* also may reflect resistance to dissolution. Having sturdy, heavily silicified valves, *Paralia sulcata* may become concentrated relative to delicate, more soluble valves of other diatom species. The resulting predominance of *Paralia sulcata* in marsh and upland deposits may be mistaken as evidence for tidal-flat conditions (Hemphill-Haley, 1995b).

These points are illustrated by *Paralia sulcata* in samples from stratigraphic sections at the Redtail and Oyster localities. For these samples we plotted relative abundance of *Paralia sulcata* valves, defined as their percentage of the total number of diatoms counted (fig. 17).

In each of three sections the abundance of *Paralia sulcata* shows no overall correlation with the depositional environment inferred from other diatom species (fig. 17*A*–*C*). These environments include upland at the Redtail locality (fig. 17*A*). On a sample-by-sample basis the environmental significance of *Paralia sulcata* also is murky in two respects (tables 4–6):

1. *Paralia sulcata* at the Redtail locality is less abundant in tidal-flat deposits than in buried soils that formed high above the levels where the species would have lived. The species makes up about half the valves in tidal-flat deposits at 0.66, 0.70, 0.74, and 1.89 m. By contrast, *Paralia sulcata* makes up nearly three-quarters of the valves high in soils N (1.97 m) and S (1.68 m). Spruce roots and a scarcity of other diatoms show that the sample from soil S represents a spruce upland, where *Paralia sulcata* probably was deposited by storm surges and later concentrated, relative to other species, by dissolution of the valves of other taxa. The sample from soil N connotes an upland or a high marsh beside an upland (p. 23).
2. At the Oyster locality, *Paralia sulcata* is most abundant (82 percent) in a tidal-flat deposit at depth 1.18 m and horizontal coordinate 25 m. However, it is also abundant (about 70 percent) in high-marsh deposits at 0.95, 0.98, and 1.44 m.

The abundance of *Paralia sulcata* varies widely depending on whether the diatom preservation is good (most valves intact, dissolution not evident), moderate (many valves broken, dissolution evident but minimal), or poor (most valves broken, dissolution severe) (fig. 17*D*–*E*). Where preservation is good or moderate, very abundant (>70 percent) *Paralia sulcata* may reflect high production of the species. Poor preservation of other diatoms, however, may also make *Paralia sulcata* relatively abundant, as shown by soil U at the Oyster locality (figs. 18, 20). Where soil U is bold and vascular-plant fossils well-preserved (horizontal coordinate 165 m), diatoms are abundant and diverse, and *Paralia sulcata* is correspondingly minor (6 percent at depth 2.01 m; table 6). By contrast, where soil U is faint and vascular-plant fossils are lacking (horizontal coordinate 25 m), diatom preservation is similarly poor, and *Paralia sulcata* predominates (69 percent at depth 1.44 m; table 5).

COMPARISONS BETWEEN DIATOMS AND VASCULAR PLANTS

Environments inferred from the fossil diatom assemblages resemble those inferred from vascular-plant fossils in most cases where the inferences can be compared (figs. 15, 20). Such comparisons can be made for fossils inferred to record upland conditions at the Redtail locality, high marsh at the Oyster locality, and transitions from tidal flat to low marsh at both these localities.

Diatom assemblages suggestive of uplands accord with vascular-plant fossils in two of three cases at the Redtail locality (fig. 15). The upland assemblages, marked by valves that are scarce and fragmented, are consistent with the presence of many spruce roots in growth position in soils S and Y (figs. 13, 14*B*). The diatom assemblage in soil Y further accords with archaeological evidence for a fishing camp on the soil (p. 30). However, the lack of tree roots in soil N seems inconsistent with the presence of only scarce, fragmented diatoms high in this soil. The lack of roots cannot be explained by decomposition after burial of soil N because, despite its typical faintness, soil N contains or is immediately overlain by well-preserved spruce cones, as shown by radiocarbon samples plotted in figure 13. Moreover, soil N locally retains a peaty surficial horizon—at the site of the cones dated 2,475±23 ^{14}C yr B.P. (fig. 13).

Comparisons between diatoms and vascular-plant fossils show general agreement in the inference of high marsh for soils S, U, and Y at the Oyster locality (fig. 20). Although soils bearing high-marsh herbs locally have brackish intertidal diatoms indices transitional between low marsh and high marsh, these indices are due to probably allochthonous valves of heavily silicified and easily reworked tidal flat diatoms (p. 48). Diatoms in soil U accord with vascular-plant evidence that soil U represents a slightly lower-level high marsh than do soils S and Y (p. 48).

Transitions from tidal flat to low marsh can be inferred both from diatom assemblages and from vascular-plant fossils in mud above soils S, U, and Y at the Oyster locality (fig. 20). Each transition is marked in outcrop by the first appearance of *Trigochin maritimum* rhizomes in soft gray mud above the buried soil. The mud lacks other vascular-plant fossils in growth position but contains rhythmic layers of organic mud ascribed to filamentous algae found today mainly at the transition between tidal flat and low marsh (p. 48). Diatom assemblages independently suggest that mud below the rhizomes represents a tidal flat or shallow subtidal conditions. However, the diatom assemblages, as summarized by the brackish intertidal diatom index, place the transition to low marsh several tenths of a meter above the lowest *Triglochin maritimum* rhizomes. This discrepancy may reflect patchy colonization of the tidal flat, which could have supported dominantly tidal-flat assemblages of diatoms until *Triglochin maritimum* patches fully coalesced. The discrepancy may also result from errors inherent in using diatom assemblages to estimate the point of transition from tidal flat to low marsh (Hemphill-Haley, 1995b).

Inferences from rhizomes and diatoms differ somewhat for a tidal-flat-to-low-marsh transition between soils J and L at the Redtail locality (fig.15). Diatoms found with the lowest *Triglochin maritimum* rhizomes (at depth 310 cm) include such low-marsh species as *Caloneis westii* and *Diploneis interrupta*. However, the assemblage contains many more valves of the high-marsh diatom *Cosmioneis pusilla* var. 1. These valves, which could have been reworked from high marsh that may have fringed the upland beside the Redtail locality (fig. 7), push the diatom index into the high-marsh range (fig. 15).

RADIOCARBON DATING

Radiocarbon ages have been measured on samples of wood, peat, and rhizomes from the Oyster, Redtail, Pool, Jensen, and Sewer localities. Most of the ages were measured by liquid scintillation methods and were calculated for an assumed fractionation ($\delta^{13}C$) of -25 parts per thousand (‰) (table 7, lab code Beta). Other samples were dated by proportional gas methods (lab codes QL and USGS). $\delta^{13}C$ was measured for all the QL ages and was assumed to be -25 ‰ for the USGS ages. Still other samples were dated by accelerator mass spectrometry (RIDDL, GX) and calculated with measured $\delta^{13}C$.

KINDS OF YEARS

Table 7 and the outcrop diagrams give ages in conventional radiocarbon years before A.D. 1950 (^{14}C yr B.P.). In the text and in interpretive diagrams, however, we mainly use calendric years before A.D. 2,000 (years ago). We converted radiocarbon ages to calendric-year ranges by means of the calibration data of Stuiver and Becker (1993) and version 3.0.3 of the radiocarbon calibration program of Stuiver and Reimer (1993).

We do not use "cal yr B.P.," the standard unit for calibrated radiocarbon ages (Stuiver and Pearson, 1986), because the "B.P." connotes "before present" but denotes "before A.D. 1950." Thus we describe A.D. 1700 as about 300 years ago, not as 250 cal yr B.P.

ANALYTICAL ERRORS IN DATING

The error quoted with each age, as listed in table 7, does not necessarily equal one standard deviation of the age measurement. Such underestimation of analytical uncertainties is common in radiocarbon dating (Scott and others, 1990). The quoted error probably exceeds 0.6–0.8 standard deviation for the QL ages (Stuiver and Pearson, 1986) but may approximate 1.0 standard deviation for the GX ages (Nelson and others, 1995). We lack such figures for the Beta, RIDDL, and USGS ages.

Figure 32 shows two calendric-age ranges for each ^{14}C age. The narrower range equals the 95-percent confidence interval if the error quoted by the lab equals one standard deviation of the age measurement. The wider range incorporates a published, maximum error multiplier of 1.6 for ages measured at the University of Washington (lab code QL; Stuiver and Pearson, 1986) and an assumed and probably excessive error multiplier of 2.0 for the other ages. In other illustrations and in the text we use the wider range, and in the text we commonly use a still broader range rounded outward to the century.

GEOLOGIC ERRORS IN DATING

The material dated formed before or after the inferred earthquakes that we sought to date. For several samples of forest-floor litter this difference is probably negligible (fig. 32, "closely limiting" ages for soils J and N), and for some tree-root samples the difference has been corrected by means of tree-ring counts (Atwater and others, 1991) (fig. 32, "closely limiting" ages for soils S and Y). For other samples, particularly of peat, the difference may amount to decades or centuries (Nelson, 1992b). Arrows in figure 32 identify ages subject to such differences. These include ages on small woody roots that may have died long before an inferred earthquake (arrow pointing upward), ages on rhizomes that may have formed long after the earthquake (arrow pointing downward), and ages on peat and sticks that may either predate or postdate the earthquake (arrows pointing both directions).

Even the carefully selected and exhaustively cleaned stems of perennial herbaceous plants appear subject to geologic errors in dating of earthquakes. Ages measured on *Potentilla pacifica* and *Juncus balticus* rooted in soil Y at the Oyster locality (table 7) average 40–50 radiocarbon years greater than the likely radiocarbon age of the earthquake (Nelson and others, 1995). Reasons for the differences may include:

1. The dated material, coming from perennial plants, largely originated decades before the earthquake.
2. Air used in photosynthesis contained old CO_2 derived from decay of organic matter in the marsh soil, including litter at the ground surface. Such uptake of old CO_2, suggested to us by Minze Stuiver (oral commun., 1995), may account for part of the photosynthate in the grass *Spartina alterniflora* at a South Carolina salt marsh (Morris and Whiting, 1986).
3. Soil water contained old carbon, in such compounds as amino acids, that was taken up by the plants (Kathleen Sayce, written commun., 1996).
4. Ages may differ systematically between radiocarbon laboratories (Scott and others, 1990).

Nelson and others (1995) found that neither the first nor the fourth of these possibilities fully explains the relatively great ages obtained from the herbaceous fossils rooted in soil Y and its inferred correlatives.

SEQUENCES OF BURIED SOILS

OVERVIEW OF EVIDENCE FOR STRATIGRAPHIC CORRELATION AND DECOMPOSITION

Buried soils at Willapa Bay are part of a regional sequence that is largely defined by a pattern of alternating bold and faint soils. This pattern is probably due, in part, to differences in decomposition of buried A or O horizons after burial.

REGIONAL SEQUENCE

Low-tide outcrops in southern coastal Washington resemble one another in their sequences of buried marsh and swamp soils of late Holocene age. The similarities, first noted in reconnaissance in 1987 (Atwater and others, 1987), create a pattern, like a bar code. In this bar code three typically bold soils (L, S, Y) alternate with faint soils (N, U). At many sites an additional faint soil (W; overlooked in 1987) is barely visible between soils U and Y.

Additional properties of the soils support such stratigraphic correlation (p. 83). Tree roots are most common in soils S and Y, and they are scarce or absent in soils N, U, and W—even where soils N and U have peaty surficial horizons. Radiocarbon ages are similar among soils correlated by abundance of peat and tree roots (fig. 32).

The combined evidence for stratigraphic correlation leads us to treat soils as mappable units that can be assigned the same name at various localities in southern coastal Washington and beyond. We also use the inferred extent of correlative soils as evidence that earthquake ruptures occurred on the Cascadia plate boundary (p. 83) and that the ruptures were long enough to have resulted from earthquakes of magnitude 8 or larger (p. 85).

DECOMPOSITION AFTER BURIAL

Decomposition of organic matter accounts for much of the typical faintness of soils N, U, and W, and it probably also explains much of the absence of soil W. We further infer that this decomposition took place after burial, in the weathering profile of soil S (in the case of soil N) and in the profile of soil Y (for soils U and W). We summarize these inferences here because they bear on the correlation and consequent naming of buried soils at the localities described below. Differences in decomposition also suggest that some recurrence intervals were much longer than others (p. 98–99).

Decomposition of organic matter is evident in modern tidal-marsh soils at Willapa Bay. Most of these soils are oxidized (Munsell colors 2.5Y to 10YR 5/4) to depths of ½ m and commonly contain rust-colored mottles to depths as great as ¾ m. Fossil rhizomes of *Triglochin maritimum* are rotten or absent in the oxidized mud. Moreover, the oxidized mud is firmer (probably, more desiccated) than underlying, gray mud that contains well-preserved fossils of vascular plants. The oxidation may occur, in large part, during neap tides. Such is inferred to be the case in a Maryland salt marsh having a mean tide range of 3 m, similar to the range at Willapa Bay. In the Maryland marsh, neap tides diminish pore-water pressure in marsh soil by failing to overtop it, the pressure falls below the threshold for entry of air into the soil, air probably enters along pathways created by plant roots, and soil thereby contains as much as 2 percent air (Hemond and Chen, 1990).

Several lines of evidence confirm that faint soils at Willapa Bay initially contained organic matter that later decomposed in weathering profiles from overlying soils:

1. Soils are faint wherever they—and the mud above and below them—are firm and lack fossil rhizomes or plant detritus. Soils that are typically bold become faint where directly overlain by firm mud without rhizomes: soil S at the Redtail locality (p. 27), soil L at the Jensen locality (p. 67), and soil Y at the Sewer locality (p. 69). Similarly at the Oyster locality, soil U is faint where associated mud is firm and vascular-plant fossils are lacking, but bold where associated with soft mud and well-preserved roots and rhizomes (p. 45).
2. Assemblages of environmentally indicative diatoms in soil U at the Oyster locality do not differ greatly between a section where the soil is bold and located 1.0 m below the top of soil Y (horizontal coordinate 165 m; BIDI =

0.80) and a section where the soil is faint and located 0.3 m below the top of soil Y (horizontal coordinate 25 m; BIDI = 0.71) (fig. 20; tables 5, 6). This similarity in diatom assemblages implies that differences in later weathering, not differences in environment of formation, account for the variation from bold to faint for soil U at the Oyster locality (p. 45). Differences in weathering of soil U at the Oyster locality are further suggested by the differences in diatom preservation (fig. 23) and by the abundance of *Paralia sulcata*, whose sturdy valves probably resist decomposition (p. 21). The ratio of *Paralia sulcata* to all other taxa is less than 1:10 where soil U is bold (table 6, depth 2.01 m) but about 1:2 where soil U is faint (table 5, depth 1.44 m).

3. Typically faint soils N and U at the Redtail locality formed in a high marsh (U) or perhaps in the transition from marsh to upland (N) (p. 27), as judged from diatom assemblages. In those settings, vascular plants should have rained much organic matter onto each soil and injected additional organic matter into it, making the soil bold before burial.

Horizons of decomposed peat have also been reported from the Holocene of coastal Germany. According to Streif (1982, p. 36), the horizons can be ascribed to "temporary lowering of the groundwater table" and consequent "oxidation of peaty matter."

NIAWIAKUM RIVER

The Niawiakum River drains 5 km² of hills composed of Pleistocene estuarine deposits and the Crescent Formation. Brackish water extends far upstream; usual freshwater inflow in late summer is probably about 0.1 m³/s. Brackish marshes therefore extend far upstream as well, grading into a tidal swamp of Sitka spruce and western crabapple 0.5 km northeast of the Pool locality (fig. 7).

Buried soils along the tidal Niawiakum River have provided much previously reported evidence for repeated prehistoric earthquakes on the Cascadia plate boundary. Gouge cores penetrated as many as eight successive buried soils along a cross section about 0.5 km northwest of the Pool locality (Atwater, 1987; location of cross section shown in our fig. 7). Downstream from this cross section the uppermost buried soil (soil Y) is widely covered by tsunami deposits that are commonly several centimeters thick (Atwater, 1987, 1996; Reinhart and Bourgeois, 1987, 1989; Hemphill-Haley, 1995b, 1996). Herbaceous stems and leaves rooted in soil Y and in another, lower soil (soil S) show that both these soils record subsidence that occurred suddenly (Atwater and Yamaguchi, 1991, their figs. 4, 5). Fossil diatoms at the Oyster and Redtail localities, and at two other sites farther upstream, independently confirm that soil Y suddenly subsided (Hemphill-Haley, 1995b; her sites 1, 2, and 3 are at the Oyster, Redtail, and Heron localities, respectively). Radiocarbon evidence for extensive plate-boundary rupture at the Cascadia subduction zone includes high-precision ages of spruce stumps rooted in soil Y near the Pool locality (Atwater and others, 1991; locations of dated stumps shown by QL symbols in our fig. 7) and accelerator-mass-spectrometry (AMS) ages on herbaceous stems and leaves rooted in soil Y at the Oyster locality (Nelson and others, 1995). The AMS ages are listed in table 7, and their approximate sample location is plotted in figure 18.

We surveyed successive buried soils along the Niawiakum River at four places where they are especially well exposed—the Redtail, Oyster, Pool, and Heron localities (figs. 6, 7). At very low tides the Redtail locality displays six buried soils from the past 3,500 years, whereas the Oyster locality has four buried soils from the past 2,000 years. Probable correlatives of five of the soils at the Redtail locality crop out at the Pool and Heron localities. We discuss the more thoroughly studied outcrops first (Redtail and Oyster localities) and the less studied outcrops second (Pool and Heron localities).

REDTAIL LOCALITY

The Redtail locality comprises 65 m of stream bank—about 30 m along the Niawiakum River, the rest along an unnamed tributary (figs. 13, 14*A*, *B*). The bank is capped by tidal marsh except at its west end, where it intersects a forested upland. The upland is made of Pleistocene estuarine deposits that were deeply dissected by the glacial-age Niawiakum River and its tributaries. These deposits form a stiff muddy foundation that descends eastward beneath a Holocene section containing seven buried soils.

BURIED SOILS

Six buried soils are exposed at the Redtail locality at tides below mean lower low water. Four of these soils are commonly peaty and (or) woody enough to form prominent ledges (fig. 14*A–C*, soils J, L, S, and Y); the other two, which are characteristically faint, lack such topographic expression (soils N and U). A seventh soil (H), observed only in core, underlies soil J near the forested upland.

All the soils dip away from the Pleistocene deposits onto which they lap. Such dips are greatest for the oldest soils (figs. 13, 14*B*; soils H, J, and L). Soil J is 1.7 m lower near the unnamed tributary than it is on Pleistocene deposits—a difference more than three times greater than undulatory relief on the nearly horizontal modern marsh along the Niawiakum River (fig. 13).

Most of the 1.7 m of relief on soil J, and most of the northeastward dip of other buried soils as well, was probably caused by settlement through compaction of soft Holocene mud. Such mud is probably many meters thick above the last-glacial thalweg of the unnamed tributary; during the last glaciation the lower Niawiakum River flowed tens of meters below modern sea level, as shown by highway borings near the Oyster locality (p. 45). Settlement caused by compaction of peat and mud is common in tidal wetlands, as recently shown for modern salt marshes of the southeastern United States (Cahoon and others, 1995).

Most of the soils are interrupted by muddy channel fills in the northeastern half of the outcrop (fig. 13). The channel fills are 2–10 m wide in the plane of the outcrop. We observed truncation of buried soils on one or both margins of each fill. The fills consist of soft gray mud; in one of them, near horizontal coordinate 35 m, the mud contains much detrital wood.

Abundance of peat in the surficial horizon varies greatly for many of the soils, as summarized simplistically by the symbols for bold and faint soils in figure 13. In soil J the surficial horizon consists of woody peat 10 cm thick near the forested upland but grades, along 20 m of continuous outcrop beside the Niawiakum River, into slightly peaty mud 2 cm thick. The woody peat abounds in forest-floor litter—sticks, spruce cones, needles. Soil L consistently contains 20 cm of muddy peat along the Niawiakum River but lacks such peat in 9 m of outcrop along the unnamed tributary. There, the surficial horizon of soil L is made of slightly peaty mud having many undulations 5–10 cm high and 5–20 cm long—elk or deer hoofprints, perhaps. The surficial horizon of soil N, though typically limited to dark brownish gray mud 2 cm thick, is composed of woody peat 5 cm thick for several meters along the Niawiakum River. Like soil J, this peat contains many sticks and spruce cones. Soil S, which typically contains a surficial horizon of woody peat 5–10 cm thick (fig. 14*C*), becomes faint where it laps onto Pleistocene deposits and thereby enters the weathering profile of soil Y.

These variations in abundance of peat are probably due to initial composition in some cases and later decomposition in others. An initial abundance of forest-floor litter in soils J and N probably accounts for the greater abundance of peat near the forested upland; these soils logically received most such litter near the forested upland. Later decomposition in the profile of soil S probably accounts for the widespread faintness of soil N, and decomposition in the profile of soil Y probably accounts for the general faintness of U and the localized faintness of soil S (p. 25–26).

TSUNAMI DEPOSIT

A tsunami deposit discontinuously overlies soil Y at the Redtail locality. The deposit consists of micaceous sandy silt about 1 mm thick. Most of the sand is very fine. The sandy layer is separated from the underlying soil by as much as 3 mm of gray mud. Such mud layers are commonly part of the tsunami deposit on soil Y elsewhere along the Niawiakum River (Reinhart and Bourgeois, 1987; Atwater and Yamaguchi, 1991, their fig. 5*B*), as illustrated at the Oyster locality (p. 45, 47; fig. 19*E*).

Several points show that a tsunami probably deposited the sandy layer:

1. The layer resulted from deposition by an unusually strong current. Other than cracked rock in cultural deposits (p. 35), the sandy layer is the coarsest inorganic material in the outcrop.
2. The unusual current approximately coincided with subsidence recorded by intertidal submergence and burial of soil Y. This coincidence, shown by the position of the sandy layer just above the top of soil Y, would not be expected of a storm but would be expected of a tsunami generated by a plate-boundary earthquake at the southern Washington part of the Cascadia subduction zone (Atwater, 1987). The coincidence is further demonstrated by the preservation of herbaceous stems and leaves, in growth position, in the sandy deposit on soil Y at the Oyster locality (p. 47–48).
3. The current entailed flow up the Niawiakum River valley, as shown by variation in thickness of correlative sand elsewhere along the Niawiakum River (Atwater, 1987, 1996; Reinhart and Bourgeois, 1987), by oriented plant fossils at the Oyster locality (p. 47–48), and by diatoms—found immediately above soil Y at four sites between the Oyster and Pool localities—that were derived from sandy tidal flats (Hemphill-Haley, 1995b, 1996).
4. The current had multiple pulses, as shown by the presence of five or six sandy layers within the sandy deposit on soil Y at the Oyster locality (p. 45, 47; fig. 19*E*). A tsunami typically comprises a train of waves; each of the sandy layers can be ascribed to a separate wave in a tsunami wave train.
5. Currents from a storm or seiche are unlikely to have been swift enough to account for the extent and grain-size trends of sandy deposits on soil Y along the Niawiakum River, according to an unpublished sediment-transport model by Reinhart and Bourgeois (1989). However, a storm surge at least 2.5 m high deposited sand, silt, and clay on tidal marshes along several kilometers of a Florida river in 1993 (Goodbred and Hine, 1995).

FOSSIL DIATOMS

Diatoms show that each of the six buried soils seen in outcrop at the Redtail locality formed higher in the intertidal zone than did mud above the soil (figs. 15, 16). In addition, diatoms provide further evidence for tsunami deposition on soil Y, and they hint at the presence of an otherwise invisible soil between soils U and Y.

Each of the six soils contains diatoms indicative of conditions at or above very high tides (figs. 15, 16). Diatoms of soils J, L, and U are dominated by species—particularly *Cosmioneis pusilla* and *Pinnularia lagerstedtii* (table 4)—indicative of tidal marsh above mean higher high water. Even higher conditions, transitional to upland, are suggested by the small number and poor preservation of diatoms in the uppermost parts of soils S and Y. Such conditions are consistent with the abundant spruce roots in these soils (p. 29) and with the presence of *Paralia sulcata* valves (fig. 17; see section "Significance of *Paralia sulcata*," p. 23). Soil N

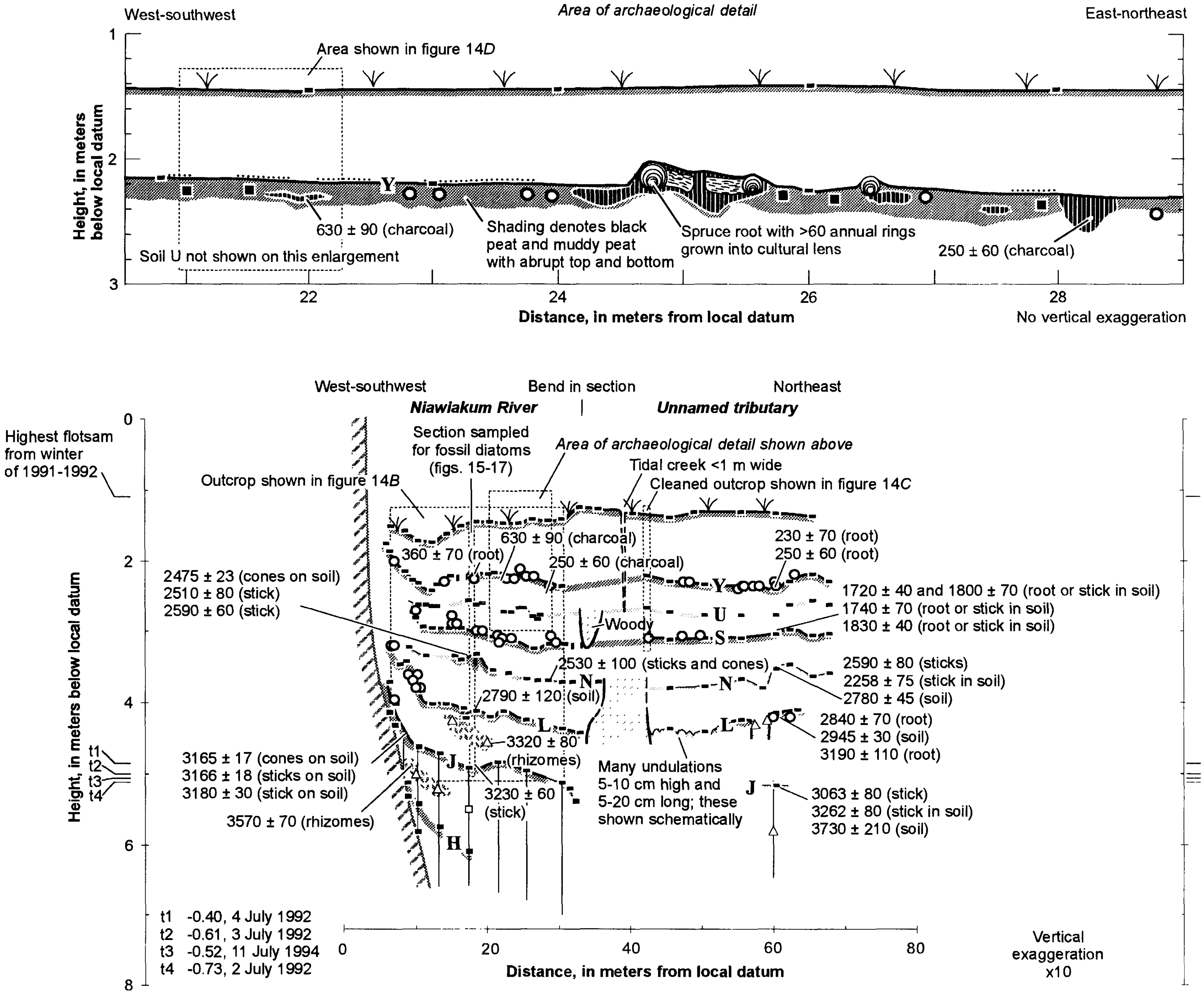

Figure 13. Statigraphy at Redtail locality, Niawiakum River.

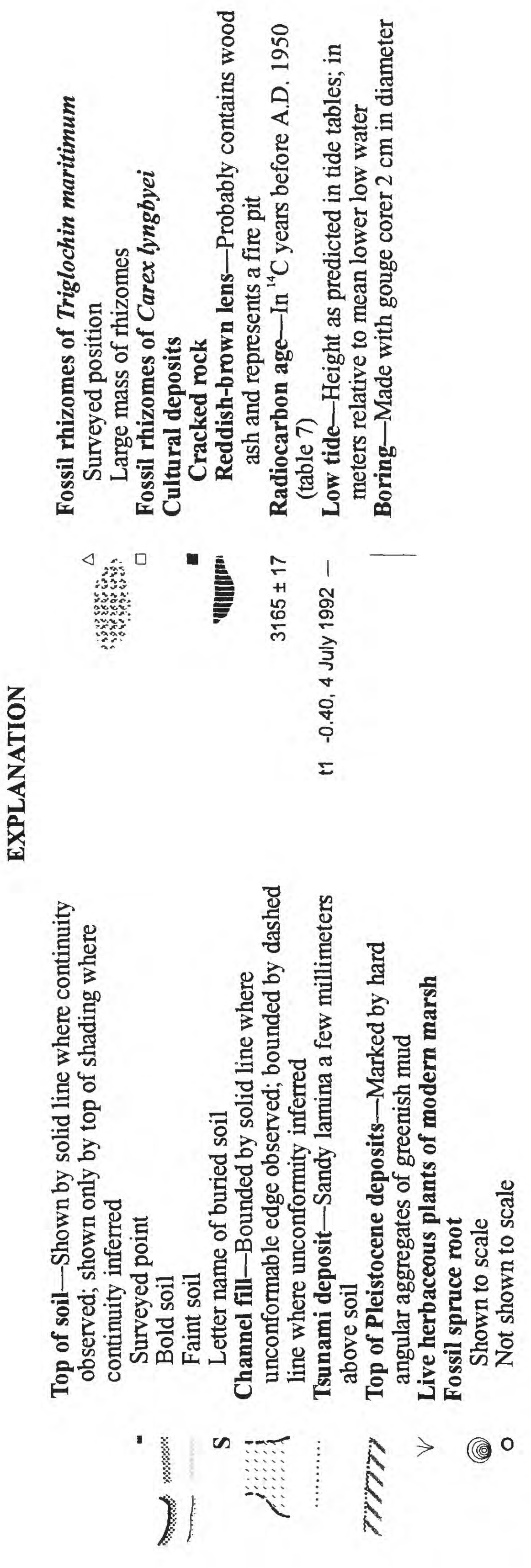

Figure 13. Continued.

contains an upland assemblage of diatoms but lacks tree roots that should accompany such an assemblage (p. 23).

For all six buried soils the transition from soil to overlying mud coincides with an abrupt shift to assemblages of diverse diatom species indicative of intertidal flats or shallow subtidal areas (table 4). For soils J, L, and U this shift bypassed low marsh, and for soils S and Y (and perhaps also soil N) it bypassed high marsh as well. The corresponding rise in relative sea level, as inferred from modern wetlands and their diatom assemblages (figs. 8, 12), is probably about 1 m or more in each case.

A vestige of a soil, invisible in outcrop, may be present between soils U and Y at the outcrop shown in figure 14*C*. Assemblages of poorly preserved diatoms are all that remain in the oxidized profile of soil Y at depths of 94–104 cm below the top of this outcrop. However, a possible tidal-flat assemblage at 96 cm overlies a sparse assemblage of poorly preserved high-marsh species at 98–100 cm—an interval located 18 cm above the top of soil U and 22 cm below the top of soil Y. This sequence provides inconclusive evidence for an otherwise invisible soil between soils U and Y. The invisible soil may be soil W, which can be seen in outcrop 1 km downstream at the Oyster locality but only where it is more than 25 cm below the top of soil Y (fig. 18).

Diatoms are part of the evidence that a tsunami deposited the discontinuous lamina of very fine sandy silt that are located a few millimeters above soil Y at the Redtail locality (p. 27). A sample from deposits just above soil Y contains well-preserved estuarine tidal flat species and lacks freshwater diatoms (table 4, sample from depth 0.74 m). More than half the tidal-flat species are diatoms typical of sandy flats of Willapa Bay. These species show that the sand was not washed down the Niawiakum River by a flood of freshwater.

Diatoms provide the only direct evidence that a tsunami overran soils S and N at the Niawiakum River. Although neither of these soils is overlain by a bed as sandy or as close to the soil as the sandy bed above soil Y, both are overlain by mud that contains high percentages of species typical of sandy tidal flats.

GROWTH-POSITION FOSSILS OF VASCULAR PLANTS

Four of the buried soils contain spruce roots suggestive of conditions within or above the upper ½ m of the intertidal zone. The roots are most widespread in soils S and Y (figs. 13, 14*A–C*). Spruce roots are also present in soil L, both at its juncture with Pleistocene deposits (fig. 14*B*) and along the tributary slough near the northeastern end of the surveyed outcrop (fig. 13). Soil J contains spruce roots only where it laps onto Pleistocene deposits (fig. 14*B*).

Mud above soils H and J contains rhizomes indicative of conditions lower in the intertidal zone. All these rhizomes are of *Triglochin maritimum* except above soil H, where the mud also contains rhizomes of *Carex*. The lack of rhizomes of mud above younger soils is probably due to

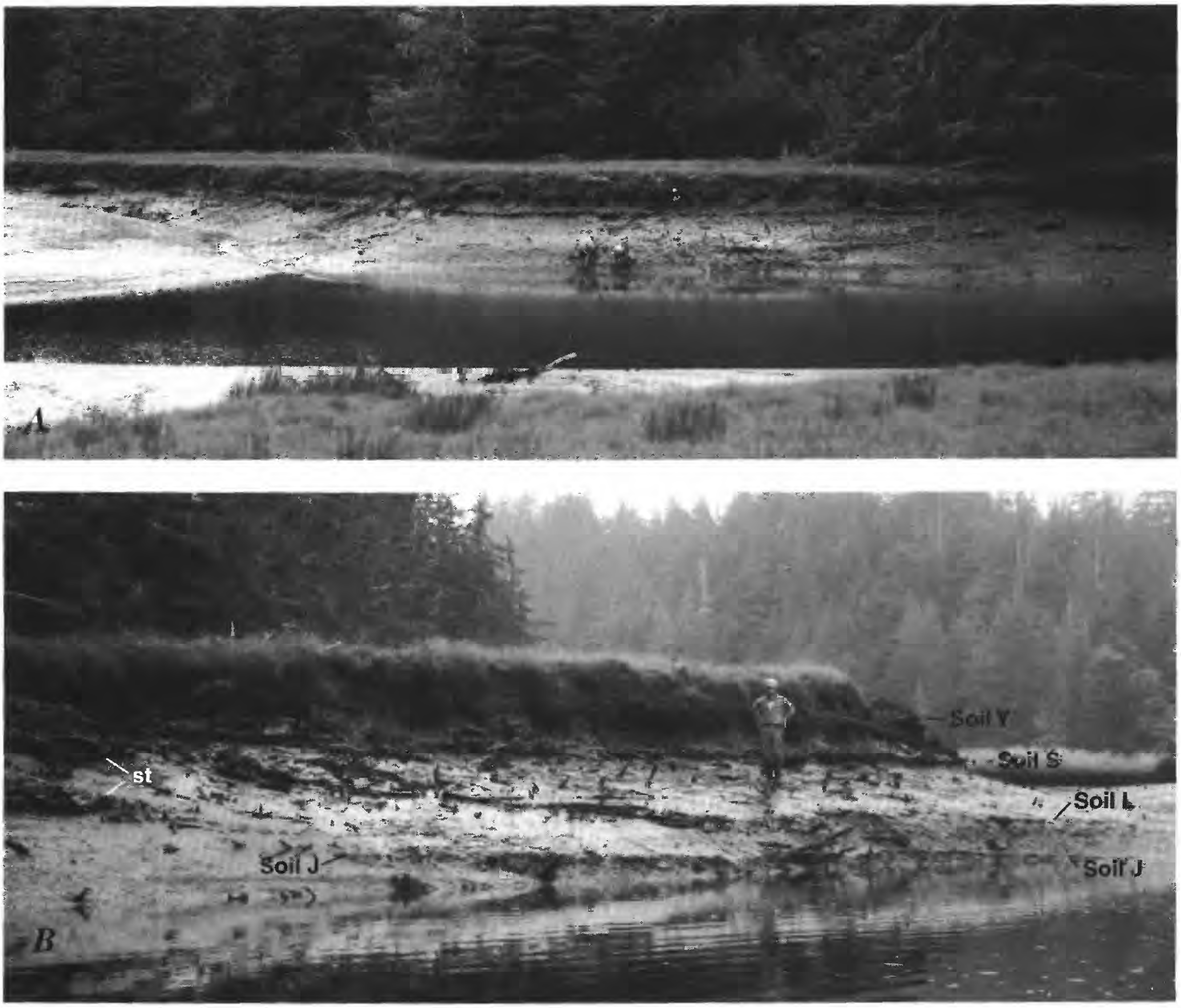

Figure 14. Redtail locality, Niawiakum River (fig. 13). *A*, Overview to north, across the Niawiakum River; tributary creek enters at right. Trees in background are rooted on upland, above level of highest tides. Tidal marsh high in intertidal zone (high marsh) forms meadow in foreground and in front of trees. Scale shown by people at center, low on far bank of river. June 1987. *B*, Closer view of outcrop along Niawiakum River. Soils J and L dip eastward, away from firm substrate of Pleistocene deposits onto which they lap. Buried soil S is prominent because of its peaty surficial horizon, abundant spruce roots, and lack of concealment by modern vegetation. Soil Y is mostly concealed by modern plants. Landward end of soils J and L marked by spruce stumps (st) rooted in them at left. August 1986.

decomposition. Mud beneath the modern marsh soil is brown and firm to within a few centimeters of the top of soil Y. We rarely found fossil rhizomes in such oxidized, desiccated mud, and where we did, they are mostly decomposed. When soil Y was at the surface, decomposition in a deeply oxidized, desiccated profile of soil Y probably destroyed rhizomes in mud above soils S and U. Such decomposition in the profile of soil S likewise helps to explain the lack of rhizomes in mud above soils N and L.

CULTURAL DEPOSITS

Remains of a human campsite at the Redtail locality add to diatom and spruce-root evidence for nearly upland conditions on soil Y. The campsite, which extended along the Niawiakum River part of the outcrop (fig. 13), is marked by charcoal, cracked rock, heated bone, and reddish-brown lenses probably composed of ash from wood fires (Cole and others, 1996) (fig. 14*D*).

Figure 14. *C*, Contrast in distinctness between faint soil U and bold soils S and Y. Shovel at horizontal coordinate 42 m; handle is 0.5 m long.

The campsite at the Redtail locality is one of several archaeological sites discovered in soil Y in southern Washington and in probably correlative soils in northern Oregon. The discoveries began in Oregon (Grant and Minor, 1991; Minor and Grant, 1996). The sites in Washington include one at the Copalis River (Cole and others, 1996) and two previously unreported sites along the Willapa River—at the Sewer locality (p. 69), and northwest of the Jensen locality

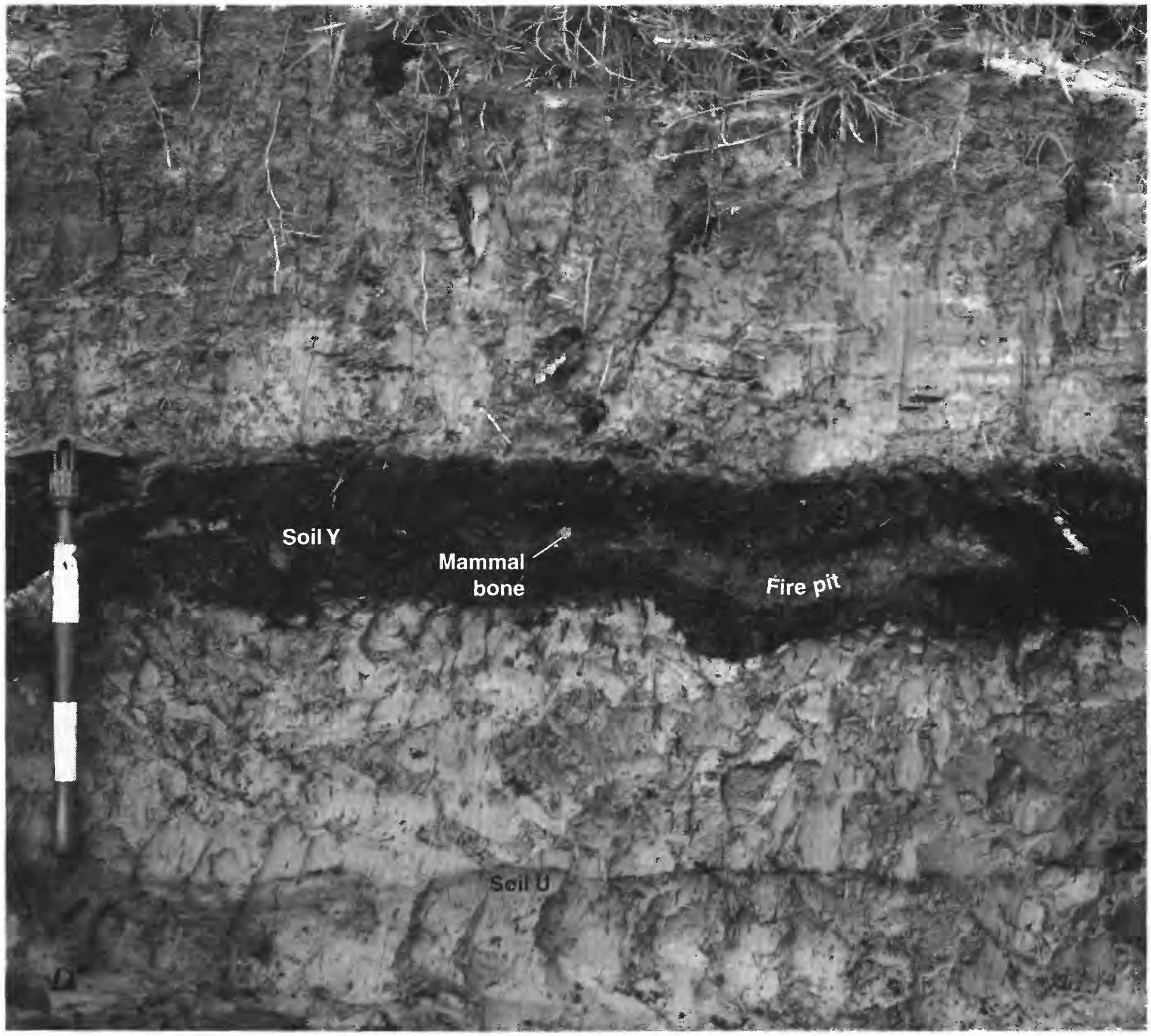

Figure 14. *D*, Black peaty horizon of soil Y, containing reddish-brown lens (light tone, in right half of photo) of probable fire ash and a mammal bone (white dot at center). Soil U faint, as in *C*. Shovel handle near horizontal coordinate 21 m; stripes on handle are 0.1 m long.

(fig. 7). The site at the Redtail locality has been assigned, by the Washington State archaeologist, Smithsonian number 45–PC–102. Stratigraphy at each of the sites shows that an earthquake about 300 years ago caused the lasting tidal submergence of land previously high enough to have been used as a campsite.

AGE

High-precision ages can be assigned to the oldest and youngest buried soils recorded in outcrop at the Redtail locality (fig. 32). Radiocarbon ages on forest-floor litter at the Redtail locality (table 7, lab numbers QL–4716, –4717, and –4718) show that the burial of soil J began 3,300–3,500 calendric years ago. Radiocarbon ages on spruce roots from nearby sites—a beach at Bay Center (fig. 6) and river banks near the Pool locality (fig. 7)—show that the burial of soil Y began about 300 years ago (Atwater and others, 1991), probably between A.D. 1700 and 1720 (Nelson and others, 1995).

Additional radiocarbon ages from the Redtail locality suggest broad calendric ranges during which some of the other burial events probably occurred (fig. 32): 2,400–4,000 years ago for soil L, 2,400–2,800 years ago for soil N, and 1,400–2,100 years ago for soil S.

A charcoal age from soil Y shows that the Redtail locality was used by people as early as A.D. 1000, while another charcoal age and a tree-ring count show that

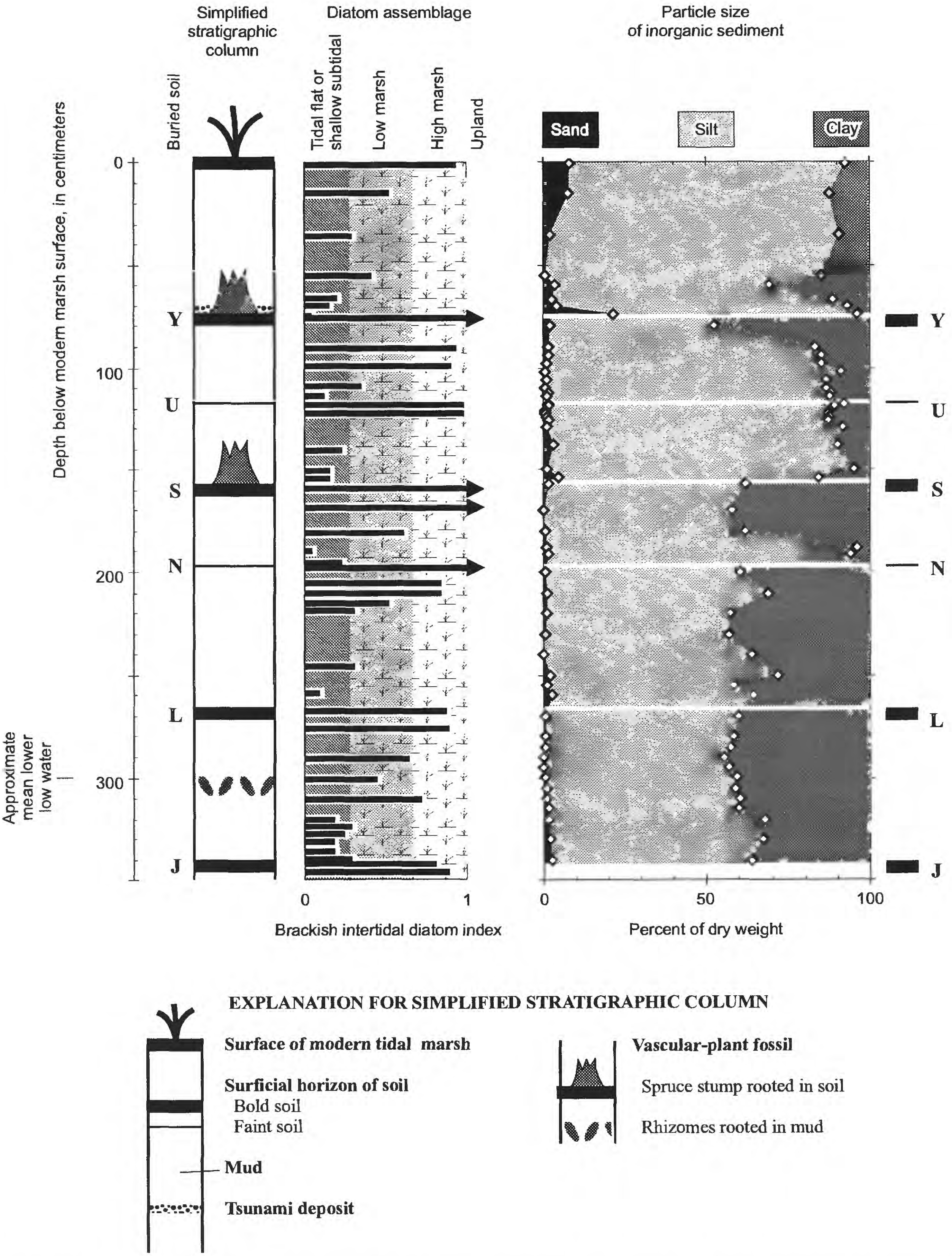

Figure 15. Summary of diatom assemblages at Redtail locality, Niawiakum River. Samples collected from section at horizontal coordinate 18 m (fig. 13).

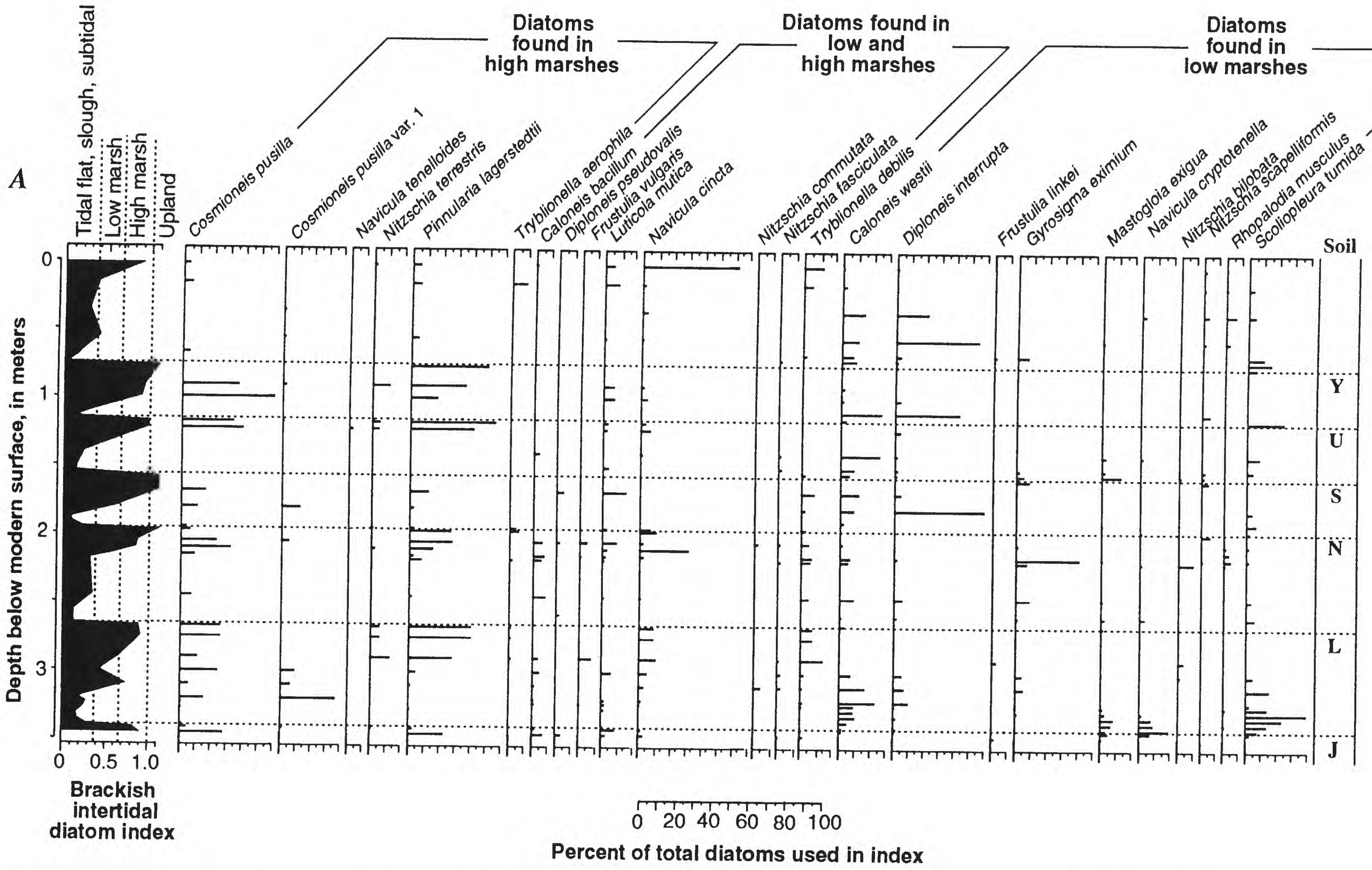

Figure 16. Relative abundances of diatom species grouped by inferred depositional environment for a stratigraphic section at the Redtail locality, Niawiakum River.

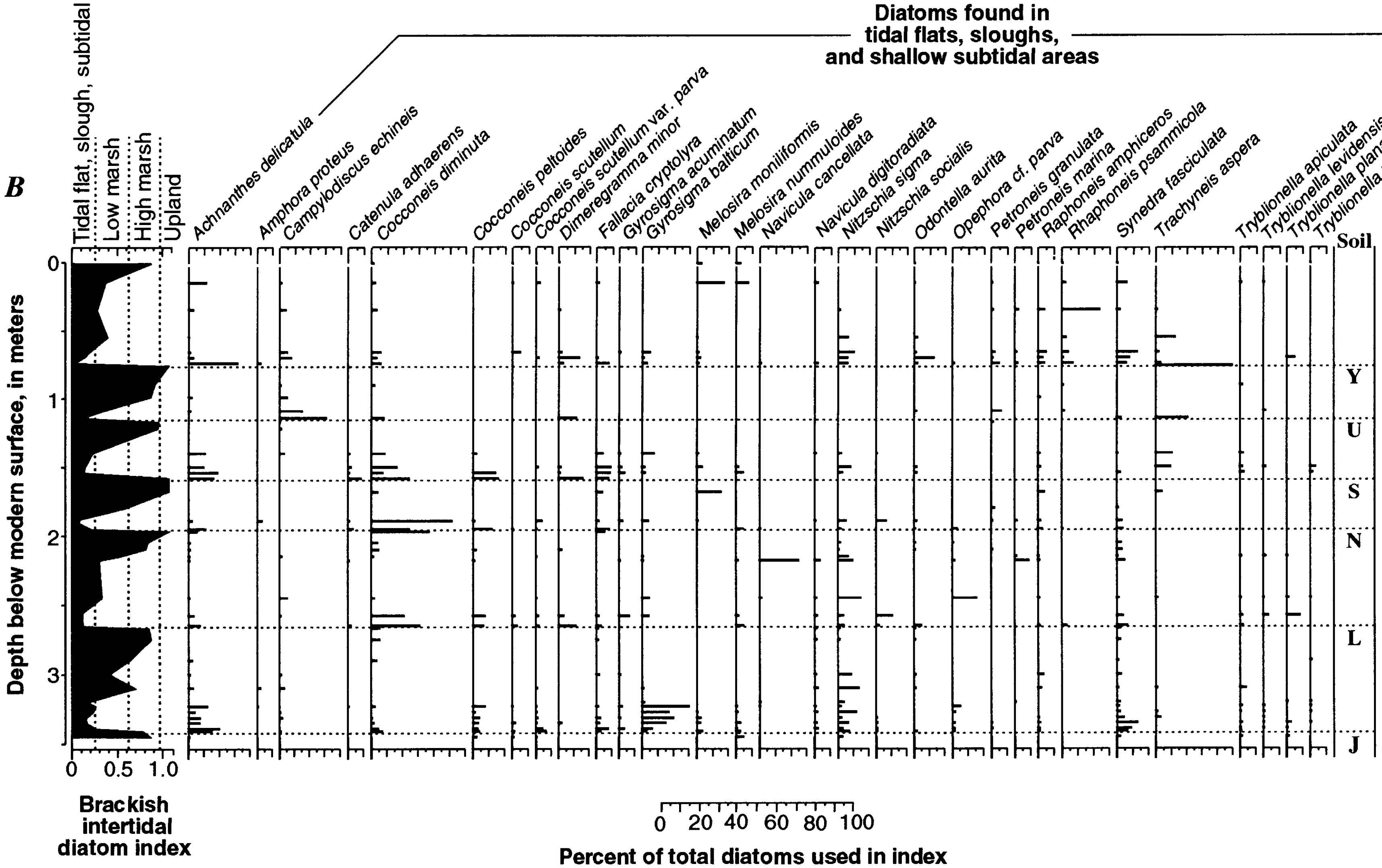

Figure 16. Continued.

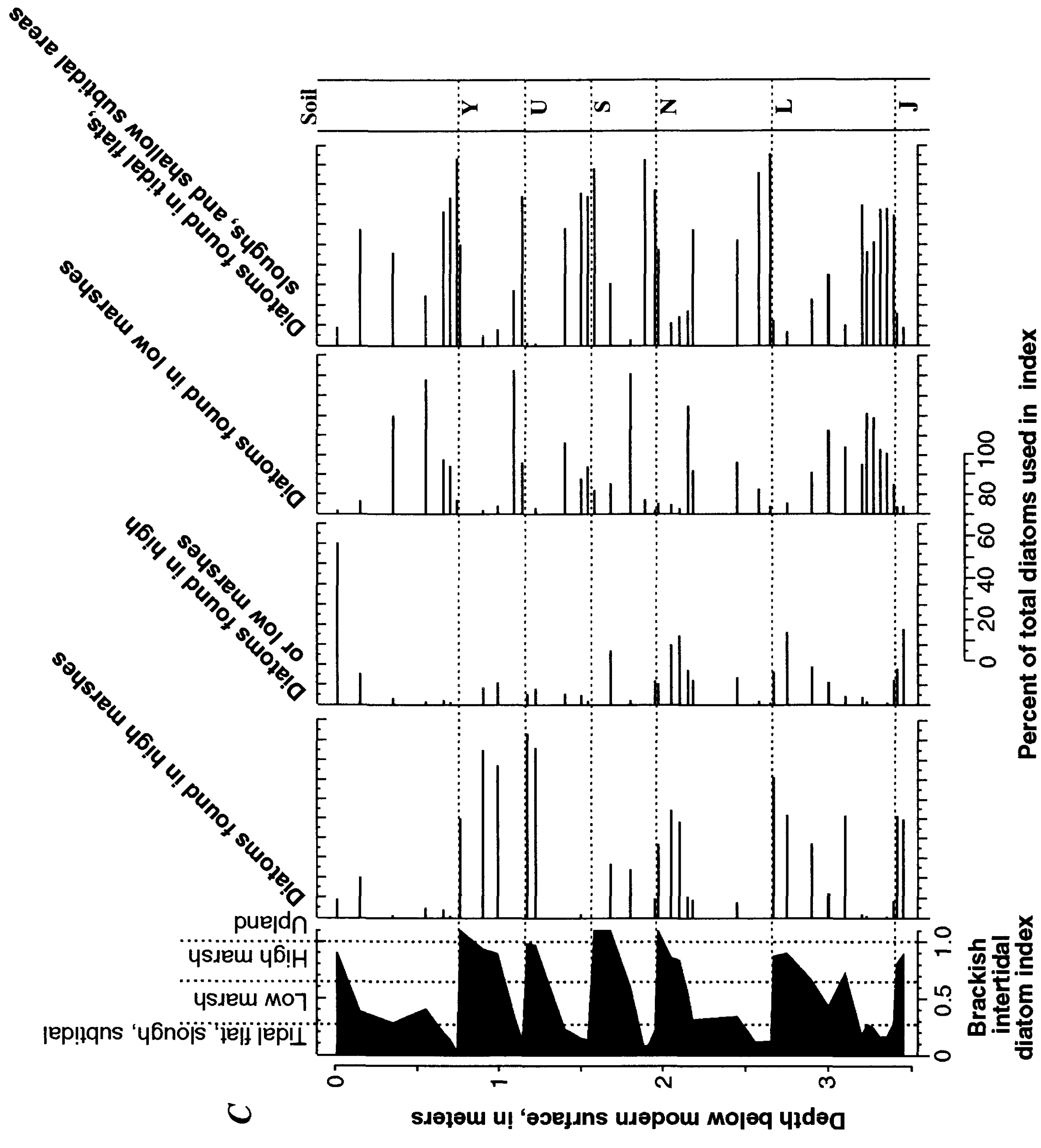

Figure 16. Continued.

humans may have abandoned the site decades before its intertidal burial in the early 1700's. The older of the dated charcoal samples—630±90 ^{14}C yr B.P., or A.D. 1000–1600 (fig. 32)—came from a cultural lens that is separated from the top of soil Y by 10 cm of archaeologically sterile peat. The younger charcoal sample gave an age of 250±60 ^{14}C yr B.P., which corresponds to a calendric range that includes A.D. 1700. Although this younger sample came from a fire pit that extends nearly to the top of soil Y, a spruce root having at least 60 annual rings grew into this fire pit (fig. 13). This spruce, like the others represented by roots in soil Y, probably died from submergence that initiated the burial of soil Y. In that case, the fire pit predates the submergence and initial burial of soil Y by at least 60 years.

OYSTER LOCALITY

The Oyster locality, located 1 km west-northwest of the Redtail locality, comprises the northeast bank of the Niawiakum River about 100–300 m upriver from U.S. Highway 101. The top of the bank is high marsh except for a mudflat 50 m wide at the confluence of two tidal creeks tributary to the river (figs. 18, 19*A*, *B*). Since 1986 the upper

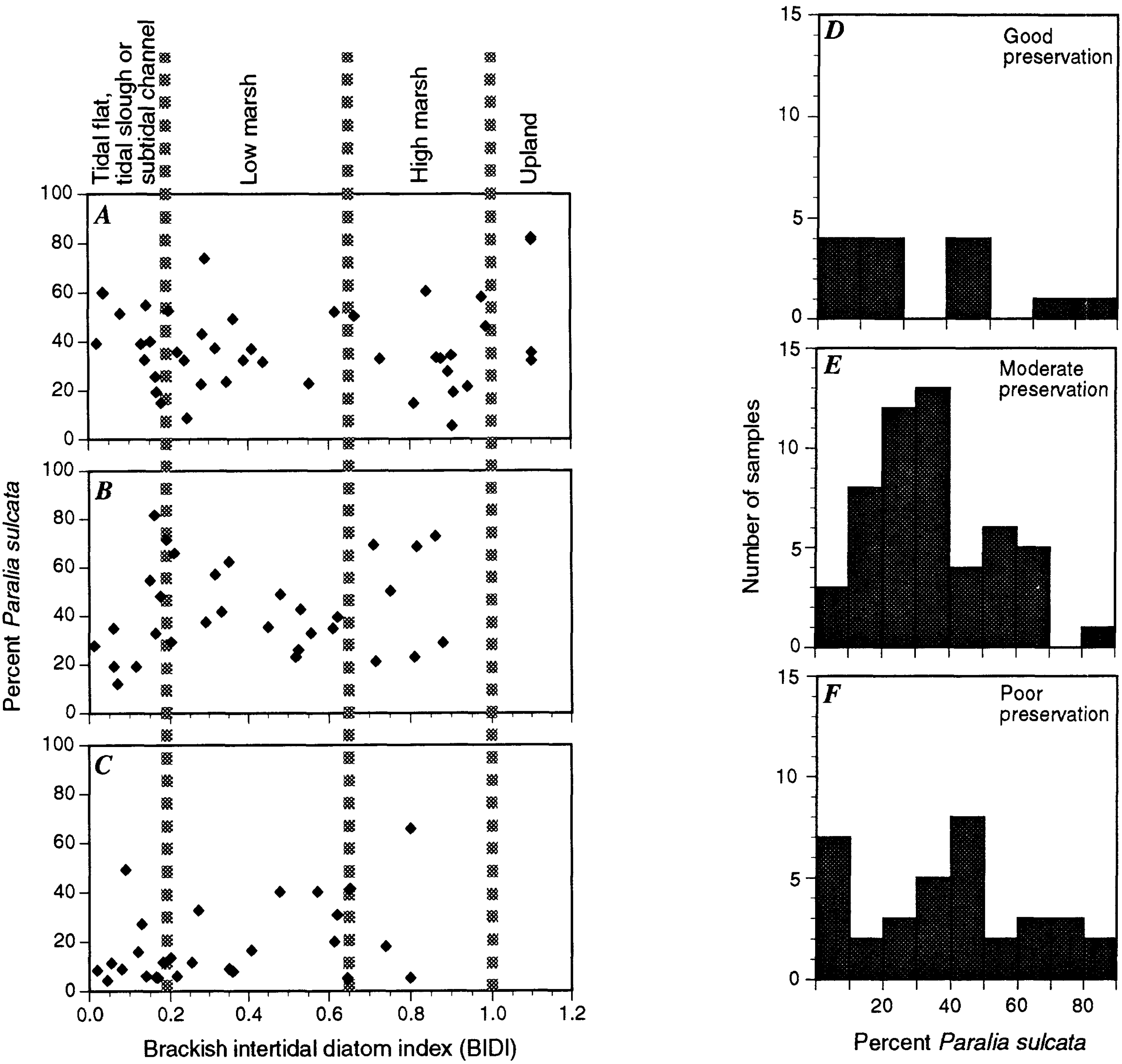

Figure 17. Abundance of the diatom *Paralia sulcata* in stratigraphic sections at the Redtail and Oyster localities, Niawiakum River. Abundance expressed as percentage of total number of diatoms counted. Data from tables 4–6. *A–C*, Comparison with depositional environment inferred from brackish intertidal diatom index at (*A*) Redtail locality, (*B*) Oyster locality, horizontal coordinates 15 and 25 m, and (*C*) Oyster locality, horizontal coordinate 165 m. *D–F*, Comparison with qualitative measures of diatom preservation.

half of the bank has been invaded by *Spartina alterniflora* (fig. 19*C*), an Atlantic-coast grass that began to spread rapidly at Willapa Bay in the early 1980's (Sayce, 1988; Mumford and others, 1990).

BURIED SOILS

Four buried soils are widely exposed at the Oyster locality. The oldest and youngest of these have ledge-forming peaty horizons (fig. 19*B–D*). The two intervening soils are characteristically faint and lack topographic expression except on well-washed, nearly vertical faces, from which they protrude a few centimeters more than does mud immediately above them. For reasons discussed under "Age and Correlation" (p. 52), we equate the bold soils with soils S and Y of the Redtail locality, and the lower of the faint soils with Redtail soil U. At the Redtail locality we did not notice evidence for a correlative of soil W, the other faint soil at the Oyster locality, except for two samples dominated by high-marsh diatoms (p. 29).

Table 4. Numbers of diatoms counted at the Redtail locality

	Depth below modern surface (m)	Diatom sample ID		**Benthic diatoms**	*Achanthes hauckiana*	*Achnanthes cf. minutissima*	*Achnanthes delicatula*	*Achnanthes lanceolata*	*Achnanthes spp.*	*Achnathes brevipes*	*Amphora libyca*	*Amphora proteus*	*Amphora spp.*	*Amphora ventricosa*	*Amphora ventricosa*	*Biddulphia spp.*	*Biremis ambiqua*	*Caloneis bacillum*	*Caloneis permagna*	*Caloneis spp.*	*Caloneis westii*	*Campylodiscus bicostatus*	*Campylodiscus echineis*	*Catenula adhaerens*	*Cerataulus turgidus*	*Cocconeis diminuta*	*Cocconeis peltoides*	*Cocconeis placentula*	*Cocconeis scutellum*	*Cocconeis scutellum v. parva*	*Cocconeis spp.*	*Cosmioneis pusilla*
	0.01	OS10x-75								4								2			1					4		4	1	2	1	10
	0.15	OS10x-60				11	22		4	4						1				2	4		2			4		2	1	5		10
	0.35	OS10x-40				1	3	1													14		4		7	3					4	
	0.55	OS10x-20			1															1	23				1							
	0.66	OS8-1				1	1												1	1	7		5		8	6		5	5			4
	0.70	OS8-3					3			2						2				2	9		8		3	3				2		
	0.74	OS8-6					32					2				1				1	1				6	6		1				
Uppermost 1 cm of soil Y	0.76	OS8-8																														
	0.90	OS10-24																			2		1			2						43
	0.99	OS10-32				1	2													3	1		5									59
	1.09	OS10-42					1														17		10									
	1.14	OS7-10																			2		24			6		4				
Uppermost 1 cm of soil U	1.17	OS10-56																					0.5									61
	1.22	OS10-61																					1									39
	1.40	930718 B3-20					20									2		6		2	46		6	2		16	4	2			2	
	1.50	930718 B3-30					12	2													10			2		20		4		2		
	1.54	OS6-4			4		17	1	8		4			1							6			1		8	16	2			1	
Uppermost 1 cm of soil S	1.58	OS6-8					2																	1		3	2					
	1.68	OS6-18						1													3					1		1				4
	1.80	930718 B4-25																			8											10
	1.89	OS5-1			2		1					4									2			1		64	1			5	1	
	1.95	OS5-7					18						3											5		39	19		1	1		5
Uppermost 1 cm of soil N	1.97	OS5-9					1																			7						1
	2.05	OS5-18					1											6			1					4					1	25
	2.10	OS5-22					1													2						5	2				6	35
	2.15	OS5-27					1			2	2							13			11		3			2		1		1		16
	2.18	OS5-30			1	3												7			7			1			1	1				
	2.45	930718 B7-1					1			1								12			13		8			3				1		10
	2.58	OS4-1					4						4								1		1			25	9		2	2		
	2.65	OS4-8					8														3			2		33	7	1	3	2		
Uppermost 1 cm of soil L	2.67	OS4-10																								7					2	36
	2.75	OS4-18			2	2	1	1	7									4								4						14
	2.90	930718 B8-1					1							1				4			7		1					1				24
	3.00	930718 B8-10			2		1					2						1			16		3							1		5
	3.10	930718 B8-20								2								1			37											25
	3.20	OS2-1				2	36		2	5		1	1					3			26			1		6	22		1	2		1
	3.23	OS2-4			3		6		5	1			1	1							19	1	1		2		3			1		1
	3.27	OS2-8			2	7	12		10	2			2								18		3		1	1	7			2		
	3.31	OS2-12					11		4												7				1	2	5	2	3	1		
	3.35	OS2-16			6		23		4				1								2					6	4	4		6		1
	3.39	OS2-20			3		20	2		2			4				2	2		2	2		1			11	6	3	2	10	2	6
Uppermost 1 cm of soil J	3.41	930718 B9-23					1											10									3		1	1		41
	3.45	OS2-26			1		4						1		2					4				1		1		2				60

Table 4. Numbers of diatoms counted at the Redtail locality—Continued

	Depth below modern surface (m)	*Cosmioneis pusilla var. 1*	*Craticula halophila*	*Cymbella spp.*	*Delphineis cf. karstenii*	*Delphineis cf. margaritalimbata*	*Delphineis cf. surirella*	*Delphineis surirella*	*Denticula subtilis*	*Dimeregramma minor*	*Diploneis didyma*	*Diploneis interrupta*	*Diploneis oblongella*	*Diploneis pseudovalis*	*Diploneis smithii v. rhombica*	*Diplonies stroemi*	*Endictya sp. 1*	*Epithemia spp.*	*Epithemia turgida*	*Eunotia pectinalis*	*Eunotia spp.*	*Fallacia cryptolyra*	*Fallacia forcipata*	*Fallacia pygmaea*	*Fragilaria construens v. venter*	*Fragilaria pinnata*	*Fragilaria spp.*	*Frickea lewisiana*	*Frustulia linkei*	*Frustulia vulgaris*	*Gomphonema parvulum*	*Gomphonema spp.*	*Grammatophora oceanica*	*Gyrosigma acuminatum*	*Gyrosigma balticum*
	0.01							1		1		2																			2	1	2		
	0.15			1		8			2										1	1		3				1		2				2	4		
	0.35	1		4		4		15		1		21					33		3							2	2						1		
	0.55	2						5			2	125					8		3														1		
	0.66			3	3	1		10		2		3					13	1	18										1				2	1	5
	0.70			2	9		1	7	1	14		1					9		3			1													1
	0.74				9			5		3		1					11		4			8													3
Uppermost 1 cm of soil Y	0.76																																		
	0.90	2		4		1		3	1								5									1									
	0.99			3								3																					1		
	1.09			7								28					4		7							1							1		
	1.14				6		6			9									4														2		
Uppermost 1 cm of soil U	1.17	1						2									3	1															1		
	1.22			3							2	3					2		3														1		
	1.40			2	4		4					2				2				2		8		4										2	14
	1.50				12		12		2	2		2					2		6			12												2	2
	1.54					10	18			1		1							1		1	10			4	2					1			5	2
Uppermost 1 cm of soil S	1.58					2	3			2												1				2									
	1.68					1						1		1			6					1		1			1						2		
	1.80	12		2	4							60																				2			
	1.89				3	1	2										4					2	4											3	5
	1.95				2	7	5															13			11								1		
Uppermost 1 cm of soil N	1.97						9												1			1													
	2.05	5			4	2								2	1		1		2					2						5				2	
	2.10			1			5			2								1								20									
	2.15		2	2	5		2					3												1						1				5	1
	2.18				2	3	1										2								1	4								1	1
	2.45				6	1	3					8				1			2																7
	2.58				9	8				4		2		2					3			2			1									8	5
	2.65			2	60	3	6			12			1									3			3								2		
Uppermost 1 cm of soil L	2.67		2			2	3						1									2													
	2.75						2						10																3	10	2			6	
	2.90	9	1	2			2					5					1		2			2									1			1	
	3.00	6			7	1	4					7							6					1							1			1	1
	3.10	61		2			1					16			1		5		3	1															2
	3.20		8	2			3		4			2					1					4								1				6	88
	3.23		3	1			12										3				1														38
	3.27		3	1	6	1	43					2					1		6			5		1			1							2	37
	3.31				2		30			3							2		1			3									1	1		1	23
	3.35		1		10	4	53					2					1					11	1									1		5	9
	3.39	2	2	1		2	16				1	1					3		3			4													4
Uppermost 1 cm of soil J	3.41				4								1	5	2														2		10				
	3.45	5			2		8				1			14	5		2	1											1	5		2			

Table 4. Numbers of diatoms counted at the Redtail locality—Continued

	Depth below modern surface (m)	*Gyrosigma eximium*	*Gyrosigma wansbeckii*	*Hannaea arcuatum*	*Hantzschia amphioxys*	*Hantzschia virgata*	*Hyalodiscus laevis*	*Hyalodiscus scoticus*	*Luticola mutica*	*Luticola muticoides*	*Lyrella lyra*	*Mastogloia exigua*	*Mastogloia smithii*	*Melosira moniliformis*	*Melosira nummuloides*	*Navicula cancellata*	*Navicula cincta*	*Navicula cryptotenella*	*Navicula digitoradiata*	*Navicula directa*	*Navicula elginensis*	*Navicula gregaria*	*Navicula libonensis*	*Navicula peregrina*	*Navicula peregrina v. kefvingensis*	*Navicula phyllepta*	*Navicula rhyncocephala*	*Navicula salinarum*	*Navicula spp.*	*Navicula tenelloides*	*Nitzschia bilobata*	*Nitzschia brevissima*	*Nitzschia cf. nana*	*Nitzschia commutata*	*Nitzschia fasciculata*
	0.01				1			3	18					8	8		197																2		
	0.15							8	17		2			33	15		3		4																
	0.35						1										3	2															2		
	0.55				1		3		2			1		1			1						1										2		
	0.66	7				2	1				2		2	1																					
	0.70				2		1							2															1						1
	0.74							1						1		1			2	1									1						
Uppermost 1 cm of soil Y	0.76																						1												
	0.90						8		8								2																1		
	0.99						10		7								4															1	5		
	1.09				1		4																										1		
	1.14						10																												
Uppermost 1 cm of soil U	1.17				1		1		5								5												1				1		
	1.22				4		1		2								6													2			2		
	1.40											4		2			2	2	2										4				2		2
	1.50	2							4			2		4	2														8				2		2
	1.54	5								2		13			5														1		1				
Uppermost 1 cm of soil S	1.58	1								5																									
	1.68								4					4																					
	1.80						2																												
	1.89		3		5									1					1																
	1.95								4						7	1	11	1											4						
Uppermost 1 cm of soil N	1.97									1							2												2						
	2.05	1							10								2				1						4		2					2	1
	2.10								3								35																2		
	2.15	77							3			1					4							4									1		
	2.18	10			1				1	9					2	37		1	5			2							2		14		3		2
	2.45	13					30		1			1				2	1		2			1		1			1								
	2.58	1								2		2			2			3	2								5		2						
	2.65						1			1	2	1			5																				
Uppermost 1 cm of soil L	2.67									22							13		2								5						4		
	2.75									17							14								3		31		10		4		10		1
	2.90	4					1		6								5		1								1				1				2
	3.00	5															3		2										3					4	2
	3.10				1		2		2		2					1	2												1						
	3.20	1	3						5	1		3			2	1	1		2								2	2	8						
	3.23	2					1		3	1		5		1	2			2	4										1						
	3.27											15		4				13											1						
	3.31			1								10		3	4			13	2										2						
	3.35								1			4			1			27	3										1						
	3.39								14			7		5	4		2	10											2				3		
Uppermost 1 cm of soil J	3.41								4	4		1			7		4							1	6				4			1			1
	3.45								43								10		1					8	11	5			2		2		2		2

Table 4. Numbers of diatoms counted at the Redtail locality—Continued

	Depth below modern surface (m)	*Nitzschia lorenziana*	*Nitzschia perminuta*	*Nitzschia scapelliformis*	*Nitzschia sigma*	*Nitzschia socialis*	*Nitzschia spp.*	*Nitzschia terrestris*	*Odontella aurita*	*Odontella longicruris*	*Odontella obtuta*	*Opephora cf. parva*	*Opephora spp.*	*Paralia sulcata*	*Paralia sulcata (small form)*	*Petroneis granulata*	*Petroneis marina*	*Pinnularia borealis*	*Pinnularia lagerstedtii*	*Pinnularia spp.*	*Pinnularia viridis*	*Plagiogramma staurophorum*	*Pleurosigma salinarum*	*Rhabdonema arcuatum*	*Rhaphoneis amphiceros*	*Rhaphoneis psammicola*	*Rhoicosphenia abbreviata*	*Rhopalodia acuminata*	*Rhopalodia gibba*	*Rhopalodia musculus*	*Rhopalodia operculata*	*Scoliopleura tumida*	*Stauroneis spp.*
	0.01			3			11	4	1					26	66				15						1	1	1	3					
	0.15			1			2		1					30	122	1			10	16						4	2	6		1		5	
	0.35	1		3	1		3							216	551	1	2			1					4	24		6		6		4	
	0.55	20		2	15		5		5					59	155				9							6		1		5			
	0.66	3			10		1		1	2	5		2	161	186	2	1			1		5		6	5	4	1	1	2			10	
	0.70				6		1		13					185	71	1						5		2	3	1		1				15	
	0.74				6		14		2			1		149	146	5	2			1	1			1	4	7	1					5	
Uppermost 1 cm of soil Y	0.76														5				1														
	0.90							13						30	23				42							1							
	0.99													38	88				17						1								
	1.09	1		3					1					75	77	4										1		2					
	1.14													26	96																	18	
Uppermost 1 cm of soil U	1.17							9						56	147	2			102	1													
	1.22							4						66	198				41	4													
	1.40				4	1	2							30	106						2				2		2					14	
	1.50			2	10		2		2		4			60	110									4	2		8					4	
	1.54		1	1	3				2					16	83			1													3		
Uppermost 1 cm of soil S	1.58			0.5										5	9																		
	1.68													53	299				3						1								
	1.80													18	150	2			2					2								3	
	1.89				6.5	8			2	1				114	197	1	2								2							7	
	1.95		1		3		8	1	1			5		54	78				4	3					4	1		5				2	
Uppermost 1 cm of soil N	1.97			1										79	91				5	2													
	2.05				1.5		1		1			1		11	60				30								2			1		1	
	2.10				0.5		8	2	1	2	1			93	222	1		1	16	11							3			3			
	2.15		2	1	12		5							19	56		2		4						1					8		2	
	2.18		2		14		3					2		26	98		13	1	11						1					1			
	2.45				23		5					24		23	49				2						1							4	
	2.58				4	13	17						2	115	109													3				6	2
	2.65				4	2	13		5					70	102										1	3		1					
Uppermost 1 cm of soil L	2.67		2		1.5		6	7.5	1					11	96				56	19							2						
	2.75		5				51	16						2	18				36	4													
	2.90				8.5		2		1					16	137				4	2					3		2					4	
	3.00				13.5				1					8	58				1					1	2							15	
	3.10				6									24	77		1						1									3	
	3.20				5		6					15		37	31								10					1		3		39	1
	3.23				26.5		5					4		62	37				1									2				88	4
	3.27				4	1								32	5									2	1			1				43	1
	3.31				10	1						2	6	61	50	1								12	2					1		20	
	3.35				4	1	1					2	3	41	39	1									1		2	1				10	
	3.39				11	1	7	1	3			2	4	123	122				4					1	1							3	
Uppermost 1 cm of soil J	3.41		5		4									20	38				33									1					
	3.45		1		8		11							58	75				52					1								1	

Table 4. Numbers of diatoms counted at the Redtail locality—Continued

	Depth below modern surface (m)	*Surirella spp.*	*Synedra fasciculata*	*Synedra spp.*	*Tabellaria fenestrata*	*Terpsinoe americana*	*Trachyneis aspera*	*Trachysphenia australis*	*Tryblionella acuminata*	*Tryblionella aerophila*	*Tryblionella apiculata*	*Tryblionella coarctata*	*Tryblionella debilis*	*Tryblionella granulata*	*Tryblionella levidensis*	*Tryblionella littoralis*	*Tryblionella navicularis*	*Tryblionella plana*	*Tryblionella punctata*	*Tryblionella vexans*		**Planktonic diatoms**	*Actinocyclus curvatulus*	*Actinocyclus kutzingii*	*Actinocyclus spp.*	*Actinoptychus senarius*	*Actinoptychus spp.*	*Actinoptychus vulgaris*	*Aulacoseira spp.*	*Chaetoceros spp.*	*Coscinodiscus spp.*	*Cyclotella spp.*	*Rhizosolenia hiemalis*	*Stephanodiscus spp.*	*Stephanopyxis spp.*
	0.01		1									1	38						1					2	3			1	2	1	2			1	
	0.15		12							17	2		10	4	1		2									2			3	9	1	1			
	0.35		2				1							18									1	11	1	9	2		11		7	8		1	
	0.55			1			29							33										2			1		6		14	2			
	0.66		13			2	2					2	2	10						1			3	9	2	7	1	2	22		18	6		1	
	0.70	1	8			2		1	1					8		1		5		1			5	4		10	2		3		5	2	1	1	
	0.74		6				3																3	3		5	1		8		5	3			
Uppermost 1 cm of soil Y	0.76						1																						6						
	0.90										2													2		4	1		37		1			1	
	0.99			1										9										1	7	2	2		77		8	3		4	
	1.09				2									2	1								1	1			7		40		2	3		2	
	1.14		2		20		16							40													4								4
Uppermost 1 cm of soil U	1.17													9										1					26			1			
	1.22													6											1				56		1	2			
	1.40	2	1				20				4			26									2	4					10	2					
	1.50	2					12				2			10	2				4					4		6	2		10	6	2	2			
	1.54		2.5								3	1	2						2	1						1			1	2	1				
Uppermost 1 cm of soil S	1.58													2																					
	1.68	1				1	1						2	8										2		7	1		9		1	3			
	1.80		1										2	14										1					18			2			
	1.89		4											24												7			8		1			1	
	1.95	2	6.5							5			4	5															2		1	2			
Uppermost 1 cm of soil N	1.97									1				3															1						
	2.05		3										5	2		1													2						1
	2.10		3.5											8										1		1			10		1	1			
	2.15		1								2		12	8	3		2	1		3			1	1							2				
	2.18		7							2			8	2										1					2						
	2.45	2	2				2				1	1	7	10	1		2	2	1				1	2		1			2						
	2.58		4.5								2				4			10								2			11		1				
	2.65		7	1		4		1			2																		6	2					
Uppermost 1 cm of soil L	2.67		3					1		1			10																						
	2.75		1	5						1			18						1																
	2.90		2.5										2	17						1				1	1	1			5						
	3.00		1				1				4	1	1	5						1				2		2									1
	3.10		3										2	2				1	1				1	4		3		1	2			2			
	3.20	1	3								4		1	2	3				2	1			1		2						1				
	3.23		4.5				2				1			3	2	2			1	2				5	1	14			7		2				
	3.27	4	8				5							4	1								1		7	39				2	3	4		1	
	3.31	1	20								2			27	1			4	1					3	1	19	1				8	1			
	3.35		13								1	1		12	1			1					4		1	8			4	1	10	1			
	3.39	2	10								1	2	1	14						2					3	15			5	2	5	3			
Uppermost 1 cm of soil J	3.41		2.5								2		2	3				2																	
	3.45	1	1						1				15	12	3											1			8						

Table 4. Numbers of diatoms counted at the Redtail locality—Continued

	Depth below modern surface (m)	*Thalassionema nitzschioides*	*Thalassiosira eccentrica*	*Thalassiosira pacifica*	*Thalassiosira spp.*	**Unidentified diatoms**		**Preservation**	**Total diatom valves counted**	**Total high marsh diatoms(1)**	**Total low/high marsh diatoms (1)**	**Total low marsh diatoms (1)**	**Total tidal flat diatoms (1)**	**Total diatoms used for index (BIDI)**	**BIDI value**	
	0.01		1		1			G	462	29	255	6	27	317	0.91	
	0.15	5	5		10			G	464	39	30	13	112	194	0.39	
	0.35		1	2	4			P	1034	1	3	50	46	100	0.29	
	0.55	1		5	11			P	571	13	3	156	57	229	0.41	
	0.66	5		3	13			M	655	4	2	28	67	101	0.20	
	0.70	3	1		5			M	464	1	1	25	75	102	0.14	
	0.74	2		1	1			G	487			7	94	101	0.03	
Uppermost 1 cm of soil Y	0.76							VP	14	1			1	#	#	
	0.90	1						P	242	101	10	2	6	119	0.94	
	0.99	1						M	364	77	11	4	8	100	0.90	
	1.09							P	307			48	18	66	0.36	
	1.14				6	4		P	309			20	57	77	0.13	
Uppermost 1 cm of soil U	1.17							M	438	173	10		2.5	185.5	0.99	
	1.22							M	450	88	8	3	1	100	0.98	
	1.40				10			M	416		10	68	108	186	0.24	
	1.50	3	2	2	8			M-G	419	2	6	22	94	124	0.15	
	1.54	8.5	1		5	7		G	300		2	27	82.5	111.5	0.14	
Uppermost 1 cm of soil S	1.58	0.5		1	1			VP	43			1.5	11	#	#	
	1.68		2					P	426	7	7	4	8	#	#	
	1.80	1		2	2			P-M	320	24	2	71	3	100	0.62	
	1.89	12			3	2		M	518			9	115.5	124.5	0.04	
	1.95	4.5			3	4		M	367	15	19	3	124.5	161.5	0.22	
Uppermost 1 cm of soil N	1.97							P	208	7	2	1	9	#	#	
	2.05							G	211	60	33	5	12.5	110.5	0.86	
	2.10					7		M	517	53	38	3	16	110	0.84	
	2.15	2		4	1	4		M-G	323	20	33	105	33	191	0.55	
	2.18	2.5			4	5		M-G	331	13	18	33	86	150	0.32	
	2.45				4	1		M-G	303	12	21	41	81	155	0.35	
	2.58	4			10	2		G	433		2	15	103.5	120.5	0.08	
	2.65	30	4		14	2		G	435			4	99	103	0.02	
Uppermost 1 cm of soil L	2.67	1.5			1	1		M	322	100.5	23		17.5	141	0.88	
	2.75	5	1		4	14		G	340	67	47	7	9	130	0.90	
	2.90	2			3	1		M	302	37	19	21	23	100	0.67	
	3.00	1			1			M	206	12	11	43	35.5	101.5	0.44	
	3.10			1				P-M	303	86	7	57	17	167	0.73	
	3.20	3		1	1	8		M	441	5	11	74	205	295	0.18	
	3.23	3		2	22	3		M	431	2	3	116	105	226	0.28	
	3.27	5	4	3	5	10		M	405			91	95	186	0.24	
	3.31	6	3	4	19	4		M	428			51	104	155	0.16	
	3.35	14		6	17	12		M	405	1	1	45	99	146	0.17	
	3.39	11	4	5	23	7		M	564	14	19	23	101	157	0.28	
Uppermost 1 cm of soil J	3.41			2	2			M	381	88	29	5	25	147	0.81	
	3.45	1			6	7		M	471	118	89	9	21	237	0.89	

(1) Individual taxa listed in Table 2

KEY:	
G	Good preservation
M	Moderate preservation
P	Poor preservation
VP	Very poor preservation
#	Upland deposit inferred from rare reworked diatoms

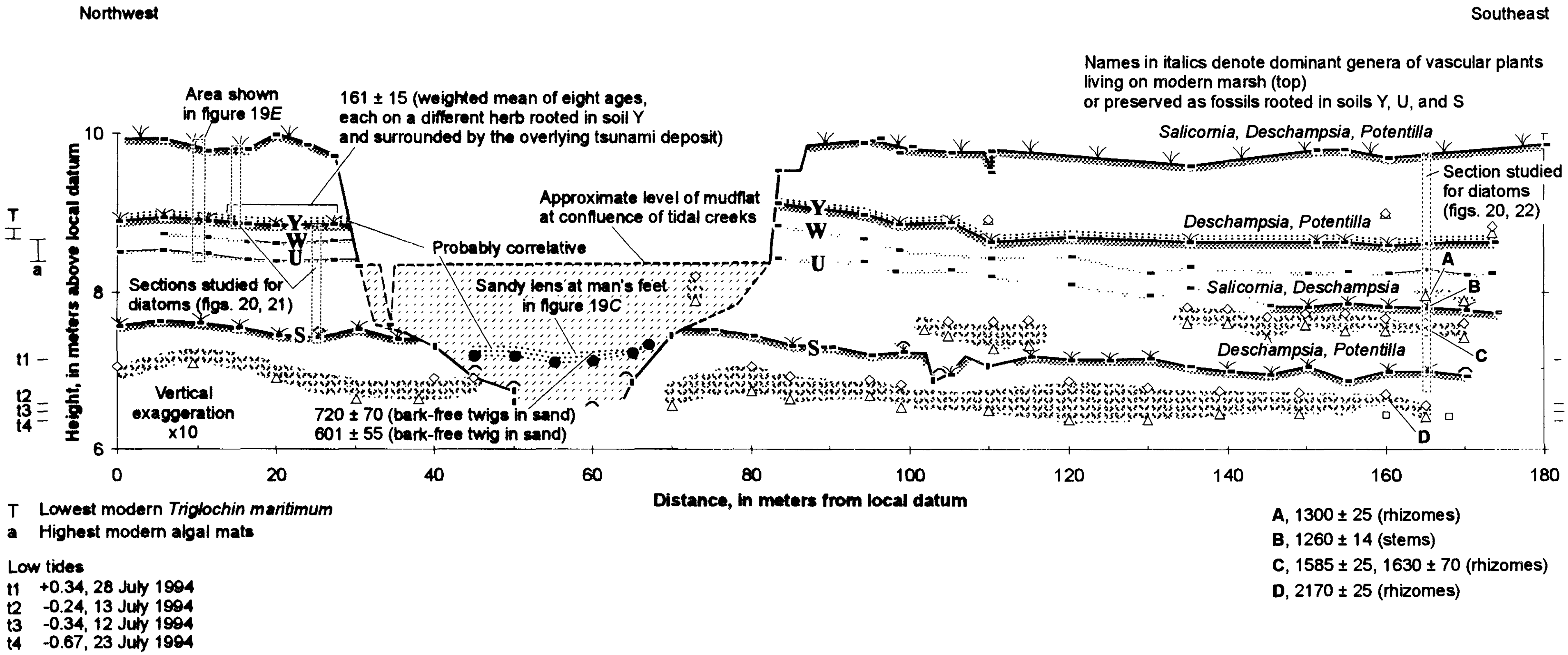

Figure 18. Stratigraphy at Oyster locality, Niawiakum River.

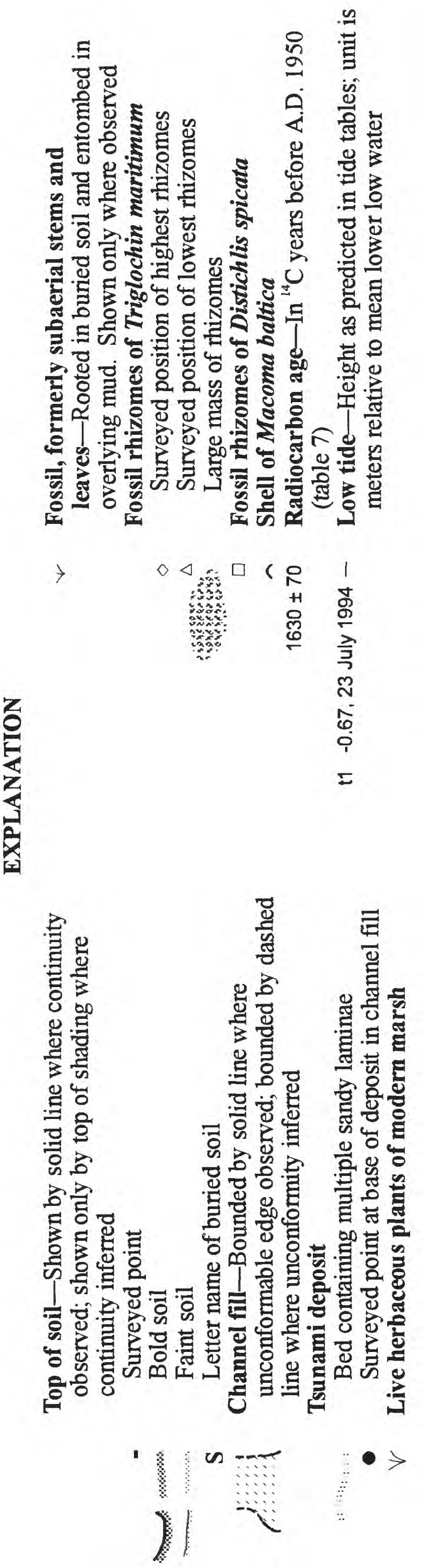

Figure 18. Continued.

All the soils at the Oyster locality dip gently southeastward (figs. 18, 19*B*), diagonally away from the nearest upland. The oldest soils dip most steeply; soils S and U are nearly 1 m lower on the southeast than on the northwest. As at the Redtail locality (p. 26), most of this relief is probably due to compaction of soft Holocene mud, which may thicken southeastward beneath the Oyster locality, the direction toward the middle of the Niawiakum River valley (fig. 7). Such thickening of soft mud has been observed in foundation borings along nearby U.S. 101 (Washington State Department of Transportation, Olympia, unpub. data, 1986). In these borings, the mud is thickest—about 30 m—about midway across the valley. Slumping along the Niawiakum River may have also contributed to relief on the buried soils at the Oyster locality. Such slumping is indicated by nearly vertical faults having less than ¼ m offset and exposed on the modern bench between soils S and W in the southeastern half of the outcrop.

Soil U varies greatly in abundance of peat at the Oyster locality. At the northwest end of the outcrop the surficial horizon of soil U is barely recognizable as a band of mud about 1 cm thick that is slightly darker (by one unit of value in the Munsell color system) than the mud above and below it (fig. 19*E*). To the southeast, however, the surficial horizon of soil U grades laterally through peaty mud into muddy peat 5 cm thick. This southeastward gradation is accompanied by the appearance of vascular-plant fossils—rhizomes below and above the soil, stems and leaves of herbaceous plants rooted within the soil—that are absent to the northwest (fig. 18). The southeastward gradation is further accompanied by softening of the mud above and below soil U. It is not accompanied, however, by any major change in diatom assemblage (fig. 20), with one main exception—the sturdy valves of *Paralia sulcata* are much more abundant, and the preservation of more delicate valves noticeably poorer, where the soil is faint than where the soil is peaty (p. 23; fig. 23). We infer that the lateral changes in vascular-plant and diatom fossils reflect differential decomposition and dissolution during the time when soil Y was at the land surface. Such diagenesis is more likely to have attacked the northwest end of the outcrop, where soil U is 0.3 m below the top of soil Y, than the southeast end, where soil U is 1.0 m below the top of soil Y.

Soil W is everywhere fainter than the underlying part of soil U. At the northwest end of the outcrop, soil W is not generally visible (fig. 19*E*), probably because of decomposition in the profile of soil Y, the top of which is 0.2 m above soil W (fig. 18). Like soil U, soil W becomes more noticeable to the southeast, where it descends to as much as 0.4 m below the top of soil Y. Nowhere at the Oyster locality, however, is soil W peaty.

TSUNAMI DEPOSIT

A tsunami deposit overlies soil Y at the Oyster locality (fig. 19*E*). The deposit comprises five or six sandy laminae

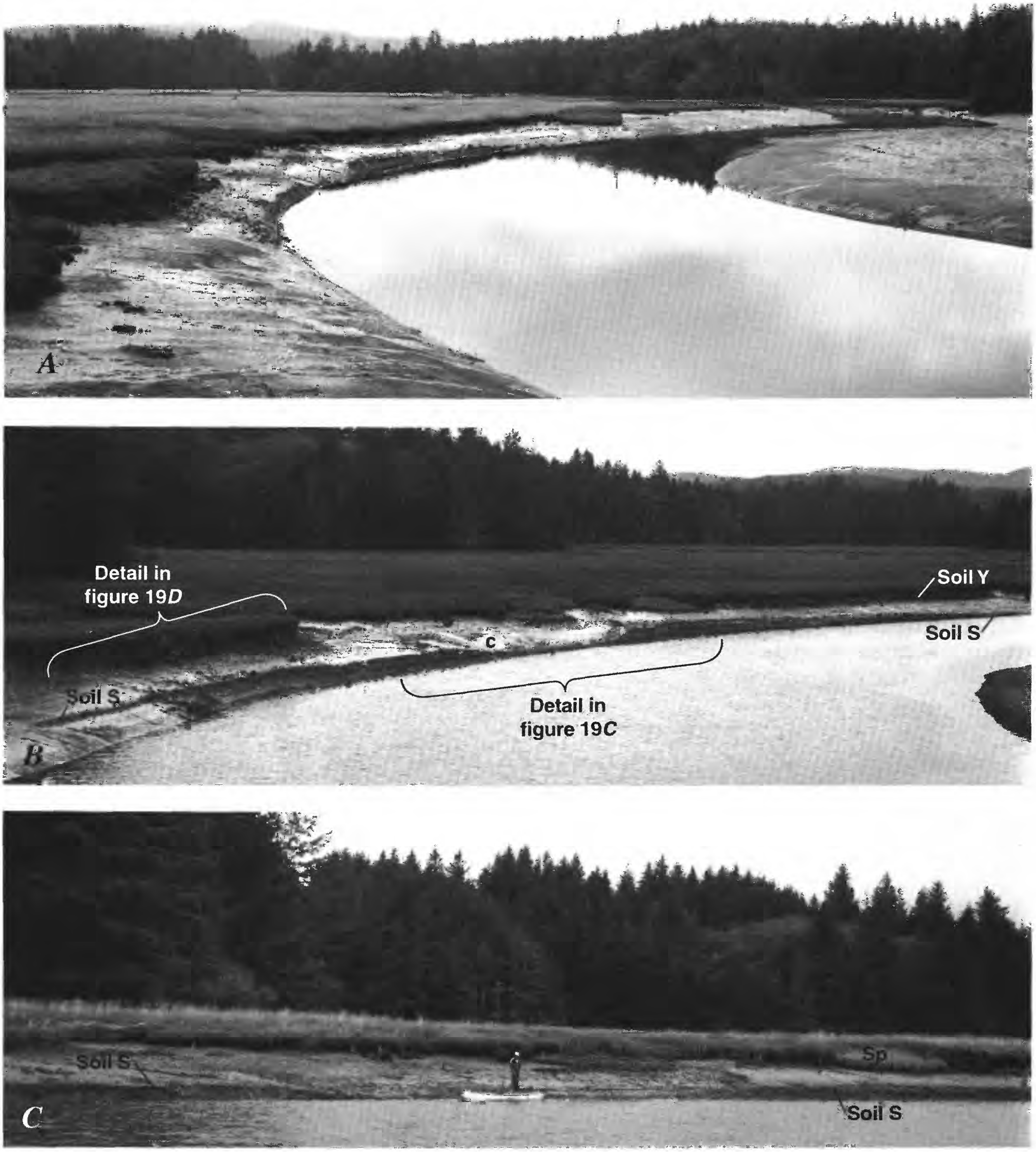

Figure 19. Oyster locality, Niawiakum River (fig. 18). *A*, Overview to the southeast (upvalley), showing tidal marsh at left and tidal flat at right. Trees in background are rooted on upland, above level of highest tides. August 1987. *B*, Closer, eastward view of surveyed outcrop. Buried soil S, which has apparent dip to the southeast, is interrupted by channel fill (c) centered near horizontal coordinate 60 m. May 1995. *C*, Closer view of channel fill shown in *B*. Horizontal layer at man's feet is sandy bed probably correlative with tsunami deposit on soil Y. Difference in lighting makes area of channel fill appear lighter toned than in *B*. Sp, *Spartina foliosa*, an introduced salt-marsh grass, on accretionary bank. Tide higher than shown in *A* and *B*. July 1994.

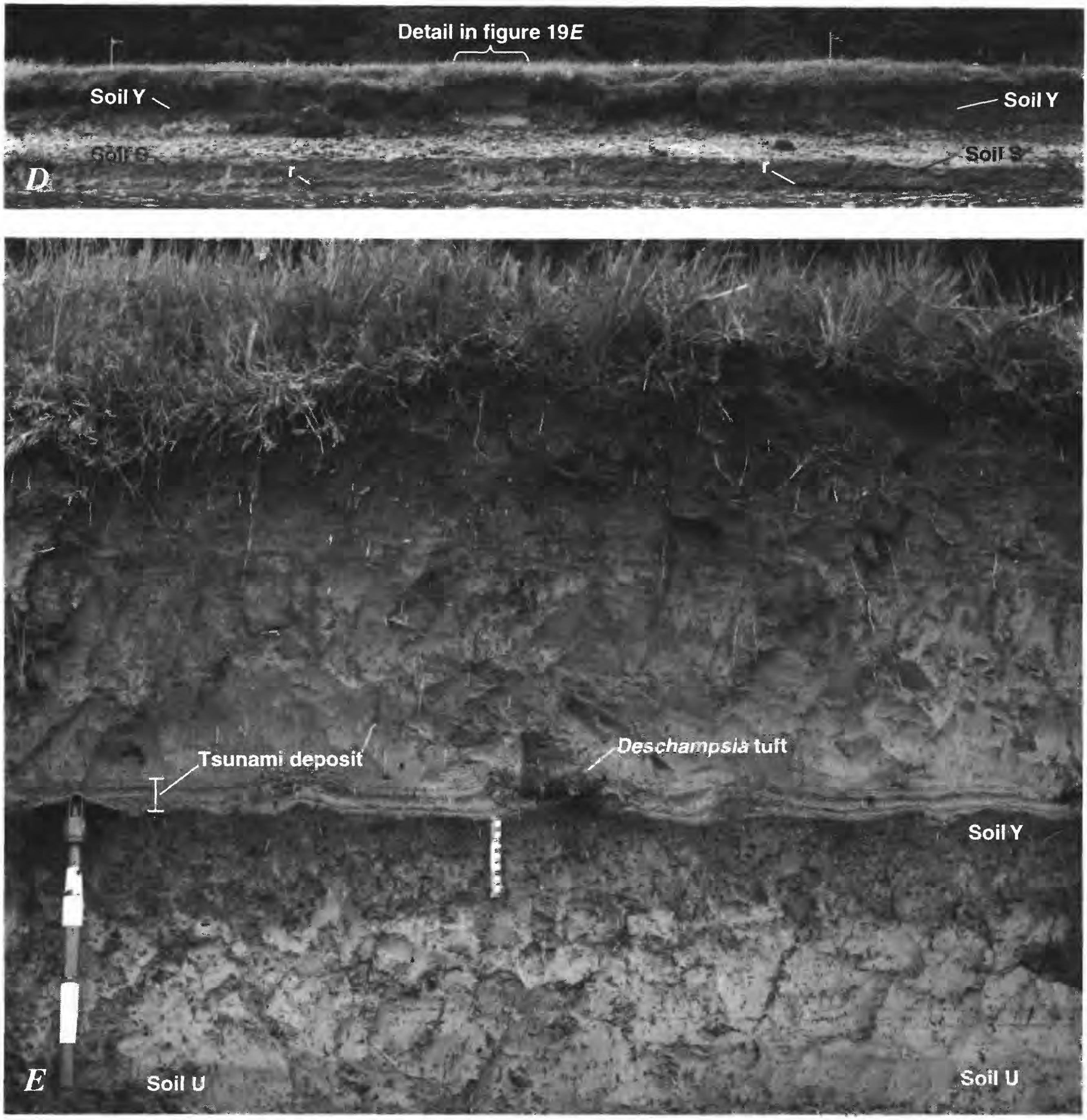

Figure 19. *D*, Buried soils S and Y downstream from channel fill. Rhizomes of *Triglochin maritimum* account for resistant layer (r) just above water line. Stakes on top of bank are 10 m apart; middle stake denotes horizontal coordinate 10 m. View across Niawiakum River; upstream to right. *E*, Tsunami deposit on soil Y at horizontal coordinate 10 m. Deposit contains sandy laminae that appear dark from shadow in recess etched by water. Above 15-cm-long scale at center the upper several laminae turn upward against tuft of *Deschampsia caespitosa*, whose leaves are flopped over to the right, upvalley. Faint soil W, which is noticeable between soils U and Y farther upstream at the Oyster locality, is too faint to show in the photograph. Shovel and centimeter scale are in same position as in *D*.

that alternate with mud (Atwater and Yamaguchi, 1991, their fig. 5). The lowest of these laminae, which is also the least distinct and least continuous, rests directly on the soil. The thickest and coarsest lamina is micaceous, silty, very fine sand 1 cm thick. The two uppermost laminae are a pair of silt partings. The total thickness of the deposit is mainly 5–7 cm.

The deposit accumulated around herbaceous plants rooted in soil Y. At the northwest end of the outcrop the surrounded tufts of *Deschampsia caespitosa* are flopped over to the east (fig. 19*E*)—upvalley (fig. 6)—as are the stems and basal leaves of *Potentilla pacifica.* The measured azimuths of 14 of these flopovers near the northwest end of the outcrop range from 065° to 120° and average 082° (M.A. Reinhart and S. McMullen, written commun., 1987). These orientations imply currents directed eastward, up the Niawiakum River valley (fig. 7).

There are no other sandy beds in the outcrop except in a probably correlative lens within the channel fill that underlies the mudflat at the confluence of tidal creeks (figs. 18, 19*C*). This sandy lens, as much as 15 cm thick, consists of micaceous, silty, very fine to fine sand interbedded with mud. Several of the sand beds in the lens abound in flat-lying plant fragments—mainly bark-free twigs, pieces of bark as much as 1 cm thick, and a few leaf bases of *Triglochin maritimum.* The twigs may have been recycled from an older deposit, as shown by their lack of bark and their radiocarbon age (p. 63).

Reasons for inferring that a tsunami deposited the sand on soil Y at the Oyster locality are listed on page 27.

GROWTH-POSITION FOSSILS OF VASCULAR PLANTS

Vascular-plant fossils and algal layers imply that burial of soils S, U, and Y at the Oyster locality resulted from lasting tidal submergence. Rooted in each soil are stems and leaves of high-marsh plants. By contrast, mud above each soil contains growth-position rhizomes of the predominantly low-marsh species *Triglochin maritimum.* The rhizomes imply a position near the lower growth limit of *Triglochin maritimum* for two reasons:

1. Though well preserved, the lowest *Triglochin maritimum* rhizomes above each of the three soils lack associated fossils of high-marsh plants.
2. These lowest rhizomes are underlain, above each of the three soils, by mud containing rhythmic organic laminae similar to those produced by filamentous algae on mudflats below the lowest *Triglochin martima* at the Oyster locality. Such laminae, which are among the geologic recorders of fully intertidal conditions at Willapa Bay (Clifton, 1983, p. 362), form today about 1.0–1.5 m below the level of high marsh at the Oyster locality (figs. 8, 18, “algal mat”).

Herbaceous plants rooted in soils S and Y probably lived higher in the intertidal zone than did the plants rooted in soil U. All three soils bear tufts of the high-marsh grass *Deschampsia caespitosa,* as shown in photographs of soils S (Atwater and Yamaguchi, 1991, their fig. 4*B*) and Y (our fig. 19*E*). But only soil U bears stems of the pickleweed *Salicornia virginica,* which tolerates higher soil salinity than do other vascular plants of tidal marshes in the western United States (Mall, 1969; Barbour and Davis, 1970). Conversely, the less saline high-marsh species *Juncus balticus* and *Potentilla pacifica* are commonly rooted in soils S and Y but appear absent from soil U. Soil U probably was inundated by salty tidewater about as frequently as the modern high marsh at the Oyster locality, on which *Salicornia* is common within 50 m of the Niawiakum River. The lack of *Salicornia* on soils S and Y implies less frequent inundation by salty tidewater. This interpretation is supported by differences in diatom assemblages (see next section).

Soil W represents a marsh above the lower growth limit of *Triglochin maritimum.* We found no growth-position remains of vascular plants that might have been rooted on soil W or which might have colonized the overlying mud. However, rhizomes of *Triglochin maritimum* are present 35 cm below the top of soil W near the southeastern end of the Oyster locality (fig. 18). These rhizomes probably formed near the lower limit of *Triglochin maritimum.* As just noted, they are underlain by algal laminae commonly found near that limit; moreover, mud among the rhizomes contains diatom assemblages indicative of the transition from tidal flat to low marsh (fig. 20, section at horizontal coordinate 165 m). After *Triglochin maritimum* became established, the marsh probably aggraded to a position higher in the intertidal zone, as shown by an overall shoaling trend in diatom assemblages between soils U and W (fig. 20).

FOSSIL DIATOMS

Diatom assemblages show that the four soils exposed at the Oyster locality represent tidal marshes, and that mud above each of these soils was deposited lower in the intertidal zone or perhaps in subtidal water (figs. 20–22). The diatoms further suggest that soils S and Y represent positions higher in the intertidal zone than do soils U and W, and that soil W represents the lowest position of any of the four soils.

Diatoms in soils S and Y are dominated by high-marsh species. However, they also contain large numbers of heavily silicified and easily reworked tidal flat diatoms (tables 5, 6). These probably allochthonous valves make the brackish intertidal diatom index lower than would be predicted for soils S and Y on the basis of vascular-plant fossils.

Diatoms in soil U imply a slightly lower-level high marsh than do diatoms for soils S and Y because, unlike soils S and Y, soil U contains a well-preserved assemblage of low-marsh species that require regular tidal inundation, particularly *Gyrosigma eximium.* Such an assemblage can be found today in stands of *Salicornia virginica* near mean higher high water on the riverward part of the modern marsh at the Oyster locality (Hemphill-Haley, 1995a). The fossil diatom assemblage thereby accords with the vascular-plant assemblage rooted in soil U; the vascular plants rooted in soil U are dominated by *Salicornia virginica.*

Soil W contains low-marsh assemblages of diatoms (fig. 20). The most important of its low-marsh taxa is *Diploneis interrupta.* Although uncommon in modern samples from Willapa Bay, *D. interrupta* is a dominant constituent of *Salicornia* and *Distichlis* low marshes in the Puget Sound

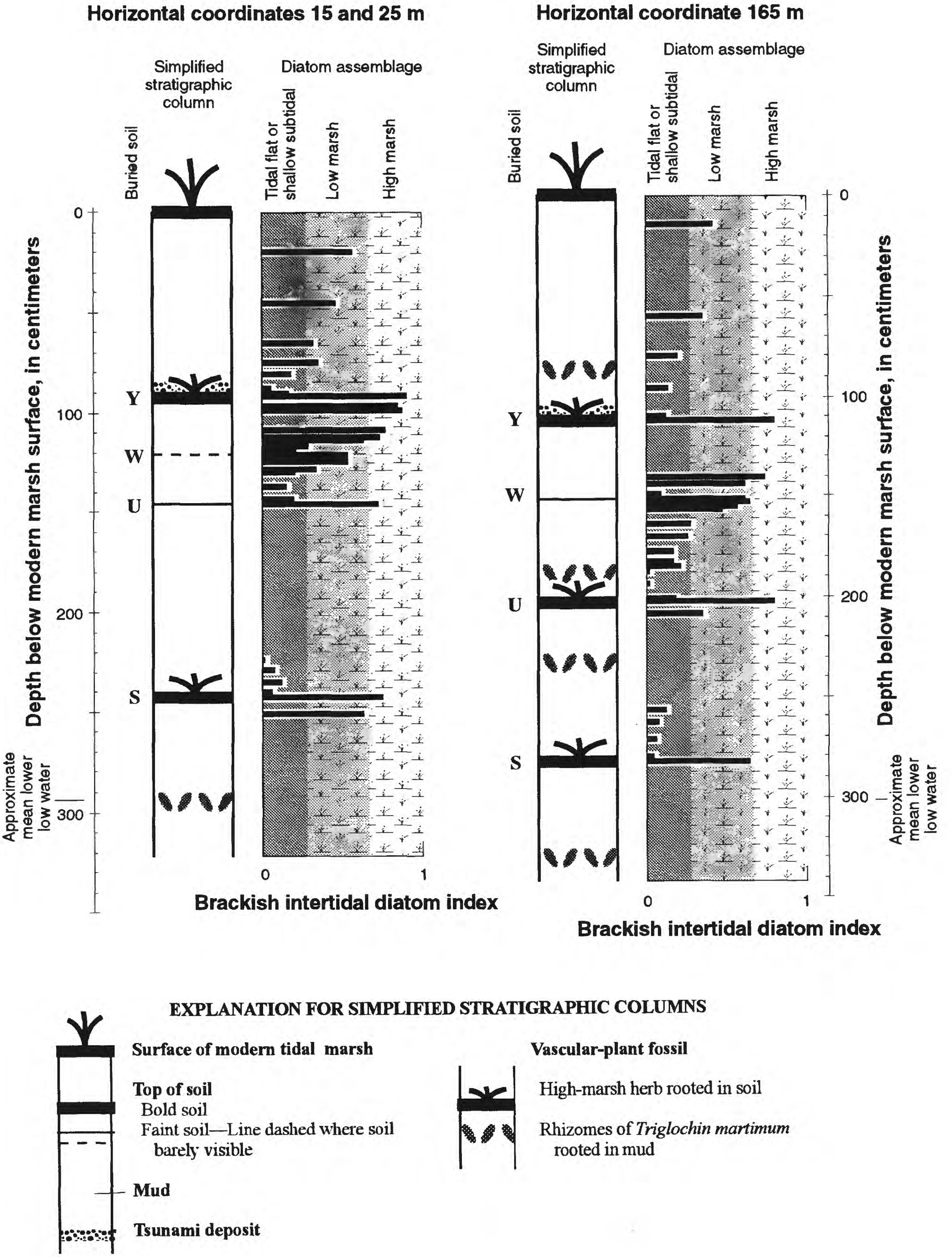

Figure 20. Summary of diatom assemblages at Oyster locality, Niawiakum River. Samples collected from sections at horizontal coordinates 20 m and 165 m (fig. 18).

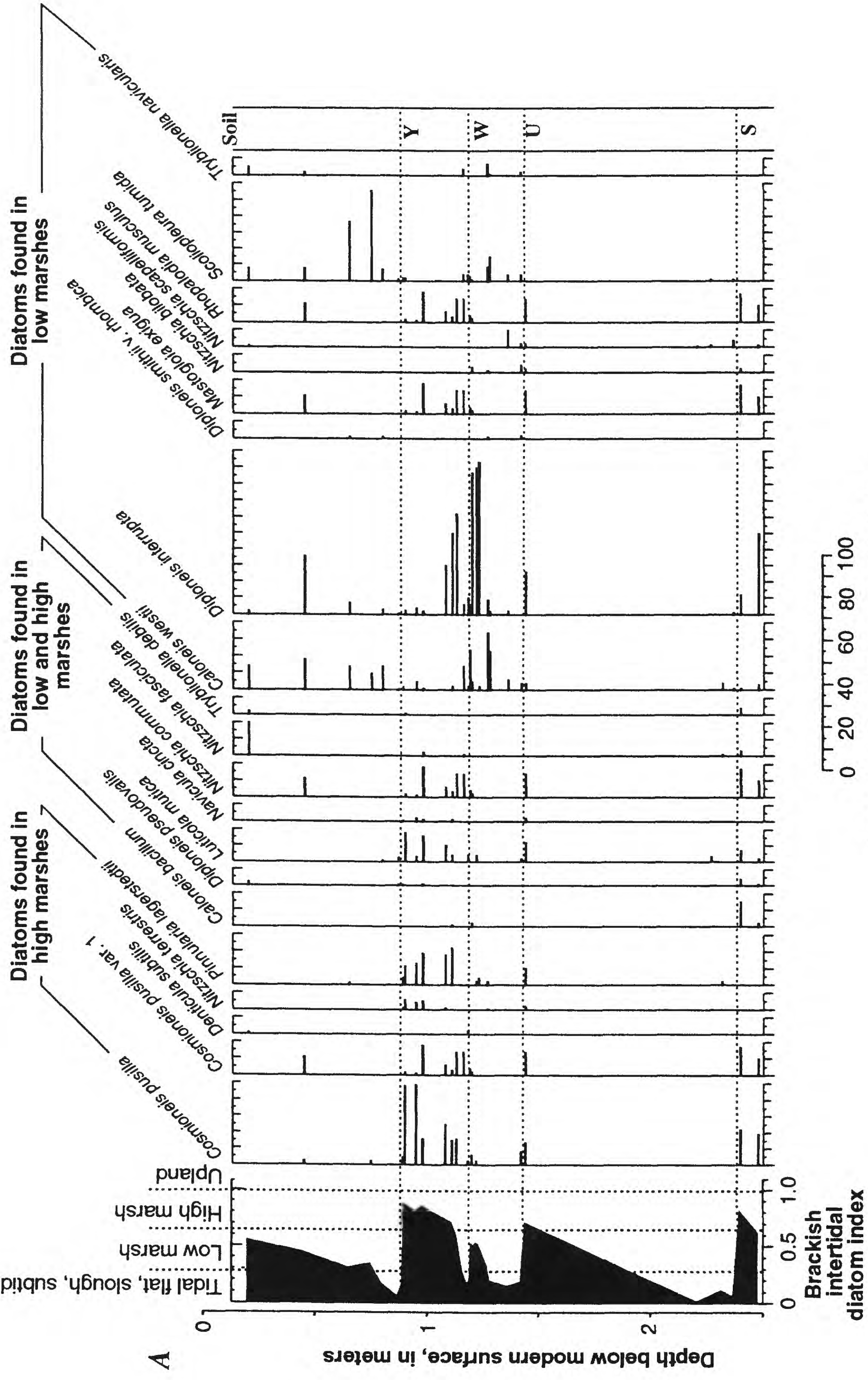

Figure 21. Relative abundances of diatom species grouped by inferred depositional environment for a stratigraphic section at horizontal coordinates 15 and 25 m, Oyster locality, Niawiakum River.

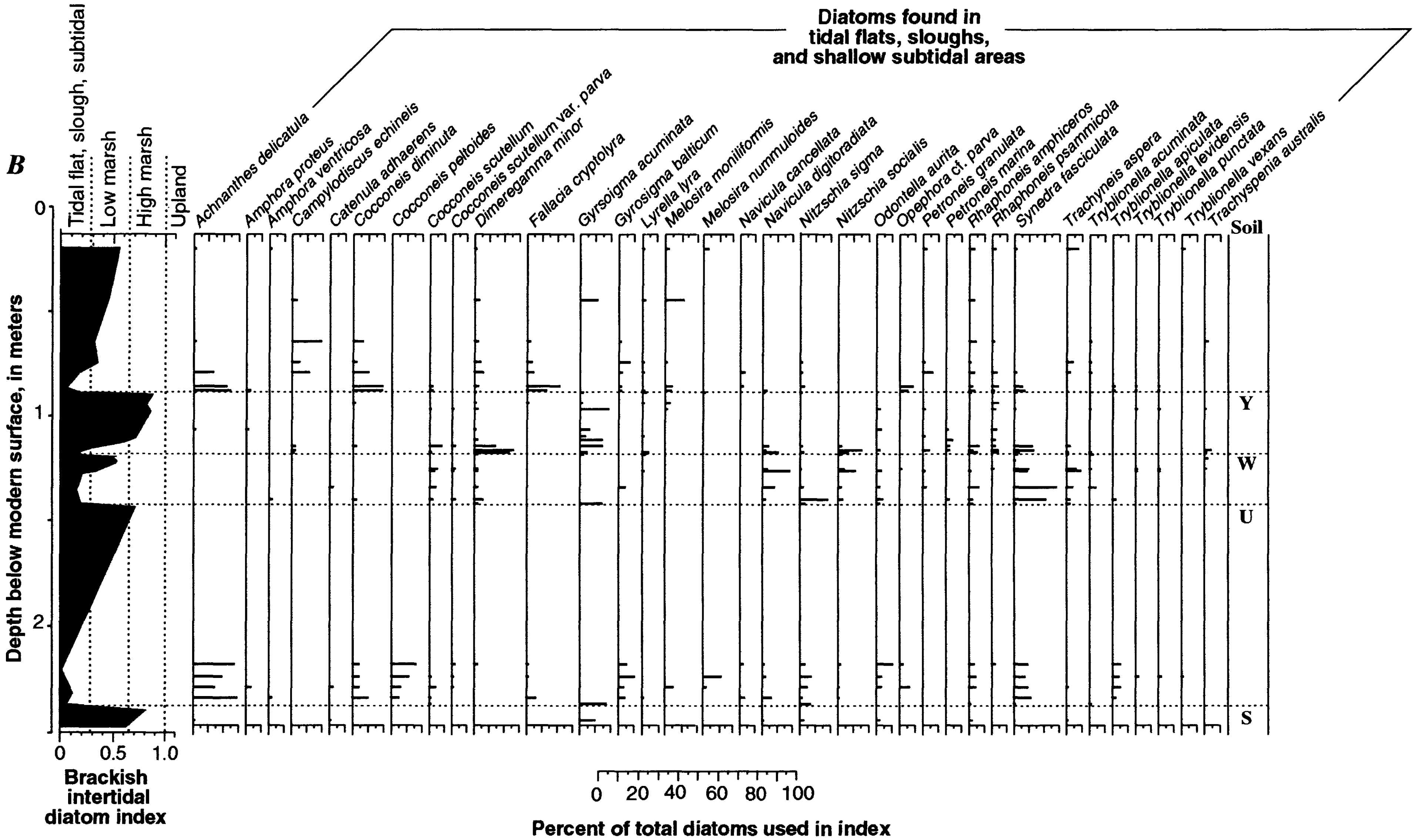

Figure 21. Continued.

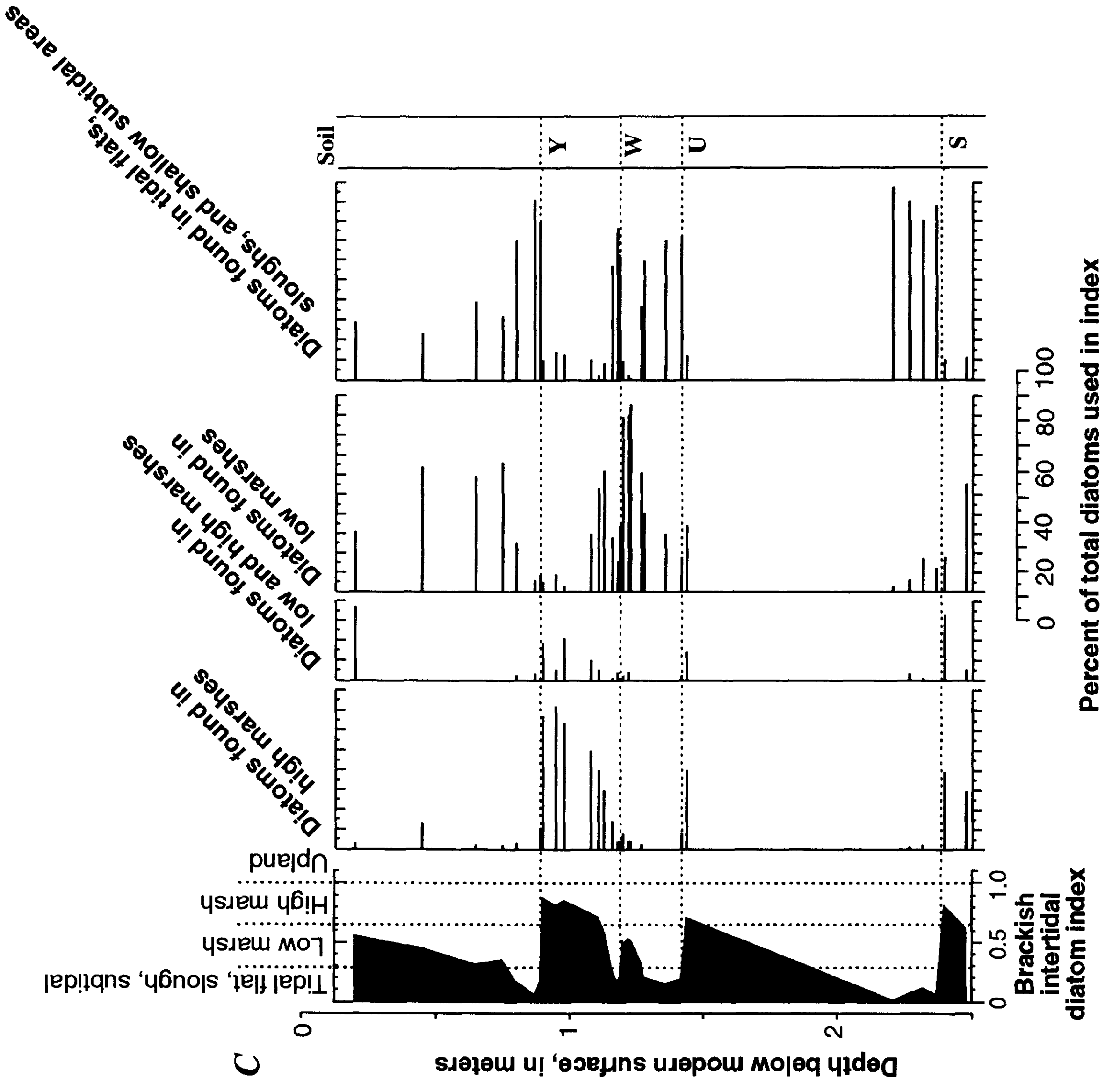

Figure 21. Continued.

region at Lynch Cove (E. Hemphill-Haley, unpub. data; location shown in fig. 1).

The tsunami deposit overlying soil Y at the Oyster locality (p. 45) contains many well-preserved diatoms typical of sandy tidal flats in Willapa Bay (sample depth 0.89 m in table 5, 1.09 m in table 6). Chief among these species are *Achnanthes delicatula* and *Cocconeis diminuta*.

Changes in diatom assemblages across the top of soil W probably did not result primarily from a tsunami. The assemblage changes from low marsh (soil W) to tidal flat (the overlying mud). Although the assemblage reverts to tidal marsh barely 10 cm above soil W (fig. 20), the mud on soil W contains few diatoms that might have been derived from sandy tidal flats of the open bay.

AGE AND CORRELATION

A radiocarbon age shows that tidal-marsh deposits exposed near the southeastern end of the Oyster locality began to form between about 2,050 and 2,350 years ago. The age was measured on *Triglochin maritimum* rhizomes collected about 50 cm below the top of soil S (age D in fig. 18). It serves as a limiting minimum age for any soil earlier than soil S, for the interval between the dated sample and the top of soil S contains no such soil yet retains many vascular-plant fossils. These fossils suggest that the interval would retain a buried soil had one ever been present.

Additional radiocarbon ages have been measured on vascular-plant fossils associated with the burial of soils S, U, and Y at the Oyster locality (table 7; figs. 18, 32).

Burial of soil S at the Oyster locality began shortly before 1,400–1,600 years ago. This estimate corresponds to the more precise of two concordant radiocarbon ages on rhizomes 45–55 cm above the soil. We assume that less than a century elapsed between the onset of burial of the soil and the inception of low marsh marked by the dated rhizomes. This assumption is supported by documentary evidence for rapid postearthquake reconstruction of tidal marshes at

Table 5. Numbers of diatoms counted at the Oyster locality, horizontal coordinates 15 and 25 m

	Depth below modern surface (m)	Diatom sample ID	**Benthic diatoms**	*Achnanthes brevipes*	*Achnanthes delicatula*	*Achnanthes spp.*	*Actinoptychus senarius*	*Actinoptychus spp.*	*Amphora coffaeiformis*	*Amphora proteus*	*Amphora spp.*	*Amphora ventricosa*	*Bacillaria paradoxa*	*Biddulphia sp.*	*Caloneis bacillum*	*Caloneis westii*	*Campylodiscus echineis*	*Catenula adhaerens*	*Cerataulus turgidus*	*Cocconeis diminuta*	*Cocconeis peltoides*	*Cocconeis placentula*	*Cocconeis scutellum*	*Cocconeis scutellum v. parva*	*Coscinodiscus spp.*	*Cosmioneis pusilla*	*Cosmioneis pusilla var. 1*	*Craticula halophila*	*Cymbella aspera*	*Cymbella silesiaca*	*Delphineis cf. karstenii*	*Delphineis cf. surirella*	*Delphineis margaritalimbata*	*Denticula subtilis*	*Dimeregramma minor*	*Diploneis didyma*	*Diploneis finnica*	*Diploneis interrupta*	*Diploneis oblongella*	*Diploneis pseudovalis*	*Diploneis smithii v. rhombica*	*Endictya sp. 1*	*Epithemia turgida*	*Eunotia spp.*	*Fallacia cryptolyra*	*Fallacia pygmaea*	*Fragilaria pinnata*	*Fragilaria spp.*
	0.20	N2-1			1		14					1				14									3					2	2	18		1	1	2		2	12	2		7	7					
	0.45	N2-10					9	2			2					18	3								17	2	11		1						3			36					7					
	0.65	N2-30		2	1		9	7			1					14	19		19	6		2			1				5		11	1			2	1		7			1	16	19		2			
	0.75	N2-40					3				4					10	5		5	2		1			8	2			1			9			4							15	5		3		2	
	0.80	N2-45			13		8	2			4			1		14	11		10	10		2			12				2			11			6	3		3			1	12	10		4			
	0.87	N2-52		1	37	4			2		6			3		1			1	32		1	3								4	7	1		4			1		1		2	1		36			
	0.89	N2-54			40	3	4		2	4	10					3				31		3	3		2	7		2			2	15								1		7	5		21		1	
Uppermost 1 cm of soil Y	0.90	N2-55			1	1	1															2				60	2				7	2			1			3				3						
	0.95	N2-60					2									5				1		2			2	49	1		2		24	1			1	3		4				9	1		1		1	
	0.98	930712 B2-1					1.5						0.5			1						1	0.5	1	2	16	18				2	2.5	1		2	5		2		1		12	1			1		1
	1.08	930712 B2-10			1		2			1												2			1	25	6			1	2	6			1		1	30				2	2			2		
	1.11	930712 B3-1					1								1	2										15	3				1							50										
	1.13	930712 B2-15																				2				16	14		2		2	2	2		2			62				2	4				2	
	1.16	930712 B2-18		6			8									14	2			2		2	8	2	18		14		4		30	6			14			6				8	8				2	
	1.18	930712 B3-8		4												2	2								2	2								2	26			10				2	2	2				
	1.19	930712 B2-21		10			3	2								24	1					3	1		1		4		1						23			6				2					2	
Uppermost 1 cm of soil W	1.20	930712 B2-22														2										6	2								2			87				2						
	1.20	930712 B3-10		2											2	5						1			1	1	2				2							76									1	
	1.22	930712 B3-12																				2			2	2												90										
	1.23	930712 B2-25						1						1		2																						93										
	1.27	930712 B3-18					1							1		34							5	2	4						31	2			2			9			1	4	2				1	
	1.28	930712 B2-29		1			8									23							3	1							4				2			2				6	1					
	1.36	930712 B3-26														6		2				2	4		2						14	2			2			2				2					2	
	1.42	930712 B3-32					2					2				4				2			2	2	2	8					26	12			6						2	8	2					
Uppermost 1 cm of soil U	1.44	930712 B3-34					2									4						4				14	14					2			2			26										
	2.21	930712 B1-1			27	5														4	16	5		2							3	3	1		2							2			1			
	2.27	930712 B1-7			19	15														4	11	2	1	1	2								2												1			
	2.32	930712 B1-12			14					3						4		2	1	4	6		4	1							3	5										4	1					
	2.37	930712 B1-17			29		1	13			8	2		1		1				10	5	1	1								8	7	1					1							6			
Uppermost 1 cm of soil S	2.40	930712 B1-20													15	1							1			22	17				1							12		4								
	2.48	930712 B1-28		1	1			1							2	3		1				1				19	10				5	1						50		1		1						

Table 5. Numbers of diatoms counted at the Oyster locality, horizontal coordinates 15 and 25 m—Continued

	Depth below modern surface (m)	*Frustulia spicula*	*Frustulia vulgaris*	*Gomphonema angustum*	*Gomphonema parvulum*	*Gomphonema spp.*	*Grammatophora oceanica*	*Gyrosigma acuminata*	*Gyrosigma balticum*	*Gyrosigma eximium*	*Hantzschia amphioxys*	*Hyalodiscus laevis*	*Luticola mutica*	*Lyrella lyra*	*Mastogloia exiguua*	*Melosira moniliformis*	*Melosira nummuloides*	*Navicula cancellata*	*Navicula cincta*	*Navicula cryptotenella*	*Navicula digitoradiata*	*Navicula lanceolata*	*Navicula spp.*	*Navicula viridula*	*Nitzschia bilobata*	*Nitzschia communtata*	*Nitzschia fasciculata*	*Nitzschia pusilla*	*Nitzschia scapelliformis*	*Nitzschia sigma*	*Nitzschia socialis*	*Nitzschia spp.*	*Nitzschia terrestris*	*Odontella aurita*	*Odontella obnuta*	*Opephora cf. parva*	*Paralia sulcata*	*Paralia sulcata (small form)*	*Petroneis granulata*	*Petroneis granulata*	*Pinnularia borealis*	*Pinnularia lagerstedii*	*Pinnularia spp.*	*Rhabdonema arcuatum*	*Rhaphoneis amphiceros*	*Rhaphoneis psammicola*	*Rhoicosphenia abbreviata*	*Rhopalodia gibba*	*Rhopalodia operculata*	*Rhopolodia musculus*	*Scoliopleura tumida*	*Stephanopyxis dimorpha*	*Surirella fatuosa*
	0.20						3	1				2		1	1	2	3						4			13	20		1								94	44	2					10	3	2	2		10		8		
	0.45											6		2		12																					75	30						1	3						8		
	0.65								1			4																									275	107				1			4	1			1		37		
	0.75					1			7			1		1		1														1							214	125	1				1	1	1						56		1
	0.80		1						2			1	1	1				3												1							165	65	6		1			4	3	3	2				7		
	0.87					2			2				4		4	7		3		1										4						14	91	57							3	7			2	1	2		
	0.89						4		2					2	4	6			1		4		2										2			8	107	35				7		1	5	2			2		3		
Uppermost 1 cm of soil Y	0.90			1			1				1		22	3			1				1		1							1			7				32	38				14			1	1					2		
	0.95										4	2	3	1		3			2				2										4				329	315				13				4							
	0.98				1								16			1			1								2						5	2	2		51	384	1			19				2	1						
	1.08			1									10																				1	3			34	121		1		18				3		2					
	1.11												4	1					1																		13	16	1			22											
	1.13				2																																28	65		4						2						2	
	1.16						6														4						1			1	2						59	114		2			2	8	6	2					4		
	1.18												4								2										15			2			192	372	4	2					2	4					4		
	1.19	1												4							10									2	6						88	190					2	1	5	4					3		
Uppermost 1 cm of soil W	1.20																																				10	28															
	1.20													2											3						2						38	70												1	1	1	
	1.22												4																								32	52				2											
	1.23																																				9	22				4											
	1.27						5														3				1					0.5	3.5		0.5			1	68	75			1	2				1					9		
	1.28													1							18										11			3	1		22	38	1				1	1	1						15		
	1.36								4												8								10	2	2			2			74	150	2						6		2			8	4		
	1.42												2								2				4				2	18	3			4			140	316		2			2		2						4		
Uppermost 1 cm of soil U	1.44												12						2						2				2	3			2	2			90	228				10			2								
	2.21								5	1								2			1		7						0.5	3	1.5	1		10		2	21	38							3	2				1			
	2.27						1		10				3		2		12				2		10					1	1	7				3			9	15							4		1			2	1		
	2.32							1	3						12	5	2						19				1			4.5	0.5	2		3		6	14	31				2			4				3	1			1
	2.37							6	4	1				1	3			3			6		20						4	1.5	0.5	10					12	41												1	1		
Uppermost 1 cm of soil S	2.40									1			7									1			2		3			6.5							10	23							1					2			
	2.48												2								1								1	2.5				2	1		16	60							2					1			

Table 5. Numbers of diatoms counted at the Oyster locality, horizontal coordinates 15 and 25 m—Continued

	Depth below modern surface (m)	*Synedra fasciculata*	*Trachyneis aspera*	*Trachysphenia australis*	*Tropidoneis spp.*	*Tryblionella acuminata*	*Tryblionella aerophila*	*Tryblionella apiculata*	*Tryblionella debilis*	*Tryblionella granulata*	*Tryblionella levidensis*	*Tryblionella littoralis*	*Tryblionella navicularis*	*Tryblionella plana*	*Tryblionella punctata*	*Tryblionella vexans*		**Planktonic diatoms**	*Actinocyclus curvatulus*	*Actinocyclus ochotensis*	*Actinocyclus kutzingii*	*Aulacoseira spp.*	*Chaetoceros spp.*	*Cyclotella sp.1*	*Cyclotella spp.*	*Stephanodiscus spp.*	*Thalassiosira spp.*	*Thalassionema nitzschioides*	Preservation	Total diatom valves counted	Total high marsh diatoms (1)	Total low/high marsh diatoms (1)	Total low marsh diatoms (1)	Total tidal flat diatoms (1)	Total diatoms used for index (BIDI)	BIDI value			
	0.20	1	7						2	20			5		2	2				9	2	24				1	2		M	415	3	37	31	29	100	0.56			
	0.45									3			2						1	5		25			2	4			M	295	13		64	23	100	0.45		(1) Individual taxa listed in Table 2	
	0.65			2		1				14									2	12	2	30			7	3	2		M	667	2		59	39	100	0.32		KEY:	
	0.75		4			1				11									2	3		14			6	1			M	542	2		66	32	100	0.35		G	Good preservation
	0.80	1	2			1				6		1							1	12	1	18			8		8	1	M	476	3	2	25	70	100	0.18		M	Moderate preservation
	0.87	9						2		6	1								2			9	3		2		14	4	M	423		5	10	155	170	0.06		P	Poor preservation
	0.89	11					2	2		6	1								1	2		6					13	5	M	428	18	2	14	132	166	0.16			
Uppermost 1 cm of soil Y	0.90	2							1	4												10			1		6	1	M	239	83	23	6	12	124	0.88			
	0.95									20										7	1	93			7	3		1	M	936	72	5	9	14	100	0.82			
	0.98	0.5		0.5		0.5				26	1										1				1	2	1.5	0.5	P	595	63	21	3	12.5	100	0.86			
	1.08									15											3	2		3	2		2		M	306	50	10	30	10	100	0.75			
	1.11				1					2																	1		M-G	135	40	5	53	2	100	0.72			
	1.13									38															2	4	6		M	265	30		62	8	100	0.61			
	1.16	12	2							52			4						2		4				6		10	1	M	458	14	1	28	57	100	0.29			
	1.18	13		4						10													2						M	688	4	4	16	76	100	0.16			
	1.19	3	1	1		1				7											1				4	1	2		M-P	420	4		34	62	100	0.21			
Uppermost 1 cm of soil W	1.20	1								5															1				M-G	146	8		89	3	100	0.53			
	1.20	2	1			2				4																			P	220	3	2	86	9	100	0.48			
	1.22			2						6																	2		P	196	4	4	90	2	100	0.53			
	1.23	0.5								1																			M-G	134	4		95	0.5	100	0.52			
	1.27	9.5	6	1	4	1				36	1		7												4	1	2		P	342	2.5		61	36.5	100	0.33			
	1.28	8.5	9		13					5	1		0.5								1				1				M-G	203			40.5	59.5	100	0.20			
	1.36	28	4			4				16												2			34		6		P	408			30	70	100	0.15			
	1.42	21	2		2			2		16			2		2				2								2	5	P	637	8	2	18	72	100	0.19			
Uppermost 1 cm of soil U	1.44	1	2							22															8		2		P	458	40	14	34	12	100	0.71			
	2.21	9						5						1	1								1		1		21	3	M	212			2.5	97.5	100	0.01			
	2.27	7						4		8	2				1	1											26	3	M	194	1	3	6	90	100	0.07			
	2.32	9	1					5		10					2										1		34	2	M	231	2	1	17	80	100	0.12			
	2.37	11						2		5																	42	2	M	272			12	88	100	0.06			
Uppermost 1 cm of soil S	2.40	0.5				1			4	3															2		2		M	142	39	33	18	10	100	0.81			
	2.48	0.5	1							3															2				M	192	29	5	55	11	100	0.62			

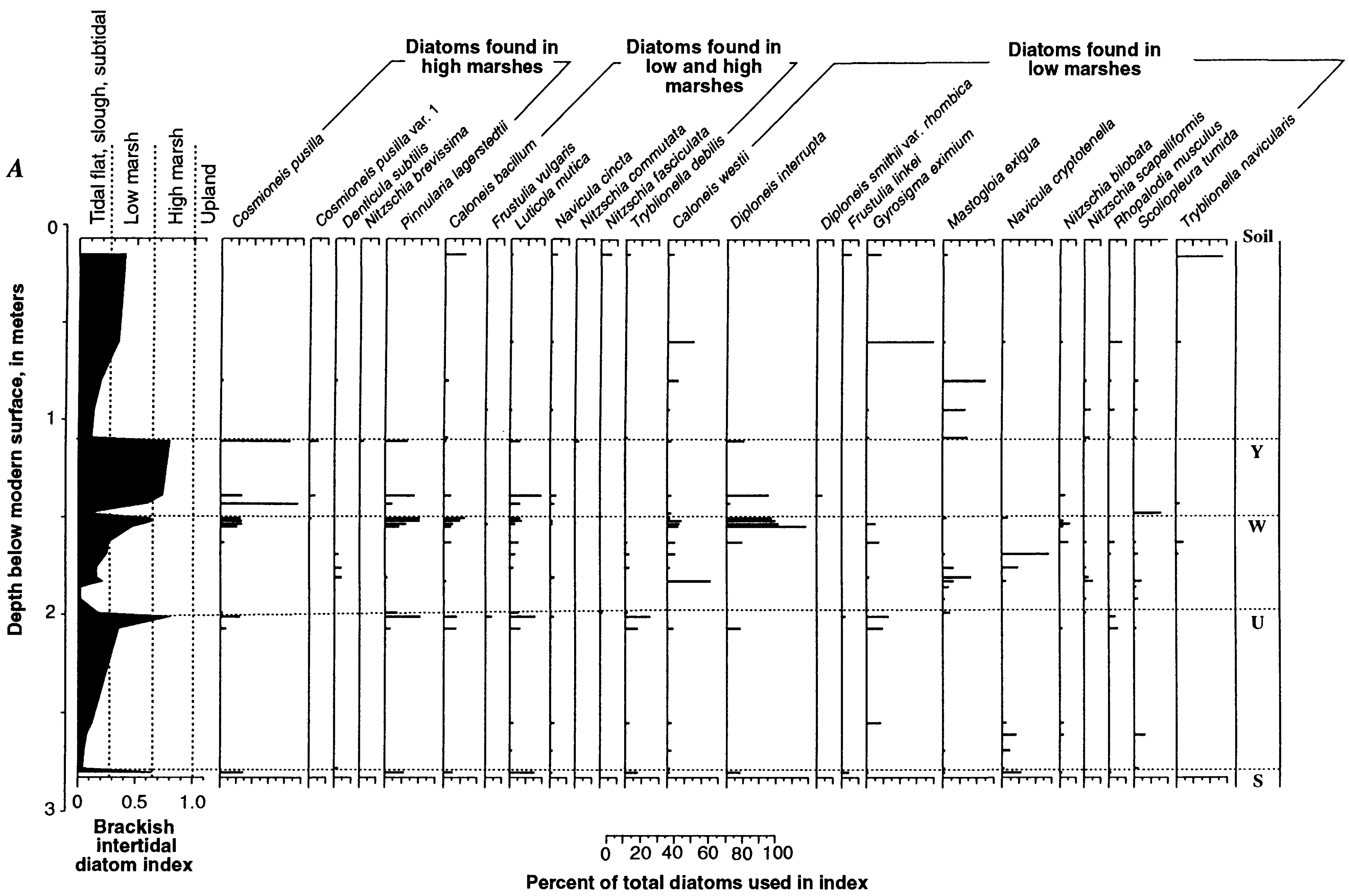

Figure 22. Relative abundances of diatom species grouped by inferred depositional environment for a stratigraphic section at horizontal coordinate 165 m, Oyster locality, Niawiakum River.

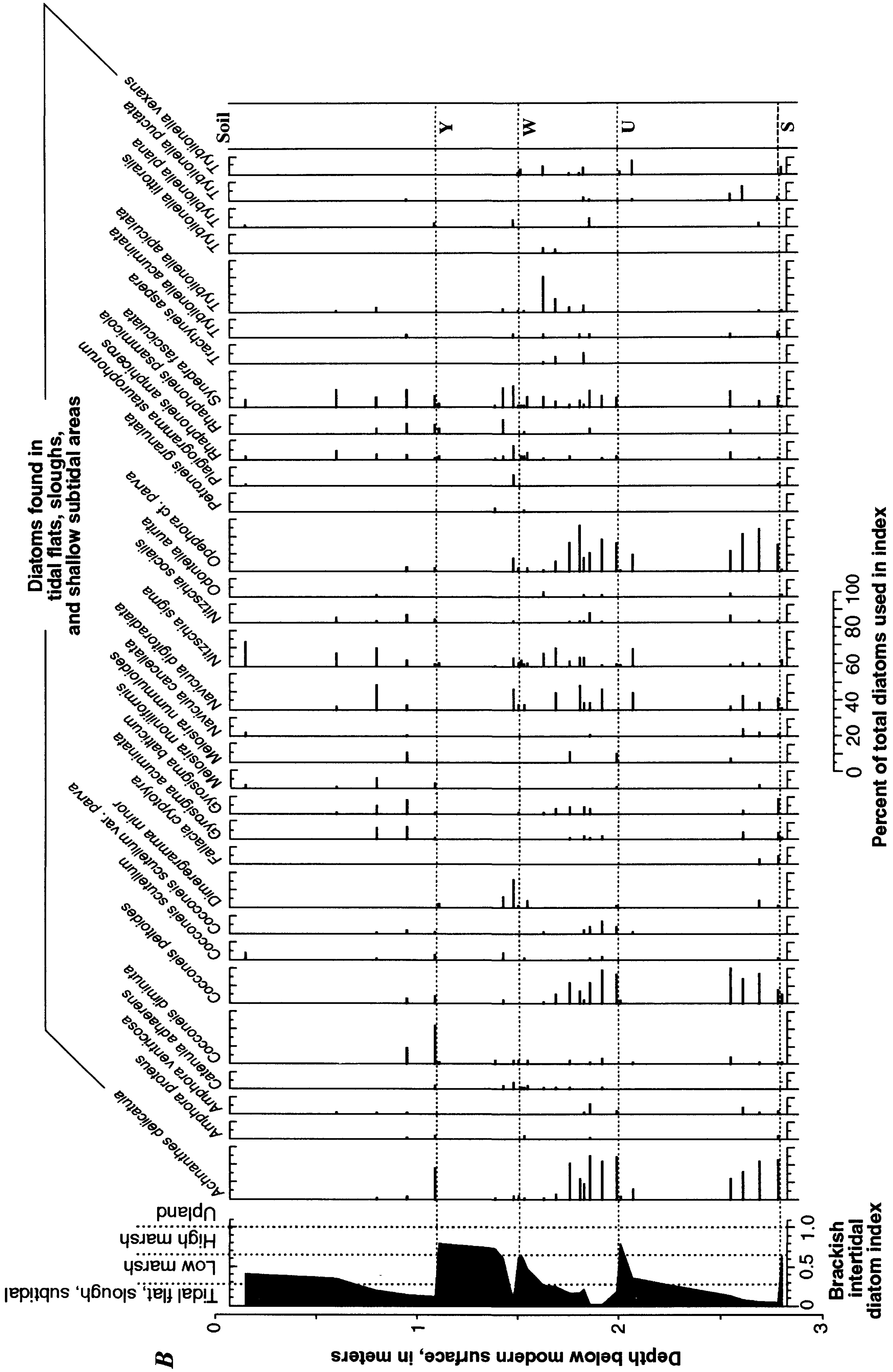

Figure 22. Continued.

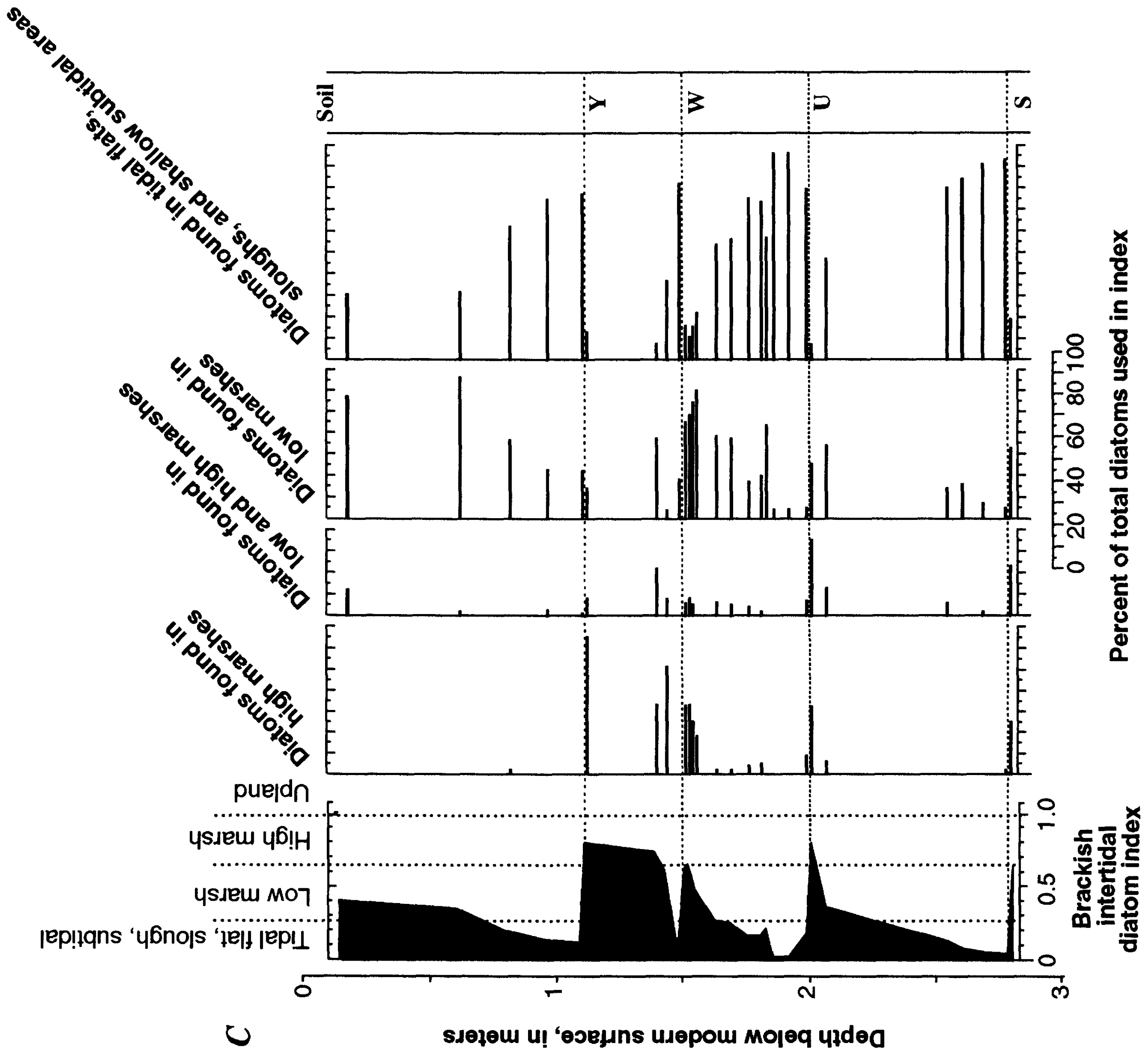

Figure 22. Continued.

Willapa Bay in the past 300 years (see section "Minimum Time for Formation of a Peaty Soil" on p. 95). Moreover, onset of burial shortly before 1,400–1,600 years ago is consistent with radiocarbon ages from other localities. Burial began between 1,520 and 1,700 years ago at the Pool locality, as judged from a high-precision age on inner rings of a red-cedar root in soil S (p. 63), and it began sometime between 1,400 and 2,100 years ago at the Redtail locality, as judged from conventional radiocarbon ages on roots and peat in the soil (fig. 32).

Two high-precision ages have been measured for soil U at the Oyster locality—one on *Salicornia virginica* stems rooted in the soil, the other on *Triglochin maritimum* rhizomes 20 cm above the soil. The ages, which are nearly identical, imply that burial of the soil began between about 1,130 and 1,350 years ago.

Burial of soil Y began no earlier than A.D. 1660, as shown by radiocarbon ages of *Potentialla pacifica* and *Juncus balticus* rooted in soil Y and surrounded by the overlying tsunami deposit (Nelson and others, 1995). The individual ages are listed in table 7, and ranges of calendric ages corresponding to their weighted mean (161±15 ^{14}C yr B.P.) are plotted in figure 32.

Several additional lines of evidence tend to confirm that the oldest and youngest buried soils exposed at the Oyster locality correlate with soils S and Y, respectively, at the nearby Redtail locality. Both soils are characteristically bold at both localities. The youngest buried soil is the only one covered by sand at either locality. Diatom assemblages at both localities suggest that soils S and Y formed higher in the intertidal zone than did the intervening soil or soils (p. 48). Finally, vascular-plant fossils rooted in both soils at both localities imply lower soil salinity than do the plants of modern marshes. At the Oyster locality, *Salicornia* is common on modern high marsh near the river but is absent from soils S and Y. Similarly at the Redtail locality, Sitka spruce

Table 6. Numbers of diatoms counted at the Oyster locality, horizontal coordinate 165 m

	Depth below modern surface (m)	Diatom sample ID	**Benthic diatoms**	*Achnanthes brevipes*	*Achnanthes delicatula*	*Achnanthes hauckiana*	*Achnanthes spp.*	*Actinoptychus senarius*	*Amphora coffaeiformis*	*Amphora proteus*	*Amphora spp.*	*Amphora ventricosa*	*Biddulphia sp.*	*Caloneis bacillum*	*Caloneis westii*	*Catenula adhaerens*	*Cerataulus turgidus*	*Cocconeis diminuta*	*Cocconeis pellucida*	*Cocconeis placentula*	*Cocconeis scutellum*	*Cocconeis scutellum v. parva*	*Coscinodiscus spp.*	*Cosmioneis pusilla*	*Cosmioneis pusilla var. 1*	*Craticula halophila*	*Cymbella pusilla*	*Delphineis cf. karstenii*	*Delphineis cf. surirella*	*Delphineis margaritalimbata*	*Denticula subtilis*	*Dimeregramma minor*	*Diploneis didyma*	*Diploneis interrupta*	*Diploneis oblongella*	*Diploneis smithii v. rhombica*	*Endictya sp. 1*	*Epithemia turgida*	*Eunotia spp.*	*Fallacia cryptolyra*	*Fallacia forcipata*	*Fallacia pygmaea*	*Fragilaria spp.*	*Frustulia spicula*	*Frustulia vulgaris*	*Gomphonema parvulum*	*Gomphonema spp.*	*Grammatophora oceanica*	*Gyrosigma acuminata*
	0.15	950521-6												12	3						4								1															5				3	
	0.60	950521-5		1							2	1			15														10						1													2	
	0.80	950521-4		2	1							1	1	2	6						1	1		1					42	1	1																	2	19
	0.95	950521-3		1	2					1		1			1			10	3	1		2				1			37												1				1			2	8
	1.09	950521-2		2	18					2				2		2		22	4		3	1							12								2												3
Uppermost 1 cm of soil Y	1.11	950521-1						3						1	2		1	1		2			1	43	5			11				2	1	10	2		1										1		
	1.39	940713 Bx7-1		2	1	1								4	2			2		1				13	3			1						25	1	3	1												
	1.43	940713 Bx7-5		8				2								2			2		4			48								6		2	2														
	1.48	940713 Bx7-10			2										2	4	2	2										6				16					4		2										
Uppermost 1 cm of soil Y	1.51	940713 Bx7-12			2						2			12	1			2						12	1			1				1		27	1		2												
	1.52	940713 Bx7-14				1								9	8	1								13				4						29	4														
	1.54	940713 Bx7-15			1	1				2				5	7	1					1			13				1		2				31	6										1	1		1	
	1.55	940713 Bx7-17												4	6	2		2						10				6				4		48	10		2												
	1.63	940713 Bx6-1		19	1		2	4	1		1			4	4	1			1			1		2			1	2						9	1		2												
	1.69	940713 Bx6-7		1	3	1		1							4	1			5								2	3	1		2										1								
	1.76	940713 Bx6-14			21				1						1	1		2	12							2		5	3	2	4				1						2	1	2						1
	1.81	940713 Bx5-1			12	4					2								7							4	61	9	2		4										1								
	1.83	940713 Bx6-21		1	9	2	20				4	1		1	25				2			2					14	2	2						1														2
	1.86	940713 Bx4-1		5	25	8	3			1	9	6						1	12		1	4				5		2		5								4			5								1
	1.92	940713 Bx4-7			22	5		1			2					1		3	19		2	7				1		4	1												2								2
	1.99	940713 Bx4-14		2	25	6	1				2	2							17	1		4		1		4		1	1	5		1									2								
Uppermost 1 cm of soil U	2.01	940713 Bx4-16			2									8					2					13				1							2							4		2	4				
	2.07	940713 Bx4-22		1	6		12							7	3			1				1		3		1								8	4			2				3							
	2.55	940713 Bx1-1		4	12	2					2				2			4	20	2						14		4		4											4								
	2.61	940713 Bx1-7			16	4					4	4							14							14		4	2	4																			4
	2.69	940713 Bx1-15			22	17						1			2			1	17	3						7		4	9			4								3	2								
	2.78	940713 Bx1-24		2	23	13				2	1	2			1			1	8		1		1			14		2	6	1	2	1								5									4
Uppermost 1 cm of soil S	2.80	940713 Bx1-26				6								5	1			1	5					14				3		1				8	2						1	4		4					1

Table 6. Numbers of diatoms counted at the Oyster locality, horizontal coordinate 165 m—Continued

	Depth below modern surface (m)	*Gyrosigma balticum*	*Gyrosigma eximium*	*Luticola mutica*	*Mastogloia exigua*	*Mastogloia smithii*	*Melosira moniliformis*	*Melosira nummuloides*	*Navicula cancellata*	*Navicula cari*	*Navicula cf. digitoradiata*	*Navicula cincta*	*Navicula cryptotenella*	*Navicula digitoradiata*	*Navicula gregaria*	*Navicula lanceolata*	*Navicula margalithii*	*Navicula meniscus*	*Navicula normalis*	*Navicula normaloides*	*Navicula radiosa*	*Navicula spp.*	*Navicula tenneloides*	*Navicula veneta*	*Navicula viridula*	*Nitzschia bilobata*	*Nitzschia brevissima*	*Nitzschia communtata*	*Nitzschia fasciculata*	*Nitzschia nana*	*Nitzschia perminuta*	*Nitzschia pusilla*	*Nitzschia scapelliformis*	*Nitzschia sigma*	*Nitzschia socialis*	*Nitzschia spp.*	*Nitzschia terrestris*	*Odontella aurita*	*Odontella obnuta*	*Opephora cf. parva*	*Paralia sulcata*	*Paralia sulcata (small form)*	*Petroneis granulata*	*Pinnularia borealis*	*Pinnularia lagerstedtii*	*Pinnularia spp.*	*Plagiogramma staurophorum*	*Rhaphoneis amphiceros*	*Rhaphoneis psammicola*	*Rhoicosphenia abbreviata*
	0.15		8	1	2		2		2			3																	6					14							2	20					1	2		
	0.60	1	39	1	1		1					1	1	2								3				1				4				7.5	3	1					1	14						5		
	0.80	5			26		6							15								5											1	11	1			1			9	20				1		3	3	
	0.95	9	1	1	14			6	1			1		3	1							21											4	4	5					3	7	7						3	6	
	1.09	1	1		14		3															6											3	1.5	2	2				2	12	15						1	5	
Uppermost 1 cm of soil Y	1.11			6												1											2	2					1	2			1				65	213			13			2	3	
	1.39			19								3										2				3								0.5					1		14	12	2		17			1		
	1.43			6								2																											2		26	10			4			2	8	4
	1.48													12		4						2												5	1					8	108	26					6	8		
Uppermost 1 cm of soil Y	1.51	1		6	2								3	3																				2		1				2	46	7			20					
	1.52			7								1				1		1				3				2								3.5							65	27			20			2		
	1.54		5	3								1		3		3		2								6								1.5							74	17	1		12			2	1	
	1.55																				2					2								2						2	78	12			8			4		
	1.63	1	7	5													2					4		1		5							1	7.5		2		3		1	72	5				1		1		
	1.69	3		3	1								28	10		1			1		1	3								1				10.5						6	15	3								
	1.76	4		2	6			6					9				5	1	1			8		2						2	1		1	3	0.5	1				17	9	1						2		
	1.81		1		16							2		14						1		13		2									2.5	5	1	2				27	13	1			1					
	1.83	4			6								2	4					1			18											5	5	1			1		8	13									
	1.86	3			3	1			1					4						5		21													5.5					11	20	1							3	
	1.92				1						81			12					8	2		12											1	1	0.5			1		19	26							1		
	1.99			5	4		1	5							•				2			3							1	5	1	1	1	1.5						17	21	5			7			2		
Uppermost 1 cm of soil U	2.01		14	17								2										5								9	9			1		8				1	8	2		1	23	1				
	2.07		9	6										10	4		10					11		1	4	1				1	4			10		1				10	14	1			3					
	2.55		8	2				2				2	2	2					4			24				2					2			1	4			2		12	68	20		4				4	2	2
	2.61	2							4				8	8							2	18				2								2						22	18	2								
	2.69			1	1		2		2			1	4	4					2			8												1.5	1					25	18	5						1		
	2.78	9			1				1				1	7					2			24									5				1					16	5	5					1	1		
Uppermost 1 cm of soil S	2.80		0.5	15	1					2		1	11	1	3		1	1				6		6		1					10			3.5		4		1		1	4	6			11					

Table 6. Numbers of diatoms counted at the Oyster locality, horizontal coordinate 165 m—Continued

	Depth below modern surface (m)	*Rhopalodia operculata*	*Rhopolodia musculus*	*Scoliopleura tumida*	*Stauroneis producta*	*Stephanopyxis dimorpha*	*Surirella fatuosa*	*Surirella ovata*	*Synedra fasciculata*	*Trachyneis aspera*	*Trachysphenia australis*	*Tryblionella acuminata*	*Tryblionella apiculata*	*Tryblionella debilis*	*Tryblionella granulata*	*Tryblionella levidensis*	*Tryblionella littoralis*	*Tryblionella navicularis*	*Tryblionella plana*	*Tryblionella punctata*	*Tryblionella vexans*		**Planktonic diatoms**	*Actinocyclus curvatulus*	*Actinocyclus ochotensis*	*Chaetoceros spp.*	*Cyclotella spp.*	*Stephanodiscus spp.*	*Thalassiosira spp.*	*Thalassionema nitzschioides*	Unidentified diatoms	Preservation	Total diatom valves counted	Total high marsh diatoms (1)	Total low/high marsh diatoms (1)	Total low marsh diatoms (1)	Total tidal flat diatoms (1)	Total diatoms used for index (BIDI)	BIDI value
	0.15	1							4.5					2				27	1										4			G	131		12	57	30.5	100	0.41
	0.60	4	7						10				1		2			2											16	2		G	163		2	66	31.5	100	0.35
	0.80		1	2			1		6				3		5														6			G	212	2		38	65	105	0.20
	0.95	1	3	2					11			2				1				1						2			18	5		M	215		3	25	82	110	0.14
	1.09	2	1	1					6.5					1	2				2										8	1		M	166		1	22	77	100	0.12
Uppermost 1 cm of soil Y	1.11								2		1				14														2	3		P	420	65	8	14	13	100	0.80
	1.39								1						2														1	1	2	M	142	33	22	37	7.5	100	0.74
	1.43								11				2		2			2									2	2	4	5	6	P-M	176	52	8	4	37	101	0.61
	1.48	2		16					12			2			2				4										6	6		P	270			18	82	100	0.09
Uppermost 1 cm of soil Y	1.51	1							1				1		6						1						2		1	0.5		P-M	171	33	6	45	16	100	0.62
	1.52	1				1			1						4						3									1.5	7	P-M	220	33	8	48	10.5	100	0.65
	1.54								1				1		6												3			0.5	7	P	224	25	5	54	15.5	100	0.57
	1.55	2							6						4										2		4					P	222	18		60	22	100	0.48
	1.63	1	3	1				1	6	1		2	21	1	5		3	4			5				1				1	0.5	1	P	232	2	6	38	53.5	100	0.27
	1.69	3	1	2					3.5	4			8	2	1		2	1										1	7	2.5	1	P	151	2	5	37	56	100	0.26
	1.76	7			1				1.5				3	2	2						1								3	1	2	P	166	4	4	17	75	100	0.17
	1.81	11							4			2			1						1								5		12	M	244	5	2	19.5	73	100	0.17
	1.83	4		4					1.5	6			4		4					2	4								4		16	P	206			43	56.5	100	0.22
	1.86			1					9.5			2			7				5	1					1	3			21	2.5	11	P-M	240			4	96	100	0.02
	1.92	2		2					6.5															1	1	1	1		31	4	4	P-M	291			4	96	100	0.02
	1.99								5.5					1	1										1			1	45	1	5	G	218	9	7	5	81	102	0.18
Uppermost 1 cm of soil U	2.01		4											16							2					2			2	0.5	8	G	174	36	39	28	8	111	0.80
	2.07		5	1										7						1	8								2		5	G	181	6	13	34	47	100	0.36
	2.55								9			2		2						4									38	7	14	P	319		6	14	80	100	0.13
	2.61			6											4					8							2		22	4	10	P	214			16	84	100	0.08
	2.69								3.5				1		2				2								1		4	2.5	10	P	195		2	7	91	100	0.06
	2.78			2					6			3			6					2							1		24	2.5	3	P	219	2		5	94	101	0.04
Uppermost 1 cm of soil S	2.80		1						0.5				1	7							4						1		3	1.5	14	P	179	25	23	32.5	19	100	0.65

(1) Individual taxa listed in Table 2

KEY:

G	Good preservation
M	Moderate preservation
P	Poor preservation

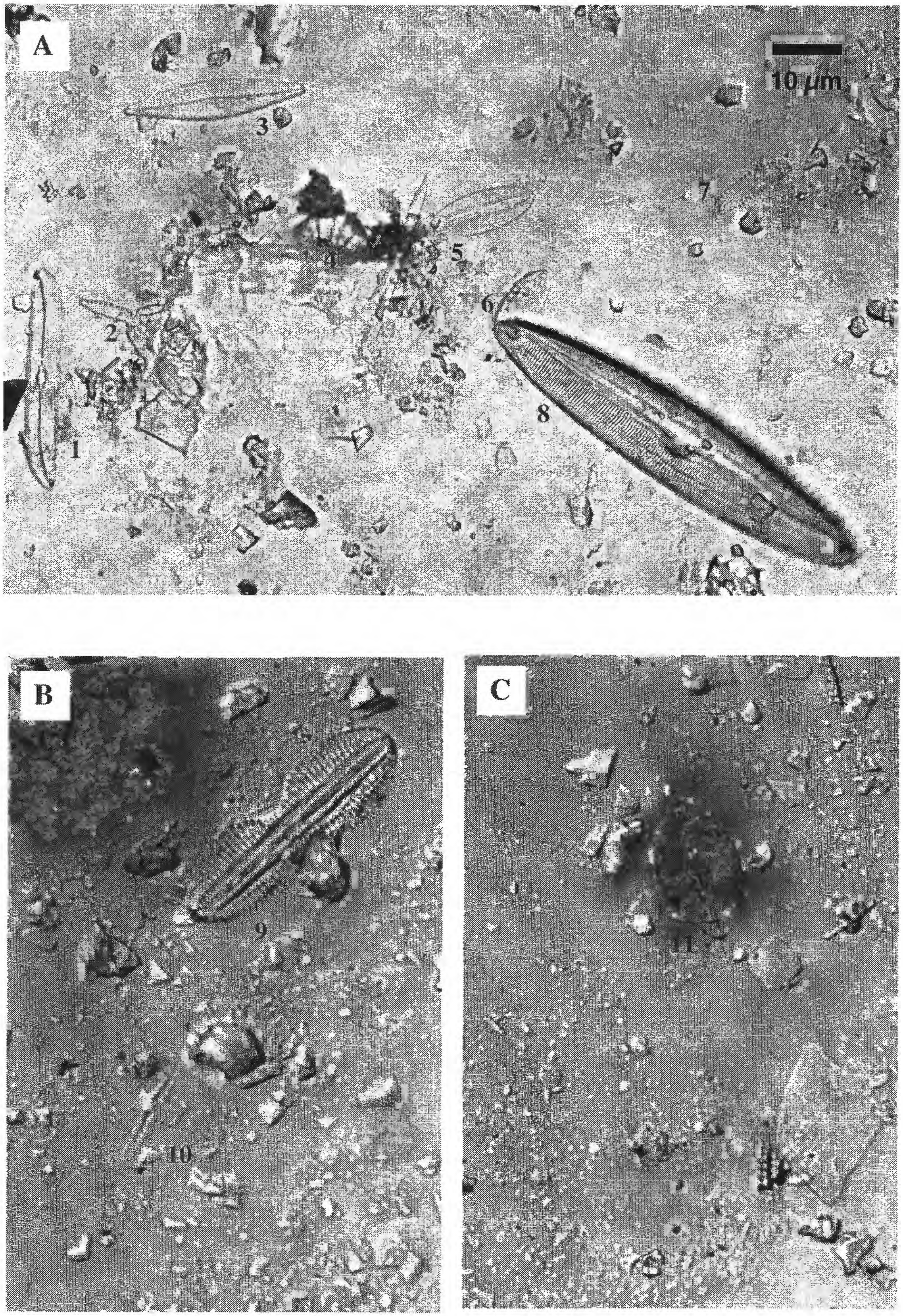

Figure 23. Differences in diatom preservation in soil U at the Oyster locality. Scale bar at upper right applies to all three photographs. *A*, Good preservation at horizontal coordinate 165 m, marked by diverse assemblage of largely intact valves. *B*, *C*, Poor preservation at horizontal coordinate 25 m, marked by sparse assemblage of largely broken valves. 1, *Gyrosigma eximium*; 2, *Nitzschia* sp.; 3, *Navicula gregaria*; 4, *Rhopalodia musculus*; 5, *Fallacia pygmaea*; 6, *Tryblionella debilis*; 7, *Pinnularia lagerstedtii*; 8, *Caloneis westii*; 9, *Diploneis interrupta*; 10, *Caloneis bacillum*; 11, *Cosmioneis pusilla*.

is absent from the modern marsh but abundant in soils S and Y.

The lower of the characteristically faint soils between soils S and Y at the Oyster locality (soil U) probably correlates with the only faint soil preserved between soils S and Y at the Redtail locality (soil U). The upper of the faint soils between soils S and Y at the Oyster locality (soil W) was probably destroyed by weathering at the Redtail locality: soil U at the Redtail locality is as high in the profile of soil Y as it is at the northwest end of the Oyster locality (fig. 18), where soil W was probably also destroyed while soil Y was at the ground surface (p. 45).

Twigs from the sand lens in the channel fill at the Oyster locality yielded radiocarbon ages that may be centuries greater than the age of the lens. Several tens of twigs collectively gave an age of about 500–1,000 years ago, and a single twig gave an age of about 500–800 years ago. However, the lens accumulated only 300 years ago if it correlates with the sandy interval on soil Y. We infer that a tsunami along the Niawiakum River about 300 years ago exhumed and redeposited twigs that had first been deposited centuries before. Such recycling of twigs and sticks best explains discordant radiocarbon ages from a tsunami deposit about 300 years old at Port Alberni, British Columbia (Clague and Bobrowsky, 1994).

POOL LOCALITY

The Pool locality comprises 20 m of bank about 10 m from an upland (fig. 7). The bank is fully exposed at many low tides because the minimum level of river water at the Pool locality is about 1 m above the level of mean lower low water (fig. 24). The water cannot drop further because, in its upper tidal reaches, the bed of the Niawiakum River is higher than the level of very low summer tides. During such tides the river trickles beneath the South Bend–Palix River Road.

Though not tall, the bank exposes five buried soils. In addition, we noted two underlying soils in a gouge core near the southwest end of the outcrop, and we found Pleistocene deposits about 1 m below the lower of these soils (fig. 24).

The sequence of five soils resembles the sequence of the five uppermost buried soils at the Redtail locality: three bold soils contain tree roots in growth position; and these soils (L, S, and Y) alternate with faint soils (N and U). Most of the tree roots at the Pool locality belong to Sitka spruce, but soil S also contains roots of western redcedar (fig. 24, horizontal coordinate 3 m).

Mud deposited by a tsunami probably mantles soil Y in the vicinity of the Pool locality (Hemphill-Haley, 1995b). This mud, like the sandy tsunami deposit on soil Y at the Redtail locality, contains diatoms typical of sandy tidal flats. The nearest sandy tsunami deposits on soil Y are nearly 0.5 km downvalley from the Pool locality, according to mapping by Atwater (1987) and by Mary Ann Reinhart and Kenneth A. Bevis (written commun., 1987; summarized by Atwater, 1996, his fig. 22C). Hemphill-Haley (1996b) reasoned that a tsunami would carry diatom valves farther upvalley than it would carry sand grains.

Inner rings of one of the redcedar roots in soil S gave a high-precision age that places the initial burial of soil S about 1,520–1,700 years ago. We selected 10 consecutive rings that formed 60–69 tree-ring years before the root stopped growing. The age obtained for this group of rings—1,740±15 ^{14}C yr B.P. (QL–4796)—corresponds to A.D. 242–408. If the tree died 65 years later, and if tree death coincided with initial burial of the soil, then burial of soil S began sometime between A.D. 307 and 473—that is, between about 1,520 and 1,700 years ago. This estimate accords with the age of 1,400–1,600 years ago inferred for the onset of burial of soil S at the Oyster locality (p. 52, 58).

High-precision radiocarbon ages were previously reported for several samples from soil Y near the Pool locality (Atwater and others, 1991). The nearby samples are from Sitka spruce stumps rooted in the soil at locations plotted in figure 7 and identified there by laboratory number (QL–). For one of these stumps, separate ages for inner and outer rings (QL–4405 and QL–4406) reduce ambiguity in converting radiocarbon ages to calendric ages; the ages limit the probable time of tree death to the first few decades of the 1700's (Nelson and others, 1995).

HERON LOCALITY

The Heron locality includes 35 m of bank between an upland and a tidal creek (figs. 7, 25). We identified eight buried soils in and beneath this bank. The widely recognized—soils J, L, N, S, and Y—spread apart from one another as they extend northward, away from the upland.

The south end of the Heron locality exposes onlap of soil Y onto stiff Pleistocene mud that makes up the upland (fig. 26). The peaty part of soil Y turns upward onto this mud (or onto colluvium derived from it) and is continuous with the O horizon of the modern upland soil.

Soil N at the Heron locality contains peat more widely than does soil N at the Redtail locality. Much of the exposed part of soil N at the Heron locality consists of peaty mud about 5 cm thick (fig. 25, horizontal coordinates 106–112 m). The soil can be correlated confidently with soil N at the Redtail locality, however, not only by stratigraphic position beneath bold soil S, but also by the presence of several partings of micaceous silt in the lowest few centimeters of mud above soil N. The mapped extent of these silt partings at the Heron locality is shown by dashed lines in the upper part of figure 25.

Hemphill-Haley (1995b, p. 372 and her fig. 6) described diatom assemblages associated with soil Y a meter or two north of the area shown in figure 26. Diatoms in the peaty surficial horizon of the soil are few and poorly preserved, as also seen in soils S and Y at the Redtail locality. This assemblage, combined with abundant spruce roots, implies conditions at or above extreme high tides. By con-

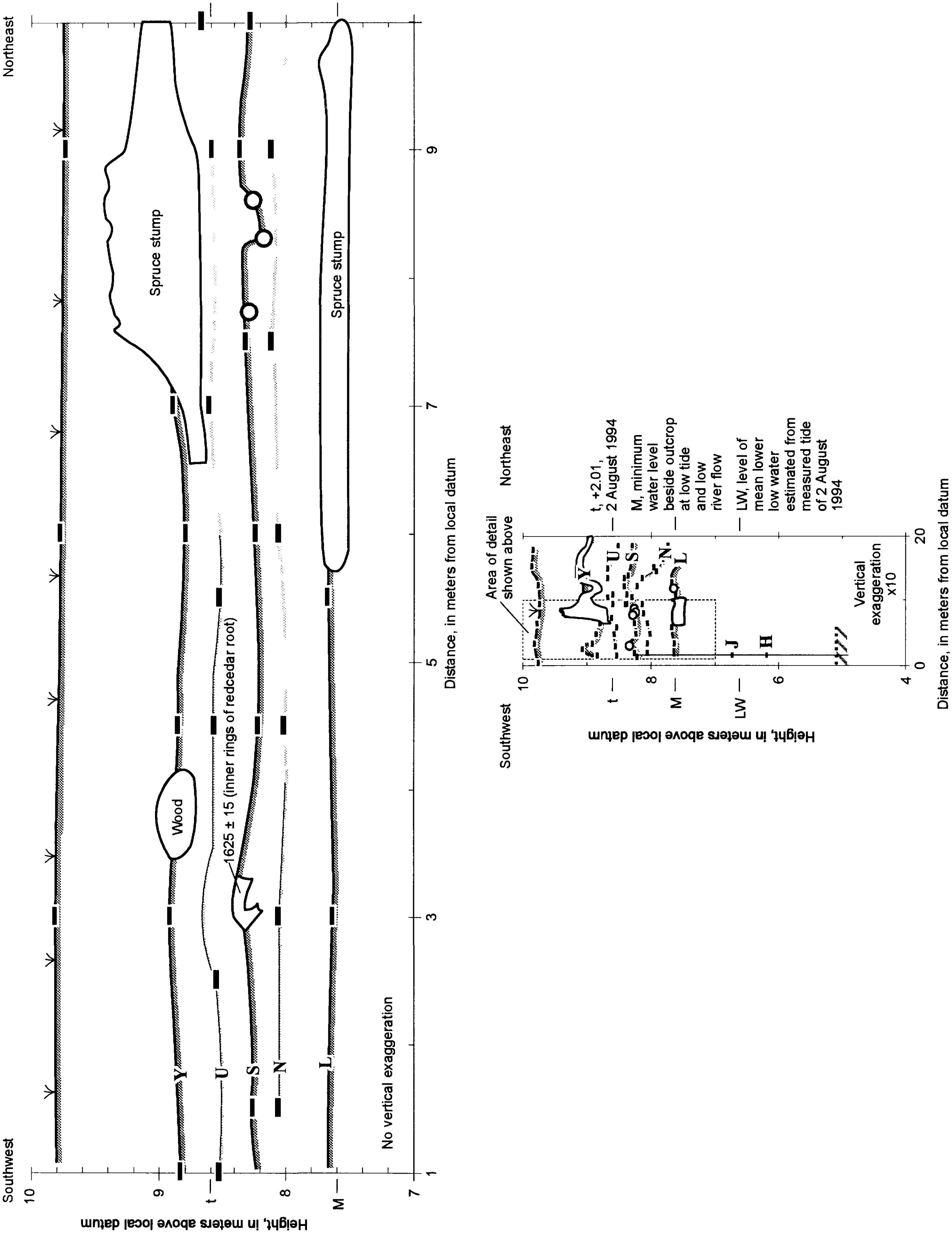

Figure 24. Stratigraphy at Pool locality, Niawiakum River.

EXPLANATION

Top of soil—Shown by solid line where continuity observed; shown only by top of shading where continuity inferred
- Surveyed point
- Bold soil
- Faint soil

S Letter name of buried soil

Top of Pleistocene deposits—Marked by hard angular aggregates of greenish mud

Fossil root—Spruce except for western redcedar labeled in soil S
- Shown to scale
- Not shown to scale

Live herbaceous plants of modern marsh

1625 ± 15 **Radiocarbon age**—In ^{14}C years before A.D. 1950 (table 7)

t, +2.01, 2 August 1994 **Low tide**—Height as predicted in tide tables; in meters relative to mean lower low water

Boring—Made with gouge corer 2 cm in diameter

Figure 24. Continued.

trast, mud above the soil contains many mudflat and low-marsh diatoms, and a tsunami deposit above the soil contains sand-flat diatom.

The section sampled by Hemphill-Haley (1995b) is complicated by what may be a sedimentary breccia between the buried soil and the tsunami deposit. This enigmatic unit, as much as 10 cm thick but exposed along only a few meters of bank, is marked by black organic slabs as much as 15 cm long. Interstices among these slabs are filled with soft gray mud that resembles mud above the tsunami deposit. The organic slabs contain abundant low-marsh diatoms. Hemphill-Haley (1995b, p. 372) inferred that a low-marsh soil was ripped up and deposited rapidly on the forest soil during or shortly before the tsunami.

WILLAPA RIVER

The Willapa River drains about 350 km^2 of mostly hilly country southeast of Raymond (fig. 6). Its lower reaches are flanked locally by tidal marshes and, upstream of Raymond, by tidal spruce swamps. In 38 years between 1947 and 1993, discharge by the main branch of the river averaged 1.8 m^3/sec and ranged from 0.4 m^3/s to about 335 m^3/s at a gage about 5 km east of Raymond (Miles and others, 1994, p. 45).

Buried soils suggestive of coseismic subsidence along the Willapa River were first studied at the South Fork locality, on the east flank of the South Bend antiform (fig. 6). At least six buried soils were identified in outcrop and two additional soils were found in boreholes (Hull, 1987; Atwater, 1992, table 1). The South Fork locality closely resembles the Redtail locality in sequence of bold and faint soils and in radiocarbon ages on spruce roots, woody detritus, and peat associated with the uppermost seven soils (Hull, 1987) (fig. 32).

Buried soils were surveyed more recently at several Willapa River outcrops on the South Bend antiform—the Jensen, Sewer, and Airport localities (figs. 6, 7, 27, 29, 31). None of these localities have been studied as thoroughly as have the Redtail and Oyster localities along the Niawiakum River. However, the sequence of eight buried soils at the Jensen locality probably spans as much time as does the sequence at the Redtail locality, and the shorter sequences of buried soils at the Sewer and Airport localities probably record most or all of the time represented in outcrop at the Oyster locality (fig. 32).

JENSEN LOCALITY

The Jensen locality comprises part of the western end of Jensen Island (fig. 7). The main outcrop is an east-west dredge cut on the north side of the island. This outcrop, surveyed for 70 m, exposes a section of natural deposits 3.5 m tall at lowest tides (figs. 27, 28*A*). Another 40 m of surveyed outcrop extends southward from the west end of the dredge

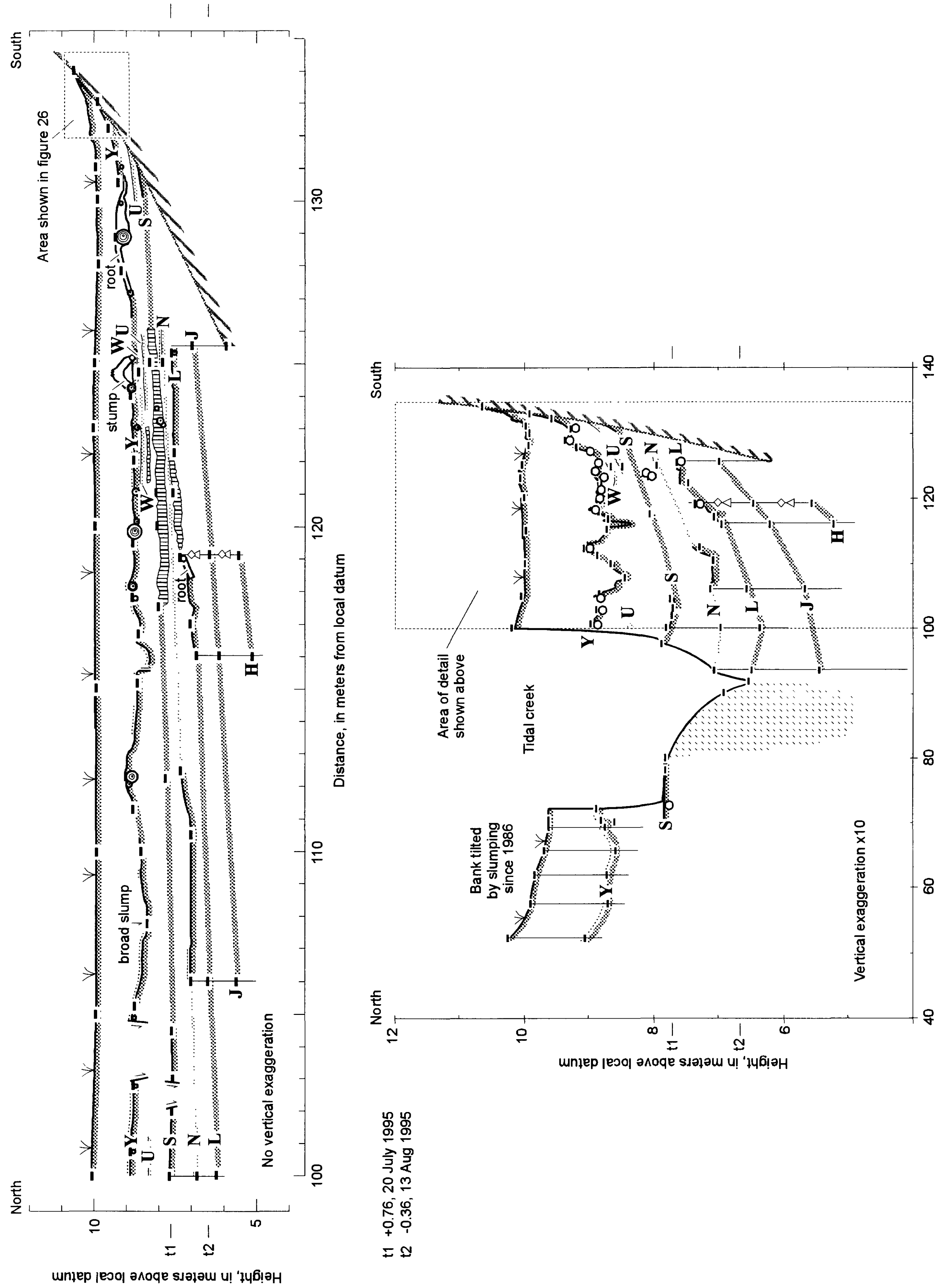

Figure 25. Stratigraphy at Heron locality, Niawiakum River.

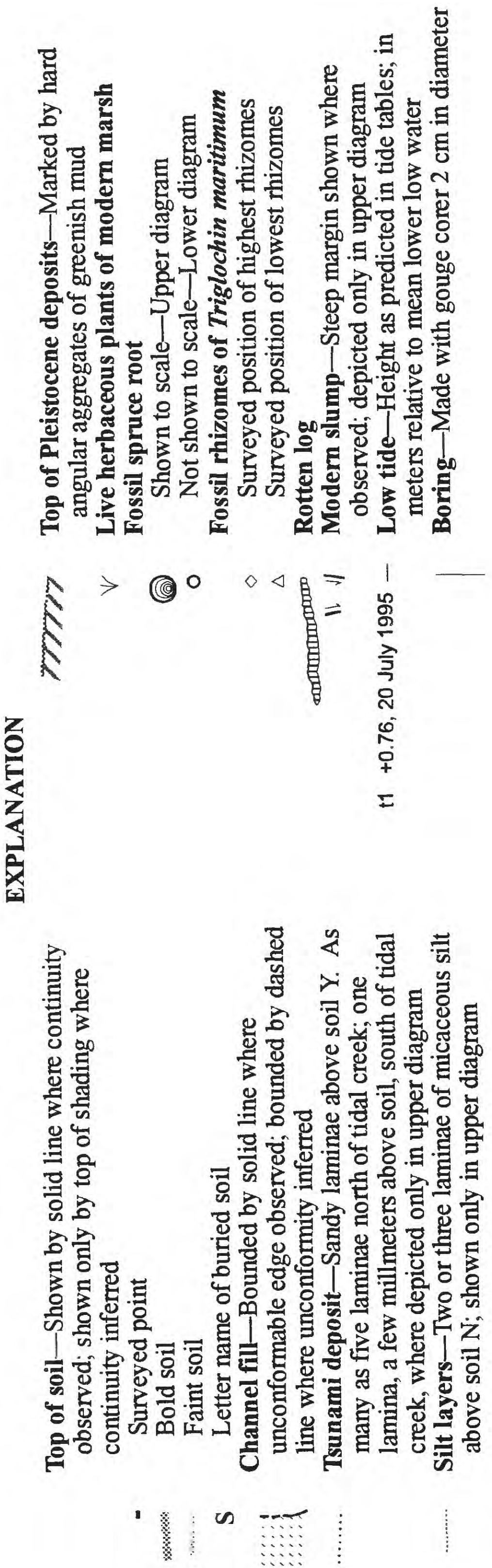

Figure 25. Continued.

cut. The bottom of this additional outcrop intersects a modern mudflat about 1 m above lowest tides.

BURIED SOILS

Eight buried soils crop out at the Jensen locality. Four are typically bold enough to form horizontal ledges that extend without interruption for tens of meters along the dredge cut—especially soil S, which has a peaty surficial horizon 15–20 cm thick. A fifth soil, termed soil L, is bold only near the spruce roots shown in figure 28*A*. The other three soils are everywhere faint and have little topographic expression.

The horizontality and close vertical spacing of the buried soils at the Jensen locality reflect a shallow, almost horizontal foundation of Pleistocene deposits. These deposits consist of stiff yellowish mud that resembles weathered Pleistocene estuarine deposits elsewhere in the Willapa Bay area. This mud lies less than ¾ m below the top of soil H and grades upward, through firm brownish gray mud, into the peaty surficial horizon of soil H (fig. 27). We speculate that the brownish gray mud was deposited by floods or extremely high tides that barely surmounted the Pleistocene deposits shortly before 3,500–4,500 years ago, which is the approximate time of burial for soil H at the Jensen and Redtail localities.

Faint soils N and W are the least traceable of the buried soils at the Jensen locality. They fade laterally like soil W at the northwest end of the Oyster locality, where soil W becomes too faint to identify readily high in the profile of the succeeding bold soil Y (fig. 19*E*). Soils N and W at the Jensen locality are high in the profiles of succeeding bold soils S and Y, respectively. Faint soils U and W are clearly exposed, bracketed by bold soils S and Y, near horizontal coordinate 30 m (fig. 28*C*).

GROWTH-POSITION FOSSILS OF VASCULAR PLANTS

Soils H, J, L, S, and Y are associated with woody roots and (or) with herbaceous rhizomes (fig. 27). Soils H and Y contain woody roots indicative of conditions high in the intertidal zone or above highest tides; in addition, mud above each of these soils contains rhizomes of *Triglochin maritimum*, an indicator of conditions lower in the intertidal zone. Soil L contains radiating roots attributable to a single Sitka spruce. Soil S lacks woody roots in growth position but is overlain by mud that contains rhizomes doubtfully identified as *Carex lyngbyei*. Soil J also lacks woody roots, but mud above it contains rhizomes of *Triglochin maritimum*.

AGE AND CORRELATION

The sequence of soils and intervening mud at the Jensen locality spans the past 3,500–4,500 years. This estimate is based on the age of a stick associated with soil H—3,640±80 ^{14}C yr B.P. This stick undulated across the top of

Figure 26. Onlap of soil Y, and of the intertidal mud that buried it, onto upland at the south end of the Heron locality (fig. 25, upper diagram). Shovel handle 0.5 m long.

the soil. Its age shows that burial of soil H began no later than 3,500–4,500 years ago. Similarly, soil H at the Redtail locality was buried shortly before 3,570±70 ^{14}C yr B.P., the age of *Triglochin maritimum* rhizomes above the soil (table 7; fig. 27).

Three points suggest that typically faint soil L at the Jensen locality correlates with typically bold soil L at the Redtail locality, despite the greater abundance of peat in the latter:

1. The outer 25 rings of a spruce root in soil L at the Jensen locality gave a radiocarbon age—2,820±50 ^{14}C yr B.P.—similar to three of the four ages for soil L at the Redtail locality (table 7; fig. 32). This age is geologically reliable because the outermost of the dated rings probably formed during the year before the tree died from earthquake-induced submergence: this ring adjoins bark; and, like several tens of preceding rings, it is wide enough to imply vigorous tree growth up to the time of an earthquake.
2. In containing spruce roots, soil L at the Jensen locality resembles soil L, but not the root-free soil N, at the Redtail locality.
3. The typical faintness of soil L at the Jensen locality may be due to weathering in the profile of soil S. Whereas the top of soil S is at least 1 m above the top of soil L at the Redtail locality (fig. 13), the corresponding distance is 0.5 m at the Jensen locality.

These correlations of soils H and L are consistent with overall similarities among the Jensen, Redtail, and South Fork localities in the sequence and age of bold and faint soils (fig. 32). The sequence at the Jensen locality differs only in the presence of a faint soil—soil W—not recognized at the Redtail and South Fork localities. But as inferred on pages 45 and 63, poor preservation limits the traceable extent of soil W at the Oyster locality and probably accounts for the absence of soil W at the Redtail locality. The survey of the South Fork locality was completed in 1987, before findings elsewhere—especially at Elliott Slough (figs. 5, 32)

(Atwater, 1996, 1996, his fig. 23*B*) and the Oyster locality—alerted us to possible destruction of soils high in the profile of soil Y.

SEWER LOCALITY

The northeast bank of the Willapa River displays buried soils for much of the 5-km distance between the South Bend sewer ponds and the Willapa Harbor airport. We surveyed outcrops near the South Bend sewer ponds (the Sewer locality) and near the airport (the Airport locality) (fig.7). The buried soils at both these localities are exposed mainly in steep banks less than 2 m high. Additional outcrop below these banks slopes gently riverward and is commonly obscured by modern mud and (or) cut by bank-parallel fractures.

The surveyed outcrop at the Sewer locality extends 500 m northwestward from the pipe that carries effluent to the sewer ponds, which are situated on former tidal marsh north of the river. We noted an uppermost buried soil, soil Y, along the entire length of this outcrop, and we found a lower buried soil, termed soil S, along its northwestern half. Figure 29 depicts the outcrop's central 180 m, which contains representative stratigraphy and all the archaeological features noted at the locality.

BURIED SOILS

The northwestern part of the Sewer locality contains four buried soils. Only the lowest of these, soil S, is characteristically peaty. Soil Y is the next-most noticeable but mainly because the lowest 10–30 cm of the overlying mud is distinctively laminated with silt that etches on wave-washed faces (fig. 30*A*, *B*). Both the remaining, intervening soils (soils U and W) are faint, particularly the upper one. Like soil S, soils U and W are probably not exposed in the southeastern ¼ km of the outcrop.

We did not observe continuity of the buried soils as widely at the Sewer locality as at the Redtail, Oyster, and Jensen localities. In general, the soils at the Sewer locality cannot be seen where outcrop has not been scraped clean. None of the soils form widely visible breaks in the slope of the outcrop: soil S is commonly at or near the bottom of steep outcrop; none of the other soils are typically peaty; and steep outcrop is commonly cluttered by modern slumps and plants.

Where seen in outcrop, soils S and Y have maximum relief of ½ m. Between horizontal coordinates 360 and 290 m, soil Y rises southeastward to an enigmatic crest on the northwest margin of a tidal creek. This crest may be a natural levee or it may mimic relief from underlying archaeological material. However, neither of these explanations accounts for the similar height of soil Y between coordinates 260 and 180 m, where nearby tidal creeks are lacking and cultural deposits are scarce (fig. 29).

The surficial horizon of soil Y ranges from peaty mud 1–2 cm thick to dark mud as little as 0.5 cm thick, probably because of variable decomposition after burial. The soil is peatiest at low altitude, where the lowest part of the overlying mud locally contains *Triglochin maritimum* rhizomes. At high altitude the surficial horizon of the soil contains no peat (fig. 30*A*, *B*), the overlying mud lacks *Triglochin maritimum* rhizomes, and mud both above and below the surficial horizon of the soil is commonly firmer and more oxidized (redder) than at low altitude. These differences imply that where soil Y is high and faint, the weathering profile of the modern marsh has extended through the surficial horizon of the underlying buried soil and has contributed to the decomposition of any peat or overlying rhizomes that may have been present soon after burial.

GROWTH-POSITION FOSSILS OF VASCULAR PLANTS

Growth-position fossils show that soil Y formed at higher altitude than did mud that overlies the soil. Whereas the soil contains sparse stumps of shrubs (perhaps western crabapple; fig.30*B*), the overlying mud locally contains growth-position rhizomes of *Triglochin maritimum*.

Vascular-plant fossils in growth position are absent within, and sparse or absent immediately above, the other buried soils. Mud above soil S contains rhizomes of *Triglochin martima* at several surveyed points, as does mud above soil U at one such point. However, we did not find remains of plants that had lived on either of these soils, nor did we find any vascular-plant fossils within or immediately above faint soil W. Like the widespread lack of preserved peat and vascular-plant fossils in overlying soil Y, and also in soil U at the Oyster locality (p. 45), this paucity or absence of vascular-plant fossils probably reflects decomposition after burial, not initial absence.

CULTURAL DEPOSITS

The Sewer locality served as a prehistoric fishing camp (Smithsonian site number 45–PC–103). Cultural deposits underlie soil Y, and stubs of probably contemporaneous fish weirs remain visible on an adjacent tidal flat.

The cultural deposits are 5–20 cm below the top of soil Y, from which they are separated by mud (figs. 29, 30*A*, *B*). The cultural deposits, in bodies as much as 18 m long and 0.4 m thick, consist of black carbonaceous mud and sand. Within this mud and sand are charcoal, cracked rock, and lenses of reddish-brown fire ash containing fish vertebrae. In places the carbonaceous deposits continue downward, into underlying mud, as filled holes about 5 cm in diameter (figs. 29, 30*A*). The holes were probably left by stakes: we found laminae bent downward beside one of the holes, and we found the charred, nearly vertical lower tip of a stake about 3 cm in diameter near a probable fire pit (fig. 29, horizontal coordinates 298.5 and 295.5, respectively).

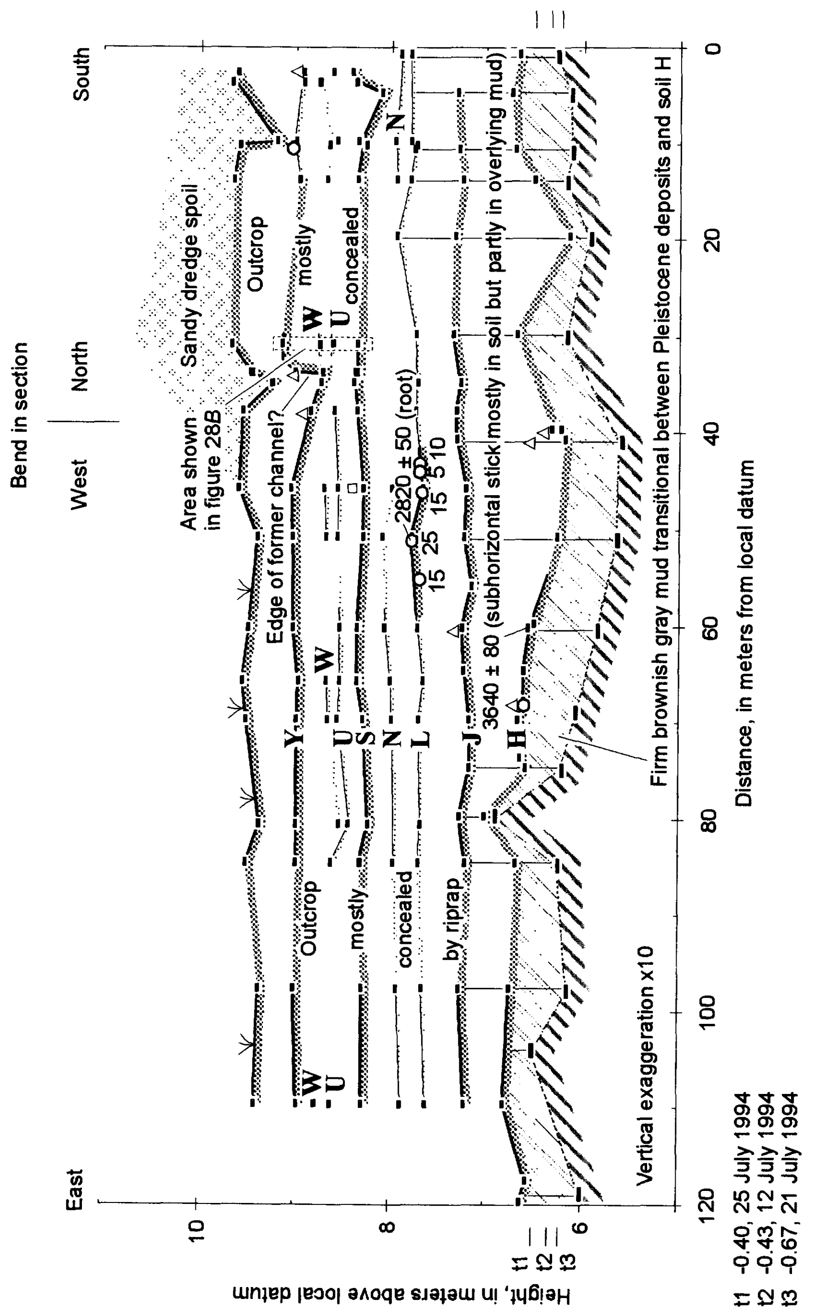

Figure 27. Stratigraphy at Jensen locality, Willapa River.

A fish weir was built or repaired at the Sewer locality between A.D. 1400 and 1650 (p. 54). The dated weir and a second, similar feature are located on a tidal flat 10–25 m southwest of (riverward from) the steep riverbank outcrop and 25–100 m southeast of (upriver from) the cultural deposits (fig. 30*C*, *D*). Their remains comprise hundreds of vertical sticks arrayed in V-shaped lines 5–15 m long. The sticks retain bark and sound wood below the soupy modern mud that veneers the tidal flat, and they protrude as rotten, worm-bored stubs as much as 15 cm above the flat.

FOSSIL DIATOMS

Diatom assemblages across the top of soil Y, sampled at horizontal coordinate 299 m (fig. 29), show that the soil formed at higher altitude than did the overlying mud. The faint surficial horizon of soil Y contains diatom fragments and abundant pollen grains suggestive of conditions near or above the level of highest tides. By contrast, mud above the soil contains many tidal-flat diatoms (for example, *Rhaphoneis psammicola*, *Synedra fasciculata*, *Thalassionema nitzs-*

EXPLANATION

	Top of soil—Shown by solid line where continuity observed; shown only by top of shading where continuity inferred
▪	Surveyed point
▨	Bold soil
░	Faint soil
S	Letter name of buried soil
////	**Top of Pleistocene deposits**—Marked by hard angular aggregates of greenish mud
>	**Live herbaceous plants of modern marsh**
15 O	**Fossil spruce root**—Numerals denote diameter, in centimeters
◇	**Fossil rhizomes of *Triglochin maritimum***
◁	Surveyed position of highest rhizomes
□	Surveyed position of lowest rhizomes
	Fossil rhizomes probably of *Carex lyngbyei*
2820 ± 50	**Radiocarbon age**—In ^{14}C years before A.D. 1950 (table 7)
t1 -0.40, 25 July 1994 —	**Low tide**—Height as predicted in tide tables; unit is meters relative to mean lower low water
|	**Boring**—Made with gouge corer 2 cm in diameter

Figure 27. Continued.

chioides, *Nitzschia sigma*), consistent with the presence of *Triglochin maritimum* rhizomes in mud above the soil 40 m to the northwest.

Diatom assemblages centimeters below the top of soil Y are too sparse to be diagnostic of any depositional environment. The few diatoms in mud between the cultural deposit and the top of soil Y are dominated by tidal-flat species (for example, *Rhaphoneis psammicola*, *Delphineis* cf. *surirella*, *Dimeregramma minor*). The cultural deposit itself contains rare fresh to brackish soil diatoms, including *Hantzschia amphioxys* and *Cosmioneis muticoides*.

AGE AND CORRELATION

We correlate buried soils at the Sewer locality with four soils at the Niawiakum River on the basis of approximate similarity in stratigraphic sequence and radiocarbon age (fig. 32). Although generally fainter than soil Y along the Niawiakum River, the uppermost buried soil at the Sewer locality resembles that soil in recording an altitude higher than is represented by overlying mud. Moreover, a radiocarbon age of 90±60 ^{14}C yr B.P. was obtained on outer rings of one of the shrub stumps rooted in soil Y at the Sewer locality (fig. 29). This age, which corresponds to A.D. 1650 or later, is indistinguishable from outer-ring ages of earthquake-killed spruce rooted in soil Y at the Niawiakum and Copalis Rivers (fig. 32). In addition, the age overlaps, at one quoted error, with the weighted-mean age of 161±15 ^{14}C yr B.P. from the eight separately dated earthquake-killed herbs rooted in soil Y at the Oyster locality (fig. 18; table 7).

Correlation of soil S at the Sewer locality with soil S at the Oyster locality is not supported by the large difference in radiocarbon ages for *Triglochin maritimum* rhizomes in overlying mud: 1,990±70 ^{14}C yr B.P. at the Sewer locality (fig. 29), as compared with ages of 1,598±23 and 1,630±70 ^{14}C yr B.P. on splits of a sample from the Oyster locality (fig. 18; table 7). However, old plant fragments may have contaminated the dated rhizomes from the Sewer locality. These rhizomes, collected rotten nearly beyond recognition, were not cleansed of interstitial mud, which may have contained older plant detritus. By contrast, the dated rhizomes from the Oyster locality were nearly as fresh as modern rhizomes, a condition that allowed vigorous cleaning under tapwater and verification that the dated material contained little or no old detritus.

The fishing camp recorded by the cultural deposits originated after A.D. 1100, and the weirs were built or repaired sometime between 1400 and 1650. These estimates are based on radiocarbon dating of the stake with the charred lower tip (710±70 ^{14}C yr B.P.) and of a bark-bearing stave from one of the weirs (380±50 ^{14}C yr B.P.) (fig. 29). The camp was abandoned years to centuries before burial of soil Y began at the Sewer locality, as shown by the mud that separates cultural deposits from the surficial horizon of the soil.

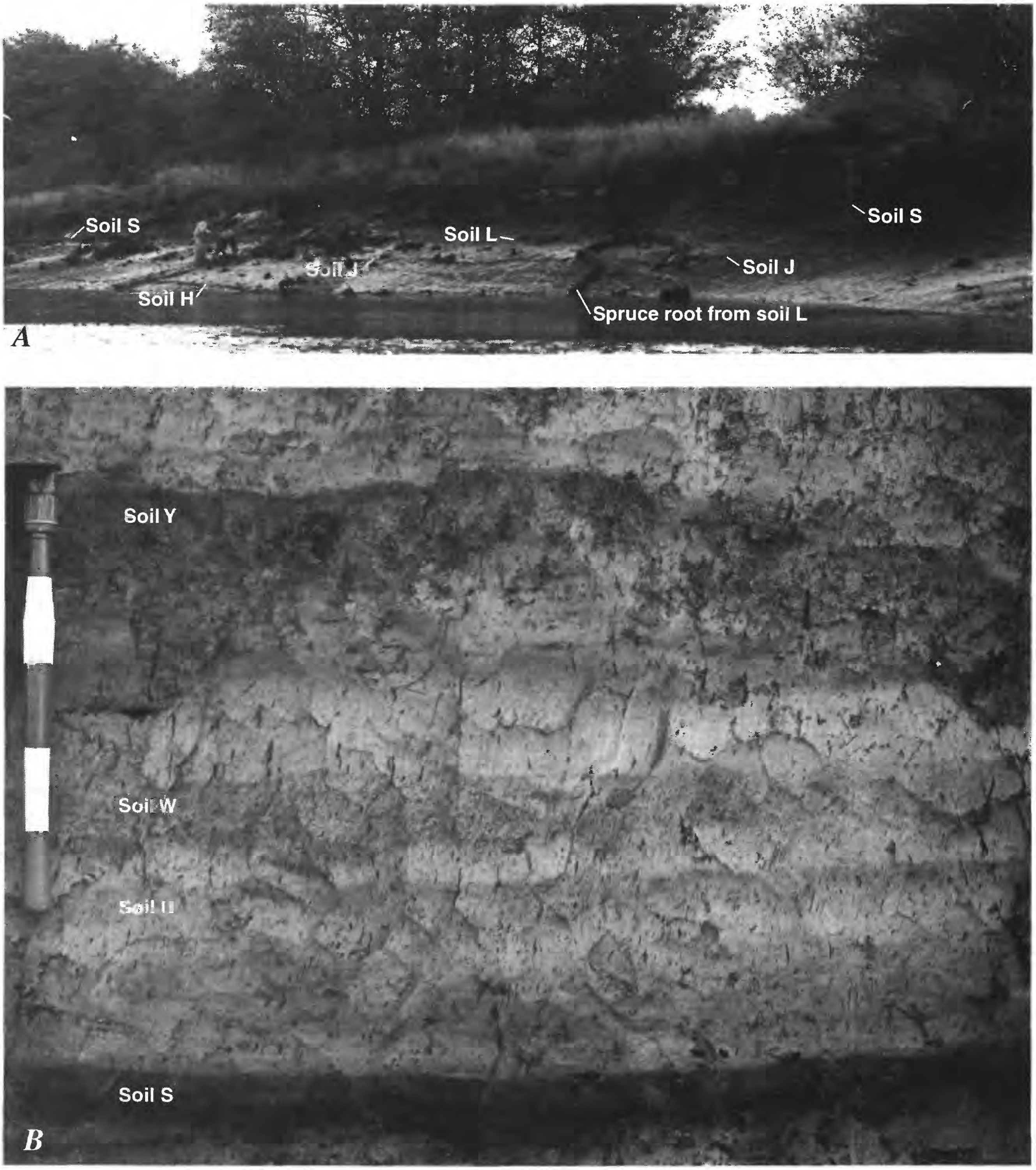

Figure 28. Jensen locality, Willapa River (fig. 27). *A*, Overview of outcrop along dredge cut (fig.7). View to southeast; horizontal coordinate 40 m is near right edge of area shown. The most extensive, resistant layer visible in the outcrop is soil S. *B*, Bold soils S and Y and intervening faint soils U and W near horizontal coordinate 32 m. Shovel handle is 0.5 m long.

AIRPORT LOCALITY

Two buried soils are widely exposed at the Airport locality and a third, intervening soil is exposed in the southeastern part of this locality (fig. 31). The uppermost soil, equivalent to soil Y at the other localities, is commonly overlain by mud that contains *Triglochin maritimum* rhizomes. Such rhizomes also overlie the lowest soil at the edge of a filled channel. This lowest soil, equivalent to soil U, is typically faint but locally retains a peaty surficial horizon and rhizomes of the high-marsh plant *Juncus balticus*. The faintness and stratigraphic position of the intervening soil suggest correlation with soil W.

Triglochin maritimum rhizomes above soil U at the Airport locality gave a radiocarbon age of 1,247±22 ^{14}C yr B.P. (table 7; fig. 31). The age resembles that obtained from stratigraphically similar rhizomes at the Oyster locality, 1,300±25 ^{14}C yr B.P. (fig. 18, age A).

DISTINCTION BETWEEN TECTONIC SUBSIDENCE DURING EARTHQUAKES AND OTHER WAYS OF PRODUCING THE BURIED SOILS

Buried soils at estuaries can record tectonic subsidence that accompanies earthquakes (fig. 2*A*). Near Anchorage, Alaska, subsidence during the great 1964 Alaska earthquake lowered marshes and forests to the level of tidal mudflats. As a result of this subsidence, peaty soils of the marshes and forests became covered by 1–2 m of tidal-flat mud by the early 1970's (Ovenshine and others, 1976).

Similar buried soils might also be produced, however, by other means (Nelson and others, 1996b; Peterson and Darienzo, 1996). These include cut and fill by migrating tidal streams, deposition by storms and floods, a fluctuating rise in sea level combined with variable sedimentation rates, breaching of bay-mouth barriers, settlement from earthquake-induced compaction, and rapid aseismic folding.

We found no evidence that alternatives to coseismic tectonic subsidence better explain any of the buried soils that we surveyed. However, criteria for identifying such subsidence can be applied more securely to some buried soils than to others. We ruled out cut and fill for most buried soils in most of the surveyed outcrops. In many cases we also ruled out deposition by storms or floods; in some cases we ruled out rise in tide level from sea-level rise and barrier breaching; and in some cases we can also show that subsidence had a tectonic, probably coseismic component. Finally, we used similarities in stratigraphic sequence and radiocarbon age to extrapolate from these various cases to all soils correlated among the surveyed outcrops.

CUT AND FILL BY TIDAL STREAMS

Most of the buried soils have less relief and more lateral continuity than is likely for a mud-over-peat contact from fluvial cutting and filling. Relief on the buried soils resembles the typically low relief on modern tidal marshes. This low relief contrasts with the unconformities observed for modern and filled channels (figs. 13, 18, 19*A–C*, 29, 31). In addition, the preservation of herbaceous stems and leaves rooted in some of the soils—particularly in soils S and Y at the Oyster locality—shows that the tops of those soils underwent little or no erosion before burial. The sole candidate for cut and fill is faint soil W at the Jensen locality, and this only because the soil is so poorly preserved that its relief and continuity are unclear.

Lateral continuity has also been checked through drilling of boreholes away from modern tidal streams at several localities in southern coastal Washington. Most such work has been done to check for tsunami deposits on soil Y along the Niawiakum River—about 50 borings in reconnaissance (Atwater, 1987) and about 200 additional borings made by M.A. Reinhart and several coworkers (compiled by Atwater, 1996, his fig. 22C). Borings have also demonstrated continuity of buried soils beneath marshes along the Johns River, at Grays Harbor (fig. 5) (M.A. Reinhart, written commun., 1993; Shennan and others, 1996).

DEPOSITION BY STORMS OR FLOODS

Fossils show that storms or floods alone cannot account for the burial of many of the soils. Burial of a soil by storm or flood deposits builds land higher. By contrast, fossils in mud above many of the buried soils record conditions of *lower* altitude than do fossils within the soils (fig. 32). Such a contrast is shown by vascular-plant fossils in growth position associated with soil J at the Redtail locality; soils S, U, and Y at the Oyster locality; soils H and Y at the Jensen locality; soil Y at the Sewer locality; and soil U at the Airport locality. Contrasting altitudes are also implied by diatom assemblages associated with soils J, L, N, S, U, and Y at the Redtail locality; by diatom assemblages associated with soils S, U, and Y at the Oyster locality; and, less dramatically, by diatom assemblages associated with soil W at the Oyster locality (p. 52). Many additional soils are associated with half the vascular-plant evidence for change in altitude: either they contain growth-position fossils of high-marsh or upland plants, or they are overlain by mud having fossils of low-marsh plants.

If the soils correlate as inferred in figure 32, the storm and flood hypotheses can be ruled out for every buried soil shown in figures 13 through 31. On the basis of preserved vascular-plant fossils alone, correlation would rule out the storm and flood hypotheses for soils H, J, S, U, and Y. Storm and flood can be further ruled out for these soils, and for soils N and W as well, by correlation with soils associated with contrasting diatom assemblages at the Redtail locality (soils J, L, N, S, U, and Y; fig. 15) and the Oyster locality (soils S, U, W, and Y; fig. 20). Similarly, the storm and flood hypotheses are precluded by changes in fossil diatom and pollen assemblages that Shennan and others (1996) found associated with soils at the Johns River (fig. 5) that probably correlate with soils L, N, S, U, and Y at Willapa Bay (fig. 32).

FLUCTUATIONS IN SEA LEVEL

Fluctuations in sea level have been implicated in the interbedding of lowland peat and tidal-flat mud in tectonically stable areas. Late Holocene peat layers intercalated

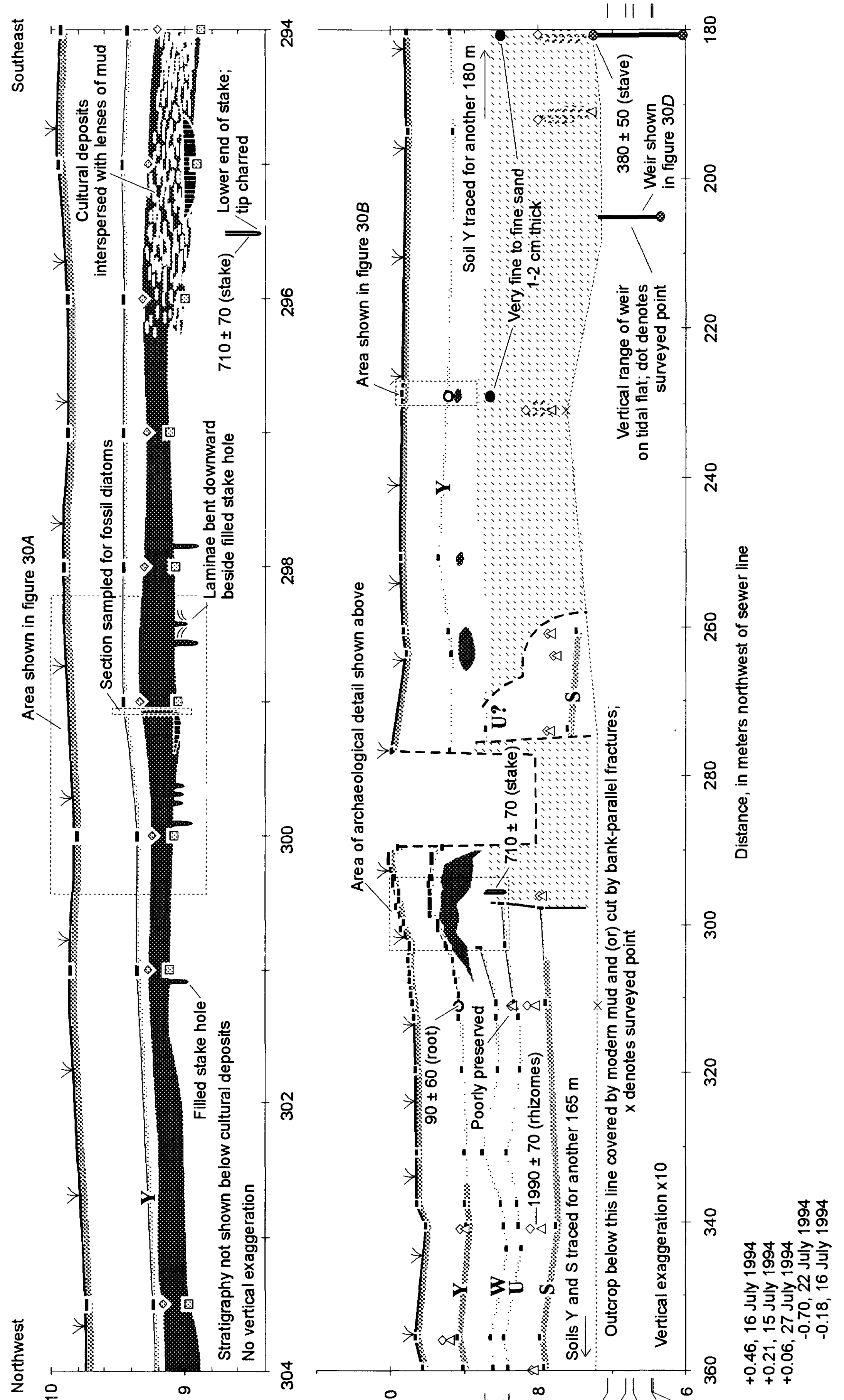

Figure 29. Stratigraphy at Sewer locality, Willapa River.

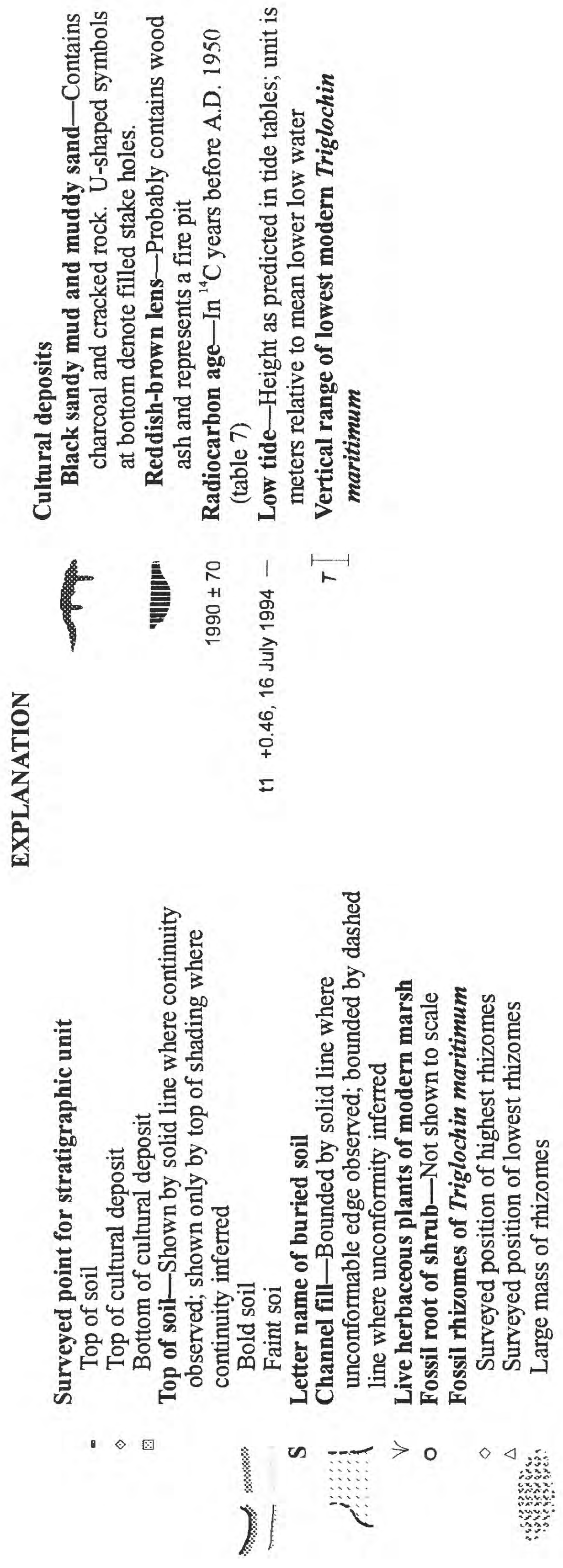

Figure 29. Continued.

with tidal-flat deposits are widespread in northwestern Europe (Jelgersma, 1961; Streif, 1972; Devoy, 1979) and the eastern United States (Johnson, 1925, his fig. 259B; van de Plassche, 1991;Varekamp and others, 1992; Fletcher and others, 1993a, b). As at Willapa Bay, peat layers locally form soils of submerged forests (Reid, 1913, p. 6–8). Also as at Willapa Bay, peat layers can be correlated regionally by stratigraphic sequence (Jelgersma and others, 1979, p. 131–134) and radiocarbon age (Geyh, 1980; Shennan and others, 1983). Sea-level fluctuations are commonly invoked to explain the alternation between peat and mud, as illustrated by Meyerson (1972), Devoy (1979, p. 388), Behre and others (1979, p. 102–103), Shennan (1986), van de Plassche (1991), Varekamp and others (1992), and Fletcher and others (1993a, b).

None of the buried soils in our surveyed outcrops, however, suggest fluctuations in sea level. Such an origin for the soils tends to be ruled out by abrupt changes in herbaceous and microscopic fossils, by the occurrence of tsunamis at the onset of burial, and by tidal-marsh deposits that record gradual submergence elsewhere in the region.

ABRUPT CHANGES IN HERBACEOUS FOSSILS

Only extremely rapid rise in sea level is likely to have allowed preservation of the herbaceous fossils that are rooted in soils S, U, and Y at the Oyster locality (fig. 18), in probable correlatives of soils L and S at the Johns River, or in soil Y at the Copalis River (Atwater, 1992, p. 1908–1909). These fossils, consisting of stems and leaves rooted in the buried soil and entombed in overlying tidal-flat mud, show that tidal submergence and consequent burial were completed before the stems and leaves had time to decompose. From casual inspection we estimate that such decomposition takes place within a few years on modern high marsh at Willapa Bay. The fossils thereby imply submergence too fast for most sea-level rise in the past few thousand years (Atwater and Yamaguchi, 1991; Jacoby and others, 1995).

There remains a possibility that rapid but nontectonic rise in sea level would allow preservation of herbaceous stems and leaves that had been above ground and in growth position as the sea began to rise. Such fossils might be present in Delaware, where “stems and roots” and “rhizomes and stalks” are preserved at a mud-over-peat contact in Holocene tidal-marsh deposits (Fletcher and others, 1993a, p. 123; Fletcher and others, 1993b, p. 185). Fletcher and his coworkers ascribed the contact to a rapid, nontectonic rise in sea level. They did not, however, show that the fossils had been subaerial when the inferred rise began.

ABRUPT CHANGES IN MICROSCOPIC FOSSILS

Sea-level rise also appears inconsistent with abrupt changes in microfossil assemblages at the contact between buried soils and overlying mud. Such changes have been

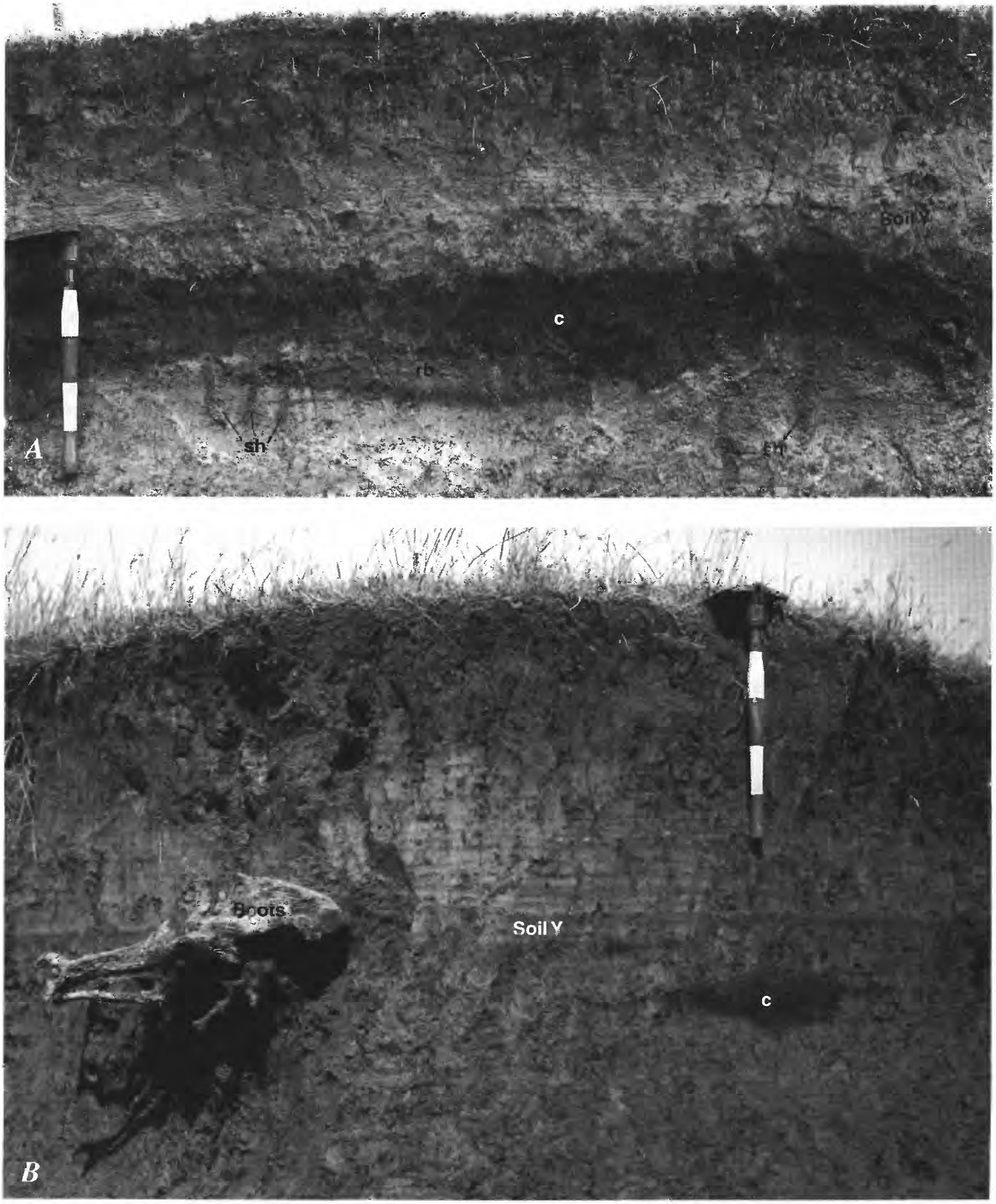

Figure 30. Sewer locality, Willapa River (fig. 29). *A*, *B*, Faint soil Y and associated cultural deposits. Top of soil Y marked by shovel blade at left in *A*; mud above soil contains laminae of silt that are particularly distinct in *B*. Modern tidal marsh at top. Darkest deposit in both photographs is carbonaceous mud and sandy mud (c) containing charcoal, cracked rock, and (in *A*) a reddish-brown lens (rb) probably made largely of ash from wood fires. These cultural deposits form a bed 25 cm thick in *A*, a lens as much as 15 cm thick below the shovel in *B*, and the fill of stake holes (sh) in *A*. Roots of a shrub, perhaps western crabapple, protrude from soil Y at left in *B*. Centers of photographs near horizontal coordinates 299 m (*A*) and 228 m (*B*).

Figure 30. *C*, *D*, Weirs on tidal flat adjacent to outcrop. View in *C* is to the southeast, upriver; outcrop is vertical bank at left, weirs are lines of stakes at center and right. View in *D* is to the southeast along long arm of weir centered near horizontal coordinate 205 m.

documented not only for diatoms at the Redtail and Oyster localities (figs. 15, 20) but also for diatoms, pollen, and foraminifera at the Johns River (Shennan and others, 1996). Shennan and his coworkers used samples collected at 1-cm intervals in the uppermost 5–15 cm of each of six buried soils and in the lowest 5 cm of mud immediately above each of these soils.

The abrupt changes in microfossil assemblages cannot have resulted from gradual rise in sea level unless gradual transitions in assemblages have been removed by widespread erosion. We recognized no widespread unconformities at the surveyed localities. Moreover, erosion can be ruled out where formerly subaerial stems and leaves of herbaceous plants are preserved in growth position on the soils. Such fossils are associated with diatom evidence for sudden submergence of soils S, U, and Y at the Oyster locality (fig. 20) and of soil L at the Johns River (Atwater, 1992, his table 1, locality 14, depth 3.0 m; Shennan and others, 1996, their horizon V).

TSUNAMIS

At least three of the buried soils are associated with evidence that a tsunami coincided with the event that caused the soil to undergo lasting submergence and consequent burial. Such coincidence would be expected of coseismic subsidence because tsunamis typically result from sudden

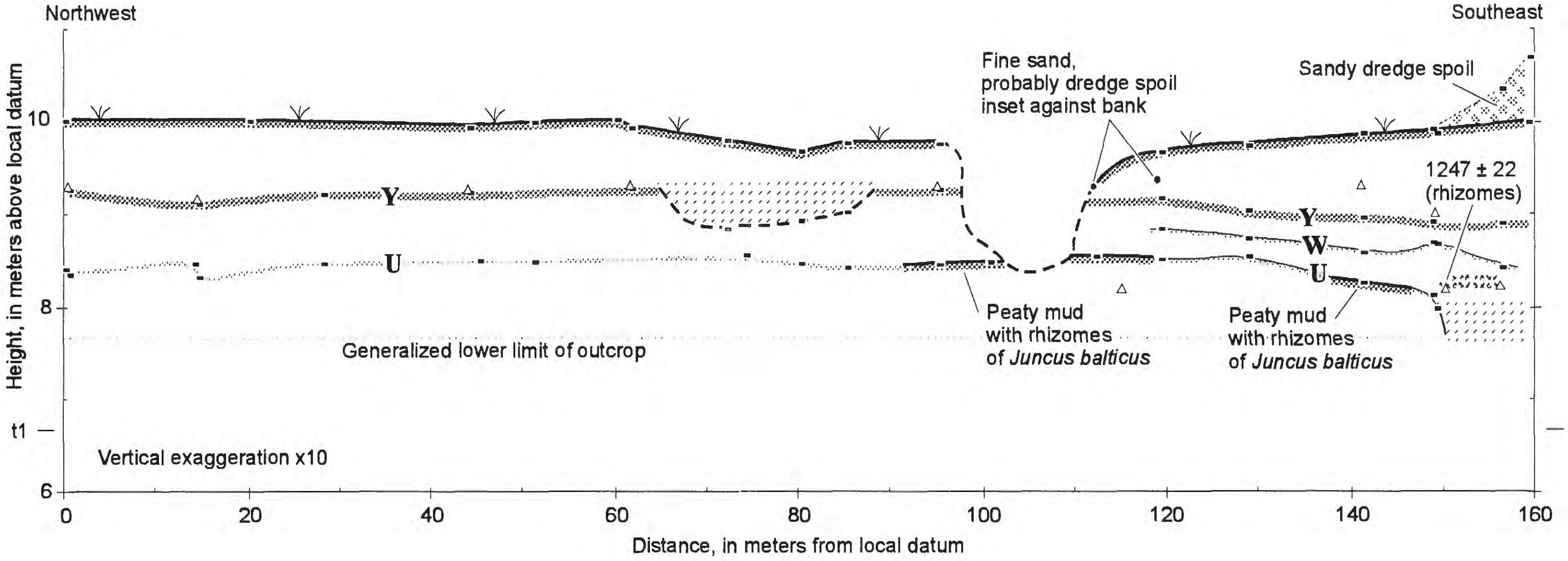

EXPLANATION

Top of soil—Shown by solid line where continuity observed; shown only by top of shading where continuity inferred
- ▪ Surveyed point
- ▨ Bold soil
- ····· Faint soil
- S Letter name of buried soil

Channel fill—Bounded by solid line where unconformable edge observed; bounded by dashed line where unconformity inferred

ѱ **Live herbaceous plants of modern marsh**

Fossil rhizomes of *Triglochin maritimum*
- △ Surveyed position
- ▨ Large mass of rhizomes

1247 ± 22 **Radiocarbon age**—In ^{14}C years before A.D. 1950 (table 7)

t1 -0.52, 8 July 1994 — **Low tide**—Height as predicted in tide tables; unit is meters relative to mean lower low water

Figure 31. Stratigraphy at Airport locality, Willapa River.

sea-floor displacement. By contrast, a tsunami need not coincide with an aseismic change in sea level.

A tsunami deposit can record coincidence with coseismic subsidence by resting on a suddenly subsided soil and by surrounding the remains of plants that had been living on the soil before it subsided (fig. 2*B*). Such is the case for the sand sheet on soil Y along the Niawiakum River (p. 27). Moreover, this sand sheet probably grades upvalley into mud that contains diatoms probably transported by tsunami (p. 63). Similar mud implies that tsunamis coincided with the subsidence marked by soils N and S along the Niawiakum River (p. 29).

The lack of recognized tsunami deposits above other buried soils in the surveyed outcrops is open to many explanations other than aseismic subsidence of the soils. Tsunami deposition should depend on the size of the tsunami, which is likely to vary with the location of earthquake ruptures (Geist and Yoshioka, 1996) and perhaps also with the size and location of coseismic submarine landslides. Tsunami deposition along the Niawiakum and Willapa Rivers may also vary with the shape of channels connecting these streams to the Pacific Ocean. Moreover, both the Niawiakum River and the Willapa River may be too far inland to have received much sand from most tsunamis generated at the Cascadia subduction zone. They are much farther from the coast than are sites having multiple sandy tsunami deposits: the Copalis River, where a probable correlative of soil S is widely overlain by sand (fig. 32; Atwater, 1992); several estuaries in northern Oregon where sand is common on such possible correlatives of soils S and U (Darienzo and others, 1994; Darienzo and Peterson, 1995); and a coastal lake near Cape Blanco, Oregon, that has been invaded by tsunami as many as 14 times in the past 7,500 years (Nelson and others, 1996c).

GRADUAL SUBMERGENCE ELSEWHERE IN THE REGION

If buried soils at Willapa Bay are due to nontectonic fluctuations of sea level in the past 3,500 years, the fluctuations did not extend into areas of Washington and Oregon that contain thick deposits of tidal-marsh peat from the past several thousand years. Such areas include a site at northern Puget Sound (Eronen and others, 1987) and sites along the south-central coast of Oregon (Nelson, 1992a; Nelson and others, 1996b).

The peat in these areas, which formed during the past several thousand years, probably resembles classic evidence for gradual submergence in Massachusetts. There, tidal-marsh peat several meters thick is pervaded by growth-position roots and rhizomes of plants that thrive only near high-tide levels; submergence occurred gradually enough for marshes to build upward apace with the sea (Mudge, 1862; Redfield, 1972, p. 210).

While gradual submergence at Puget Sound and southern Oregon was allowing tidal marshes to persist, jerky submergence in southern coastal Washington abruptly changed tidal marshes into tidal flats. The coexistence of these two styles of submergence can be explained most simply by gradual submergence throughout the region and by coseismic subsidence of more limited extent (Atwater, 1987).

BREACHING OF BAY-MOUTH BARRIERS

If Willapa Bay had a barrier at its mouth that limited the tidal range behind it, the breaching of such a barrier might cause high-tide levels to rise, thereby producing buried soils similar to those produced by subsidence during earthquakes. Such tide-level rise "has, for a long time, been the mechanism used to explain the intercalated peats and clays" of northwestern Europe (Shennan, 1986, p. 121), as illustrated by Jelgersma and others (1979, p. 139). It has also been invoked for some of the interbedding of peat and mud at Coos Bay, Oregon (Nelson and others, 1996a, p. 151–152). But neither historical records nor fossils imply that barrier breaching contributed to the episodic late Holocene submergence and burial of wetland soils in southern coastal Washington.

Historical records provide no basis for inferring past blockage of the largest estuaries in southern coastal Washington. Although associated with treacherous offshore bars, Willapa Bay, Grays Harbor, and the Columbia River have stayed fully open to the sea since Euro-Americans first entered them about 200 years ago. A likely explanation is that the estuaries discharge too much freshwater to the sea, and tidally exchange too much water with it, to have been blocked by barrier sand. The tidal prisms are huge—½ km^3 for Willapa Bay and Grays Harbor, 1 km^3 for the Columbia River (Johnson, 1973)—and so is the freshwater discharge of the Columbia River.

Fossils preclude bay-mouth blockage if such blockage would have turned Willapa Bay into a freshwater lake in the years just before buried soils were submerged and buried. Instead of freshwater plants like cattails and willows, soils S and Y at the Oyster locality supported the brackish-water tidal assemblage of *Deschampsia caespitosa*, *Potentilla pacifica*, and *Juncus balticus*. Moreover, soil U at the Oyster locality was largely covered by the halophyte *Salicornia virginica*. Inflow of seawater is further implied by diatom assemblages in the surficial horizon of soils S, U, W, and Y at the Oyster locality; in the surficial horizon of soils J, L, and U at the Redtail locality; and just beneath the surficial horizon of soil N at the Redtail locality. None of the diatom assemblages studied at either of these localities are consistent with prevalence of standing freshwater.

Fossils similarly imply seawater inflow to the Copalis River and Grays Harbor just prior to the burial of one or more soils at these estuaries. *Deschampsia caespitosa*, *Potentilla pacifica*, and *Juncus balticus* were living along the Copalis River when a probable correlative of soil Y was suddenly submerged (Atwater, 1992, p. 1908–1909). These species also lived on probable correlatives of soils L and Y at Grays Harbor, along the Johns River (Atwater, 1992, localities 13 and 14 of his table 1 and his figs. 6, 7). Moreover, the mouth of the Johns River was also bordered by a *Triglochin maritimum* low marsh at the time of the submergence marked by soil Y (Atwater, 1992, locality 12 in his table 1 and his figs. 6, 7). Annual freshwater inflow to Grays Harbor averages about 10 km^3 (Peterson and others, 1984, p. 88), 10 times the high-tide volume of Grays Harbor (Barrick, 1975, p. A–6). If a barrier greatly limited seawater inflow to Grays Harbor before sudden submergence of soil Y, salinity along the Johns River should have been low enough to favor freshwater plants over *Triglochin maritimum.*

SETTLEMENT FROM COMPACTION DURING SHAKING

Seismic shaking can produce localized submergence through compaction and consequent settlement of unconsolidated deposits. Such settlement from the 1964 Alaska earthquake widely affected estuarine and alluvial deposits (Plafker and Kachadoorian, 1966, p. D13–D18; Plafker, 1969, his plate 4B and fig. 27) and locally doubled the total subsidence near Portage (McCulloch and Bonilla, 1970, p. D81). Settlement may also have contributed to coastal submergence in Chile during the 1960 Chile earthquake (Plafker and Savage, 1970, p. 1006, their table 1, and their fig. 5A).

Although settlement may have augmented tectonic subsidence in southern coastal Washington, it cannot account for all the evidence for subsidence. If most or all the subsidence were due to settlement, buried soils would merge where they are underlain, at shallow depth, by well-consolidated Pleistocene deposits. Such is not the case, however, at the Jensen locality, where successive, distinct soils have a shallow, subhorizontal foundation of stiff Pleistocene mud (fig. 27). Moreover, buried soils remain distinct where they lap onto uplands made of well-consolidated Pleistocene deposits, as shown along the Niawiakum and Copalis Rivers (Atwater, 1992, p. 1909). Such onlap is conspicuous at the Heron locality (fig. 26; p. 63), where soil Y, covered by tidal deposits, ascends a valley wall composed of stiff Pleistocene mud. This evidence shows that the upland, as well as soil Y, subsided into the intertidal zone, consistent with tectonic subsidence but not with subsidence limited to poorly consolidated valley fill.

TECTONIC SUBSIDENCE NOT ATTENDED BY SEISMIC SHAKING

Two lines of evidence suggest that none of the buried soils at northeastern Willapa Bay are likely to record rapid tectonic subsidence that was not attended by seismic shaking. First, as discussed on pages 100 and 102, subsidence marked by soils J and younger may correlate with turbidity currents that probably resulted from shaking about 50 km west of Willapa Bay. Second, as discussed here, subsidence marked by buried soils Y and S probably correlates with liquefaction a few tens of kilometers to the south. Liquefaction has also been inferred to correlate with the subsidence marked by soil W, but shaking was not necessarily involved in this case.

A buried soil probably correlative with soil Y is widely associated with liquefaction features along the lower Columbia River about 30–45 km east of the Pacific coast. The features, discovered by Obermeier (1995), are further documented in observations compiled by Atwater (1994). Although most of the liquefaction features are dikes that do not extend to the top of the soil, some of the intrusions appear continuous with sand lenses that rest directly on the soil. The stratigraphic position of the sand lenses, which resembles that of the tsunami deposits at the Oyster and Redtail localities, implies that the sand was vented during or soon after the land subsided (fig.2*C*).

A buried soil probably correlative with soil S is associated with several gravelly dikes along the Naselle River of southern Willapa Bay. These dikes, discovered in 1995 by Alan Mortimer, Judith Boughner, and Brian Atwater, are a few tens of meters downstream from locality 20 of Atwater (1992), which is the outcrop described by Ota and Umitsu (1995). At least one of the dikes is low in a mud-filled crack that extends upward to, but not above, a buried tidal flat continuous with the probable correlative of soil S. Mud-filled cracks continuous with dikes below are among the geologic features near Anchorage, Alaska, that record liquefaction from the 1964 Alaska earthquake (Walsh and others, 1995, their figs. 15, 17, 21, 24, 33, 34, and 55). We infer that the similar crack at the Naselle River records lateral spreading that coincided with the sudden subsidence marked by soil S.

Enigmatic sand bodies mistakenly ascribed to liquefaction are present along the Copalis River, where they formed between 900 and 1,300 years ago (Atwater, 1992). Although probably caused by an earthquake and perhaps correlative with submergence marked elsewhere by soil W and its correlatives, these sand bodies do not appear to record seismic shaking (p. 83).

DISTINCTION BETWEEN PLATE-BOUNDARY AND UPPER-PLATE SOURCES FOR THE EARTHQUAKES

Geophysics provides starting points for implicating plate-boundary earthquakes in coseismic subsidence along the Pacific coast at the Cascadia subduction zone:

1. Plate-boundary earthquakes could have caused widespread, sudden subsidence by elastically thinning the North America plate. Possible analogs include the sudden subsidence of coastal areas hundreds of kilometers long during great historical earthquakes at subduction zones in Alaska, Chile, and Japan (Heaton and Hartzell, 1986).
2. The Cascadia plate boundary resembles, in age of subducting lithosphere and rate of convergence, some plate

boundaries elsewhere on which great earthquakes have occurred historically (Heaton and Hartzell, 1987; Rogers, 1988).

3. A large fraction of the shallow slip between the Juan de Fuca and North America plates should occur during earthquakes, according to a recent hypothesis about forces from plate motions (Scholz and Campos, 1995, p. 22112).
4. The Cascadia subduction zone is likely to be accumulating energy for release in future plate-boundary earthquakes, according to interpretation of geodetic surveys and heat-flow models (Savage and others, 1991; Hyndman and Wang, 1993, 1995; Dragert and others, 1994; Mitchell and others, 1994; Dragert and Hyndman, 1995).

The alternative of upper-plate earthquakes arises where sudden coastal subsidence may have been limited to areas along faults or folds in the North America plate. Such localized subsidence has been documented for a syncline in northern California that trends approximately parallel to nearby thrust faults having Holocene slip (Clarke and Carver, 1992). Farther north, subsidence during the past few thousand years may have been localized along coastal synclines in south-central Oregon (McInelly and Kelsey, 1990; Nelson, 1992a; Nelson and Personius, 1996). In addition, upper-plate faults off the Pacific coast of Oregon and Washington have slipped in the past 10,000 years, and some of the estuaries having evidence for sudden subsidence have been correlated with such youthful structures mapped offshore (Goldfinger and others, 1992a, b; McNeill and others, 1994; McCaffrey and Goldfinger, 1995). The subduction zone along the North Island, New Zealand, may contain analogs for land-level change during upper-plate earthquakes at the Cascadia subduction zone. Some of the prehistoric, Holocene marine terraces on the North Island represent coseismic uplift that was not necessarily accompanied by seismic slip on the subduction boundary between the Pacific and Australian plates (Berryman and others, 1989; Berryman, 1993).

Coastal geology provides at least two criteria for distinguishing between plate-boundary earthquakes and upper-plate earthquakes as causes of coseismic subsidence at the Cascadia subduction zone. One of these is the extent of subsidence having the same approximate age. Unlike a single plate-boundary rupture at the Cascadia subduction zone, a series of earthquakes on faults in the North America plate could be distributed through enough time for radiocarbon detection of differences in dates of subsidence. Such differences have not been detected for the best dated and most recent of the prehistoric sudden subsidence (Nelson and others, 1995). Instead, high-precision radiocarbon dating shows that the most recent sudden subsidence at Willapa and Humboldt Bays, 625 km apart along the subduction zone, occurred during the same few decades in the early 1700's (fig. 33). Additional radiocarbon dating of lower resolution, employing subsidence-killed herbaceous plants, shows that the most recent coseismic subsidence postdates A.D. 1660 at the six estuaries where such plants have been dated: the Copalis River and Willapa Bay, Washington; and Netarts Bay and the Nehalem, Salmon, and Coquille Rivers, Oregon (localities shown by herb symbols in fig. 1).

The sense of coseismic land-level change on anticlines provides a second criterion for distinguishing between plate-boundary earthquakes and upper-plate earthquakes. This criterion is based on two assumptions:

1. An anticline can subside during a plate-boundary earthquake at a subduction zone by participating passively in the coseismic thinning of the upper plate. In a well-studied example, a magnitude-9.2 earthquake on the subduction zone in Alaska in 1964 was accompanied by subsidence throughout an Alaskan area 800 km long and more than 100 km wide (Plafker, 1969), apparently irrespective of many late Cenozoic folds and faults (Plafker and others, 1994).
2. An anticline is unlikely to subside during an upper-plate earthquake that causes localized subsidence along adjacent synclines of similar age and trend. Rather, the anticline may undergo uplift, as during the folding at Puget Sound during one or more earthquakes on faults in the North America plate about 1,000–1,100 years ago (Bucknam and others, 1992).

The Cascadia subduction zone contains at least three anticlines having buried soils indicative of coseismic subsidence. One of these, located near Cape Blanco, Oregon, deforms Pleistocene marine terraces that have been uplifted at net rates of nearly 1 m per 1,000 years, which is among the highest rates of net Quaternary uplift along the Pacific coast at the Cascadia subduction zone (Kelsey, 1990; Kelsey and others 1994, their fig. 4). Despite this history of late Quaternary uplift, the south flank of the anticline contains several successive buried soils suggestive of coseismic subsidence during the past 5,000 years (Kelsey and others, 1993, 1996).

The Coquille River estuary, about 30 km north-northeast of Cape Blanco, shows evidence for coseismic subsidence that also may have occurred on a Quaternary anticline. The evidence for subsidence was described by Nelson (1992a, p. 298) as the best yet found in south-central Oregon. It consists of a buried soil that contains rooted stumps and herbs entombed in overlying mud. The subsidence recorded by the soil has been dated to sometime after A.D. 1660 and probably resulted from the same earthquake, or swift series of earthquakes, as the subsidence marked by soil Y in southern coastal Washington (p. 81; Nelson and others, 1995). The subsided site is located in line with the southern projection of the axis of an anticline that warps a marine terrace about 100,000 years old (McInelly and Kelsey, 1990, their fig. 5).

Buried soils also show that coseismic subsidence has occurred in the Holocene on the largest structural uplift in southern Washington—the South Bend antiform (fig. 5; p. 8). Buried soils further imply that coseismic uplift has not occurred on this structure in the past 3,500 years or more. The soils are present not only in the Holocene deposits surveyed at the Jensen, Sewer, and Airport localities (figs. 27–

31) but also in estuarine deposits of Pleistocene age (p. 9; table 1). Structural setting has had little effect on the amount or timing of coseismic subsidence in southern coastal Washington, except perhaps about 1,000–1,100 years ago. These findings, summarized below, show that most or all coseismic subsidence in southern coastal Washington results from plate-boundary earthquakes, not from earthquakes on faults in the North America plate.

SENSE OF LAND-LEVEL CHANGE

The South Bend antiform is similar to other parts of southern coastal Washington in its evidence for coseismic subsidence. Buried soils are present in estuarine deposits of Pleistocene age (table 1) and Holocene age (fig. 34), both on and off the antiform. Where preserved, vascular-plant fossils in Holocene soils on the antiform show that lasting tidal submergence, not just storms or floods, caused burial of the soils (p. 73). The probable correlation between buried Holocene soils on and off the antiform (fig. 32) further implies that this submergence resulted from sudden tectonic subsidence, at least in the case of soils L, S, U, and Y; herbaceous fossils rooted in these soils off the antiform demonstrate sudden submergence followed by rapid burial (p. 75). Although we did not find such herbaceous fossils rooted in any buried soil on the South Bend antiform, this lack of entombed herbs is probably due to decomposition after burial (p. 29–30) rather than lack of coseismic subsidence on the antiform. For example, we found no entombed herbs rooted in any of the buried soils at the Redtail locality, nor did we find them rooted in soils J, N, or W at any other locality off the antiform.

We recognized no evidence for coseismic uplift at Willapa Bay, either on or off the South Bend antiform. As little as 0.5 m of uplift would suffice to change tidal marshes into upland forests containing not only Sitka spruce but also other trees typical of uplands beside Willapa Bay: red alder, big leaf maple, western redcedar, western hemlock. On the antiform, however, growth-position remains of trees of any species are sparse or absent in all buried soils at the Airport, Sewer, and Jensen localities (figs. 27, 29, 31). Most or all of the woody roots and stumps at the Jensen locality are of Sitka spruce (p. 67), the dominant tree of tidal wetlands in southern coastal Washington (p. 11). Roots and stumps at the Sewer locality belong to an unidentified shrub that may be western crabapple (p. 69), which is also a tidal-wetland species (p. 11). Off the antiform, soils S and Y were wooded by Sitka spruce beside uplands (Redtail and Heron localities; figs. 13, 25) and along the upper reaches of tidal streams. In addition, forests on these soils contained western redcedar among some of the Sitka spruce (at and near the Pool locality, for example; p. 63). But nearer the sea, even soils S and Y represent brackish-water tidal marshes, as at the Oyster locality (fig. 18).

Coseismic subsidence on the South Bend antiform might result from earthquakes in the North America plate if a Quaternary syncline crosses the antiform near the Willapa River. The only reported candidate for such a structure is a shallow syncline several tens of kilometers wide that McNeill and others (1994) projected toward Willapa Bay from seismic-reflection profiles about 10 km off the Pacific coast (Goldfinger and others, 1997). If this syncline controls coseismic subsidence at Willapa Bay, the syncline should be bounded to the north and south by relatively uplifted areas that escaped coseismic subsidence. There is little room, however, to thread such areas among coseismically subsided sites in southern coastal Washington (fig. 34).

AMOUNT OF LAND-LEVEL CHANGE

The South Bend antiform probably resembles adjacent areas not only in subsiding during earthquakes but also in the amount of this subsidence. The amount is difficult to determine because the indicator fossils have large vertical ranges (fig. 8; Hemphill-Haley 1995a) and because local settlement can augment tectonic subsidence (p. 80). However, if the amount of subsidence depended on location with respect to the South Bend antiform, so would vascular-plant assemblages and the thickness of mud between soils. We found no such dependence on location with respect to the South Bend antiform.

VASCULAR-PLANT ASSEMBLAGES

Where vascular-plant fossils are preserved in growth position both within a buried soil and in mud above the soil, the fossils show that a high marsh, or a forest near extreme high water, became a tidal flat or a low marsh—both on and off the antiform. Examples include soil Y on the antiform at the Jensen, Sewer, and Airport localities, and off the antiform at the Oyster locality; soil U at the Airport and Oyster localities; and soil H at the Jensen locality.

Soil S at the Oyster locality may record greater subsidence than does soil S at other localities; several tens of centimeters of tidal-flat mud accumulated on this soil before *Triglochin maritimum* became established (fig. 20). However, this greater subsidence may be due to settlement from compaction of tens of meters of soft Holocene fill (p. 45).

THICKNESS OF MUD BETWEEN SOILS

The thickness of mud between buried soils at the surveyed localities varies mainly with the presence or absence of Pleistocene deposits at shallow depth beneath them. Mud between soils is thin where their Pleistocene foundation lies just a few meters beneath, both on the antiform (Jensen locality; fig. 27) and off the antiform (west end of Redtail locality, south end of Heron locality; figs. 13, 25). Conversely for sites probably underlain by many meters of soft Holocene mud, buried soils are more widely spaced, whether on the antiform at the Sewer and Airport localities (figs. 29, 31), or off the antiform at the Oyster locality (fig.

18) and away from uplands at the Redtail and Heron localities (figs. 13, 25).

The thickness of intertidal mud above a buried soil can serve as a rough indicator of the amount of coseismic subsidence because subsidence makes room for tides to deposit mud on the soil. The thickness of mud is unlikely to equal the amount of coseismic subsidence, however, if tidal inundation subsequently decreases during interseismic uplift or increases during interseismic subsidence (Darienzo and Peterson, 1990; Hemphill-Haley, 1995b, p. 377; Guilbault and others, 1995).

NUMERICAL ESTIMATES OF SUBSIDENCE

We do not compare structural setting with numerical estimates of subsidence because, at present, such estimates would be unreliable for the South Bend antiform. Estimates of coseismic subsidence at the Cascadia subduction zone are best made at sites studied carefully for microscopic fossils (Mathewes and Clague, 1994; Hemphill-Haley, 1995b; Guilbault and others, 1995; Nelson and others, 1996a, b; Shennan and others, 1996). Microfossils have not yet been studied for most soils on the South Bend antiform. However, they have been studied abundantly for soils off the antiform, along the Niawiakum River.

Subsidence of at least 1 m was previously inferred for soil Y at the Redtail and Oyster localities, mainly on the basis of diatom assemblages (Hemphill-Haley, 1995b). Here we extend this estimate to most soils at the Redtail and Oyster localities. The estimates are based on inferred differences in depositional environment between buried soils and the mud immediately above them (figs. 15, 20). We inferred the environmental differences from stratigraphy and from species of vascular plants and diatoms that are vertically zoned in modern tidal wetlands (figs. 8, 11, 12).

Subsidence of at least 1 m is probably recorded by soils J, L, N, S, U, and Y at the Redtail locality because all these soils probably contain high marsh or upland assemblages of diatoms and because mud above each of them contains diatom assemblages suggestive of widely unvegetated mudflats (p. 29). The modern difference between these environments is rarely less than 0.5 m and commonly exceeds 1 m (fig. 8, parameter D). The evidence for at least 1 m of subsidence is strongest for soils S and Y, whose spruce roots corroborate diatom evidence for conditions transitional to upland (p. 29).

The Oyster locality also has strong evidence that soils S and Y record at least 1 m of subsidence (p. 48). This evidence consists of high-marsh plants rooted in the soils, algal lamination and *Triglochin maritimum* rhizomes in mud above the soils, and diatom assemblages compatible with these features.

Only soil W has evidence against subsidence greater than 1 m. At the Oyster locality this soil represents a tidal marsh above the lower limit of *Triglochin maritimum* but probably below the transition from low marsh to high marsh (p. 48). Moreover, after soil W subsided it did not remain a tidal flat for long, as judged from the thickness of mud dominated by tidal-flat diatoms (p. 52). In that case it may have subsided only through the vertical range of low marsh, or as little as about 0.5 m.

COEVALITY OF LAND-LEVEL CHANGE

Buried soils of the past 2,000 years on the South Bend antiform do not appear to differ—either in stratigraphic sequence or in radiocarbon age—from buried soils at nearby sites off the antiform (fig. 32). All these soils appear to be part of a regionally correlative sequence previously reported from many estuarine localities along the southern 100 km of the Washington coast (Atwater, 1992). In this sequence, two bold soils (herein, soils S and Y) bracket one or two faint soils (U and W). Soils S and Y commonly contain more fossil tree roots than do soils U and W, and only soil Y is commonly covered by a tsunami deposit at Willapa Bay and Grays Harbor. Ages determined by radiocarbon dating (chiefly for soils S and Y; Atwater, 1992) and by tree-ring pattern matching (soil Y only; Yamaguchi and others, 1997) are consistent with correlations inferred from these various stratigraphic clues. Additional radiocarbon dating of soils in the stratigraphic position of soils S, U, and Y is consistent with correlation between a typical southern-Washington sequence of buried soils at the Naselle River (fig. 5) and a sequence of buried soils at Netarts Bay, Oregon (fig. 1) (Nelson and others, 1996b, their fig. 6).

Buried soils 2,000–3,500 years old also show no major differences in stratigraphy or approximate age between the South Bend antiform and the handful of sites at which such soils have been dated in southern coastal Washington. The four lowest soils on the antiform at the Jensen locality probably correlate with soils H, J, L, and N off the antiform at the Redtail locality (p. 67–69). Soils low in the section at the Jensen locality probably also correlate with soils off the anticline at Willapa Bay (South Fork locality) and Grays Harbor (Johns River and Blue Slough localities) (fig. 32).

POSSIBLY UNUSUAL CHANGES IN LAND LEVEL 1,000–1,100 YEARS AGO

The subsidence marked by soil W at Willapa Bay may have coincided, to the nearest century or less, with unusual faulting in the North America plate. Such faulting probably occurred some 50 km to the north, at the Copalis River. There, vented sand covers a soil, possibly correlative with soil W (fig. 32), that underwent little or no subsidence at the time of venting. This lack of subsidence implies localized deformation in the North America plate because the venting, which is not readily explained by shaking-induced liquefaction, probably resulted from faulting or folding of an aquifer beneath the Copalis River (Atwater, 1992, p. 1917, "Note added in proof"). Such faulting or folding could have been part of widespread movement on structures high in the

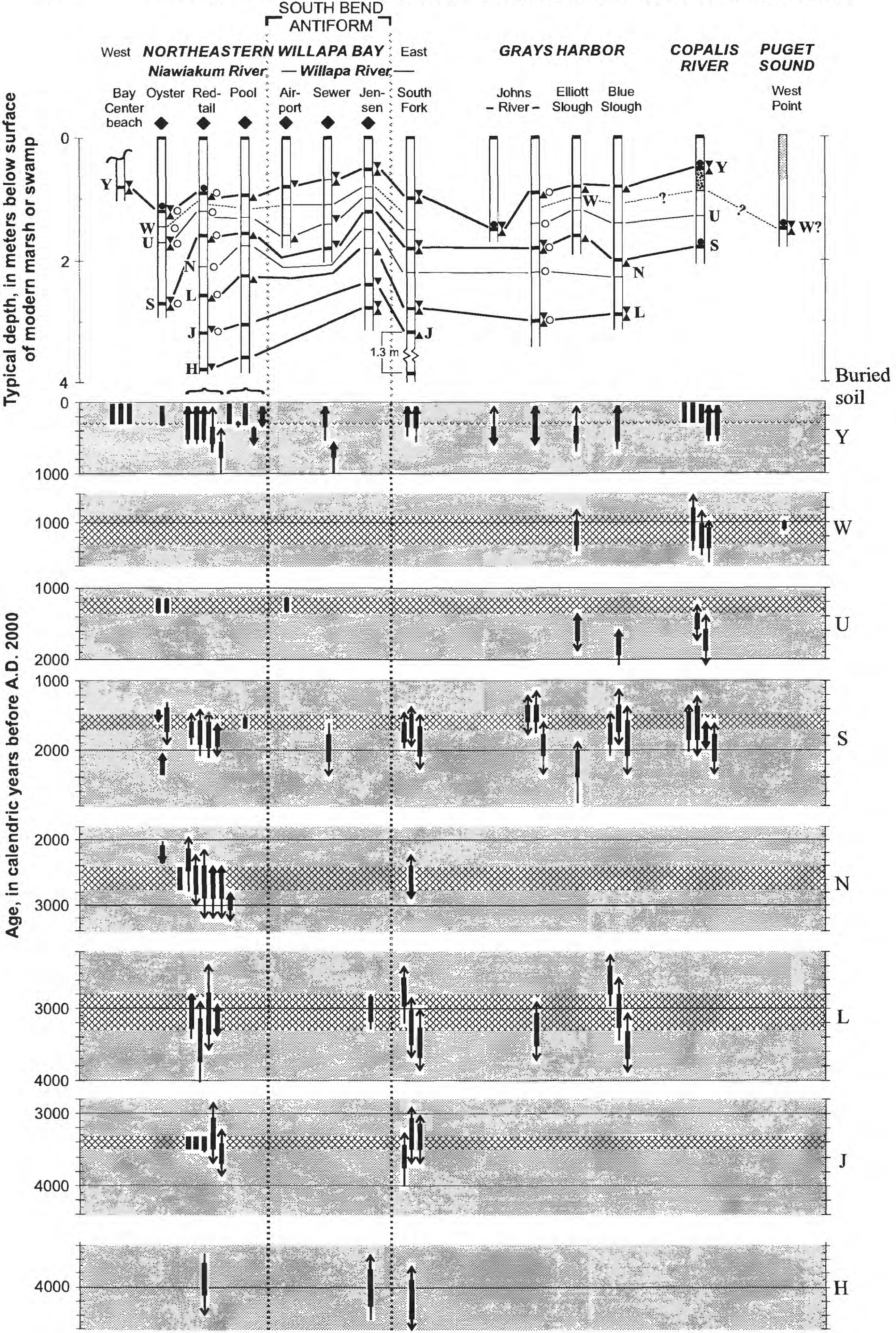
SOUTH BEND ANTIFORM
West
NORTHEASTERN WILLAPA BAY
Niawiakum River
— Willapa River —
East
GRAYS HARBOR
COPALIS RIVER
PUGET SOUND
Bay Center beach
Oyster
Red-tail
Pool
Air-port
Sewer
Jen-sen
South Fork
Johns – River –
Elliott Slough
Blue Slough
West Point
Typical depth, in meters below surface of modern marsh or swamp
0
2
4
Y
W
U
S
N
L
J
H
W?
?
1.3 m
Buried soil
Age, in calendric years before A.D. 2000
0
1000
2000
3000
4000

← **Figure 32.** Inferred correlations among buried Holocene soils at estuaries in southern coastal Washington and at Puget Sound. Individual age ranges calculated from radiocarbon ages in Atwater and others (1991), Atwater (1992), Atwater and Moore (1992), and table 7 of this report. Vertically ruled bands denote likely age ranges explained in section "Number and Ages of Earthquakes" (p. 91). Age range for soil Y at Oyster locality corresponds to weighted mean age of 161±15 ^{14}C yr B.P.

EXPLANATION

Columnar sections

◆ **Section described in this report**—Column generalized from outcrop drawing (figs. 13, 18, 24, 27, 29, and 31)

Soil—Categorized by surficial horizon

▮ **Bold**—Peaty mud or peat

▯ **Faint**—Dark mud

Deposits between successive soils

□ **Mud**

● **Probable tsunami deposit on soil**

▨ **Vented sand on soil**—Erupted from >35 m below land surface (Atwater, 1992, p. 1917)

▒ **Muddy peat**—>0.3 m thick; records gradual submergence in the past 1000 years (Atwater and Moore, 1992)

Vascular-plant fossils in growth position

▼ **Rhizomes in mud above soil**—*Triglochin maritimum* or, at South Fork, *Carex lyngbyei*

▲ **Plant remains rooted in buried soil**—Herbs, shrubs, or trees

○ **Microscopic fossils**—Diatoms at Redtail and Oyster localities (figs. 15, 16, and 20-23); diatoms and pollen at Johns River (Shennan and others, 1996)

~ **Unconformity on modern beach**

Correlations—Dashed where drawn through section in which soil is not recognized; queried where speculative. Letter gives name for soils inferred to correlate with one another

Y —— **Soil typically bold**

W ‒‒?‒‒ **Soil typically faint**

Ages of inferred earthquakes

Thick line gives 95-percent confidence interval calculated from error reported by laboratory; thin line increases this error by 1.6 or 2.0 (see text section "Radiocarbon Dating")

| **Closely limiting age**—Obtained from earthquake-killed plants (soils S, U, W, Y) or forest litter from uppermost 0.5 cm of buried soil (soils J, N); ages for soils S and Y denote inferred time of plant death

↓ **Minimum age**—Measured on rhizomes of *Triglochin maritimum* above soil

↑ **Maximum age**—Measured on woody root, plant detritus, or archaeological charcoal in buried soil

↕ **Minimum or maximum age**—Measured on peat in soil or on plant detritus in mud less than 20 cm above soil

✕✕✕✕ **Likely age range for inferred earthquake or earthquake series**

Figure 32. Continued.

North America plate in western Washington 1,000–1,100 years ago. At that time, movement on one or more faults in the North America plate farther inland, in the Puget Sound area, generated 5–7 m of coseismic uplift near Seattle and several meters of coseismic uplift in an area 30–50 km to the southwest (Bucknam and others, 1992).

Despite this evidence for upper-plate seismicity, soil W at Willapa Bay probably represents an earthquake on the plate boundary. Radiocarbon-dated soils show that coseismic subsidence occurred elsewhere along the Washington coast between 900 and 1,300 years ago (Atwater, 1992, his figs. 6, 7)—at Neah Bay (location shown in fig. 1), at Grays Harbor along Elliott Slough, and at southern Willapa Bay along the Bear River (locations shown in fig. 5). We speculate that movement on faults and folds in the North America plate of western Washington accompanied—or shortly preceded or followed—one or more plate-boundary earthquakes 1,000–1,100 years ago, and that this plate-boundary seismicity is recorded at northeastern Willapa Bay by soil W.

SIZES OF THE EARTHQUAKES

Although their sizes are difficult to estimate, most or all of the earthquakes represented by buried soils H through Y were probably great earthquakes—of moment magnitude 8 or larger. Such magnitudes are suggested by geologic evidence for large ruptures and by a tradeoff between size and frequency.

DIMENSIONS OF PLATE-BOUNDARY RUPTURES

RUPTURE WIDTH

Wide ruptures are likely because, as shown in the section "Distinction Between Plate-Boundary and Upper-Plate Sources for the Earthquakes" (p. 80), the earthquakes marked by the buried soils probably occurred on the boundary between the Juan de Fuca plate and the North America plate. Ruptures on the Washington part of this plate boundary are likely to exceed 50 km in width, according to interpretation of geodetic and heat-flow data (Savage and others, 1991; Dragert and others, 1994; Hyndman and Wang, 1995). A potential rupture width of more than 100 km has been estimated from satellite measurements of deformation between 1992 and 1994 near the border between Washington and British Columbia (Dragert and Hyndman, 1995, p. 756).

High temperatures and fluid pressures may preclude ruptures much wider than 100 km on the Washington part of

Table 7. Radiocarbon ages of samples from the Oyster, Redtail, Jensen, Sewer, and Airport localities, northeastern Willapa Bay

Age ± quoted error[1]	Material	Soil	Stratigraphic setting	Locality	River	Lab number[2]	Field number
90 ± 60	Outer part of bark-bearing root 10 cm in diameter without conspicuous rings; probably western crabapple	Y	10 cm below top of soil; root attached to bark-bearing trunk about 15 cm in diameter that extends into silt above soil	Sewer	Wil	Beta 76289	J13A
120 ± 41	Leaf base of *Potentilla pacifica*	Y	Rooted in soil and entombed in overlying tsunami deposit	Oyster	Nia	GX 17927	ARN91-37
135 ± 42	Leaf base of *Potentilla pacifica*	Y	Rooted in soil and entombed in overlying tsunami deposit	Oyster	Nia	GX 17852	ARN91-36
139 ± 40	Leaf base of *Potentilla pacifica*	Y	Rooted in soil and entombed in overlying tsunami deposit	Oyster	Nia	GX 17946	ARN91-40
155 ± 47	Leaf base of *Potentilla pacifica*	Y	Rooted in soil and entombed in overlying tsunami deposit	Oyster	Nia	GX 17846	ARN91-34
156 ± 43	Leaf base of *Potentilla pacifica*	Y	Rooted in soil and entombed in overlying tsunami deposit	Oyster	Nia	GX 17838	ARN91-32
162 ± 49	Culm base of *Juncus balticus*	Y	Rooted in soil and entombed in overlying tsunami deposit	Oyster	Nia	GX 17828	ARN91-31
174 ± 43	Leaf base of *Potentilla pacifica*	Y	Rooted in soil and entombed in overlying tsunami deposit	Oyster	Nia	GX 17942	ARN91-39
230 ± 70	Spruce root 1.0-1.5 cm diameter	Y	Uppermost 1 cm of soil; from same tree as Beta-19840?	Redtail	Nia	Beta 19839	SL86-106O
250 ± 60	Spruce root 1.0-1.5 cm diameter	Y	Uppermost 1 cm of soil; from same tree as Beta-19839?	Redtail	Nia	Beta 19840	SL86-106P
250 ± 60	Charcoal	Y	Fire pit that extends to top of soil	Redtail	Nia	Beta 63220	F14B
272 ± 47	Culm base of *Juncus balticus*	Y	Rooted in soil and entombed in overlying tsunami deposit	Oyster	Nia	GX 17933	ARN91-38
360 ± 70	Spruce root 3.5 cm diameter, containing about 15 rings	Y	Top of root 1 cm below top of soil	Redtail	Nia	Beta 22368	A1F
380 ± 50	Stave. Dated portion—consisting of branched, bark-covered stick—was 4 cm in maximum diameter and contained about 15 annual rings	--	Weir on mudflat	Sewer	Wil	Beta 74541	J4A
601 ± 55	Bark-free twig	--	Probable tsunami deposit in channel fill	Oyster	Nia	GX 20307-AMS	J10A2
630 ± 90	Charcoal	Y	Fire pit 10-20 cm below top of soil	Redtail	Nia	Beta 49195	A1
710 ± 70	Stake 5 cm in diameter; lower end charred, hard, and sharp	--	Vertical in mud to depth of 1.0 m below top of soil Y; charred end down	Sewer	Wil	Beta 76290	J14A
720 ± 70	Bark-free twigs	--	Probable tsunami deposit in channel fill	Oyster	Nia	Beta 76685	J10A1
1,247 ± 22	*Triglochin maritimum* rhizomes	U	In mud above filled channel	Airport	Wil	QL 4822	J2A
1,260 ± 14	*Salicornia virginia* stems and attached roots	U	Stems in mud 0-3 cm above top of soil; roots in peaty mud 0-2 cm below top of soil	Oyster	Nia	QL 4795	J9C

Table 7. Radiocarbon ages of samples from the Oyster, Redtail, Jensen, Sewer, and Airport localities, northeastern Willapa Bay—Continued

Age ± quoted error[1]	Material	Soil	Stratigraphic setting	Locality	River	Lab number[2]	Field number
1,302 ± 21	*Triglochin maritimum* rhizomes	U	In mud about 20 cm above top of soil	Oyster	Nia	QL 4798	J9D
1,598 ± 23	*Triglochin maritimum* rhizomes; split into roughly identical sample for Beta-76633	S	In mud 45-55 cm above top of soil	Oyster	Nia	QL 4797	J9B
1,630 ± 70	*Triglochin maritimum* rhizomes; split into roughly identical sample for QL-4797	S	In mud 45-55 cm above top of soil	Oyster	Nia	Beta 76633	J9B1
1,720 ± 40	Root or stick 3 cm diameter; split into more or less identical sample for Beta-19837	S	Top of soil	Redtail	Nia	USGS 2540	SL86-106K2
1,740 ± 15	*Thuja plicata* (western redcedar) root; rings number 60-69, where ring number 1 adjoins bark	S	One of a forked pair of redcedar roots high in soil	Pool	Nia	QL 4796	J12A
1,740 ± 70	Root or stick 2 cm diameter	S	Top of soil	Redtail	Nia	Beta 19838	SL86-106L
1,800 ± 70	Root or stick 3 cm diameter; split into more or less identical sample for USGS-2540	S	Top of soil	Redtail	Nia	Beta 19837	SL86-106K1
1,830 ± 40	Root or stick	S	Uppermost 1 cm of soil	Redtail	Nia	USGS 2541	SL86-106M
1,990 ± 70	*Triglochin maritimum* rhizomes	S	Mud 20-30 cm above top of soil	Sewer	Wil	Beta 76291	J18A
2,170 ± 25	*Triglochin maritimum* rhizomes	S	Mud 50 cm below top of soil	Oyster	Wil	QL 4823	J9A
2,258 ± 75	Rotten stick 0.5-1.0 cm diameter	N	Uppermost 0.5 cm of soil	Redtail	Nia	RIDDL 686	SL86-106I
2,475 ± 23	Spruce cones	N	Resting on top of soil; probably part of forest-edge litter at time of subsidence	Redtail	Nia	QL 4715	F19A1
2,510 ± 80	Stick	N	Mud 1-2 cm above top of soil	Redtail	Nia	Beta 22371	A1N2
2,530 ± 100	Sticks and spruce cones	N	Uppermost 1 cm of soil	Redtail	Nia	Beta 21826	A2A+B
2,590 ± 80	Sticks	N	Top of soil	Redtail	Nia	Beta 19836	SL86-106H
2,590 ± 60	Stick	N	Mud 1-2 cm above top of soil	Redtail	Nia	Beta 22370	A1N1
2,780 ± 45	Peat	N	Uppermost 1 cm of soil	Redtail	Nia	USGS 2539	SL86-106J
2,790 ± 120	Peat	L	Uppermost 1-2 cm of soil	Redtail	Nia	Beta 21824	A1D
2,820 ± 50	Spruce root, outer 25 rings	L	Part of a large root system in soil (fig. 13*B*)	Jensen	Wil	Beta 81551	J8A
2,840 ± 70	Root	L	In soil	Redtail	Nia	Beta 19835	SL86-106G
2,945 ± 30	Peat	L	Uppermost 1 cm of soil	Redtail	Nia	USGS 2538	SL86-106E
3,063 ± 80	Bark-free twig 0.2 cm diameter	J	Top of soil	Redtail	Nia	RIDDL 684	SL86-106B
3,165 ± 17	Spruce cones	J	Resting on top of soil; probably part of forest-edge litter at time of subsidence	Redtail	Nia	QL 4718	F16A1
3,166 ± 18	Twigs	J	Identical to QL-4718	Redtail	Nia	QL 4717	F16A2
3,180 ± 30	Stick	J	Identical to QL-4718	Redtail	Nia	QL 4716	F16C
3,190 ± 110	Root	L	In soil	Redtail	Nia	Beta 19834	SL86-106F
3,230 ± 60	Stick	J	Top of soil	Redtail	Nia	Beta 21822	A-1B

Table 7. Radiocarbon ages of samples from the Oyster, Redtail, Jensen, Sewer, and Airport localities, northeastern Willapa Bay—Continued

Age ± quoted error[1]	Material	Soil	Stratigraphic setting	Locality	River	Lab number[2]	Field number
3,262 ± 80	Bark-free twig 0.5 cm diameter	J	Uppermost 0.5 cm of soil	Redtail	Nia	RIDDL 685	SL86-106C
3,320 ± 80	Rhizomes	J	Mud 20-40 cm above top of soil	Redtail	Nia	Beta 21823	A1C
3,570 ± 70	Rhizomes	H	Mud 20-30 cm below top of soil J and about 30 cm above top of soil H	Redtail	Nia	Beta 21825	A1E
3,640 ± 80	Bark-free stick	H	In upper few centimeters of soil and in lower few centimeters of overlying mud	Jensen	Wil	Beta 76288	J8E1
3,730 ± 210	Peat	J	Uppermost 1-2 cm of soil	Redtail	Nia	USGS 2537	SL86-106A

[1] Ages in radiocarbon years before A.D. 1950 (yr B.P.)

[2] Beta, Beta Analytic, Inc., Coral Gables, Florida. GX, target prepared by Geochron Laboratories, Cambridge, Massachusetts; age measured by accelerator mass spectrometry by Institute of Geology and Nuclear Sciences, Ltd., Lower Hutt, New Zealand. QL, Quaternary Isotope Lab, University of Washington, Seattle, Washington. RIDDL, Radioisotope Direct Detection Laboratory, McMaster University, Hamilton, Ontario.

the Cascadia subduction zone. High temperatures at depth should limit the landward extent of brittle failure (Hyndman and Wang, 1993). High fluid pressures may limit release of seismic energy from displacement on the seaward part of the plate boundary (Byrne and others, 1992; Goldfinger and others, 1996).

RUPTURE LENGTH

Ruptures at least 50 km wide at the Cascadia subduction zone can be as short as 200 km and still have enough area to produce a magnitude-8 earthquake, if a magnitude-area correlation for mostly smaller ruptures (Wells and Coppersmith, 1994) applies to the Cascadia subduction zone.

The most recent coseismic subsidence, which probably dates to 300 years ago, struck estuaries as much as 625 km apart during the same few decades (fig. 33; Nelson and others, 1995). This degree of coevality implies either a single rupture at least 600 km long or a swift series of shorter ruptures. A long single rupture at Cascadia best explains a tsunami in Japan in January 1700 (Satake and others, 1996). This correlation is supported by tree-ring dating in southern Washington, as summarized on page 94.

Earlier coseismic subsidence, though not so precisely dated, may have also resulted from long ruptures. Largely overlapping age ranges spanning about 150–250 calendric years, obtained from multiple radiocarbon ages on earthquake-killed herbs or delicate plant detritus on probable correlatives of soils S, U, and Y (Nelson and others, 1996b, their fig. 6), suggest correlation of two stratigraphic sequences 110 km apart—at the Naselle River, Washington (fig. 5) and at Netarts Bay, Oregon (fig. 1). Widespread subsidence is further suggested by similarities among ages for soil S throughout southern coastal Washington (fig. 32). Moreover, a long apparent interval without buried soils, centered about 2100 years ago, is indicated by a gap in radiocarbon ages both in southern Washington (see section "Interval Between Events Marked by Soils N and S," p. 98) and in northern Oregon (fig. 4 of Darienzo and Peterson, 1995; gap between ages for their events 5 and 6).

TRADEOFF BETWEEN SIZE AND FREQUENCY

If plate-boundary earthquakes at the Cascadia subduction zone are typically smaller than moment magnitude (M_w) 8, the earthquakes should happen more often than is indicated by historical seismic quiescence or implied by geologic estimates of recurrence intervals. Table 8 illustrates this tradeoff between size and frequency of earthquakes for various degrees of coupling at the plate boundary. From this table we conclude that maximum earthquakes of M_w 7.5 or 8.0 would require many more such events than are allowed by historical and geological records. We further infer that this problem cannot be solved through creep at the plate boundary or permanent deformation within the North America and Juan de Fuca plates.

Plate convergence creates seismic moment, which is related to seismic energy and is defined as the product of rigidity, rupture area, and average fault displacement (Hanks and Kanamori, 1979). Given estimates of rigidity and rupture area, one can deduce combinations of earthquake size and frequency that produce average displacement consistent with plate convergence at the Cascadia subduction zone. Only some of these combinations, however, are consistent with the lack of thrust earthquakes on most of the Cascadia plate boundary in the past 150–200 years, and with geologic

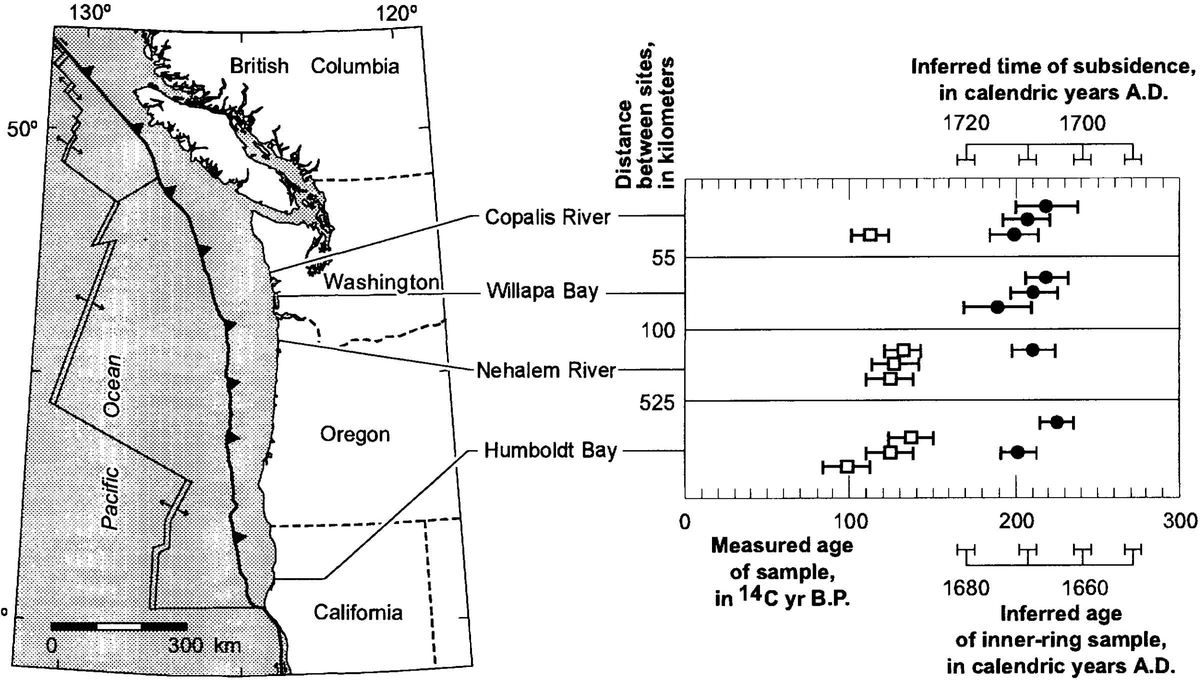

EXPLANATION

▲ Seaward edge of subduction zone
╪ Spreading ridge
— Transform fault

Average number of tree-ring years before death, for tree probably killed by effects of subsidence
□ 5 — Outer-ring sample
● 40 — Inner-ring sample

Error bars for sample ages and for calendric-year scales represent at least 0.6-0.8 standard deviation

Figure 33. Comparison of high-precision radiocarbon ages measured on inner and outer rings from spruce stumps in southern Washington, northern Oregon, and northern California. Washington ages tabulated by Atwater and others (1991); Oregon ages, Nelson and Atwater (1993); California ages, Carver and others (1992). All ages summarized by Nelson and others (1995). Calendric time scale at bottom, based on calibration data of Stuiver and Becker (1993), applies to inner-ring samples if they formed before the early 1700's. Such timing has been demonstrated for one stump at Willapa Bay (Atwater and others, 1991, their fig. 3b) and for one stump at Humboldt Bay (Nelson and others, 1995, their fig. 2). For these stumps, calendric dates younger than the early 1700's have been disallowed through matching of distinctive wiggles in radiocarbon time scales. Years for calendric time scale at top are 40 years later than those for the calendric scale at bottom because the trees died 40 tree-ring years after formation of the middle ring in the inner-ring samples. Error bars on calendric scales show two-standard-deviation uncertainty in converting from radiocarbon years to calendric years for wood formed between 1650 and 1680.

evidence that earthquakes on this plate boundary recur hundreds of years apart.

We obtained minimum estimates of seismic moment by using several estimates treated here as constants. For rigidity we use 3×10^{10} N/m^2, at the low end of the range that Kanamori (1977, p. 2983) used to calculate sizes of great earthquakes. For rupture area we use 50,000 km^2, well under the 90,000 km^2 estimated by Hyndman and Wang (1995, p. 22152) on the basis of geodetic and heat-flow data. For plate convergence we use 3.5 cm/yr, the component orthogonal to the strike of the plate boundary off Oregon and Washington; the component parallel to strike is excluded because most or all of this component is probably expended on permanent deformation in the North America plate (McCaffrey and Goldfinger, 1995). Orthogonal convergence probably exceeds 3.5 cm/yr off northern Washington and southern British Columbia, where the convergence direction is nearly orthogonal (Wilson, 1993, p. 16069), and off northern California, where the orthogonal component of plate convergence is increased by spreading in the Basin and Range province (Pezzopane and Weldon, 1993, p. 1164–1165). Modern earthquakes in the North America and Juan de Fuca plates account for no more than about one-tenth of the convergence (Hyndman and Weichert, 1983).

The calculated seismic moment varies largely with coupling—the fraction of plate convergence that becomes

Table 8. Hypothetical sizes and numbers of earthquakes resulting from 300, 500, and 1,000 years of plate convergence at the Casadia subduction zone

[For assumptions see section, "Tradeoff Between Size and Frequency"]

Coupling[1]	Seismic moment[2], in 10^{29} dyne-cm	Corresponding size of single earthquake (M_w)	Corresponding number of lesser earthquakes[3]		
			M_w 8.5	M_w 8.0	M_w 7.5
		300 years of plate convergence			
1	1.56	8.8	2	14	79
3/4	1.18	8.7	2	11	59
1/2	0.79	8.6	1	7	39
1/4	0.39	8.4	1	4	20
		500 years of plate convergence			
1	2.63	8.9	4	23	132
3/4	1.97	8.8	3	18	99
1/2	1.31	8.7	2	12	66
1/4	0.66	8.5	1	6	33
		1,000 years of plate convergence			
1	5.25	9.1	8	47	263
3/4	3.94	9.0	6	35	197
1/2	2.63	8.9	4	23	132
1/4	1.31	8.7	2	12	66

[1] Fraction of plate convergence that becomes seismic slip at the plate boundary.

[2] Product of rigidity, rupture area, and average displacement (Hanks and Kanamori, 1979).

[3] Rounded to nearest whole number.

seismic slip on the plate boundary. At many subduction zones this fraction has been shown to be less than one-fourth (Pacheco and others, 1993), and such weak coupling in northern Japan has been shown to reflect aseismic creep in the first year after a large plate-boundary earthquake (Heki and others, 1997). Coupling has not been measured for the Cascadia subduction zone, owing to the lack of plate-boundary earthquakes in the zone's instrumental history. However, because of their motions with respect to the mantle, the Juan de Fuca and North America plates may be strongly coupled (Scholz and Campos, 1995, p. 22112). Strong coupling at Cascadia is consistent with heat-flow and geodetic data (Savage and others, 1991; Hyndman and Wang, 1993, 1995; Dragert and others, 1994). It is also consistent with the lack of small modern earthquakes on the plate boundary—earthquakes that could demonstrate present-day creep (Heaton and Hartzell, 1987; Rogers, 1988).

The other main variable in table 8 is the amount of time during which the seismic moment accumulates. We illustrate three values: 300, 500, and 1,000 years. Three hundred years approximates the time since the most recent great earthquake inferred for the Cascadia subduction zone (see section "Soil Y" on p. 94) as well as the shortest average recurrence interval estimated for plate-boundary earthquakes at Cascadia (p. 7; fig. 3). Five hundred years approximates the average of six intervals between great plate-boundary earthquakes of the past 3,500 years at northeastern Willapa Bay, as inferred in this report (see p. 99). The longest of these intervals—between earthquakes marked by soils N and S—spanned about 1,000 years (p. 98).

The three right-hand columns in table 8 show that the seismic moment from centuries of plate convergence at the Cascadia subduction zone would produce very large numbers of earthquakes if the maximum earthquake size is M_w 7.5 or 8.0. The M_w 7.5 earthquakes are so numerous, even for just 300 years of plate convergence, that many such earthquakes should have occurred historically if plate-boundary earthquakes at the Cascadia subduction zone do not exceed M_w 7.5. The numbers of M_w 8 earthquakes are also too large to agree with recurrence intervals of 300–500 years unless only about one-quarter of the plate convergence becomes seismic slip at the plate boundary. In that case, all the convergence could be accounted for by a series of four to six adjacent M_w 8 ruptures each about 200 km long and adjoined like sausage links along the 1,000-km-long subduction zone. The stronger coupling inferred above requires earthquakes of M_w 8.5 or larger to obviate average recurrence intervals shorter than those summarized in figure 3.

NUMBER AND AGES OF EARTHQUAKES

Seven great plate-boundary earthquakes probably struck southern coastal Washington between 3,300–3,500 years ago and 300 years ago. A great earthquake, or a pair of such earthquakes having adjacent ruptures on the southern Washington part of the Cascadia plate boundary, probably corresponds to each buried soil that we observed in outcrop along the Niawiakum River (figs. 13–26) and correlated with buried soils elsewhere in southern coastal Washington (figs. 32, 34). More than seven great earthquakes (or series) may have struck southern coastal Washington in the past 3,500 years if the buried-soil record is incomplete.

EVENTS RECORDED BY BURIED SOILS

For convenience we use "event" for the earthquake or series of earthquakes represented by a buried soil and its probable correlatives. The term is useful because latitudinally adjacent parts of the Cascadia plate boundary may rupture all together in a single earthquake, or they may rupture individually in an earthquake series that spans too little time for the individual ruptures to be distinguished from one another by conventional geologic dating.

Such variable rupture—sometimes a single earthquake, other times a series of smaller earthquakes—is common at subduction zones (Thatcher, 1989), including several zones that have been likened to Cascadia (Heaton and Hartzell, 1986, 1987). A single earthquake ruptured about 500 km of subduction zone off Columbia and Ecuador in 1906, but this same area then ruptured piecemeal in a series of three earthquakes between 1942 and 1979 (Kanamori and McNally, 1982). Similarly at the Nankai Trough off southwest Japan, about 500 km of subduction zone ruptured as a whole in 1707 but piecemeal, in a pair of adjacent earthquakes 32 hours apart in 1854 and in another pair of earthquakes two years apart in the 1940's (Ando, 1975). In the language used below, the Nankai example comprises three events—the first in 1707, the second in 1854, the third in the 1940's.

SOIL J

The earliest well-dated event in southern coastal Washington is marked by soil J. We observed this soil in outcrop at the Redtail locality (figs. 13, 14*B*) and saw probable correlatives exposed at two other sites in northeastern Willapa Bay—at the Jensen locality (figs. 27, 28*A*) and along the South Fork Willapa River (Hull, 1987). We have also found a probable correlative of soil J along the Naselle River, about 200 m downstream from the outcrop studied by Ota and Umitsu (1995).

Low altitude, not small rupture area, probably accounts for the limited extent of soil J depicted in figure 34. At most places the present altitude of the soil is too low for exposure at even the lowest of tides. We infer that soil J exists in many areas where it is below lowest tides and therefore can only be seen in core. One such area may be the Johns River (fig. 5), where a possible correlative of soil J was observed in borings by Shennan and others (1996).

The event marked by soil J probably occurred between 3320 and 3,500 years ago (fig. 34). This estimate is based on three concordant ages on forest-floor litter at the Redtail locality (p. 32).

SOIL L

Soil L, the oldest soil widely exposed at Willapa Bay and Grays Harbor, records a poorly dated event that probably happened between 2,800 and 3,300 years ago. The soil, which is typically bold and commonly contains spruce roots seaward of modern spruce swamps, is conspicuous in outcrop at Willapa Bay along the Niawiakum and Willapa Rivers, and at Grays Harbor along the Johns River and Blue Slough (fig. 34). A probable correlative of soil L also crops out along the Naselle River, about 200 m downstream from the outcrop studied by Ota and Umitsu (1995).

The estimated age of 2,800–3,300 years is based on three kinds of evidence: conventional radiocarbon dating of materials that did not necessarily form close to the time of the event; conventional radiocarbon dating of wood that probably formed in the last 25 years before the event; and stratigraphic position between the two better-dated soils that bracket soil L. The conventional ages—on peat and sticks, and on small woody roots sampled without regard to the number or position of rings—together provide broadly limiting ages of 2,200 and 3,800 years ago (fig. 32). The outer 25 rings of a bark-bearing spruce root at the Jensen locality gave a conventional age (p. 68) that narrows the range to 2,800–3,300 years ago. This narrower range fits in the gap between events marked by soil J (3,300–3,500 years ago) and soil N (2,400–2,800 years ago).

SOIL N

Soil N has about the same mapped distribution in southern coastal Washington as does soil L (fig. 34). Typically faint, soil N rarely contains growth-position remains of woody plants, even where its surficial horizon retains peat, as shown at the Redtail and Heron localities (figs. 13, 25).

Nearly all the ages for the event marked by soil N were measured at the Redtail locality and nearly all of these are concordant (fig. 32). One is a high-precision age on forest-floor litter (2,475±23 ^{14}C yr B.P.; table 7). Its corresponding range of calendric ages is broad—between 2,400 and 2,780 years ago—because of a plateau in radiocarbon ages for that period of calendric time (Stuiver and Pearson, 1986). At the Oyster locality, an age on rhizomes gives soil N a limiting minimum age between about 2,050 and 2,350 years ago (p. 52).

SOIL S

Bold soil S is widely and conspicuously exposed not only at Willapa Bay and Grays Harbor but also at estuaries having smaller tidal ranges. Likely correlatives of soil S have been documented in outcrop at the Copalis River (fig. 34; Atwater, 1992, his "lower bold soil"), at Netarts Bay, Oregon (Darienzo and others, 1994; Nelson and others,

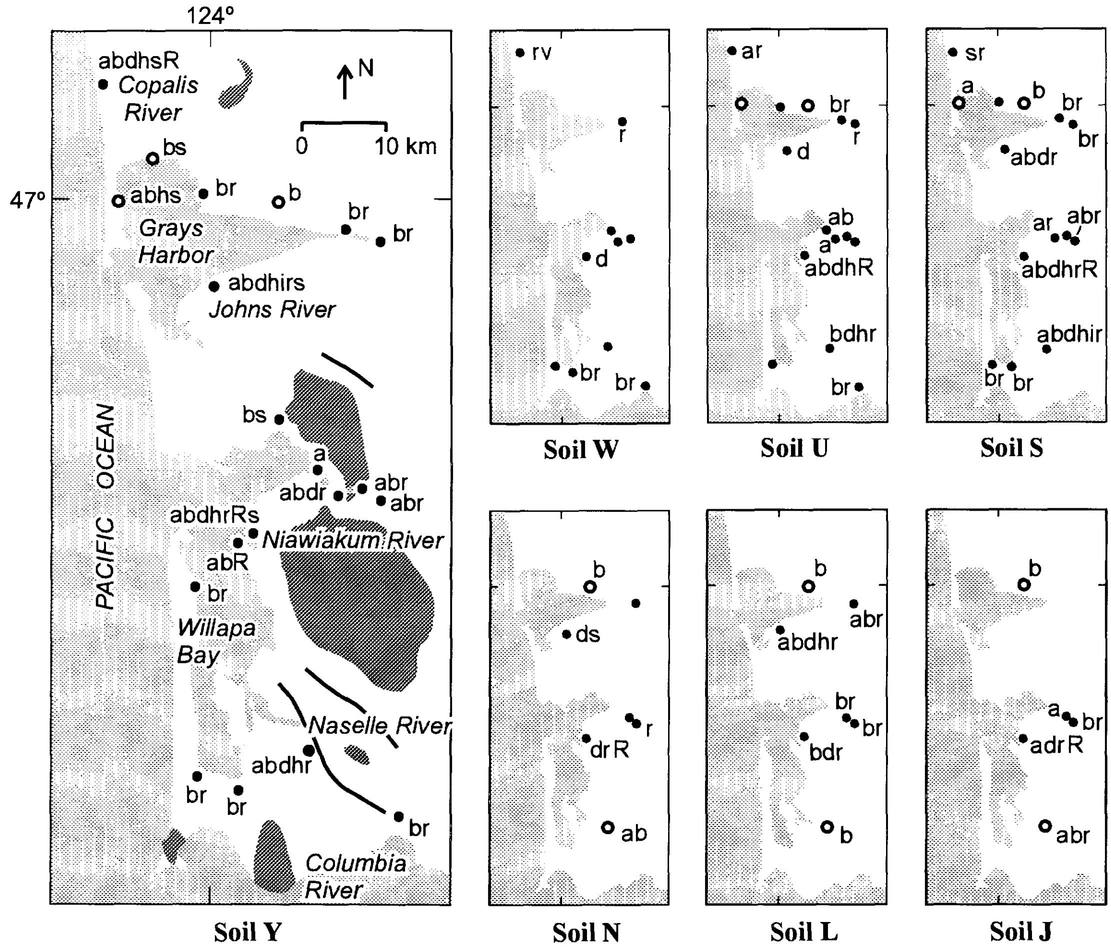

Figure 34. Geographic distribution of well-exposed evidence for earthquakes in the past 3,500 years in southern coastal Washington. Sources: Atwater (1987), Reinhart and Bourgeois (1987), Atwater and Yamaguchi (1991), Atwater and others (1991), Atwater (1992), Hemphill-Haley (1995b), Ota and Umitsu (1995), Shennan and others (1996), B.F. Atwater, M.A. Reinhart, and D.K. Yamaguchi (unpub. data, 1987–1990), and this report.

1996b), and perhaps as far south as Coos Bay, Oregon (Nelson and others, 1996a, their couplet 4) and Humboldt Bay, California (Clark and Carver, 1992). The soil is typically the most conspicuous of all the buried soils seen in many Washington outcrops, as illustrated at the Redtail (fig. 14*A*, *B*), Oyster (fig. 19*B*), and Jensen (fig. 28*A*) localities. A common characteristic is spruce roots in growth position at least as far downstream as any other exposed soil, and farther downstream than modern spruce swamps.

The event marked by soil S probably occurred between 1,500 and 1,700 years ago. This estimate is based on concordant high-precision ages of two samples collected along the Niawiakum River—rhizomes that probably formed soon after the event (p. 52, 58), and tree rings that probably formed about 65 years before the event (p. 63).

The range of 1,500–1,700 years accords with conventional radiocarbon ages on material associated with soil S in southern coastal Washington. Most of these ages were measured on the peaty surficial horizon of the soil, on rings of unknown position in roots within the soil, and on sticks and cones directly above the soil (table 7; Atwater, 1992, his table 1). Such material provides maximum limiting ages for the event; these ages are between 1,400 and 2,100 years ago (fig. 32).

The range of 1,500–1,700 years ago probably accords with problematic ages of five carefully selected samples from the Naselle River of southeastern Willapa Bay (fig. 5). These ages, reported by Nelson and others (1996b), were measured on thoroughly cleaned stems and (or) leaves of herbaceous fossils (four *Potentilla pacifica*, one *Juncus balticus*) rooted in a probable correlative of soil S. The individual ages range from 1,680±40 ^{14}C yr B.P. to 1,910±50 ^{14}C yr B.P (table 7 of Atwater and Hemphill-Haley, 1996). The weighted mean age, 1,797±23 ^{14}C yr B.P., corresponds to about 1,600–1,900 years ago. But the mean is questionable because the five ages are significantly different at the 95-percent level, according to the chi-squared test of contemporaneity of Ward and Wilson (1978).

We obtained another potentially conflicting age from the Sewer locality. This age—1,990±70 ^{14}C yr B.P. (table

EXPLANATION

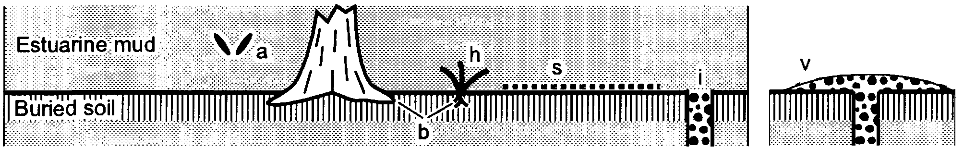

Evidence for Holocene earthquakes

Buried soil observed in outcrop—Typically in one or more low-tide exposures at least 30 m long. Letters beside dot denote associated evidence for subsidence, tsunami, shaking, and stratigraphic correlation

● **From published report**

○ **From unpublished data**

Subsidence—Inferred from paleontologic evidence that mud above soil represents a lower altitude than does the soil itself

a **Remains of herbs rooted in mud above buried soil**—Species typical of low parts of tidal marshes

b **Remains of herbs or trees rooted in buried soil**—Species typical of high parts of tidal wetland or of upland.

h Locally include herbaceous stems and leaves entombed in tsunami and (or) tidal-flat deposits above soil (h)

d **Microscopic fossils in soil and in mud**—Diatoms, pollen, and foraminifera at Johns River (Shennan and others, 1996); diatoms only at other localities

s **Tsunami**—Indicated by sand sheet on buried soil

i **Shaking**—Inferred from intrusive and extrusive sand. Excludes sand that vented

v from depths probably too great for ordinary earthquake-induced liquefaction (v)

Correlation of buried soils—Tested by radiocarbon dating

r **Conventional dating**—Quoted error typically 50-100 radiocarbon years

R **High-precision dating**—Quoted error 10-25 radiocarbon years

Evidence for net Cenozoic uplift or subsidence

▲ **Structural high**—Eocene Crescent Formation mapped at surface

\ **Syncline**—Mapped in rocks as young as Miocene

Figure 34. Continued.

7)—was measured on rotten, possibly contaminated rhizomes above soil S (p. 71).

SOIL U

Soil U appears to be widespread in southern Washington (fig. 34) and may have correlatives at least as far south as Netarts Bay, Oregon (Darienzo and others, 1994; Nelson and others, 1996b). The soil is typically faint and rarely contains woody roots in growth position, even where peaty or in an area of modern tidal spruce.

The event recorded by soil U probably occurred between 1,130 and 1,350 years ago. This range corresponds to two high-precision ages on growth-position herbaceous fossils at the Oyster locality—1,260±14 and 1,300±25 ^{14}C yr B.P. (p. 58). These ages are compatible with the age of 1,247±22 ^{14}C yr B.P. obtained on rhizomes above soil U at the Airport locality (p. 73). They are also close to 1,364±21 ^{14}C yr B.P., the weighted mean of six concordant radiocarbon ages each measured on a different herbaceous plant rooted in a probable correlative of soil U at the Naselle River (Nelson and others, 1996b; individual ages listed in table 7 of Atwater and Hemphill-Haley, 1996). The mean Naselle River age corresponds to a calendric range of about 1,200–1,400 years ago.

Ages greater than 1,400 years ago were reported by Atwater (1992) for conventionally dated material associated with soil U at Grays Harbor and the Copalis River (fig. 32). The conventional ages, however, were measured on peat (Elliott Slough and Copalis River) and on an upright but possibly detrital stump (Blue Slough). Both the peat and the stump could have originated centuries before the event recorded by the soil.

SOIL W

Soil W is barely preserved at some Washington localities and is absent, probably because of decomposition (p. 25), at some localities where soils U and Y are both present (fig. 34).

The event marked by soil W probably occurred between 900 and 1,300 years ago. This range is consistent with conventional ages on peaty mud at Grays Harbor, on a spruce root at southern Willapa Bay, and on sticks and a willow(?) root along a tributary to the Columbia River (Atwater, 1992, his table 1). It is further consistent with ages on peat and roots in a soil covered by vented sand at the Copalis River (fig. 32).

As speculated on page 83, the event marked by soil W may have occurred at or about a time of unusual faulting in the North America plate at Puget Sound. High-precision dating of earthquake-killed herbs and trees shows that this Puget Sound seismicity occurred between 1,000 and 1,100 years ago (Bucknam and others, 1992; Atwater and Moore, 1992; Jacoby and others, 1992; Huntley and Clague, 1996, their table 1).

SOIL Y

Soil Y is distinctive, like soil S, for containing spruce roots far downstream from modern spruce swamps (Atwater, 1992). It is further marked at Willapa Bay by a widespread mantle of tsunami-laid sand (Atwater, 1987, 1996; Reinhart and Bourgeois, 1987, 1989). Probable correlatives of soil Y have been identified along at least 900 km of the Cascadia subduction zone (Nelson and others, 1995).

The likely time of the event marked by soil Y is close to 300 years ago. Conventional radiocarbon ages show that the event happened after about A.D. 1500 (fig. 32). This window was narrowed to post-1680 by Yamaguchi and others (1989, 1997), who matched ring-width patterns in western redcedar snags rooted in soil Y in southern coastal Washington. Atwater and others (1991) obtained high-precision ages on selected rings of earthquake-killed spruce along the Niawiakum River, at nearby Bay Center, and at the Copalis River. The corresponding time of tree death is between about A.D. 1700 and 1720 (fig. 33), if calculated with the corrected radiocarbon calibration data of Stuiver and Becker (1993).

Among radiocarbon estimates for the time of the event marked by soil Y, the narrowest published ranges have been obtained from six ages for inner-ring samples of spruce stumps rooted in the soil (Atwater and others, 1991; Nelson and others, 1995). Each sample contains 10 or 20 rings that average 40 tree-ring years before tree death, and each comes from a different spruce stump: three stumps at the Copalis River, and three stumps 55 km to the south at Bay Center (two stumps) and the Niawiakum River (one stump). The six ages can be averaged if the trees probably died from the same earthquake or from a series of earthquakes within a few years of one another (Atwater and others, 1991). Their weighted mean—209±6 ^{14}C yr B.P.—has been converted to two different calendric age ranges intended to include the 95-percent confidence interval for tree death. The first reported, A.D. 1695–1710 (Atwater and others, 1991), is based the calibration data of Stuiver and Becker (1986). In this calibration, 209±6 ^{14}C yr B.P. corresponds to a 95-percent confidence interval of A.D. 1655–1669 if ±6 ^{14}C yr equals at least 0.6 standard deviation. Stuiver and Becker (1993) corrected the calibration data for slight contamination by radon. With this corrected data the weighted mean age implies tree death between 1703 and 1715 (Nelson and others, 1995).

The event consisted of a single magnitude-9 earthquake close to 9 p.m. local time on January 26, 1700, according to Satake and others (1996). Satake and his coworkers studied written records of a tsunami that struck Japan 10 hours later. They showed that earthquakes capable of generating this tsunami probably did not occur in Japan, Kamchatka, Alaska, or South America during January 1700. Using a numerical model of tsunamis, they also showed that the tsunami in Japan could have resulted from an earthquake that ruptured most of the length of the Cascadia subduction zone.

Correlation of the January 1700 tsunami in Japan with a great earthquake at Cascadia was first tested at Cascadia through study of living, presently tidal Sitka spruce (*Picea sitchensis*) that survived the submergence about 300 years ago in southern Washington and northern Oregon. Several dozen such trees have been found at the transition between floodplain and tidal swamp at the Copalis River, Willapa Bay, and the Columbia River. Annual rings in a third of them show changes in width and anatomy consistent with disturbance—tilting, increased flooding, or both—in the first few years after 1699 (Jacoby and others, 1997).

Further support for correlation with the January 1700 tsunami has come from tree-ring dating of redcedar that were killed or damaged by the most recent event in southern Washington. Among eight redcedar retaining bark despite centuries of decay, at least six died sometime between August 1699 and May 1700; they contain a complete 1699 ring but no younger ring (Yamaguchi and others, 1997). The five trees come from four estuaries along nearly 100 km of the Cascadia subduction zone: Copalis River, Grays Harbor, Willapa Bay, and Columbia River.

ADDITIONAL, UNRECORDED EVENTS

Buried soils do not necessarily record all the great plate-boundary earthquakes that have struck southern Washington during the past 3,500 years. The buried-soil record is most likely to be incomplete for earthquakes comparable to the 1944 and 1946 earthquakes in southwest Japan. These earthquakes, which caused a maximum of ½ m of tectonic subsidence (Ando, 1975, p. 122), were probably close to M_w 8.0 (Heaton and Hartzell, 1986, p. 693–694).

Such an earthquake could fail to register as a buried soil for two reasons:

1. If the earthquake occurs soon after a preceding great earthquake, there may be no peaty soil to bury; tidal flats resulting from the preceding earthquake may not have had time to grow upward into marshes and swamps having peaty soils.

2. If the earthquake is followed by a long period without great earthquakes in the area, the buried soil that records the earthquake may be destroyed by decomposition after burial (p. 27; fig. 35).

Both these problems probably contribute to the spotty distribution and typical faintness of soil W. Little time may have elapsed between the earthquake marked by soil U (1,130–1,350 years ago) and soil W (900–1,300 years ago, perhaps 1,000–1,100 years ago). Soil W, where studied at the Oyster locality, had not yet become a high marsh at its time of subsidence and burial (p. 48). For many centuries thereafter the soil resided high in the profile of soil Y, where it was subject to decomposition before being lowered far into the intertidal zone about 300 years ago. This decomposition allowed destruction of soil W at the northwestern part of the Oyster locality (p. 45) and throughout the Redtail locality (p. 29).

We doubt, however, that any great earthquake of the past 3,500 years at northeastern Willapa Bay completely failed to leave a trace. Rather, we infer that a buried soil should be preserved, at least locally, for every earthquake that caused more than ½ m of widespread coseismic subsidence at northeastern Willapa Bay in the past 3,500 years—provided the soil had many decades to form.

MINIMUM TIME FOR FORMATION OF A PEATY SOIL

Nineteenth-century writings and maps suggest that 150 years is ample for reconstructing high marshes from muddy tidal flats at Willapa Bay. The writings come from one of the first Euro-American settlers of Willapa Bay, James G. Swan. Swan resided at the marshy mouth of the Querquelin (now Bone) River (fig. 6) in the early 1850's, barely 150 years after the most recent great earthquake in southern coastal Washington changed Willapa Bay's marshes into tidal flats. Though tinged with boosterism, Swan's account leaves little doubt that the bay's tidal marshes ("prairie-land") had already become high marsh in those 150 years:

> "...all the rivers, large and small, run through fine prairie-land, exceedingly rich. That portion nearest the Bay is liable to be overflowed one or twice during the highest tides of winter, and are termed tide lands. This overflowing is, however, of no great detriment, although the water is salt, as, wherever the lands have been properly cultivated, they have yielded heavy crops. These prairies are all covered with grass of an excellent quality, making good grazing for stock, or a nutritious fodder when cut and made into hay." (Swan, 1857, p. 28).

Swan's account is consistent with depiction of tidal marshes on 1:10,000-scale plane-table maps of the bay's margins in the 1870's. These so-called T sheets, made by the U.S. Coast Survey, are on file with the National Oceanic and Atmospheric Administration in Rockville, Maryland; in addition they can be viewed and reproduced from microfilm at this agency's library in Seattle. The maps show tidal marshes similar in extent to those of modern Willapa Bay. Symbols on the maps further imply that most of these marshes stood about as high as they do today. The symbols include a solid line that separates marsh from mudflat except for a few small patches of marsh surrounded by mudflat. Whereas the patches of marsh consisted of *Triglochin maritimum* that was colonizing the mudflat in the 1870's, the solid line connotes the landward limit of ordinary high tides—tides that failed to cover most of the marshes.

EVENTS FOR WHICH SOILS WERE DESTROYED

Although centuries of decomposition may suffice to cause total destruction of shallowly buried soils at Willapa Bay, even 1,000 years is not enough for such destruction if the soil is more than about 0.3 m below the surface of the postearthquake marsh or swamp.

A postearthquake interval of 700–800 years is probably long enough to destroy a buried soil within 0.2–0.3 m of a high-marsh or spruce-swamp surface at northeastern Willapa Bay. Such an interval, as discussed on page 85, allowed destruction of soil W at part of the Oyster locality and throughout the Redtail locality.

Slightly deeper burial, however, allowed preservation of soil N during a postearthquake interval of about 1,000 years. The soil, which is barely visible where 0.2–0.3 m below soil S at the Jensen locality, is locally bold where 0.4 m below soil S at the Redtail locality (fig. 13, horizontal coordinate 18 m) and widely bold where 0.5 m below soil S at the Heron locality (fig. 25, horizontal coordinate 106–112). The interval during which soil N could have been destroyed by decomposition began soon after 2,400–2,800 years ago (the time of the event marked by soil N) and lasted until 1,500–1,700 years ago (the event marked by soil S).

Such minimum depths of burial to preserve a soil are probably smaller than the amounts of coseismic subsidence that the soil represents, for two reasons:

1. Amounts of subsidence along the Niawiakum River are probably 1 m or more for all but soil W, as inferred from the paleoecologic contrast between soil W and immediately overlying mud (p. 83).
2. Burial depth should be smaller than coseismic subsidence where interseismic uplift reduces the thickness of postseismic mud needed to rebuild a high marsh (p. 83). Interseismic uplift, which within 15 years undid as much as one-third of the 1964 subsidence in Alaska (Brown and others, 1977), should be the norm at northeastern Willapa Bay, particularly where soils cannot settle because they are underlain, at shallow depth, by scarcely compressible Pleistocene deposits. Pleistocene deposits at Willapa Bay record net late Quaternary uplift that cannot have been accomplished without interseismic uplift (p. 9).

INTERVALS BETWEEN GREAT EARTHQUAKES

The intervals between great earthquakes inferred from the buried soils can be portrayed simplistically as centuries of tectonic uplift and tidal sedimentation between instants of tectonic subsidence. We depict such history schemati-

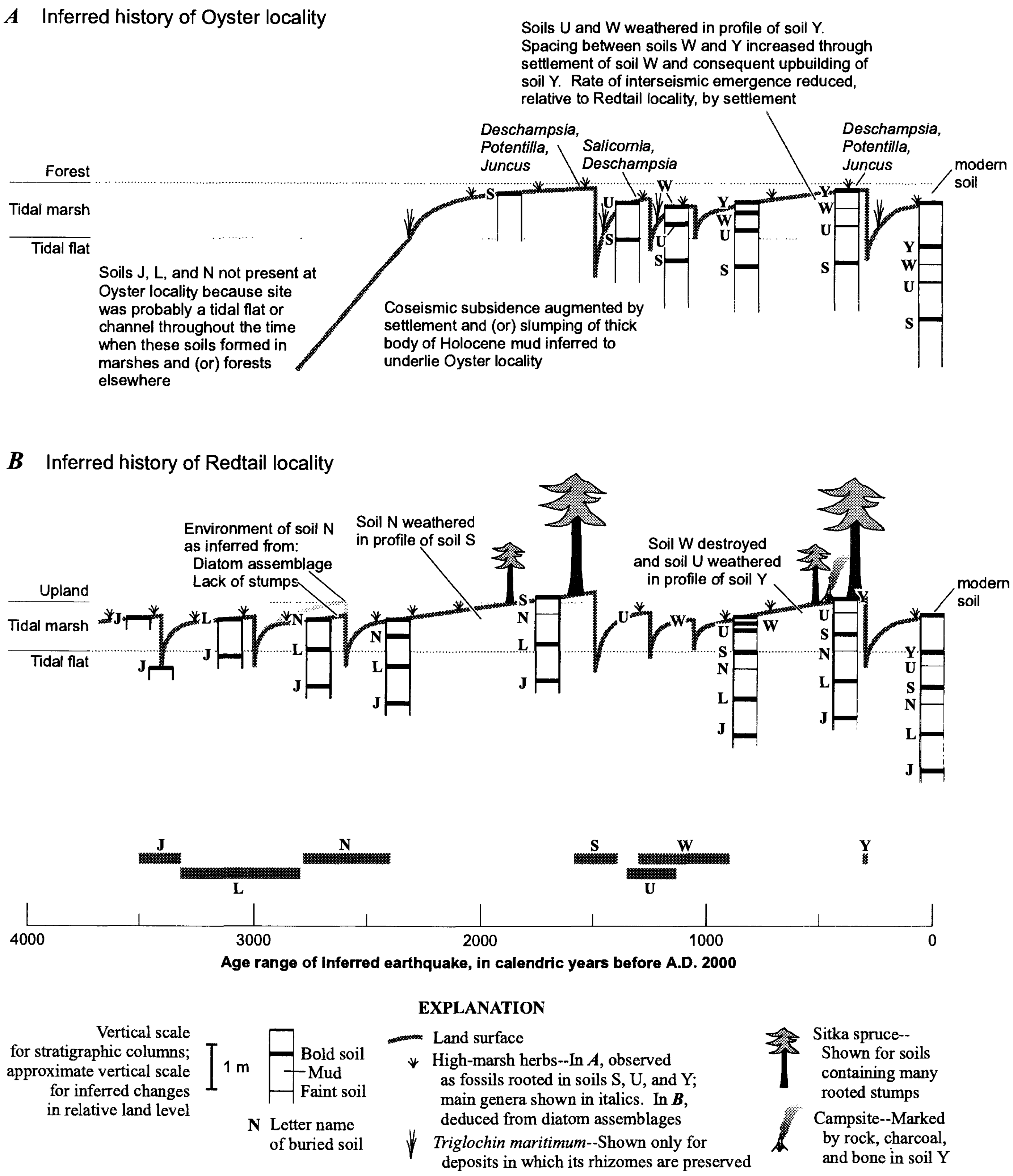

A Inferred history of Oyster locality

Soils U and W weathered in profile of soil Y. Spacing between soils W and Y increased through settlement of soil W and consequent upbuilding of soil Y. Rate of interseismic emergence reduced, relative to Redtail locality, by settlement

Soils J, L, and N not present at Oyster locality because site was probably a tidal flat or channel throughout the time when these soils formed in marshes and (or) forests elsewhere

Coseismic subsidence augmented by settlement and (or) slumping of thick body of Holocene mud inferred to underlie Oyster locality

B Inferred history of Redtail locality

Environment of soil N as inferred from:
Diatom assemblage
Lack of stumps

Soil N weathered in profile of soil S

Soil W destroyed and soil U weathered in profile of soil Y

Age range of inferred earthquake, in calendric years before A.D. 2000

EXPLANATION

Vertical scale for stratigraphic columns; approximate vertical scale for inferred changes in relative land level

Land surface

High-marsh herbs--In *A*, observed as fossils rooted in soils S, U, and Y; main genera shown in italics. In *B*, deduced from diatom assemblages

Triglochin maritimum--Shown only for deposits in which its rhizomes are preserved

Sitka spruce--Shown for soils containing many rooted stumps

Campsite--Marked by rock, charcoal, and bone in soil Y

Figure 35. Diagrammatic history of land-level change, vegetation, and decomposition inferred from buried soils at Niawiakum River at Oyster locality (*A*) and Redtail locality (*B*). Sawtooth curve displays land-level changes associated only with sedimentation, settlement, and tectonic uplift and subsidence directly related to earthquakes. Diagram ignores changes in sea level and permanent crustal uplift or subsidence. Time scale and explanation at bottom applies to both *A* and *B*. For details see first few paragraphs in section "Intervals Between Great Earthquakes" (p. 95, 97).

cally for the Oyster and Redtail localities (fig. 35). In this figure the heavy sawtooth line for each locality represents wetland height relative to a sea-level datum. We inferred wetland height from vascular-plant fossils and diatom assemblages (p. 83). The graph shows no overall trend in wetland height; we neglect eustatic and isostatic changes in sea level, and we further neglect fall in sea level from permanent tectonic uplift. Rather, the graph shows only the combined effects of the elastic component of interseismic uplift, sedimentation during this uplift, settlement from interseismic compaction, and tectonic coseismic subsidence

We assume that the combined effect of interseismic uplift and sedimentation is rapid at first but slow later, in keeping with the high initial rates of interseismic earthquake uplift (Brown and others, 1977; Savage and Plafker, 1991) and sedimentation (Ovenshine and others, 1976; Bartsch-Winkler and Garrow, 1982) documented for parts of Alaska that subsided during the 1964 Alaska earthquake. Rapid postearthquake sedimentation is further suggested by historical evidence from Willapa Bay, as discussed in the section "Minimum Time for Formation of a Peaty Soil" (p. 95).

The overall sawtooth shape of the land-level curves in figure 35 is based partly on analogy with cyclic vertical deformation related to great earthquakes in southwest Japan (Thatcher, 1984). The gentler interseismic slope of the wetland-level line for the Oyster locality represents settlement from interseismic compaction of peat and mud (p. 26–27). We infer that such settlement has counteracted tectonic uplift and sedimentation more effectively at the Oyster locality, where soft underlying mud may be as much as 30 m thick (p. 45), than at the Redtail locality, where buried soils lap onto stiff Pleistocene deposits (fig. 13).

UNCERTAINTIES IN THE ESTIMATED INTERVALS

Our estimates for recurrence intervals may contain errors from buried soils that do not represent great earthquakes, from earthquakes not recorded by buried soils, and from problems with dating the inferred earthquakes (fig. 4).

DOES EVERY BURIED SOIL REPRESENT A GREAT EARTHQUAKE?

As shown schematically in figure 4*B* and *C*, some buried soils may represent events other than great earthquakes. We evaluate this possibility in the sections "Distinction Between Tectonic Subsidence During Earthquakes and Other Ways of Producing the Buried Soils" (p. 73) and "Distinction Between Plate-Boundary and Upper-Plate Sources for the Earthquakes" (p. 80). We conclude that a great plate-boundary earthquake probably accounts for each of the buried soils in the surveyed outcrops.

This general conclusion does not apply equally to all soils. The case for a great plate-boundary earthquake at northeastern Willapa Bay is strongest for soil Y. Its shallow depth allows alternative explanations to be tested more readily than for less accessible soils; it is the only soil shown to be widely accompanied by evidence for tsunami and liquefaction in southern coastal Washington; and it is the only soil for which rupture length has been investigated through high-precision radiocarbon dating. The case is weakest for soil J, whose great depth limits its exposure and dating to a few outcrops, and for soil W, owing to its faintness and widespread absence.

IS EVERY GREAT EARTHQUAKE REPRESENTED BY A BURIED SOIL?

We evaluate possible incompleteness from long intervals and short intervals in the section "Additional, Unrecorded Events" (p. 94). There, we conclude that the buried-soil record at northeastern Willapa Bay is likely to include every great earthquake that caused widespread coseismic subsidence in the area during the past 3,500 years, except for earthquakes close to M_w 8.0 that caused less than about 0.5 m of subsidence and occurred within the first decades after a preceding great earthquake in the same area.

Some pairs of earthquakes may be represented by a single, widely correlated soil. Such would be the case if a soil, as correlated widely in southern coastal Washington, records a pair of great earthquakes—say, one from a rupture mainly north of the latitude of central Willapa Bay, the other from a rupture to the south of that latitude. To cover this possibility we refer to each soil as recording an "event," each of which comprises one or more great earthquakes (p. 91).

HOW PRECISELY ARE THE EARTHQUAKES DATED?

The age range assigned to each event on the basis of radiocarbon dating is summarized in the section "Events Recorded by Buried Soils" (p. 91). Each such range probably includes the 95-percent confidence interval (p. 24). The range spans about 400 years for the events marked by soils L, N, and W; about 200 years for soils J, S, and U; and about 20 years for soil Y. The broad range for soil W can be narrowed to 100 years if the event represented by soil W correlates with a better dated earthquake at Puget Sound (p. 94). The event marked by soil Y has been tree-ring dated to an interval less than a year and correlated with a tsunami that pins an earthquake to the day and approximate hour (p. 94).

To estimate recurrence intervals we compare full ranges of allowable age, not midpoints of ranges. Such comparison yields awkwardly broad ranges of recurrence intervals but propagates numerical uncertainties in dating.

HOW ACCURATELY ARE THE EARTHQUAKES DATED?

The accuracy of our numerical estimates of individual recurrence intervals can be checked, to some degree, against relative lengths of intervals. To infer relative lengths we use extent of trees and preservation of buried soils as guides to the duration of interseismic time. The approach is based on two premises summarized in figure 4*G* and illustrated in figure 35:

1. Passage of time at Willapa Bay helps change a tidal flat into a spruce forest rarely inundated by tides. Such vegetational succession is likely because Willapa Bay is subject to tectonic uplift between earthquakes (p. 9). The rate of uplift, if as high as estimated for the past 50 years by Hyndman and Wang (1995), is several times the average rate of late Holocene submergence, which is close to 1 mm/yr at northern Puget Sound (Eronen and others, 1987). The net result should be interseismic emergence, at least at sites where shallow depth to Pleistocene deposits permits little interseismic settlement from compaction of Holocene deposits. Such sites include the Jensen locality (fig. 27) and landward parts of the Redtail and Heron localities (figs. 13, 25).
2. Passage of time provides greater opportunity for a buried soil to decompose in the profile of the active soil above it. Such decomposition probably accounts for much of the scarcity of organic matter and lack of large vascular-plant fossils in the faint soils (p. 25).

We thus presume that the extent of trees and decomposition of buried soils are related more to the passage of time than to the occurrence of unusually rapid uplift. This presumption is supported by radiocarbon dating and perhaps also by correlation with turbidites.

Radiocarbon estimates of recurrence intervals correspond well with the extent of trees and the decomposition of buried soils, as shown in figure 35. The longest intervals inferred from numerical ages correspond to the longest intervals implied by abundance of trees and decomposition of soils—the intervals between the events marked by soils N and S and between W and Y. Soils S and Y were more widely forested than any of the others, and they are the only soils widely underlain by one or more faint soils. Conversely for a short interval—the one between the events marked by soils S and U—vascular-plant fossils and diatoms indicate tidal inundation more frequent for soil U than for soils S and Y (p. 48), and underlying soil S is well preserved. During what may be the shortest interval—the time between the events marked by soils U and W—soil W merely reached the transition between low marsh and high marsh (p. 48). Underlying soil U is rarely well preserved, but this poor preservation probably resulted from prolonged weathering high in soil Y.

Maximum extent of trees and decomposition of soils at Willapa Bay may correlate with maximum burrowing into turbidites on the floor of Cascadia Channel. This correlation is discussed in the section "Comparison with Intervals Estimated from Deep-Sea Turbdites" (p. 100).

INDIVIDUAL INTERVALS

Six individual recurrence intervals can be estimated from the seven inferred events—earthquake or earthquake series—marked by soils J, L, N, S, U, W, and Y.

INTERVALS BETWEEN EVENTS MARKED BY SOILS J, L, AND N

The two intervals among these events together span somewhere between 540 and 1,100 years; their average length is between 270 and 550 years.

The first of the intervals was probably longer than the second. Such a difference cannot be discerned from numerical ages, owing to large uncertainties for the events marked by soils L and N (p. 91). However, roots at the Redtail, Pool, Heron, and Jensen localities imply that spruce may have been more widespread on soil L than on soil N (figs. 13, 24, 25, 27)—evidence for greater interseismic emergence of soil L. Greater emergence of soil L is also suggested by microscopic fossils in probable correlatives of soils L and N at the Johns River (Shennan and others, 1996, their horizons V and IV). It appears to conflict, however, with the presence of an upland diatom assemblage in soil N at the Redtail locality (p. 23).

INTERVAL BETWEEN EVENTS MARKED BY SOILS N AND S

This interval, the longest one that we infer, spans somewhere between 700 and 1,300 years. In keeping with such a duration, soil S has fossils indicative of prolonged interseismic emergence: abundant spruce roots at many localities and a nearly upland assemblage of diatoms documented at the Redtail locality. Moreover, underlying soil N is commonly faint, as should be the case if it weathered for a long time in the profile of soil S.

INTERVAL BETWEEN EVENTS MARKED BY SOILS S AND U

A much shorter interval, of somewhere between 150 and 570 years, separated the events marked by soils S and U. The interval was long enough for rebuilding of a high marsh at the Oyster and Redtail localities (figs. 15, 20). However, at the Oyster locality it was not long enough for *Salicornia virginica* to be replaced by the fresher-water assemblage of vascular plants found rooted there in soils S and Y (p. 48).

A relatively short interval between soils S and U can also be inferred from microscopic fossils at the Johns River. Shennan and others (1996), citing assemblages of diatoms, pollen, and foraminifera at the Johns River, inferred that a soil U (their horizon II) represents a lower level in the intertidal zone than do soils S and Y (their horizons I and III).

INTERVAL BETWEEN EVENTS MARKED BY SOILS U AND W

An interval no longer than 450 years separates the events marked by soils U and W. The interval spans somewhere between 30 and 350 years if the event marked by soil W coincided, as speculated on page 94, with faulting in the Puget Sound region 1,000–1,100 years ago.

Fossils in soil W at the Oyster locality imply that the interval lasted no more than a century or two. The fossils imply that the event marked by soil U produced a tidal flat

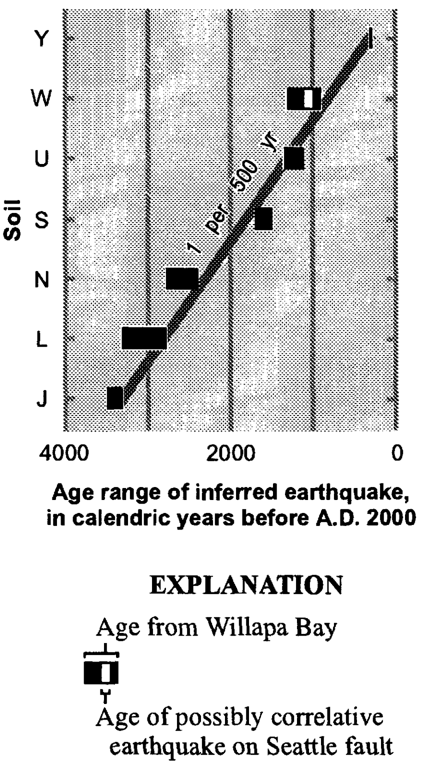

Figure 36. Inferred history of great earthquakes at northeastern Willapa Bay in the past 3,500 years. Age ranges described in section "Events Recorded by Buried Soils" (p. 91).

that shoaled into a *Triglochin maritimum* low marsh but did not become a high marsh before the event marked by soil W (p. 48). By contrast, the event marked by soil Y produced a tidal flat that probably became a high marsh within 150 years (see section "Minimum Time for Formation of a Peaty Soil" on p. 95).

INTERVAL BETWEEN EVENTS MARKED BY SOILS W AND Y

The final recorded interval lasted as little as 600 years and as much as about 1,000 years. If the event marked by soil W occurred 1,000–1,100 years ago, the interval lasted somewhere between 700 and 800 years.

A long interval before the event marked by soil Y is consistent with several kinds of evidence for emergence that could have been accomplished through prolonged interseismic uplift: spruce rooted in the soil in upstream and forest-edge areas where spruce is absent today (as near the Pool locality and at the Redtail and Heron localities); western redcedar similarly rooted downstream of its modern limits (Atwater, 1992, his fig. 5); diatom assemblages in the soil that suggest conditions transitional to upland (fig. 15); and remains of fishing camps high in the profile of the soil (Cole and others, 1996; our p. 30, 69, and figs. 13, 14*D* 29, 30*A*, *B*).

AVERAGE INTERVAL

The six recurrence intervals since 3,500 years ago have an average length of 500–540 years (fig. 36). This range includes one-sixth of 3,020–3,200 years, which is the difference in ages between the event marked by soil J (3,320–3,500 years ago) and the event marked by soil Y (300 years ago).

The average is sensitive to uncertainties in the counting of earthquakes (see sections "Does Every Buried Soil Represent a Great Earthquake?" and "Is Every Great Earthquake Represented by a Buried Soil?" on p. 97). The average increases to 600–645 years if soil W does not represent a great plate-boundary earthquake. Conversely, the average decreases to 430–460 years if one such earthquake left no lasting soil.

VARIABILITY AMONG INDIVIDUAL INTERVALS

Individual intervals between great plate-boundary earthquakes (or earthquake series) recorded by buried soils at northeastern Willapa Bay have been far from uniform during the past 3,500 years. Intervals between recorded events range from about one to three centuries (the interval between events marked by soils U and W) to about a millenium (the interval between events marked by soils N and S).

This variability might be reduced, but probably not much, by a great earthquake that was nowhere recorded by a lasting buried soil. Such an unrecorded earthquake would probably occur within a century of the preceding great earthquake (see section "Additional, Unrecorded Events", p. 94). Consequently, the unrecorded earthquake need not greatly shorten a long recurrence interval, and it would *increase* variability among recurrence intervals if it followed an especially short recurrence interval.

The event marked by soil W illustrates this problem with using unrecorded events to reduce the inferred variability among recurrence intervals. Soil W represents an event that is widely unrecorded, probably owing to decomposition of a shallowly buried soil during a long interval before the event marked by soil Y. Without soil W the time between the events marked by soils U and Y could be mistaken for a single interval about 1,000 years long. Soil W divides this time into two shorter intervals. But such division increases variability among intervals because the interval between events marked by soils U and W lasted several centuries less than the average interval.

COMPARISON WITH INTERVALS ESTIMATED FROM BURIED SOILS AT OTHER COASTAL ESTUARIES

The average interval of 500–540 years at Willapa Bay overlaps with all the ranges estimated from buried soils at other coastal estuaries with one exception (fig. 3). This exception is at Humboldt Bay, where the average interval for the past 1,450–1,750 years ranges from about 300 to 500 years. The possible explanations include:

1. Some of the inferred earthquakes at Humboldt Bay were limited to faults in the North America plate (Clarke and Carver, 1992).
2. Great earthquakes happen more often on the California part of the plate boundary than elsewhere on the plate boundary.
3. In the past 1,750 years, great Cascadia earthquakes have occurred more often than usual, regardless of location along the subduction zone. For example, the average of the three full recurrence intervals in the past 1,750 years at Willapa Bay is between 400 and 480 years (intervals between the events marked by soils S and U, soils U and W, and soils W and Y).

The exceptionally long interval between events marked by soils N and S may correlate with the longest recurrence interval inferred from buried soils at estuaries in northern Oregon. This Oregon interval, perhaps 1,000 years long and centered about 2,000 years ago, separates events 5 and 6 of Darienzo and Peterson (1995).

COMPARISON WITH INTERVALS ESTIMATED FROM DEEP-SEA TURBIDITES

A great plate-boundary earthquake accompanied by tectonic subsidence at Willapa Bay is well situated to send a turbidity current down Cascadia Channel (fig. 37). Though 200 km off the Oregon coast, Holocene turbidites in Cascadia Channel were derived primarily from canyon heads a mere 50 km west of Willapa Bay (Griggs and Kulm, 1970, p. 1381–1382). These canyon heads probably shook hard during great Holocene earthquakes on the southern Washington part of the Cascadia plate boundary: the canyon heads are located directly above the probable area of shallow rupture on the Cascadia plate boundary (Hyndman and Wang, 1995).

Given this connection, recurrence intervals recorded by buried soils at Willapa Bay ought to resemble recurrence intervals recorded by turbidites in Cascadia Channel. Adams (1990, p. 579) noted such a resemblance in average recurrence interval. Citing preliminary studies of buried soils, he estimated an average of 625 years for the last five to eight times of coseismic subsidence at Willapa Bay and likened it to his average of 590 years for the last 13 turbidity currents down lower Cascadia channel. Though the average interval at Willapa Bay now appears somewhat shorter than 625 years, it is probably compatible with the turbidite average, as we show in the next section “Average Interval.”

We then consider evidence for and against one-for-one correspondence between recurrence intervals for coseismic subsidence at Willapa Bay and recurrence intervals for turbidity currents in Cascadia channel. Adams (1990) interpreted similar thicknesses of pelagic clay between turbidites as evidence for earthquake-recurrence intervals less varied than those we now infer for Willapa Bay. However, successive turbidites differ from one another in abundance of burrows, and these differences suggest varied recurrence intervals that individually correlate with recurrence intervals at Willapa Bay.

AVERAGE INTERVAL

The average interval of 500–540 years at Willapa Bay is slightly less than the average that Adams (1990) inferred from turbidites in Cascadia Channel and other deep-sea channels off the Washington and Oregon coast (figs. 1, 3). Adams's 590-year average is plotted in figure 3 as a range of 550–630 years to express uncertainties in age of the earliest of the 13 great earthquakes that he inferred (see section “Turbidites in Deep-Sea Channels Off Washington and Oregon,” p. 7).

Several possibilities could explain why the Willapa Bay average is slightly less than the offshore turbidite average. Two arise from the difference in period of record—about 7,500 years for the turbidites ascribed to earthquakes by Adams (1990), versus 3,500 years for well-dated buried soils at Willapa Bay (fig. 36). Perhaps great Cascadia earthquakes have occurred more often in the past 3,500 years than in the preceding 4,000 years. Or perhaps Cascadia earthquakes were recorded by turbidites more completely in the past 3,500 years than in the preceding 4,000 years. Either of these possibilities is consistent with a post-Mazama increase in frequency of turbidity currents. As noted by Griggs and Kulm (1970, p. 1375–1376), average pre-Mazama intervals between Holocene turbidites were about 750–1,500 years in the same areas where post-Mazama intervals are less than 600 years.

Another possibility is that the turbidite record of great earthquakes in Cascadia Channel is incomplete because some earthquake-induced turbidites failed to travel beyond its tributaries. Average intervals between turbidity currents are about 100 years shorter in tributary channels; conversely, they exceed 1,000 years in the lowermost reaches of Cascadia Channel (Griggs and Kulm, 1970, p. 1375–1376), beyond the southern limit of the channel shown in figure 37. Cores from tributary channels contain as many as 16 turbidites less than about 7,500 years old (Adams, 1990, his fig. 1). If these tributary-channel sequences record 14–16 great earthquakes, the average recurrence intervals overlap with the Willapa Bay range of 500–540 years.

Finally, the buried-soil record at Willapa Bay may include an earthquake too small to produce any of the 13

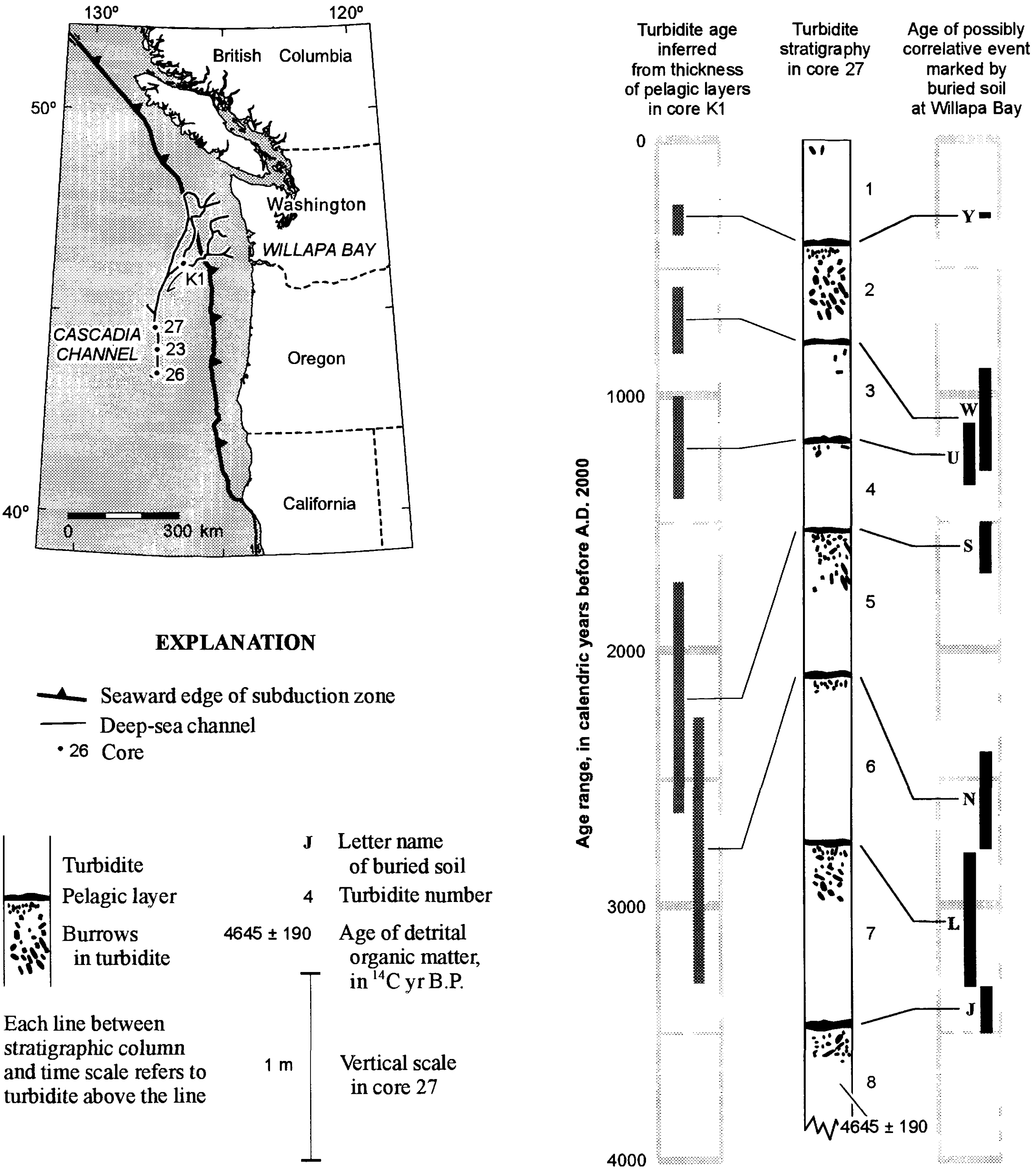

Figure 37. Turbidite stratigraphy of lower Cascadia Channel and ages inferred for individual turbidites. Burrows in turbidites suggest variability among recurrence intervals and correlation with recurrence intervals inferred from buried soils at Willapa Bay (p. 102). Stratigraphic column from Griggs and others (1969, their fig. 6). Ages based on pelagic-layer thickness are from Adams (1990, his table 3); all were estimated from pelagic layers in core K1 except for the age of the youngest turbidite, whose age Adams estimated from pelagic layers in six other cores (his table 2). Ages of events marked by buried soils at Willapa Bay are from figures 32 and 36.

turbidites in the turbidite record of Griggs and Kulm (1970) and Adams (1990). Soil W might represent such an earthquake because fossils associated with the soil imply less than 1 m of coseismic subsidence (p. 83).

VARIABILITY AMONG INTERVALS

INTERVALS IMPLIED BY DEPOSITS BETWEEN TURBIDITES

Turbidites of Cascadia Channel are separated from one another by layers of gray clay—termed pelagic (Griggs and others, 1969; Adams, 1990) or hemipelagic (Griggs and Kulm, 1970)—each of which probably represents at least the early part of the time between successive turbidity currents. The thickness of these pelagic layers is fairly uniform: on average, at least three-quarters of the pelagic layers in a single core differ in thickness by no more than a factor of two (Griggs and Kulm, 1970, p. 1375). Griggs and Kulm therefore inferred that the "time intervals between flows were of a similar duration."

Adams (1990, p. 578) used thickness of pelagic layers as evidence that only one of the intervals in the past 7,500 years is likely to be shorter than 300 years or longer than 900 years. He deduced this range from a standard deviation of 170 years, calculated from average rates of pelagic sedimentation and from the standard deviation of pelagic thickness in three cores selected for their pelagic layers of fairly uniform thickness.

Such statistics do not necessarily express uncertainties in measuring pelagic thickness in cores and in accounting for thickness lost to erosion. These uncertainties may be large (Griggs and others, 1969, p. 167). However, Adams (1990, p. 577) viewed them as tending to add to the real variability among recurrence intervals. He inferred this variability to be small (p. 576), in accord with his presumption that earthquakes on a plate-boundary recur at regular intervals and resemble one another in size (p. 578).

INTERVALS IMPLIED BY BURROWS IN TURBIDITES

Griggs and others (1969) showed that the abundance of burrows varies among successive turbidites of Cascadia Channel. They found such variability in three cores along 65 km of channel—cores 23, 26, and 27 in figure 37. They used the variability to correlate individual turbidites among these cores. A sketch of core 27, reproduced in figure 37, illustrates the correlative variability: "The second, fifth and seventh graded layers [turbidites 2, 5, and 7 in fig.37] contain abundant and distinct burrows to depths of 25 cm or greater. In intervening flows, however, they are much less abundant and are restricted primarily to the upper 5 or 10 cm" (Griggs and others, 1969, p. 165).

The abundance of burrows in these turbidites may increase with the time between turbidites. Griggs and others (1969, p. 167) contrasted this hypothesis with the uniform thickness of pelagic layers. But they also cited grooves eroded into many of the pelagic layers as evidence that preserved pelagic thickness represents only part of the time between successive turbidity currents. Further, Griggs and his coworkers described the turbidites as too similar to one another for variable abundance of burrows to be explained by differences in texture and organic content of the burrowed sediment.

If burrows in the turbidites became more abundant with time, recurrence intervals implied by the turbidite sequence of Griggs and others (1969) may correlate, one for one, with intervals inferred from buried soils at Willapa Bay (fig. 37). By this correlation, turbidites 5 and 2 were heavily burrowed in lower Cascadia Channel during the exceptionally long intervals when soils S and Y, respectively, formed at Willapa Bay. Conversely, light burrowing of turbidites 4 and 3 coincided with the short intervals preceding the events marked by soils U and W. Heavy burrowing of turbidite 7 would have occurred during the interval between events J and L, whose duration is poorly known but may be long on the basis of fossils (p. 98).

These correlations between Cascadia Channel and Willapa Bay are consistent with the sole available radiocarbon age from the sequence of correlated turbidites. The age, reported by Griggs and others (1969, their fig. 6), was measured on organic silt containing plant fragments probably recycled from older deposits. The age shows that turbidite 8 formed no earlier than 4,645±190 ^{14}C yr B.P., or no more than about 5,000–6,000 calendric years ago. If generated by the event marked by soil H, turbidite 8 should be 3,500–4,500 calendric years old (fig. 32). Alternatively, turbidite 8 correlates with an earlier buried soil (Adams, 1990, p. 579). Peat from this soil, which underlies soil H at the South Fork locality (fig. 6), gave an age of 4,290±80 ^{14}C yr B.P. (Atwater, 1992, his table 2).

Our correlations between Cascadia Channel and Willapa Bay are inconsistent with many of the ages and individual recurrence intervals estimated by Adams (1990, p. 581) from core K1 (fig. 37). One of the largest inconsistencies involves the youngest complete recurrence interval. Adams, citing a pelagic layer 19–25 mm thick, estimated that this interval lasted about 300–500 years. By contrast, we estimate that the youngest complete recurrence interval at Willapa Bay lasted 600–1,000 years—the interval between the events marked by soils W (900–1,300 years ago) and Y (300 years ago) (p. 99; fig. 36). We speculate that the pelagic layer was much thicker than 19–25 mm before it was eroded by the current that deposited the youngest turbidite at the site of core K1.

John Adams (written commun., 1996) suggested to us that highly varied recurrence intervals might produce fairly uniform pelagic thickness if the depth of erosion of a pelagic layer increases with the size of the turbidity current, which in turn may increase with the length of the recurrence interval. Adams also pointed out, however, that some pelagic layers should have been removed altogether had deep erosion occurred widely in Cascadia Channel. Perhaps the typical pelagic layer accumulated more rapidly at first, while the water column retained particles from the preceding turbidite. In that case, the lower part of the layer might be compact enough to resist erosion, however short or long the interval during which the rest of the layer accumulates.

PATTERN OF RECURRENCE

The likely variability among recurrence intervals of the past 3,500 years shows that great earthquakes at Willapa Bay do not happen on a regular schedule. The least regularity is implied by the three successive intervals between soils N and S, S and U, and U and W. Whereas the first of these intervals spanned 700–1,300 years, the other two *together* spanned no more than 800 years. The interval between the events marked by soils J and L may also have been much longer than the succeeding interval, between the events marked by soils L and N (fig. 36).

Such highly irregular recurrence of earthquakes on one part of a fault has been inferred for the southern San Andreas fault (Sieh and others, 1989), for a thrust fault in Algeria (Swan, 1987), and for normal faults near the Dead Sea (Marco and others, 1996) but not for great plate-boundary earthquakes at subduction zones other than Cascadia. For most subduction zones the reported record of great earthquakes spans only one or a few earthquake cycles (Thatcher, 1989), where "cycle" denotes the interval between "events" as defined on page 91. The main exception is southwest Japan, where historical records since A.D. 684 suggest cycle lengths of 90–264 years but no strong clustering of the cycles (Ando, 1975). Identification and dating of earthquakes are too uncertain to show whether recurrence intervals vary greatly in the region of the 1964 Alaska earthquake (Plafker and others, 1992).

SPECULATIONS ABOUT THE NEXT GREAT EARTHQUAKE IN SOUTHERN COASTAL WASHINGTON

The next great earthquake at northeastern Willapa Bay need not be as large as the largest Cascadia earthquakes of the past 3,500 years. This speculation is based on several kinds of evidence that soils S and Y represent exceptionally great earthquakes:

Exceptional subsidence during the events marked by soils S and Y.—Because they were more widely forested than other soils of the past 3,500 years in southern coastal Washington, soils S and Y had to subside farther to become tidal flats (figs. 15, 20, 35).

A long rupture during the event marked by soil Y.—A single M_w 9 earthquake best explains radiocarbon and tree-ring correlation with a tsunami that damaged Japan in January 1700 (p. 94).

Long recurrence intervals.—The events marked by soils S and Y followed recurrence intervals long enough to generate earthquakes of M_w 9 on a strongly coupled Cascadia plate boundary, under conservative assumptions stated in the section "Tradeoff Between Size and Frequency" (p. 90).

Alternatively, the event marked by soil Y failed to expend a large fraction of the plate convergence accumulated in the preceding centuries, in which case the stored convergence could allow the next great Cascadia earthquake to be as large as any Cascadia earthquake of the past 3,500 years. Such storage probably contributed to the size of the M_w 9.5 1960 Chile earthquake. Plate-boundary slip during this earthquake widely exceeded 20 m, according to interpretation of land-level changes that accompanied the earthquake (Plafker and Savage, 1970; Barrientos and Ward, 1990). However, the preceding great earthquake occurred only 123 years earlier (Lomnitz, 1970). This interval is too short for accumulation of 20 m of slip at 0.1 m/yr, the average rate of plate convergence in the region of the 1960 earthquake (DeMets and others, 1990).

REFERENCES CITED

Adams, J., 1990, Paleoseismicity of the Cascadia subduction zone: evidence from turbidites off the Oregon-Washington margin: Tectonics, v. 9, p. 569–583.

———Great earthquakes recorded by turbidites off the Oregon-Washington coast, *in* Rogers, A.M., Walsh, T.J., Kockelman, W.J., and Priest, G.R., eds., Assessing earthquake hazards and reducing risk in the Pacific Northwest: U.S. Geological Survey Professional Paper 1560, p. 147–158.

Ando, M., 1975, Source mechanism and tectonic significance of historic earthquakes along the Nankai Trough, Japan: Tectonophysics, v. 27, p. 119–140.

Ando, M., and Balazs, E.I., 1979, Geodetic evidence for aseismic subduction of the Juan de Fuca plate: Journal of Geophysical Research, v. 84, p. 3023–3028.

Atwater, B.F., 1987, Evidence for great Holocene earthquakes along the outer coast of Washington State: Science, v. 236, p. 942–944.

———1992, Geologic evidence for earthquakes during the past 2000 years along the Copalis River, southern coastal Washington: Journal of Geophysical Research, v. 97, p. 1901–1919.

———compiler, 1994, Geology of liquefaction features about 300 years old along the lower Columbia River at Marsh, Brush, Price, Hunting, and Wallace Islands, Oregon and Washington: U.S. Geological Survey Open-File Report 94–209, 64 p.

———1996, Coastal evidence for great earthquakes in western Washington, *in* Rogers, A.M., Walsh, T.J., Kockelman, W.J., and Priest, G.R., eds., Assessing earthquake hazards and reducing risk in the Pacific Northwest: U.S. Geological Survey Professional Paper 1560, p. 77–90.

Atwater, B.F., and Hemphill-Haley, E., 1996, Preliminary estimates of recurrence intervals for great earthquakes of the past 3500 years at northeastern Willapa Bay, Washington: U.S. Geological Survey Open-File Report 96–001, 88 p.

Atwater, B.F., Hull, A.G., and Bevis, K.A., 1987, Aperiodic Holocene recurrence of widespread, probably coseismic subsidence in southwestern Washington [abstract]: Eos, v. 70, p. 1330–1331.

Atwater, B.F., and Moore, A.L., 1992, A tsunami 1000 years ago in Puget Sound, Washington: Science, v. 258, p. 1614–1617.

Atwater, B.F., Nelson, A.R., Clague, J.J., Carver, G.A., Yamaguchi, D.K., Bobrowsky, P.T., Bourgeois, J., Darienzo, M.E., Grant, W.C., Hemphill-Haley, E., Kelsey, H.M., Jacoby, G.C., Nishenko, S.P., Palmer, S.P., Peterson, C.D., and Reinhart, M.A., 1995, Summary of coastal geologic evidence for past great earthquakes at the Cascadia subduction zone: Earthquake Spectra, v. 11, p. 1–18.

Atwater, B.F., Stuiver, M., and Yamaguchi, D.K., 1991, Radiocarbon test of earthquake magnitude at the Cascadia subduction zone: Nature, v. 353, p. 156–158.

Atwater, B.F., and Yamaguchi, D.K, 1991, Sudden, probably coseismic submergence of Holocene trees and grass in coastal Washington State: Geology, v. 19, p. 706–709.

Barbour, M.G., and Davis, C.B., 1970, Salt tolerance of five California salt marsh plants: American Midland Naturalist, v. 84, p. 262–265.

Barrick, R.C., 1975, Hydrodynamics of Grays Harbor estuary, *in* Maintenance dredging and the environment of Grays Harbor, Washington: Seattle, U.S. Army Corps of Engineers, Appendix A.

Barrientos, S.E., and Ward, S.N., 1990, The 1960 Chile earthquake: inversion for slip distribution from surface deformation: Geophysical Journal International, v. 103, p. 589–598.

Bartsch-Winkler, S.R., and Garrow, H.C., 1982, Depositional systems approaching maturity at Portage Flats, *in* Coonrad, W.L., ed., The United States Geological Survey in Alaska: accomplishments during 1980: U.S. Geological Survey Circular 844, p. 115–117.

Behre, K.-E., Menke, B., and Streif, H., 1979, The Quaternary geological development of the German part of the North Sea, *in* Oele, E., Schttenhelm, R.T.E., and Wiggers, A.J., eds., The Quaternary History of the North Sea: Acta Universitatis Upsaliensis, Symposia Universitatis Upsaliensis Annun Quingentesimum Celebrantis, v. 2, p. 85–113.

Benson, B.E., Grimm, K.A., and Clague, J.J., 1997, Tsunami deposits beneath tidal marshes on northwestern Vancouver Island, British Colombia: Quaternary Research (in press).

Berryman, K.R., 1993, Age, height, and deformation of Holocene marine terraces at Mahia Peninsula, Hikurangi subduction margin, New Zealand: Tectonics, v. 12, p. 1347–1364.

Berryman, K.R., Ota, Y., and Hull, A.G., 1989, Holocene paleoseismicity in the fold and thrust belts of the Hikurangi subduction zone, eastern North Island, New Zealand: Tectonophysics, v.163, p. 185–195.

Brown, L.D., Reilinger, R.E., Holdahl, S.R., and Balazs, E.I., 1977, Postseismic crustal uplift near Anchorage, Alaska: Journal of Geophysical Research, v. 82, p. 3369–3378.

Bucknam, R.C., Hemphill-Haley, E., and Leopold, E.B., 1992, Abrupt uplift within the past 1700 years at southern Puget Sound, Washington: Science, v. 258, p. 1611–1614.

Byrne, D.E., Sykes, L.R., and Davis, D.M., 1992, Great thrust earthquakes and aseismic slip along the plate boundary of the Makran subduction zone: Journal of Geophysical Research, v.97, p. 449–478.

Cahoon, D.R., Reed, D.J., and Day, J.W., Jr., 1995, Estimating shallow subsidence in microtidal salt marshes of the southeastern United States: Kaye and Barghoorn revisited: Marine Geology,v. 128, p. 1–10.

Carver, G.A., Stuiver, M., and Atwater, B.F., 1992, Radiocarbon ages of earthquake-killed trees at Humboldt Bay, California [abstract]: Eos, v. 73, no. 43, p. 398.

Clague, J.J., and Bobrowsky, P.T., 1994, Tsunami deposits beneath tidal marshes on Vancouver Island, British Columbia: Geological Society of America Bulletin, v. 106, p. 1293–1303.

Clarke, S.H., Jr., and Carver, G.A., 1992, Late Holocene tectonics and paleoseismicity, southern Cascadia subduction zone: Science, v. 255, p. 188–192.

Clifton, H.E., 1983, Discrimination between subtidal and intertidal facies in Pleistocene deposits, Willapa Bay, Washington: Journal of Sedimentary Petrology, v. 53, p. 353–369.

Cole, S.C., Atwater, B.F., McCutcheon, P.T., Stein, J.K., and Hemphill-Haley, E., 1996, Earthquake-induced burial of archaeological sites along the southern Washington coast about A.D. 1700: Geoarchaeology, v. 11, p. 165–177.

Cowan, D.S., and Potter, C.J., 1986, Juan de Fuca spreading ridge to Montana thrust belt: Geological Society of America Continent-ocean transect B3.

Darienzo, M.E., and Peterson, C.D., 1990, Episodic tectonic subsidence of late Holocene salt marshes, northern Oregon coast, central Cascadia margin, U.S.A.: Tectonics, v. 9, p. 1–22.

———1995, Magnitude and frequency of subduction-zone earthquakes along the Oregon coast in the past 3,000 years: Oregon Geology, v. 57, p. 3–12.

Darienzo, M.E., Peterson, C.D., and Clough, C., 1994, Stratigraphic evidence for great subduction-zone earthquakes at four estuaries in northern Oregon: Journal of Coastal Research, v. 10, p. 850–876.

DeMets, C., Gordon, R., Argus, D.F, and Stein, S., 1990, Current plate motions: Geophysical Journal International, v. 101, p. 425–478.

Denys, L., 1984, Diatom analysis of coastal deposits: methodological aspects: Bulletin van de Belgische Vereniging voor Geologie, v. 93, p. 291–295.

Devoy, R.J.N., 1979, Flandrian sea level changes and vegetational history of the lower Thames estuary: Philosophical Transactions of the Royal Society of London, B, v. 285, p. 355–407.

Dragert, H., and Hyndman, R.D., 1995, Continuous GPS monitoring of elastic strain in the northern Cascadia subduction zone: Geophysical Research Letters, v. 22, p. 755–758.

Dragert, H., Hyndman, R.D., Rogers, G.C., and Wang, K., 1994, Current deformation and the width of the seismogenic zone of the northern Cascadia subduction zone: Journal of Geophysical Research, v. 99, p. 653–668.

Eronen, M., Kankainen, T., and Tsukada, M., 1987, Late Holocene sea-level record in a core from the Puget lowland, Washington: Quaternary Research, v. 27, p. 147–159.

Fletcher, C.H., III, Pizzuto, J.E., John, S., and van Pelt, J.E., 1993a, Sea-level rise acceleration and the drowning of the Delaware Bay coast at 1.8 ka: Geology, v. 21, p. 121–124.

Fletcher, C.H., III, van Pelt, J.E., Brush, G.S., and Sherman, J., 1993b, High-resolution stratigraphic framework, Holocene sea-level and climate history, and evolution of a tidal wetland: Palaeogeography, Palaeoclimatology, Palaeoecology, v. 102, p. 177–213.

Geomatrix Consultants, 1995, Seismic design mapping: prepared for Oregon Department of Transportation, Salem, Oregon, personal services contract no. 11688, project no. 2442, various pagination.

Geist, E., and Shoichi, Y., 1996, Source parameters controlling the generation and propagation of potential local tsunamis along the Cascadia margin: Natural Hazards, v. 13, p. 151–177.

Geyh, M.A., 1980, Holocene sea-level history: case study of the statistical evaluation of ^{14}C dates: Radiocarbon, v. 22, p. 695–704.

Goldfinger, C., Kulm, L.D., Yeats, R.S., Appelgate, B., MacKay, M., and Moore, G.F., 1992a, Transverse structural trends along the Oregon convergent margin: implications for Cascadia earthquake potential: Geology, v. 20, p. 141–144.

Goldfinger, C., Kulm, L.D., Yeats, R.S., Mitchell, C., Weldon, R., Peterson, C.D., Darienzo, M.E., Grant, W.C., and Priest, G.R., 1992b, Neotectonic map of the Oregon continental margin and adjacent abyssal plain: Oregon Department of Geology and Mineral Industries Open-File Report 0–92–4, scale 1:500,000.

Goldfinger, C., Kulm, L.D., Yeats, R.S., McNeill, L., and Hummon, C., 1997, Oblique strike-slip faulting of the central Cascadia submarine forearc: Journal of Geophysical Research, v. 102, p. 8217–8243.

Goldfinger, C., McNeill, L.C., Kulm, L.D., and Yeats, R.S., 1996, Width of the seismogenic plate boundary in Cascadia: structural indicators of strong and weak coupling [abstract]: Geological Society of America, Abstracts with Programs, v. 28, no. 5, p. 69.

Goodbred, S.L., Jr., and Hine, A.C., 1995, Coastal storm deposition: salt-marsh response to a severe extratropical storm, March 1993, west-central Florida: Geology, v. 23, p. 679–682.

Grant, W.C., and Minor, R., 1991, Paleoseismic evidence and prehistoric occupation associated with late Holocene sudden submergence, northern Oregon coast [abstract]: Eos, v. 72, no. 44, p. 313.

Griggs, G.B., Carey, A.G., and Kulm, L.D., 1969, Deep-sea sedimentation and sediment-fauna interaction in Cascadia Channel and on Cascadia Abyssal Plain: Deep-Sea Research, v. 16, p. 157–170.

Griggs, G.B., and Kulm, L.D., 1970, Sedimentation in Cascadia deep-sea channel: Geological Society of America Bulletin, v. 81, p. 1361–1384.

Guilbault, J.-P., Clague, J.J., and Lapointe, M., 1995, Amount of subsidence during a late Holocene earthquake—evidence from fossil tidal marsh foraminifera at Vancouver Island, west coast of Canada: Palaeogeography, Palaeoclimatology, Palaeoecology, v. 118, p. 49–71.

Hanks, T.C., and Kanamori, H., 1979, A moment magnitude scale: Journal of Geophysical Research, v. 84, p. 2348–2350.

Heaton, T.H., and Hartzell, S.H., 1986, Source characteristics of hypothetical subduction earthquakes in the northwestern United States: Bulletin of the Seismological Society of America, v. 76, p. 675–708.

———1987, Earthquake hazards on the Cascadia subduction zone: Science, v. 236, p. 162–168.

Heki, K., Miyazaki, S., and Tsuji, H., 1997, Silent fault slip following an interplate thrust earthquake at the Japan Trench: Nature, v. 386, p. 595–598.

Hemphill-Haley, E., 1993, Occurrences of Recent and Holocene intertidal diatoms (Bacillariophyta) in northern Willapa Bay, Washington: U.S. Geological Survey Open-File Report 93-284, 94 p.

———1995a, Intertidal diatoms from Willapa Bay, Washington: application to studies of small sea-level changes: Northwest Science, v. 69, p. 29–45.

———1995b, Diatom evidence for earthquake-induced subsidence and tsunami 300 yr ago in southern coastal Washington: Geological Society of America Bulletin, v. 107, p. 367–378.

———1996, Diatoms as an aid in identifying late-Holocene tsunami deposits: The Holocene, v. 6, p. 439–448.

Hemond, H.F., and Chen, D.G., 1990, Air entry in salt marsh sediments: Soil Science, v. 150, p. 459–468.

Hitchcock, C.L., and Cronquist, A., 1973, Flora of the Pacific Northwest: Seattle, University of Washington Press, 730 p.

Holdahl, S.R., Faucher, F., and Dragert, H., 1989, Contemporary vertical crustal motion in the Pacific Northwest, *in* Cohen, S.C., and Vanicek, P., eds., Slow Deformation and Transmission of Stress in the Earth: American Geophysical Union Geophysical Monograph 49, p. 17–29.

Hull, A.G., 1987, Buried lowland soils from Willapa Bay, southwest Washington: further evidence for recurrence of large earthquakes during the past 5000 years [abstract]: Eos, v. 68, p. 1469.

Huntley, D.J., and Clague, J.J., 1996, Optical dating of tsunami-laid sands: Quaternary Research, v. 46, p. 127–140.

Hyndman, R.D., and Wang, K., 1993, Thermal constraints on the zone of major thrust earthquake failure: the Cascadia subduction zone: Journal of Geophysical Research, v. 98, p. 2039–2060.

———1995, The rupture zone of Cascadia great earthquakes from current deformation and thermal regime: Journal of Geophysical Research, v. 100, p. 22133–22154.

Hyndman, R.D., and Weichert, D.H., 1983, Seismicity and rates of relative motion on plate boundaries of western North America: Geophysical Journal of the Royal Astronomical Society, v. 72, p. 59–82.

Jacoby, G.C., Bunker, D.E., and Benson, B.E., 1997, Tree-ring evidence for an A.D. 1700 Cascadia earthquake in Washington and northern Oregon: Geology, v. 25, p. 999–1002.

Jacoby, G.C., Carver, G., and Wagner, W., 1995, Trees and herbs killed by an earthquake ~300 yr ago at Humboldt Bay, California: Geology, v. 23, p. 77–80.

Jacoby, G.C., Williams, P.L., and Buckley, B.M., 1992, Tree ring correlation between prehistoric landslides and abrupt tectonic events in Seattle, Washington: Science, v. 258, p. 1621–1623.

Jelgersma, S., 1961, Holocene sea level changes in the Netherlands: Mededelingen van de Geologische Stichting, Serie C, VI, v. 7, p. 1–100.

Jelgersma, S., Oele, E., and Wiggers, A.J., 1979, Depositional history and coastal development in the Netherlands and the adjacent North Sea since the Eemian, *in* Oele, E., Schttenhelm, R.T.E., and Wiggers, A.J., eds., The Quaternary History of the North Sea: Acta Universitatis Upsaliensis, Symposia Universitatis Upsaliensis Annun Quingentesimum Celebrantis, v. 2, p. 115–142.

Jennings, A.E., and Nelson, A.R., 1992, Foraminiferal assemblage zones in Oregon tidal marshes—relation to marsh floral zones and sea level: Journal of Foraminiferal Research, v. 22, p. 13–29.

Johnson, D.W., 1925, The New England–Acadian Shoreline: New York, John Wiley, 608 p.

Johnson, J.W., 1973, Characteristics and behavior of Pacific Coast tidal inlets: Journal of the Waterways, Harbors, and Coastal

Engineering Division, Proceedings of the American Society of Civil Engineers, v. 99, p. 325–339.

Kanamori, H., 1977, The energy release in great earthquakes: Journal of Geophysical Research, v. 82, p. 2981–2987.

Kanamori, H., and McNally, K.C., 1982, Variable rupture mode of the subduction zone along the Ecuador-Colombia coast: Bulletin of the Seismological Society of America, v. 72, p. 1241–1253.

Karlin, R.E., and Abella, S.E.B., 1992, Paleoearthquakes in the Puget Sound region recorded in sediments of Lake Washington, U.S.A.: Science, v. 258, p. 1617–1620.

Kelsey, H.M., 1990, Late Quaternary deformation of marine terraces on the Cascadia subduction zone near Cape Blanco, Oregon: Tectonics, v. 9, p. 983–1014.

Kelsey, H.M., Engebretson, D.C., Mitchell, C.E., and Ticknor, R.L., 1994, Topographic form of the Coast Ranges of the Cascadia Margin in relation to coastal uplift rates and plate subduction: Journal of Geophysical Research, v. 99, p. 12245–12255.

Kelsey, H.M., Witter, R.C., and Hemphill-Haley, E., 1996, Record of plate boundary earthquakes near Cape Blanco, Oregon [abstract]: Geological Society of America Abstracts with Programs, v. 28, no. 5, p. 80.

Kelsey, H.M, Witter, R.C., and Polenz, M., 1993, Cascadia paleoseismic record derived from late Holocene fluvial and lake sediments, Sixes River valley, Cape Blanco, south coastal Oregon [abstract]: Eos, v. 74, no. 43, p. 199.

Kunze, L.M., and Cornelius, L.C., 1982, Baseline inventory of rare, threatened and endangered plant species/communities along Washington's Pacific coast: Washington Department of Ecology, National Oceanic and Atmospheric Administration Coastal Zone Management Grant G68–029.

Lomnitz, C., 1970, Major earthquakes and tsunamis in Chile during the period 1535 to 1955: Geologische Rundschau, Band 59, p. 938–960.

Mall, R.E., 1969, Soil-water-salt relationships of waterfowl food plants in the Suisun marsh of California: California Department of Fish and Game, Wildlife Bulletin 1, 59 p.

Marco, S., Stein, M., Agnon, A., and Ron, H., 1996, Long-term earthquake clustering: a 50,000-year paleoseismic record in the Dead Sea Graben: Journal of Geophysical Research, v. 101, p. 6179–6191.

Mathewes, R.W., and Clague, J.J., 1994, Detection of large prehistoric earthquakes in the Pacific Northwest by microfossil analysis: Science, v. 264, p. 688–691.

McCaffrey, R., and Goldfinger, C., 1995, Forearc deformation and great subduction earthquakes: implications for Cascadia offshore earthquake potential: Science, v. 267, p. 856–859.

McCulloch, D.S., and Bonilla, M.G., 1970, Effects of the earthquake of March 27, 1964, on The Alaska Railroad: U.S. Geological Survey Professional Paper 545–D, 161 p.

McInelly, G.W., and Kelsey, H.M.,1990, Late Quaternary tectonic deformation in the Cape Arago–Bandon region of coastal Oregon as deduced from wave-cut platforms: Journal of Geophysical Research, v. 95, p. 6699–6714.

McNeill, L.C., Goldfinger, C., Kulm, L.D., and Yeats, R.S., 1994, Tectonics of the Washington continental margin, Cascadia subduction zone [abstract]: Geological Society of America Abstracts with Programs, Annual Meeting 1994, p. A–523.

Meyers, R.A., Smith, D.G., Jol, H.M., and Peterson, C.D., 1996, Evidence for eight great earthquake-subsidence events detected with ground-penetrating radar, Willapa barrier, Washington: Geology, v. 24, p. 99–102.

Meyerson, A.L., 1972, Pollen and paleosalinity analyses from a Holocene tidal marsh sequence, Cape May County, New Jersey: Marine Geology, v. 12, p. 335–357.

Miles, M.M., Wiggins, W.D., Ruppert, G.P., Smith, R.R., Reed, L.L., Hubbard, L.E., and Courts, M.L., 1994, Water resources data Washington water year 1993: U.S. Geological Survey Water-Data Report WA–93–1, 408 p.

Minor, R., and Grant, W.C., 1996, Earthquake-induced subsidence and burial of late Holocene archaeological sites, northern Oregon coast: American Antiquities, v. 61, p. 772–781.

Mitchell, C.E., Vincent, P., and Weldon, R.J., 1994, Present-day vertical deformation of the Cascadia margin, Pacific Northwest, United States: Journal of Geophysical Research, v. 99, p. 12257–12277.

Morris, J.T., and Whiting, G.J., 1986, Emission of gaseous carbon dioxide from salt-marsh sediments and its relation to other carbon losses: Estuaries, v. 9, p. 1–19.

Mudge, B.F., 1862, The salt marsh formations of Lynn: Proceedings of the Essex Institute, v. 2, p. 117–119.

Mumford, T.F., Jr., Peyton, P., Sayce, K.R., and Harbell, S. (eds.). 1990. Spartina workshop record. Seattle, Washington, University of Washington, Washington Sea Grant Program, WSG-WO 91–01, 73 p.

Nelson, A.R., 1992a, Holocene tidal-marsh stratigraphy in south-central Oregon evidence for localized sudden submergence in the Cascadia subduction zone, *in* Fletcher, C.P., and Wehmiller, J.F., eds., Quaternary coasts of the United States: marine and lacustrine systems: Society for Sedimentary Geology Special Publication 48, p. 287–301.

———1992b, Discordant ^{14}C ages from buried tidal-marsh soils in the Cascadia subduction zone, southern Oregon coast: Quaternary Research, v. 38, p. 75–90.

Nelson, A.R., and Atwater, B.F., 1993, Radiocarbon ages of earthquake-killed plants along the Cascadia subduction zone [abstract]: Eos, v. 74, no. 43, p. 199–200.

Nelson, A.R., Atwater, B.F., Bobrowsky, P.T., Bradley, L.-A., Clague, J.J., Carver, G.A., Darienzo, M.E., Grant, W.C., Krueger, H.W., Sparks, R., Stafford, T.W., and Stuiver, M., 1995, Radiocarbon evidence for extensive plate-boundary rupture about 300 years ago at the Cascadia subduction zone: Nature, v. 378, p. 371–374.

Nelson, A.R., Hemphill-Haley, E., and Witter, R.C., 1996c, A 7500-year lake record of Cascadia tsunamis in southern coastal Oregon [abstract]: Geological Society of America, Abstracts with Programs, v. 28, no. 5, p. 95.

Nelson, A.R., Jennings, A.E., and Kashima, K., 1996a, Holocene intertidal stratigraphy, microfossils, rapid submergence, and earthquake recurrence at Coos Bay, southern coastal Oregon, USA: Geological Society of America Bulletin, v. 108, p. 141–154.

Nelson, A.R., and Kashima, K., 1993, Diatom zonation in southern Oregon tidal marshes relative to vascular plants, foraminifera, and sea level: Journal of Coastal Research, v. 9, p. 673–697.

Nelson, A.R., and Personius, S.F., 1996, The potential for great earthquakes in Oregon and Washington—an overview of recent geologic studies and their bearing on segmentation of Holocene ruptures, central Cascadia subduction zone, *in* Rogers, A.M., Walsh, T.J., Kockelman, W.J., and Priest, G.R., eds., Assessing earthquake hazards and reducing risk in the

Pacific Northwest: U.S. Geological Survey Professional Paper 1560, p. 91–114.

Nelson, A.R., Shennan, I., and Long, A.J., 1996b, Identifying coseismic subsidence in tidal-wetland stratigraphic sequences at the Cascadia subduction zone of western North America: Journal of Geophysical Research, v. 101, p. 6115–6135.

Obermeier, S.F., 1995, Preliminary limits for the strength of shaking for the Columbia River valley and the southern half of coastal Washington for the Cascadia subduction zone earthquake of about 300 years ago: U.S. Geological Survey Open-File Report 94–589.

Ota, Y., and Umitsu, M., 1995, Stratigraphic, radiocarbon and diatom indicators of sudden submergence along the Nesselle [sic] River mouth, Washington, USA: Journal of Geography, v. 104, p. 107–112 (in Japanese).

Ovenshine, A.T., Lawson, D.E., and Bartsch-Winkler, S.R., 1976, The Placer River Silt—an intertidal deposit caused by the 1964 Alaska earthquake: Journal of Research of the U.S.Geological Survey, v. 4, p. 151–162.

Pacheco, J.F., Sykes, L.R., and Scholz, C.H., 1993, Nature of seismic coupling along simple plate boundaries of the subduction type: Journal of Geophysical Research, v. 98, p. 14133–14159.

Palmer, S.P., and Lingley, W.S., Jr., 1989, An assessment of the oil and gas potential of the Washington outer continental shelf: Washington Sea Grant Program, University of Washington, Seattle, 83 p.

Peterson, C.D., and Darienzo, M.E., 1989, Potential evidence of subduction zone tectonics from stacked peat horizons in late Pleistocene coastal terraces of the northern Cascadia margin [abstract]: Eos, v. 70, p. 1331.

———1996, Discrimination of climatic, oceanic, and tectonic mechanisms of cyclic marsh burial, Alsea Bay, Oregon, *in* Rogers, A.M., Walsh, T.J., Kockelman, W.J., and Priest, G.R., eds., Assessing earthquake hazards and reducing risk in the Pacific Northwest: U.S. Geological Survey Professional Paper 1560, p. 115–146.

Peterson, C.D., Scheidegger, K., Komar, P., and Neim, W., 1984, Sediment composition and hydrography in six high-gradient estuaries of the northwestern United States: Journal of Sedimentary Petrology, v. 54, p. 86–97.

Pezzopane, S.K., and Weldon, R.J., II, 1993, Tectonic role of active faulting in central Oregon: Tectonics, v. 12, p. 1140–1169.

Plafker, G., 1969, Tectonics of the March 27, 1964 Alaska earthquake: U.S. Geological Survey Professional Paper 543–I, 74 p.

Plafker, G., and Savage, J.C., 1970, Mechanism of the Chilean earthquakes of May 21 and 22, 1960: Geological Society of America Bulletin, v. 81, p. 1001–1030.

Plafker, G., Gilpin, L.M., and Lahr, J.C., 1994, Neotectonic map of Alaska, *in* Plafker, George, and Berg, H.C., eds., The Geology of Alaska: Geological Society of America, The Geology of North America, v. G1, Plate 12, scale 1:2,500,000 with 3 tables and text.

Plafker, G., and Kachadoorian, R., 1966, Geologic effects of the March 1964 earthquake and associated seismic sea waves on Kodiak and nearby island, Alaska: U.S. Geological Survey Professional Paper 543–D, 46 p.

Plafker, G., Lajoie, K.R., and Rubin, M., 1992, Determining recurrence intervals of great subduction zone earthquakes in southern Alaska by radiocarbon dating, *in* Taylor, R.E., Long, A., and Kra, R.S., eds., Radiocarbon after four decades, an interdisciplinary perspective: New York, Springer-Verlag, p. 436–453.

Redfield, A.C., 1972, Development of a New England salt marsh: Ecological Monographs, v. 42, p. 201–237.

Reid, C., 1913, Submerged forests: Cambridge, University Press, 129 p.

Reinhart, M.A., and Bourgeois, J., 1987, Distribution of anomalous sand at Willapa Bay, Washington—evidence for large-scale landward-directed processes [abstract]: Eos, v. 68, p. 1469.

———1989, Tsunami favored over storm or seiche for sand deposit overlying buried Holocene peat, Willapa Bay, WA [abstract]: Eos, v. 70, p. 1331.

Rogers, G.C., 1988, An assessment of the megathrust earthquake potential of the Cascadia subduction zone: Canadian Journal of Earth Sciences, v. 25, p. 844–852.

Satake, K., Shimazaki, K., Tsuji, Y., and Ueda, K., 1996, Time and size of a giant earthquake in Cascadia inferred from Japanese tsunami record of January 1700: Nature, v. 379, p. 246–249.

Savage, J.C., Lisowski, M., and Prescott, W.H., 1991, Strain accumulation in western Washington: Journal of Geophysical Research, v. 96, p. 14493–14507.

Savage, J.C., and Plafker, G., 1991, Tide gage measurements of uplift along the south coast of Alaska: Journal of Geophysical Research, v. 96, p. 4325–4336.

Sayce, K., 1988, Introduced cordgrass, *Spartina alterniflora* Loisel. in saltmarshes and tidelands of Willapa Bay, Washington: Ilwaco, Washington, Willapa National Wildlife Refuge, U.S. Fish and Wildlife Service contract FWSI-87058(TS), 70 p.

Scholz, C.H., and Campos, J., 1995, On the mechanism of seismic decoupling and back arc spreading at subduction zones: Journal of Geophysical Research, v. 100, p. 22103–22115.

Scott, E.M., Aitchison, T.C., Harkness, D.D., Cook, G.T., and Baxter, M.S., 1990, An overview of all three stages of the international radiocarbon intercomparison: Radiocarbon, v. 32, p. 309–319.

Shennan, I., 1986, Flandrian sea-level changes in the Fenland. I: The geographical setting and evidence of relative sea-level changes: Journal of Quaternary Science, v. 1, p. 119–154.

Shennan, I., Long, A.J., Rutherford, M.M., Green, F.M., Innes, J.B., Lloyd, J.M., Zong, Y., and Walker, K.J, 1996, Tidal marsh stratigraphy, sea-level change and large earthquakes, I: a 5000 year record in Washington, USA: Quaternary Science Reviews, v. 15, p. 1023–1059.

Shennan, I., Tooley, M.J., Davis, M.J., and Haggart, B.A., 1983, Analysis and interpretation of Holocene sea-level data: Nature, v. 302, p. 404–406.

Sherrod, B.L., Rollins, H.B., and Kennedy, S.K., 1989, Subrecent intertidal diatoms from St. Catherine Island, Georgia: taphonomic implications: Journal of Coastal Research, v. 5, p. 665–677.

Sieh, K., Stuiver, M., and Brillinger, D., 1989, A more precise chronology of earthquakes produced by the San Andreas fault in southern California: Journal of Geophysical Research, v. 94, p. 603–623.

Snavely, P.D., Jr., and Wells, R.E., 1996, Cenozoic evolution of the continental margin of Oregon and Washington, *in* Rogers, A.M., Walsh, T.J., Kockelman, W.J., and Priest, G.R., eds., Assessing earthquake hazards and reducing risk in the Pacific

Northwest: U.S. Geological Survey Professional Paper 1560, p. 161–182.

Streif, H., 1972, The results of stratigraphical and facial investigations in the coastal Holocene of Woltzeten/Ostfriesland, Germany: Geologiska Foreningens i Stockholm Forhandlingar, v. 94, p. 280–299.

———1982, Review of chapter 1: The occurrence and significance of peat in the Holocene deposits of the German North Sea coast, *in* de Bakker, H., and van den Berg, M.W., eds., Proceedings of the symposium on peat lands below sea level: Wageningen, The Netherlands, International Institute for Land Reclamation and Improvement, p. 31–41.

Stuiver, M., and Becker, B., 1986, High-precision decadal calibration of the radiocarbon time scale, AD 1950–6000 BC: Radiocarbon, v. 28, p. 863–910.

———1993, High-precision decadal calibration of the radiocarbon time scale, AD 1950–6000 BC: Radiocarbon, v. 35, p. 35–67.

Stuiver, M., and Pearson, G.W., 1986, High-precision calibration of the radiocarbon time scale AD 1950–500 BC: Radiocarbon, v. 28, p. 805–838.

Stuiver, M., and Reimer, P.J., 1993, Extended ^{14}C data base and revised CALIB 3.0 ^{14}C age calibration program: Radiocarbon, v. 35, p. 215–230.

Swan, F.H., 1987, Temporal clustering of paleoseismic events on the Oued Fodda fault, Algeria, *in* Crone, A.J., and Omdahl, E.M., eds., Directions in Paleoseismology: U.S. Geological Survey Open-File Report 87–673, p. 239–248.

Swan, J.G., 1857, The Northwest Coast or, Three Years' Residence in Washington Territory: Harper & Brothers, 435 p. (reprinted in 1972 by University of Washington Press, Seattle).

Thatcher, W., 1984, The earthquake deformation cycle at the Nankai Trough, southwest Japan: Journal of Geophysical Research, v. 89, p. 3087–3101.

———1989, Earthquake recurrence and risk assessment in circum-Pacific seismic gaps: Nature, v. 341, p. 432–434.

Torresan, M.E., 1987, Review and comparison of hydrophotometer and pipette method in analysis of fine grained sediment: U.S. Geological Survey Open-File Report 87–514, p. 1–38.

van de Plassche, O., 1991, Late Holocene sea-level fluctuations on the shore of Connecticut inferred from transgressive and regressive overlap boundaries in salt-marsh deposits: Journal of Coastal Research, special issue 11, p. 159–179.

Varekamp, J.C., Thomas, E., and Van de Plassche, O., 1992, Relative sea-level rise and climate change over the last 1500 years, *in* Wezel, F.-C., ed., Global Change Special Issue: Terra Nova, v. 4, p. 293–304.

Wagner, H.C., 1967a, Preliminary geologic map of the Raymond quadrangle, Pacific County, Washington: U.S. Geological Survey Open-File Report 67–265, scale 1:62,500.

———1967b, Preliminary geologic map of the South Bend quadrangle, Pacific County, Washington: U.S. Geological Survey Open-File Report 67–266, scale 1:62,500.

Walsh, T.J., Combellick, R.A., and Black, G.L., 1995, Liquefaction features from a subduction zone earthquake: preserved examples from the 1964 Alaska earthquake: Washington Division of Geology and Earth Resources, Report of Investigations 32, 80 p.

Walsh, T.J., Korosec, M.A., Phillips, W.M., Logan, R.L., and Schasse, H.W., 1987, Geologic map of Washington—southwest quadrant: Washington Division of Geology and Earth Resources Geologic Map GM–34, scale 1:250,000.

Ward, G.K., and Wilson, S.R., 1978, Procedures for comparing and combining radiocarbon age determinations: a critique: Archaeometry, v. 20, p. 19–31.

Weichert, D.H., and Adams, J., 1995, Non-parametric estimates of Cascadia earthquake hazard [abstract]: Seismological Research Letters, v. 66, no. 2, p. 49.

Weinmann, F., Boulé, M., Brunner, K., Malek, J., and Voshino, V., 1984, Wetland plants of the Pacific Northwest: Seattle, Washington, U.S. Army Corps of Engineers, 85 p. and others, 1984.

Wells, D.R., and Coppersmith, K.J., 1994, New empirical relationships among magnitude, rupture length, rupture width, rupture area, and surface displacement: Bulletin of the Seismological Society of America, v. 84, p. 974–1002.

Wells, R.E., 1989, Geologic map of the Cape Disappointment–Naselle River area, Pacific and Wahkiakum Counties, Washington: U.S. Geological Survey Miscellaneous Investigations Map I–1832, scale 1:62,500.

Wilson, D.S., 1993, Confidence intervals for motion and deformation of the Juan de Fuca plate: Journal of Geophysical Research, v. 98, p. 16053–16071.

Yamaguchi, D.K., Atwater, B.F., Bunker, D.E., Benson, B.E., and Reid, M.S., 1997, Tree-ring dating the 1700 Cascadia earthquake: Nature, v. 389, p. 922–923.

Yamaguchi, D.K., Woodhouse, C.A., and Reid, M.S., 1989, Tree-ring evidence for synchronous rapid submergence of the southwestern Washington coast about 300 years ago [abstract]: Eos, v. 70, p. 1332.

☆ U.S. GOVERNMENT PRINTING OFFICE: 1997 - 673-048 / 20088 REGION NO. 8

SELECTED SERIES OF U.S. GEOLOGICAL SURVEY PUBLICATIONS

BOOKS AND OTHER PUBLICATIONS

Professional Papers report scientific data and interpretations of lasting scientific interest that cover all facets of USGS investigations and research.

Bulletins contain significant data and interpretations that are of lasting scientific interest but are generally more limited in scope or geographic coverage than Professional Papers.

Water-Supply Papers are comprehensive reports that present significant interpretive results of hydrologic investigations of wide interest to professional geologists, hydrologists, and engineers. The series covers investigations in all phases of hydrology, including hydrogeology, availability of water, quality of water, and use of water.

Circulars are reports of programmatic or scientific information of an ephemeral nature; many present important scientific information of wide popular interest. Circulars are distributed at no cost to the public.

Fact Sheets communicate a wide variety of timely information on USGS programs, projects, and research. They commonly address issues of public interest. Fact Sheets generally are two or four pages long and are distributed at no cost to the public.

Reports in the **Digital Data Series (DDS)** distribute large amounts of data through digital media, including compact disc–read-only memory (CD-ROM). They are high-quality, interpretive publications designed as self-contained packages for viewing and interpreting data and typically contain data sets, software to view the data, and explanatory text.

Water-Resources Investigations Reports are papers of an interpretive nature made available to the public outside the formal USGS publications series. Copies are produced on request (unlike formal USGS publications) and are also available for public inspection at depositories indicated in USGS catalogs.

Open-File Reports can consist of basic data, preliminary reports, and a wide range of scientific documents on USGS investigations. Open-File Reports are designed for fast release and are available for public consultation at depositories.

MAPS

Geologic Quadrangle Maps (GQ's) are multicolor geologic maps on topographic bases in 7.5- or 15-minute quadrangle formats (scales mainly 1:24,000 or 1:62,500) showing bedrock, surficial, or engineering geology. Maps generally include brief texts; some maps include structure and columnar sections only.

Geophysical Investigations Maps (GP's) are on topographic or planimetric bases at various scales. They show results of geophysical investigations using gravity, magnetic, seismic, or radioactivity surveys, which provide data on subsurface structures that are of economic or geologic significance.

Miscellaneous Investigations Series Maps or Geologic Investigations Series (I's) are on planimetric or topographic bases at various scales; they present a wide variety of format and subject matter. The series also includes 7.5-minute quadrangle photogeologic maps on planimetric bases and planetary maps.

INFORMATION PERIODICALS

Metal Industry Indicators (MII's) is a free monthly newsletter that analyzes and forecasts the economic health of five metal industries with composite leading and coincident indexes: primary metals, steel, copper, primary and secondary aluminum, and aluminum mill products.

Mineral Industry Surveys (MIS's) are free periodic statistical and economic reports designed to provide timely statistical data on production, distribution, stocks, and consumption of significant mineral commodities. The surveys are issued monthly, quarterly, annually, or at other regular intervals, depending on the need for current data. The MIS's are published by commodity as well as by State. A series of international MIS's is also available.

Published on an annual basis, **Mineral Commodity Summaries** is the earliest Government publication to furnish estimates covering nonfuel mineral industry data. Data sheets contain information on the domestic industry structure, Government programs, tariffs, and 5-year salient statistics for more than 90 individual minerals and materials.

The Minerals Yearbook discusses the performance of the worldwide minerals and materials industry during a calendar year, and it provides background information to assist in interpreting that performance. The Minerals Yearbook consists of three volumes. Volume I, Metals and Minerals, contains chapters about virtually all metallic and industrial mineral commodities important to the U.S. economy. Volume II, Area Reports: Domestic, contains a chapter on the minerals industry of each of the 50 States and Puerto Rico and the Administered Islands. Volume III, Area Reports: International, is published as four separate reports. These reports collectively contain the latest available mineral data on more than 190 foreign countries and discuss the importance of minerals to the economies of these nations and the United States.

PERMANENT CATALOGS

"Publications of the U.S. Geological Survey, 1879–1961" and **"Publications of the U.S. Geological Survey, 1962–1970"** are available in paperback book form and as a set of microfiche.

"Publications of the U.S. Geological Survey, 1971–1981" is available in paperback book form (two volumes, publications listing and index) and as a set of microfiche.

Annual supplements for 1982, 1983, 1984, 1985, 1986, and subsequent years are available in paperback book form.